FINAL Report A

TRyy1110

Project Title: Design and Evaluation of High-Volume Fly Ash (HVFA) Concrete Mixes

Report A: Evaluation of HVFA Cementitious Paste and Concrete Mixtures

Prepared for
Missouri Department of Transportation
Construction and Materials

Missouri University of Science and Technology, Rolla, Missouri

October 2012

ABSTRACT

In the Paste Screening Study, 25 combinations of five Type I/II portland cements and five Class C fly ashes commonly used in Missouri were tested in paste form with no chemical or powder additives. Testing procedures included semi-adiabatic calorimetry, Vicat setting time, miniature slump, and compressive strength at one and 28 days. The two most reactive and two least reactive combinations (defined by one day strengths) were further evaluated in the Paste Main Effects Study. Eighty mixtures were examined.

In the Paste Main Effects Study, the effects of two levels each of WR/HRWR, gypsum, calcium hydroxide (lime), rapid set cement (RSC), and gypsum-lime, and gypsum-RSC were determined. Except for the WR/HRWR dosage level experiment, all other mixtures contained a low WR/HRWR dosage. Except for the gypsum level experiment, all other mixtures contained 4% gypsum. The lime levels were 5 and 10% and the RSC levels were 10 and 20%. All percentages are by mass of fly ash. Sixty-four mixtures were examined.

The objective of the Concrete Properties Study was to scale up from paste to concrete the most promising powder additive combinations and then evaluate the mixtures in terms of plastic and hardened properties. Thus the mixture matrix included ordinary portland cement (OPC)-fly ash blends at two levels (same as in the Paste Main Effects Study) and fly ash at three levels (zero, 50 and 70%). WR dosage (nominal dosage), gypsum content (4%), lime content (10%), and RSC content (20%) were held constant. Ten concrete mixtures were evaluated.

At the 50% fly ash level, one day strengths were low no matter which powder additives was used, but good strengths were achieved by day 3. At the 70% fly ash level,

the concrete was weaker than at zero and 50% fly ash, but reasonable strengths were reached at 28 days. At 50% fly ash, abrasion resistance was somewhat lower. At 70% the effect was much worse. In regard to drying shrinkage, it appears that HVFA mixtures shrink less than their OPC counterparts. In a comparison to OPC mixtures, rapid chloride permeability (RCP) was lower for 50% fly ash mixtures, but 70% fly ash mixtures are more permeable. All HVFA mixtures had greater freeze-thaw Durability Factors than the OPC mixtures, and were at 93 or above. However, all fly ash mixtures did poorly in regard to salt scaling. Reaction time (calorimeter curve time, setting time, stiffening time) varied as a function of characteristics of the OPC and fly ash in conjunction with each other, type and level of powder additives used, dosage of WR/HRWR, and the type of test method used for evaluation.

TABLE OF CONTENTS

Page

LIST OF ILLUSTRATIONS

Figure Page

LIST OF TABLES

1. INTRODUCTION

1.1. BACKGROUND

Missouri S&T was contracted by MoDOT to determine the feasibility of using high substitution rates of fly ash for portland cement in concrete used for structural purposes. Using a large amount of fly ash in concrete typically results in slower setting times, reduced early strength (and sometimes reduced ultimate strength), salt scaling issues, and incompatibilities with other concrete components which sometimes result in unexpected and severe early stiffening and delayed strength gain. Although concrete with high replacement levels of fly ash were studied over 30 years ago, methods of mitigation of these problems has recently centered on use of activator powders. The current interest in HVFA concrete stems from an increased interest in sustainability, determining the upper limit of replacement level issues that can be mitigated, and dealing with incompatibilities, especially for materials common in Missouri. As a part of the overall study being conducted by Missouri S&T, the present portion of the study deals with producing a variety of mixture designs and determining the plastic and hardened properties of the high volume fly ash (HVFA) concrete.

1.2. OBJECTIVES

The objectives of this portion of the study was to select portland cement, fly ash, and several powder activators for use in HVFA concrete, and to develop several mixtures for further testing.

1.3. SCOPE

The scope of this study was limited to sources of portland cement and fly ash commonly used in Missouri. The powder activators were limited to gypsum, hydrated lime, and commercially available rapid set cement, and to specific percentages as used in previous studies (Marlay, 2011), which have been shown to be effective in reducing the harmful effects of high volumes of fly ash in concrete (Bentz, 2010).

2. LITERATURE REVIEW

2.1. HIGH VOLUME FLY ASH MIXTURES

2.1.1. High Volume Fly Ash Hydration. High volume fly ash (HVFA) concrete mixes are typically defined as concrete mixes containing larger than normal replacements of cement with fly ash. This replacement is typically greater than or equal to 30% replacement (Naik, et al., 1995). Others have defined HVFA as 50% fly ash or more. Replacing large volumes of cement with fly ash in this manner, however, drastically influences the hydration curve of the cementitious system. Wang, et al. investigated the effects of fly ash and admixtures on the hydration curve of cement. They replaced Type I and II cement with 20% of Class F and Class C fly ash. Class F fly ash served only to reduce the heat release, while Class C fly ash reduced the heat release as well as delaying the peak of the hydration curve, effectively serving to retard the set of the concrete mixture. When combining substitution of fly ash with the addition of a water reducing (WR) admixture and a retarding admixture, the Class C mixes were more significantly affected than any other combination, impeding hydration for an extended time (Wang, et al., 2006).

Sulfate is required in order to force the reaction of tricalcium aluminate (C_3A) and tetracalcium aluminoferrite (C_4AF) to ettringite. Ettringite requires a significant concentration of sulfate in order to form and remain stable—once the sulfate level drops below the level required to maintain stable formation of ettringite, it undergoes conversion to monosulfate. In addition, the sulfate level affects the reaction of the silicates (tricalcium silicate, C_3S and dicalcium silicate, C_2S) in cement, more fully hydrating the silicates and resulting in higher strengths. If not enough sulfate is present

in the cement, ettringite will be unable to slow the reaction of C_3A, which will consume the calcium in solution, slowing or stopping the hydration of silicates, and resulting in retardation of set, or failure to set (Roberts & Taylor, 2007).

In regard to WR, as dosages of water reducing admixtures increase, the silicate hydration peak is retarded, resulting in retarded set. Beyond a point, the sulfate depletion occurs before the silicate hydration peak, resulting in the formation of monosulfate, and the consumption of calcium in C_3A hydration, leading the silicate peak to be severely retarded and depressed. Combining this effect with substitution of Class C fly ash, which depresses the silicate hydration peak, set may not occur (Roberts and Taylor, 2007).

Jiang, et al. investigated the hydration of HVFA pastes using replacement rates of 40% or greater. They found that as the fly ash content increased and as the *w/cm* increased, the total porosity increased. At a fly ash content of 70%, mixes with a larger *w/cm* showed a higher permeability, suggesting that the fly ash content should be limited to less than 70% in HFVA concrete. However, with increase of age, the porosity decreased, with pore volumes in HVFA mixes being of a smaller size. This was because the hydration of fly ash particles leads to a denser microstructure with an improved pore size distribution. However, using a scanning electron microscope, the authors noted that even at 90 days, many unreacted fly ash particles were found embedded in hydration products, which suggests that the fly ash in HVFA concrete cannot be fully hydrated (Jiang, et al., 1999).

Hübert, et al. examined the hydration products in HVFA binders. Three blended cements were examined containing 60%, 70%, and 85% replacement of portland cement by weight with two different fly ashes. Hydration was halted after 3, 7, 28, 90, and 300

days to characterize the hydration products. For every HVFA mix the calcium hydroxide content was lower than the baseline cement-only mix at all ages. For several of the mixes, complete depletion of calcium hydroxide occurred, likely due to the high reactivity of the fly ash. Ettringite content was also examined in the mixes, with evidence that ettringite was also a product of the hydration of the fly ash in these systems. The two different fly ashes showed that differing fly ash contents were required to attain the greatest amount of additional C-S-H. This is likely due to the varying consumption of calcium hydroxide. The reactivity of the fly ash used in a concrete mix needs to be adapted to the amount of available calcium hydroxide for optimal increase in strength (Hübert, et al., 2001). This leads to an examination of the concept of adding supplementary powder additives.

2.1.2. Powder Activators. Bentz examined HVFA mixes with a 50% replacement of cement with Class C fly ash, which resulted in a loss of compressive strength in the paste cubes. The addition of one and five % gypsum increased early age hydration and strength but did nothing to influence the retardation in set. Powder additions are necessary to restore the "normal" hydration and strength development, though some may not serve to mitigate the retardation influence of the fly ash. Bentz examined several powder additions with the intent of mitigating the retardation. Dosages for these powders were in percentage of total solids of the mix. A dosage of 5% of the mass of total solids of limestone powder showed a minimal effect on the hydration curve. Ten% aluminum hydroxide increased the heights of the hydration peaks, but did not accelerate the occurrence of the peaks. In particular, aluminum hydroxide increased the height of the second peak, corresponding to secondary aluminate hydration. A dosage of

10% cement kiln dust only accelerated the curves minimally, though Bentz notes that it increased the early-age hydration. Five % condensed silica fume accelerated the hydration, but failed to restore the curve to the condition of the baseline curve. Of the powders examined, the two that showed a marked degree of success in restoring the normal hydration were calcium hydroxide and rapid set cement (Bentz, 2010). It has been shown that that these two activators serve to decrease set times of HVFA mixes back to set times similar to a control mix, or in some cases resulting in faster setting than the baseline, while still resulting in an initial set of greater than three hours, allowing for time to transport and place the concrete (Bentz and Ferraris, 2010).

2.1.2.1. Calcium Hydroxide. If insufficient calcium is available and is consumed by C_3A reactions, the silicate reactions will be slowed or halted. The addition of calcium hydroxide, then, provides a source of calcium ions to restore the normal silicate reactions (Roberts and Taylor, 2007). Calcium is already being restored to the mixture in the form of gypsum, however, it is likely that the calcium and sulfate provided by gypsum are both being utilized in aluminate reactions, leading to the formation of ettringite rather than aiding in the silicate hydration. In Bentz' study of 5% calcium hydroxide addition, the hydration curve accelerated by 1.5 hours; this acceleration increased when a high range water reducer (HRWR) was present in the mixture, nearly restoring the curve to the same position as the control mixture. However, it was suggested that calcium hydroxide may reduce compressive strengths (Bentz, 2010).

2.1.2.2. Rapid Set Cement. Rapid set cement contains calcium sulfoaluminate, dicalcium silicate, and gypsum. The chemistry of rapid set cement may be unaffected by the retarding action of the fly ash. A three-component blend would utilize rapid set

cement to contribute to early age strength development and set, while fly ash would contribute to the longer term performance and strength gain. Rapid set cement was used at a dosage of 10% of the total mass of cementitious materials. Rapid set cement provides two separate contributions to the mix: both the hydration reactions of the rapid set cement, and the accelerated hydration of the cement/fly ash mixture due to the rapid set cement. With a HRWR, retardation was reduced by four hours, with the rapid set cement reacting nearly immediately after contact with water. In addition, he writes that initial compressive strengths were five % greater than those with no rapid set cement addition at 28 days. There is some concern that at a replacement level of 20%, the hydration may be excessive, and lead to setting occurring too rapidly (Bentz, 2010).

2.1.3. Mixture Proportioning. Bentz, et al. present a method for optimizing HVFA concrete mixes; the method consists of four stages: checking compatibility, attaining acceptable setting times, attaining acceptable strengths, and attaining acceptable autogenous shrinkage. After selecting potential fly ash and cement sources, compatibility should be determined by calorimetry. If the cement and fly ash combination are deemed incompatible, then this incompatibility must be rectified by addition of gypsum in order to optimize sulfate balance. Then, retardation should be mitigated by means of either powder addition to the mix, or admixture replacement. Calcium hydroxide and rapid set cement have been found to have potential for restoring setting time at levels of 5% to 10% per mass of binder. Adjustment of the dosage of water reducer, if applicable, may be necessary at this level. Though long term strengths of HVFA mixtures may approach or exceed those of control mixtures, short term strengths may suffer. If higher one day strengths are required from the HVFA mix, switching to a Type III cement may provide

increased early strengths. Changing from a Type II/V cement to a Type III cement resulted in a compressive strength increase of 60% at one day. It is critical to maintain saturation of the capillary pores in order to not only hydrate the long term strength products, but also to reduce autogenous shrinkage. External curing may not be enough, due to the limited travel distance of water once the capillary porosity becomes severely limited due to hydration. Internal curing seems effective in providing a long term source of hydration for pozzolanic reactions. However, if this method is chosen, the cost of materials will significantly increase. By following this method of proportioning HVFA concrete mixes, benefits will include a lowered tendency toward thermal cracking due to the lower heat release of HVFA concrete mixes, as well as a cost savings at the time of placement and over a life-cycle (Bentz, et al., 2010).

2.2. PASTE CONSIDERATIONS

2.2.1. Compressive Strength. The rate of strength gain in mixtures containing high volumes of Class C fly ash will be slower due to the slow rate of the pozzolanic reaction. This results in lower early strengths. However, the pozzolanic reaction will also generally produce greater strengths at later ages. This is due to the replacement of the weak CH products with C-S-H, which is stronger, and the filling of pores with pozzolanic reaction products, which reduces the overall porosity of the paste and leads to an increase in strength (Detwiler, et al., 1996).

2.2.2. Methods of Evaluating Heat Evolution. There are many calorimetry methods and tools used to evaluate the heat evolution of cementitious mixtures. Some of the more widely used calorimeters include isothermal, semi-adiabatic, adiabatic, and

solution calorimeters. The type of calorimetry device, mixing method, temperature of mixing environment, and sample size can all affect the results for a given mixture. Also, calorimetry results are reported in different ways, depending on the type of calorimeter being used. Therefore, it is necessary to have an understanding of the method behind varying calorimetry techniques when interpreting the results of heat of hydration experiments (Wang, 2006).

2.2.2.1. Isothermal Calorimetry. Isothermal calorimetry is used to measure the rate of heat production of a specimen kept at near-isothermal conditions. This means that the temperature of the specimen is kept at a near constant temperature during hydration. A typical isothermal calorimeter employs two heat flow sensors, each with an attached specimen vial holder, and a heat sink with a thermostat. A prepared sample is placed in one of the vials and an inert specimen is placed in the other vial. Each vial is then placed into one of the vial holders. The heat released during hydration then passes to the heat flow sensors. The output of the inert specimen sensor is subtracted from the output of the test specimen sensor to result in the calorimeter output. The heat production is measured in watts (W) or joules per second (J/s). The results are usually reported in relation to the specimen mass as mW/g or J/s/g (ASTM C 1679, 2009). Isothermal calorimetry is used as a precise means of determining the heat produced solely by the cementitious materials at a given temperature. The results are generally used quantitatively.

2.2.2.2. Semi-Adiabatic Calorimetry. Semi-adiabatic calorimetry measures the temperature of a partially insulated specimen over time. There are a variety of semi-adiabatic systems available that differ in the size of sample used and the degree of insulation. The objective for a given system is to insulate the sample in a way that

minimizes the influence of the ambient temperature, but also does not retain excessive heat that would accelerate the hydration of the specimen and distort the thermal profile. One common system uses plastic cylinder molds as the specimen container. The container is placed in a cylindrical receptacle in the device, which consists of an insulated box with a thermocouple at the bottom, so that the thermal readings are taken from the bottom of the specimen. Another common method uses thermocouples or thermistors, which are inserted into the center of the specimen. With this method, the specimen container is anything that can hold an appropriately sized sample, such as plastic cylinders or even coffee cups (Cost, 2009).

Semi-adiabatic calorimetry is generally used as an economical alternative to isothermal calorimetry that can also be used in field conditions. The results are generally used for comparative and qualitative evaluation. However, some researchers have used more elaborate semi-adiabatic methods to achieve quantitative results, such as the adiabatic temperature rise or predicted setting times. Also, semi-adiabatic conditions may provide a better model for the thermal conditions inside a non-massive concrete structure, where gradual heat loss occurs.

2.2.2.3. Adiabatic Calorimetry. In adiabatic calorimetry, there is no heat loss or gain experienced by the specimen and the temperature of the specimen is measured during hydration. An economical adiabatic calorimeter used by Gibbon, et al. consisted of a large tank with heater elements, a temperature probe, and stirrers. Inside of the tank, the specimen container was placed with a temperature probe inserted in the center of the specimen. The water temperature was controlled to be maintained at the same temperature as the hydrating sample. After completion of a test, the temperature readings

were used to determine the specific heat and heat of hydration. The heat of hydration curve was then integrated to give a plot of total heat produced over time (Gibbon, et al., 1997).

This type of calorimetry is often used to determine the cumulative temperature rise of the concrete over time. It provides a model of the heat conditions in massive concrete structures, where there is little or no dissipation of heat.

2.2.2.4. Solution Calorimetry. Solution calorimetry is most often used to determine the adherence of a hydraulic cement to ASTM specifications on heat of hydration requirements at 7 and 28 days. However, it may also be used for research purposes to determine the heat of hydration at any age. The method involves dissolving two samples in a solution of nitric acid and hydrofluoric acid. One of the samples consists of the dry cementitious materials, while the other is a corresponding, partially hydrated paste specimen. The paste specimen is prepared ahead of time and stored in a sealed vial and placed in a water bath. At the time of testing, the paste specimen is removed from the vial and crushed with a mortar and pestle until all of the material passes through a No. 20 sieve. The heat of solution of the dissolving specimens is measured and the difference between the dry and partially hydrated specimens is taken as the heat of hydration (ASTM C 186, 2005).

2.2.3. Evaluation of Heat Evolution to Avoid Incompatibilities. The composition of mineral admixtures varies considerably, even between those that fall under the same classification. This leads to complexity in cementitious systems, as the use of one or more mineral admixtures in a single concrete mixture is commonplace. Due to this complexity, problems such as slump loss, delayed setting, and slow rates of

strength gain, are more likely to occur as a result of incompatibilities between the materials. The most common cause of incompatibility is related to the sulfate concentration in a system. If there is not a sufficient amount of sulfate, the aluminates (C_3A and C_4AF) will react rapidly and consume a large portion of the available calcium in the system. This will cause the hydration of the silicates (C_3S and C_2S) to slow down and possibly stop completely. Using isothermal calorimetry, Lerch (1946) illustrated the effect of insufficient sulfate levels on cement. The results showed that as the sulfate level decreased, the second peak of the hydration curve decreased. This was attributed to a depletion of available calcium for hydration of the silicates. A similar effect was found by Roberts and Taylor (2007) for concrete mixtures with Class C fly ash, which is known to commonly cause incompatibility related problems, due to relatively high levels of aluminates. The results show a decrease and delay in the silicate hydration curve.

Cost and Knight (2007) also discussed the use of Class C fly ash as a common cause of abnormal behavior in concrete, due to increased aluminate levels, along with high temperatures, sulfate levels, chemical admixtures, and hot-weather concreting practices. It was noted that the potential for erratic behavior may increase in hot-weather concrete operations if the dosage of Class C fly ash is increased to utilize the retarding effect of the material. As part of the study, the heat generation of several paste mixtures was evaluated, using semi-adiabatic calorimetry, to detect incompatibilities. The concrete was made with a Type II cement at varying sulfate levels and a Class C fly ash at varying replacement levels. The results showed that the only combination to generate a typical silicate peak was the 3.3% sulfate cement with 10% fly ash. The combinations of this cement with 25% and 35% fly ash both showed extremely depressed silicate hydration

peaks. The 3.7% sulfate cement with 25% fly ash showed improvement in the silicate peak, but at 35% fly ash only a small peak was developed. To investigate an additional increase in sulfate, the sulfate content of the cement was increased to 4.1% in combination with the 35% replacement level of Class C fly ash. This seemed to somewhat restore the silicate peak, but it was delayed significantly (Cost and Knight, 2007).

As can be seen, the use of Class C fly ash can cause significant problems in concrete when the sulfate balance has been compromised. High temperatures and the use of chemical admixtures, such as water reducers, can increase the magnitude of incompatibility related problems as these can affect the solubility and reaction rate of compounds in the system (Cost and Knight, 2007). Generally, the adverse effects of incompatibilities are accompanied by changes in heat evolution. Therefore, investigating the heat producing behavior of cementitious system can assist in avoiding incompatibilities in the field.

2.2.4. Miniature Slump. Kantro (1980) discussed the use of the miniature slump test as a rapid means of determining the effects of admixtures on the rheological properties of cement pastes. In this study, a miniature slump cone was made of Lucite with a height of 2.25 inches, top diameter of 0.75 inches, and bottom diameter of 1.50 inches. These dimensions were chosen to be in proportion to the dimensions of the traditional slump cone used for ASTM C 143. After performing the test, the area of the paste pat was determined. The miniature slump test was used on paste mixtures with varying water-cement ratios and various admixtures. It was found that the method was suitable for comparative testing and evaluating loss in workability. Also, though it was

determined that the miniature slump test was more sensitive, it was found that the overall effects observed with the paste testing correlated with the results of corresponding concrete testing.

Other researchers have utilized the miniature slump cone to evaluate the early stiffening behavior of pastes (Bhattacharja and Tang, 2001; Roberts and Taylor, 2007). In these studies, the paste was mixed following a standard procedure and the miniature slump test was performed at 2, 5, 15, and 30 minutes after the start of mixing. It was noted that later times, such as 45 minutes, may also be used. Roberts and Taylor discussed the use of an early stiffening index, which was calculated by dividing the pat area at 30 minutes by the pat area at 5 minutes. They noted that calculated indices less than 0.85 are generally considered to indicate rapid stiffening behavior. It was also noted by these researchers that since pastes are more sensitive to incompatibilities, paste systems that indicated potential problems may behave normally in concrete mixtures.

2.3. PLASTIC CONCRETE PROPERTIES

2.3.1. Slump. In a study involving the influence of varying fly ash contents on slump and required dosage of HRWR, the mix using unground fly ash required less HRWR to achieve a given slump than the mix using fly ash which had been interground with the cement. The increase in required HRWR was due primarily to the increased fineness of the interground fly ash (Bouzoubaa, et al., 2001).

Bouzoubaa, et al. (2007) investigated the use of 30%, 40%, and 50% by mass replacement of cement with fly ash. Three concrete mixtures were of different grades: 20, 40, and 60 MPa achieved by varying the cement content. As fly ash content

increased, the water requirement to attain a given slump decreased, and consequently the *w/cm* decreased as well (Bouzoubaa, et al., 2007).

2.3.2. Air Content. In regard to the influence of varying fly ash content on air content and required dosage of air entraining agents, fly ash which had been interground with the cement required a higher dosage of air entraining agent than the mix using an unground fly ash. This was also primarily due to the increased fineness of the interground fly ash (Bouzoubaa, et al., 2001).

Bilodeau, et al. noted that the amount of air entraining agent required to attain the desired air content was greatly influenced by both the fly ash and the cement used in the mix. Differing dosages were due to the carbon, alkali contents, and the fineness of the fly ash, and the alkali content of the cement used (Bilodeau, et al., 1994).

2.3.3. Time of Set. Mehta and Monteiro note that the initial setting and final setting times are arbitrarily defined in test methods, and they do not mark a specific physical or chemical change in the cement paste, but rather "the former defines the limit of handling and the latter defines the beginning of development of mechanical strength".

In a study of HVFA concretes, the setting times for HVFA concrete mixtures were 30 minutes to 3 ½ hours longer than those of the baseline mixes. The fly ash mixes used in this study consisted of 45% by mass of cement, and 55% by mass of a Class F fly ash (Bouzoubaa, et al., 2001).

2.3.4. Microwave Water Content. The method used for determining water content of fresh concrete by the microwave method comes from work done by Nagi and Whiting. The authors used a 900 W microwave oven to dry a 1500 g sample of concrete. They developed a schedule for microwaving the sample and breaking it up in order to

achieve full recovery of water content within a reasonable amount of time. A delay of up to 30 minutes from initial mixing showed no effect on the results of microwave water content determination. There was good agreement between multiple operators after only a brief instruction in the test method. In addition to being reproducible, the test is also independent of absorption of aggregates or the consistency of the concrete, having tested it on mixes ranging from a 0.2 in. (5 mm) slump to a 6.6 in. (168 mm) slump (Nagi and Whiting, 1994).

2.4. HARDENED CONCRETE PROPERTIES

2.4.1. Compressive Strength. Compressive strength of HVFA mixtures typically suffers in the short term, as highly reactive cement is replaced with less reactive fly ash. One study showed 55% Class F fly ash mixtures obtained around half the strength of ordinary portland cement (OPC) mixtures at one day. The fly ash mixtures only begin to match or exceed the strength of control mixes between 14 and 28 days, with substantial strength gains still occurring out to one year. This is due to the pozzolanic activity of the fly ash present in the mix reacting to continue to form C-S-H (Bouzoubaa, et al., 2001).

Another study showed strengths of Class F fly ash mixes at 30%, 40%, and 50% replacement by mass of cement with fly ash lagging behind their control mix counterpart in strengths. The difference between the control mix and the HVFA mixtures lessens as the specimens age, and at one year of age, the 40% fly ash mix has exceeded the control mix in compressive strength (Galeota, et al., 1995).

In regard to long term effects of high volumes of both Class C and Class F fly ashes on concrete mixtures, it has been found that increasing volumes of both Class C

and Class F fly ashes resulted in a similar decrease in early strengths, although Class F fly ashes show a better long term strength gain correlation with increased fly ash volume. Class C fly ashes performed better at early age strength gain than Class F fly ashes, due to the pozzolanic activity imparted by the higher calcium content of Class C fly ashes (Naik, et al., 2003).

2.4.2. Flexural Strength. Bouzoubaa, et al. investigated the use of 30%, 40%, and 50% by mass replacement of cement with fly ash. Three concrete mixtures of different grades were studied: 20 MPa, 40 MPa, and 60 MPa. Splitting tensile and flexural strength increased with age and with increasing grade of concrete, however, the effect of fly ash was more varied. At the 20 MPa grade, fly ash content did not seem to affect the flexural strength significantly until 91 days of age, however at 40 MPa there were noticeably higher flexural strengths compared to the control concrete, and at 60 MPa, higher fly ash content resulted in a general decrease in flexural strengths (Bouzoubaa, et al., 2007).

A study by Naik, et al. examined three different fly ash mixes: 20% Class C fly ash, 50% Class C fly ash, and 40% Class F fly ash. As fly ash content increased for Class C ashes, the flexural strength suffered at earlier ages, though as the age approached a year the flexural strength of the 50% Class C fly ash mix approached and then exceeded the flexural strength seen by the 20% Class C fly ash mix. Flexural strength development curves followed a similar curve shape as that of compressive strength (Naik, et al., 1995).

2.4.3. Splitting Tensile Strength. Bouzoubaa, et al. investigated the use of 30%, 40%, and 50% by mass replacement of cement with fly ash. Three concrete mixtures of different grades were studied: 20 MPa, 40 MPa, and 60 MPa. Splitting tensile and

flexural strength increased with age and with increasing grade of concrete, however, the effect of fly ash was more varied. At the 20 MPa grade, fly ash content did not seem to affect the splitting tensile strength significantly, however at 40 MPa there were noticeably higher splitting tensile strengths compared to the control concrete, and at 60 MPa, higher fly ash content resulted in a decrease in splitting tensile strengths, with lower splitting tensile strengths than the control concrete at 91 days of age (Bouzoubaa, et al., 2007).

Rivest, et al. cast large monoliths of control concretes and a 56% fly ash HVFA mixture with accompanying specimens to test mechanical properties. Splitting tensile strengths were expected to fall in the range of 8% to 10% of the compressive strength as published data predicted (Rivest, et al., 2004).

A study by Naik, et al. examined three different fly ash mixtures: 20% Class C fly ash, 50% Class C fly ash, and 40% Class F fly ash. As fly ash content increased for Class C ashes, splitting tensile strengths decreased, following similar strength development curves as expected of compressive strength (Naik, et al., 1995).

2.4.4. Modulus of Elasticity. Rivest et al. found that the modulus of elasticity for the HVFA concrete mix was generally higher than both control concretes made with Type I and with Type II cement. They suggest that this is due to unreacted glassy fly ash particles acting as very fine aggregates rather than hydration products, thereby increasing the rigidity of the concrete. Also, the filler effect of the fly ash contributes to a stronger transition zone, subsequently increasing the rigidity of the concrete (Rivest, et al., 2004).

2.4.5. Abrasion Resistance. Cabrera and Atis note that there are no guidelines on values from abrasion tests that ensure whether a concrete will perform adequately or

not, thus, abrasion results may only be used on a comparative basis. The authors used a British abrasion standard typically used for abrasion characteristics of aggregates in their study; findings confirmed other studies that abrasion is closely related to compressive strength (Cabrera & Atis, 1999).

Three Class C fly ashes were investigated in concrete mixes at replacement rates of 40%, 50%, and 60%. A modified version of ASTM C 944 involved the addition of silica sand to the surface at one minute intervals while abrading the specimen, and measuring the resulting depth of wear with time. The resistance to abrasion increased with age, and decreased with both time abraded and fly ash content, although a 40% replacement of cement with fly ash seemed to perform as well as the control mixture with no ash. A correlation between abrasion resistance and compressive strength existed. The source of fly ash showed a significant effect on hardened concrete properties, though no definite trend was established by the authors between fly ash properties and abrasion resistance (Naik, et al., 2002).

2.4.6. Rapid Chloride Permeability. Rapid Chloride Permeability is measured by means of ASTM C 1202, which notes that the test measures electrical conductance of concrete, which is a rapid method of indicating concrete's resistance to chloride ion penetration, not a direct measure of chloride ion penetration (ASTM, 2012).

Gu, et al. examined the performance of steel reinforcement in HVFA concretes when exposed to chloride solutions. Two mixes in this study incorporated 58% by mass of both Class F and Class C fly ash. There was greater resistance to chloride ion permeability than control concretes, even at only 28 days of age (Gu, et al., 1999).

HVFA concrete mixes containing 58% replacement of cement by mass with fly ash were studied by Bilodeau et al. The resistance of concrete to chloride ion penetration from 28 days out to 1 year showed high resistance to chloride ion penetration, with values at one year being rated ‘very low’, or less than 1000 coulombs passed. There was a relationship between chloride ion penetration and compressive strength of concrete. The differences between two mixes using two different cements were likely due to differences in porosity as a result of differing rates of hydration and pozzolanic reaction in different cement and fly ash combinations (Bilodeau, et al., 1994).

Bouzoubaa, et al. investigated the use of 30%, 40%, and 50% by mass replacement of cement with fly ash with three concrete mixtures of different grades. While satisfactory chloride ion permeability could be achieved simply by reducing the *w/cm* ratio, the addition of fly ash drastically reduced chloride ion permeability as soon as 28 days, with 91 day tests showing coulomb values of less than 300, or almost negligible permeability (Bouzoubaa, et al., 2007).

2.4.7. Freeze-Thaw Resistance. Bilodeau, et al. examined a number of HVFA (58% fly ash) concrete mixes. After 300 cycles of freezing and thawing, all combinations of cement and fly ash showed durability factors of greater than or equal to 96. Freezing and thawing tests were extended to 1000 cycles, an extremely severe condition, and all but one mix retained durability factors of greater than or equal to 93 (Bilodeau, et al., 1994).

Galeota, et al. examined four concrete mixtures—one control mix with no fly ash, and three HVFA concrete mixes—at 30%, 40%, and 50% replacement of cement with fly ash. A Class F fly ash was used with no air entrainment. The control mixture with no fly

ash and the 30% fly ash mix failed earlier than did their counterparts containing more fly ash, showing that increased fly ash content seems to increase freeze-thaw resistance (Galeota, et al., 1995).

2.4.8. Scaling Resistance. The freeze-thaw resistance of concrete when in contact with deicing salts is generally lower than the resistance to freezing and thawing alone, with the most damage occurring to concrete surfaces at a salt concentration of 4-5 percent (Mehta & Montiero, 1993). Rosli and Harnik examined the possible reasons for scaling to occur when concrete is subjected to a combination of freezing and deicing salts. The inhomogeneity of concrete at the surface, namely that the cement gel, fine aggregate particles, and capillarity, is more concentrated than through the rest of the concrete, and there are less coarse aggregate particles. This means that concrete properties differ at this 'transitional zone', including *w/cm*, modulus of elasticity, and pore volume.

There are several gradients in concrete, leading to a "layer by layer" freezing effect which can cause cracking and spalling of the concrete when subjected to deicing salts and freezing. The first gradient is water content, with the highest concentration of water being present at the surface of the concrete, with the gradient tapering off further into the concrete due to the lowered permeability of concrete. The presence of this gradient means that a "water front" will form. This water front is the boundary between frozen and unfrozen concrete, as the outer saturated layer will freeze earlier than the less saturated inner layers. Ice formation, then, is restrained to the outer layer until the temperature drops enough to freeze the inner layers of the concrete, which contributes to surface damage of the concrete.

The second gradient is the gradient of salt concentration. Salt concentration is typically low directly on the surface of the concrete, as salt is generally washed off of the surface of the concrete by rain. The peak salt concentration, then, exists within the concrete due to chloride diffusion through the concrete. Upon freezing, the outer layers will be able to freeze sooner, due to lower chloride content, and the higher chloride content inner layers will remain unfrozen. This freezing mechanism also contributes to damage of the outer layers.

The final gradient is the thermal gradient through the concrete. Concrete surfaces undergo "temperature shock" when ice is rapidly thawed by salt, as the heat required for spontaneous melting of ice is extracted from the concrete. This "temperature shock" leads to the formation of a large thermal gradient within the concrete. The conclusion is that this rapid cooling causes tensile stresses on the order of the tensile strength of the concrete, contributing to microcracking which could lead to macrocracks after occurring repeatedly. The inhomogeneous properties of the outer layers of the concrete, combined with the three gradients discussed lead to the deterioration of the concrete in the form of scaling (Rosli & Harnik, 1980).

Bilodeau, et al. examined a number of HVFA (58% fly ash) concrete mixes. When examining resistance to deicer salt scaling, it was found that all HVFA concretes showed a poor resistance to deicer salt scaling. All tested combinations of cement and fly ash by Bilodeau et al. showed a rating of 5 at 50 cycles, or severe scaling, with the exception of one mix showing a rating of 4, or moderate to severe scaling. The specimens were all air entrained, and showed good performance against repeated freezing and thawing, as well as showing good air void parameters in specimens cut from concrete

prisms. There were no observable difference between concrete made with different cement brands, although the scaling residue collected differed considerably depending upon the fly ash used (Bilodeau, et al., 1994).

Naik, et al. investigated long term pavement performance of HVFA concrete pavements containing up to 70% cement replacement with Class C fly ash, and up to 67% cement replacement with Class F fly ash. To the contrary of Bilodeau et al.'s results, Naik et al. found comparatively less scaling. Through a visual observation of the surface of in-use pavements, an 18 year old pavement containing 70% Class C fly ash rated at 3+, or moderate to heavy scaling, and a 12 year old pavement containing 50% Class C fly ash received a rating of 2, representing very slight to slight scaling. These results indicate a difference in field performance and laboratory scaling results (Naik, et al., 2003).

Another study reveals the scaling susceptibility of a 55% fly ash mix exhibited severe scaling, showing a visual rating (ASTM C672) of 5. However, experimental HVFA concrete sidewalks in Halifax, Canada were subjected to four winters and over 400 freezing and thawing cycles, combined with numerous applications of deicing salts, but have shown satisfactory performance. It was suggested that ASTM C 672 may be overly severe in its assessment of concrete's performance in field applications (Bouzoubaa, et al., 2001).

2.4.9. Shrinkage. In a study of a 56% fly ash HVFA mix with accompanying specimens, shrinkage strains were recorded out to one year for the HVFA concrete mix as well as control mixes made with Type I and Type II cement. The control concretes showed more shrinkage (strains of 0.069 and 0.059 mm/mm respectively) compared to

the HVFA concrete, which had a strain of only 0.048 mm/mm. It was suggested that this was due to the lower water content requirement of HVFA concretes, as well as greater unhydrated cementitious material in the HVFA mix which serves to act as aggregate, restraining shrinkage (Rivest, et al., 2004).

2.4.10. Summary. High replacement rate of cement with fly ash tends to lower the water requirement to achieve slump, reduce early strength, retard setting times, increase slump loss, but increase later strengths. Restoration of strength of may occur as early as 14 days. Beneficial consequences of up to 50% replacement can be increased modulus of elasticity and freeze-thaw durability, lower rapid chloride permeability and less shrinkage. Typical detrimental effects are lower abrasion resistance and laboratory salt scaling resistance, although field studies do not wholly support problems with scaling. Sometimes incompatibilities arise in the cement-fly ash-water reducer system. Severe retardation or even acceleration of set time, extremely low early strengths and delayed or severely diminished later strengths may occur. These problems are many times related to an imbalance of aluminate/sulfate brought on by significant levels of aluminate in some Class C fly ashes, which consumes the available calcium, making it unavailable for silicate reactions. Various powder activators have been tried to address the above issues. The most promising appear to be calcium hydroxide and rapid set cement.

3. TECHNICAL APPROACH

The study was divided into two parts, termed Phase I and Phase II. Phase 1 involved working with cementitious paste mixtures to examine the effect of water reducer dosages, fly ash substitution rates, cement brands, fly ash sources, and powder additive types and amounts. Once the paste results pointed the way toward the optimum levels of these components, Phase II began, which dealt with examining the effect of the above variables on the plastic and hardened properties of concrete.

4. PHASE I – PASTE STUDY

4.1. EXPERIMENTAL DESIGN

A variety of decisions had to be made in setting up the experimental design. Fly ash class, source, percent replacement, cement type and source, *w/cm*, admixture type and dosage, powder activator types and contents, test types, test equipment, and paste mixing methods were variables that needed to be examined.

Ultimately, it was decided to use fly ash and cement sources that were commonly used in MoDOT projects. Thus, five type I/II cement brands all were chosen, three from the east side of the state and two from the west side. The predominant fly ash class produced by Missouri power plants is Class C. Five sources were chosen, three from plants from the east side of the state, and two from the west side. Because the present study was in many ways a continuation of a previous study done at Missouri S&T, replacement levels for the HVFA were set at 50 and 70% by mass of total cementitious material. Additionally, the literature has shown that about 25% replacement is the upper bound on "normal" behavior of concrete, and is a common maximum allowable value in many specifications, including MoDOT's. Including the straight ordinary portland cement (OPC) control mixture, the fly ash levels were zero, 25, 50, and 70% replacement. The five cements were designated as numbers 1 through 5, and the fly ashes the same. Thus, a combination of cement 1 and fly ash 3 was termed combination "1-3".

The choice of *w/cm* involved several factors: workability, choice of admixture, early and late strength, and realism. The literature showed that other studies utilized fairly low *w/cm's*, in the range of 0.26 to 0.50. A review of typical structural and paving mixtures used on MoDOT projects revealed *w/cm's* of 0.45 and 0.40, respectively.

Because there was a concern that at 70% fly ash substitution strengths would be low, it was preferred that a somewhat low *w/cm* should be used, but not unrealistically low. Thus, a *w/cm* of 0.40 was chosen. The total cementitious material content of 564 lbs (255 kg) was used, which is a typical value used by contractors on MoDOT projects (and exceeds MoDOT specifications for both structural and pavement mixtures).

Recognizing that mixtures of this *w/cm* would encounter workability issues for the straight OPC mixtures, it was decided to use a water reducer (WR). Although a traditional Type A may have been less problematic, a WR was chosen that was advertised as being able to function as both an A and as an F high range water reducer (HRWR). Because it has been shown that WR will affect setting time (usually retard), and may cause early stiffening because of an interaction with a particular sources of cement and fly ash, it was decided to explore the effect of several levels of WR. Three dosage levels were selected: zero, low, and high. "Low" was defined as the dosage necessary to achieve the required design slump of the concrete control mix. The "high" level was selected at an arbitrarily greater value compared to the low dosage. Actual dosages were determined experimentally and are discussed later in this report.

As mentioned, the previous HVFA study conducted on campus was based on work done by Bentz (Bentz, 2010). As a continuation of both studies, the type and initial amounts of powder additives were fixed: gypsum, calcium hydroxide, and rapid set cement (RSC). Gypsum was used to restore the aluminate/sulfate balance in the HVFA mixtures made necessary because of the high aluminate-low sulfate levels in fly ash which would upset the carefully determined proper balance in straight OPC's. Calcium hydroxide has been used to restore the delayed setting time from use of large

substitutions of fly ash in mixtures. The third powder admixture was rapid set cement (calcium sulfoaluminate-dicalcium silicate- gypsum) and has been used to restore early strengths in HVFA mixtures. Several levels of each were utilized, again based on the previous studies: 2 and 4 % gypsum, 5 and 10% lime, and 10 and 20% RSC. Percents refer to percent of fly ash, not total cementitious material. This is an important distinction from other studies reported in the literature, where the latter definition is used. Thus, 4% in this study would be a numerically smaller value if reported as others have done (e.g. 1.87 to 2.63%). In **Table 4.1** is shown a comparison of percentages as defined by the two methods. Mixtures in this study are designated as follows:

PC-FA-%FA-%PC-%G-%L-%RSC-WR

An example would be for cement #4, fly ash #1, 70% fly ash, 30% cement, 4% gypsum, 5% lime, zero % RSC, zero WR/HRWR dosage:

4-1-70-30-4-5-0-Z

Table 4.1 - Percentages of powder admixtures by mass of fly ash and by total cementitious material

Mixture	Powder	% by Fly ash mass	% by TCM mass
PC-FA-50-50-0-5-0-Z	lime	5.0	2.44
PC-FA-70-30-0-5-0-Z	lime	5.0	3.38
PC-FA-50-50-0-10-0-Z	lime	10.0	4.76
PC-FA-70-30-0-10-0-Z	lime	10.0	6.54
PC-FA-50-50-0-0-10-Z	RSC	10.0	4.76
PC-FA-70-30-0-0-10-Z	RSC	10.0	6.54
PC-FA-50-50-0-0-20-Z	RSC	20.0	9.09
PC-FA-70-30-0-0-20-Z	RSC	20.0	12.28
PC-FA-50-50-4-0-0-Z	Gyp	4.0	1.96
PC-FA-70-30-4-0-0-Z	Gyp	4.0	1.96
PC-FA-50-50-4-5-0-Z	Gyp & lime	4.0, 5.0	1.91, 2.39
PC-FA-70-30-4-5-0-Z	Gyp & lime	4.0, 5.0	2.63, 3.29
PC-FA-50-50-4-10-0-Z	Gyp & lime	4.0, 10.0	1.87, 4.67
PC-FA-70-30-4-10-0-Z	Gyp & lime	4.0, 10.0	2.55, 6.37
PC-FA-50-50-4-0-10-Z	Gyp & RSC	4.0, 10.0	1.87, 4.67
PC-FA-70-30-4-0-10-Z	Gyp & RSC	4.0, 10.0	2.55, 6.37
PC-FA-50-50-4-0-20-Z	Gyp & RSC	4.0, 20.0	1.79, 8.93
PC-FA-70-30-4-0-20-Z	Gyp & RSC	4.0, 20.0	2.40, 11.99

The properties of the paste that were of interest included some measure of early stiffening and fluidity, setting time, strength at a full range of ages, and reaction characteristics. Based on recommendations in the literature (NCPTC, 2007), the test

methods chosen were the miniature slump for fluidity and early stiffening, Vicat setting time, compressive strengths using 2 in. (50 mm) cubes at ages between one and 56 days, and semi-adiabatic calorimetry. The semi-adiabatic method was selected because of its relative low cost equipment, ease of use, and general acceptance of use in the literature for comparative studies such as the present study. Thus, behavior over a full range of time would be provided, as shown in **Figure 4.1**.

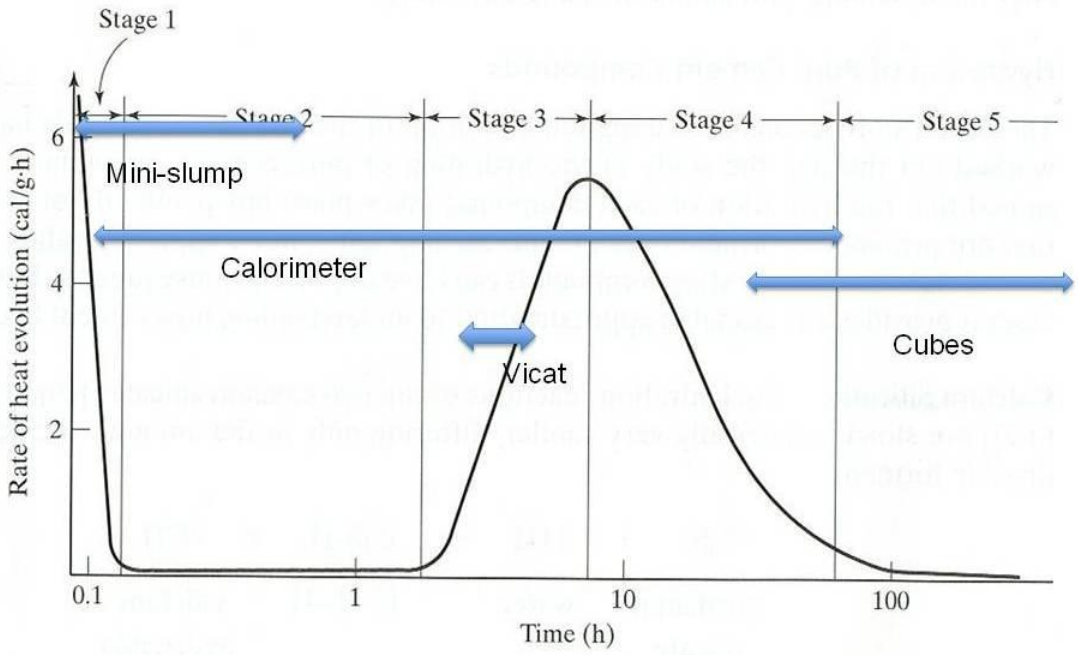

Figure 4.1- Typical calorimeter curve with testing intervals shown

The literature showed that the type of mixing method used for the cementitious paste has a significant effect on the test results. After a review of previous studies and consulting with experts in the field, it was decided to batch the cubes, mini-slump, and calorimeter specimens together using a hand-held kitchen-type mixer and bowl in a very prescribed and controlled time-wise method, and to use the standard Hobart-type mixer for the Vicat setting time specimens.

Because a full factorial experiment involving five levels of cement source, five levels of fly ash source, four levels of fly ash replacement rate, three levels of gypsum, three levels of lime, three levels of RSC, and three levels of WR/HRWR would result in over a thousand different mixtures, it was decided to use a screening study followed by more specific examination of effects. The screening study was designed to narrow the combinations of cement source and fly ash source to two: the most reactive and the least reactive. Reactivity was defined as one day compressive strengths at 70% fly ash replacement without any powder additives or WR/HRWR. The other paste tests were also performed (mini-slump, Vicat setting time, and 28 day compressive strengths) for additional information. All five cements and all five fly ashes in combination with each were tested, along with the five cements by themselves, at zero, 25, 50, and 70% fly ash replacements, resulting in 80 mixtures. Details of the testing are discussed later in this report.

Once the two combinations were determined, the second portion of the paste study was initiated (Main Effects Study). In this effort, the levels of fly ash were limited to zero, 50, and 70%. All mixtures contained the "low" WR/HRWR dosage level, because this had been determined in a different part of the study to be necessary to bring the control concrete mixture to the design slump. However, a greater level of WR/HRWR was also tested (at all four levels of fly ash but with no powder additives). Two levels of gypsum (2 and 4 %) were tried at the 50 and 70% fly ash rates to determine the optimum level of gypsum. Four % was chosen. Finally, at the low level of WR/HRWR and at 4% gypsum, the level of lime (5 and 10 %) and RSC (10 and 20%) was varied for fly ash levels of zero, 50, and 70%. This partial factorial experimental design resulted in 48

mixtures. An additional 16 mixture experiment with no gypsum was also conducted (eight with lime, eight with RSC at 50 and 70% fly ash). Thus, including the screening study, 144 mixtures were examined in Phase I (the paste study). The test methods were the same as in the screening study: miniature slump, Vicat setting time, calorimetry, and compressive strength. However, the compressive strength testing was expanded to include more ages: 1, 3, 7, 28, and 56 days. From all this, 10 concrete mixtures were selected for Phase II with the optimum WR/HRWR, gypsum, lime, and RSC levels at zero, 50, and 70% fly ash levels.

4.2. REPLICATE SPECIMENS

For each mixture, there were three replicate specimens for both compressive strength and calorimeter testing, with one mini-slump and one Vicat specimens.

4.3. MATERIALS

4.3.1. Portland Cement. The five portland cements (all Type I/II) were ones that have been commonly used on MoDOT projects. Preliminary chemical and physical analyses were obtained from MoDOT. Later, mill certifications from the producers, which are more specific to the materials used in this study, were supplied when the cements were delivered. Additionally, the research team at Missouri S&T's department of Civil, Architectural, and Environmental Engineering (CArE) did some physical testing as well. Interestingly, no two laboratories performed the exact same set of test methods. In **Table 4.2** are the results from the cement producers. The cement oxide analyses were

performed on materials that were produced at a similar time as those received during the first shipment of materials.

Table 4.2 – Analyses from cement producer mill certifications (Screening Study)

Cement	SiO_2 %	Al_2O_3 %	Fe_2O_3 %	CaO %	SO_3 %	Na_2O %	K_2O %	EqAlk %	C_3S %	C_3A %	Fineness cm^2/g
1	20.4	4.21	3.62	63.83	2.49	0.20	0.45	0.52	58	5	3980
2	19.90	5.1	3.8	62.6	3.00	---	---	0.5	62	7.1	3920
3	20.3	4.69	3.22	63.0	2.82	---	---	0.50	56	7	3839
4	19.85	4.63	3.23	64.08	3.28	0.177	0.481	0.493	60	7	3856
5	19.8	4.8	3.1	63.2	3.1	---	---	0.55	53	8	3710

A second shipment of Cement 1 and Cement 4 were received approximately six months after the first delivery, shown in **Table 4.3**. As can be seen, the analyses are quite similar.

Table 4.3 – Analyses from cement producer mill certifications (Main Effects Study)

Cement	SiO_2 %	Al_2O_3 %	Fe_2O_3 %	CaO %	SO_3 %	Na_2O %	K_2O %	EqAlk %	C_3S %	C_3A %	Fineness cm^2/g
1	20.29	4.05	3.64	63.43	2.91	0.20	0.47	0.54	57	4	4000
4	20.0	4.6	3.1	63.9	3.1	---	---	0.53	61	7	3900

4.3.2. Fly Ash. The five Class C fly ash sources were also ones that were commonly used on MoDOT projects. Preliminary chemical and physical analyses were obtained from MoDOT; more specific mill certifications were supplied from some of the

producers upon delivery of materials. Additionally, the Materials Research Center (MRC) at Missouri S&T performed chemical analyses and the particle size distributions were analyzed by the Ash Grove Cement Company Technical Center on the initial shipment of materials.

In **Table 4.4** are the oxide results from the MRC and the PSD results from the Ash Grove laboratories. The Missouri S&T results are from the delivered materials. All of the fly ashes conformed to the requirements for ASTM Class C fly ash.

Table 4.4 – MRC and Ash Grove laboratory analyses of fly ashes

Fly ash	SiO_2 %	Al_2O_3 %	Fe_2O_3 %	CaO %	SO_3 %	Na_2O %	K_2O %	EqAlk %	Retained #325 %	LOI %
1	33.72	21.9	7.15	25.31	2.25	1.40	0.41	1.68	11.16	0.37
2	33.34	20.57	6.15	26.34	1.87	1.63	0.43	1.92	11.17	0.49
3	35.42	16.88	7.97	23.21	3.46	1.40	0.56	1.78	19.37	3.05
4	30.55	18.78	7.48	28.43	3.33	1.50	0.45	1.81	10.17	0.57
5	32.26	19.03	6.24	27.94	2.40	2.20	0.33	2.43	13.04	0.26

During the course of the study, several of the cements and fly ash stocks were exhausted and new samples obtained. These were not tested. A second shipment of Fly Ash 3 was received approximately six months after the first shipment and was used primarily in the Main Effects Study and in Phase II (concrete). Fly Ash 1 was continually resupplied from bulk shipments to Missouri S&T and was used primarily in the Main Effects Study and in Phase II (concrete).

4.3.3. Gypsum. Gypsum was used to restore the aluminate/sulfate balance in the HVFA mixtures made necessary because of the high aluminate-low sulfate levels in fly ash which would upset the carefully determined proper balance in straight OPC's. The gypsum was commercially available recycled drywall called "Ultrafine Gypsum", manufactured by USA Gypsum. The analysis provided in the company's literature states it is 96.0% calcium sulfate. It was assumed that the wallboard is essentially calcium sulfate dihydrate (CaSO4·2 H20), commonly known as gypsum.

4.3.4. Lime. Calcium hydroxide has been used to restore the delayed setting time from use of large substitutions of fly ash in mixtures. The calcium hydroxide used in this study was "Standard Hydrated Lime" as manufactured by Mississippi Lime. The advertised analysis was 98.0% $Ca(OH)_2$ with a specific gravity of 2.34. The calcium hydroxide will be referred to as "lime" in other parts of this study.

4.3.5. Rapid Set Cement. The third powder admixture was rapid set cement (calcium sulfoaluminate-dicalcium silicate- gypsum) and has been used to restore early strengths in HVFA mixtures. The particular material used in this study was called "Rapid Set Cement" as manufactured by CTS Cement Manufacturing Corporation. The advertised oxide analysis is shown in **Table 4.5**.

4.3.6. Water Reducer/High Range Water Reducer. The WR/HRWR was essentially a polycarboxylate material (BASF Glenium 7500) and was advertised as meeting both Type A and F admixture requirements.

4.3.7. Water. Deionized water was used throughout the paste study.

Table 4.5 - Oxide analysis of RSC

Parameter	Percent
Calcium oxide (CaO)	50.87
Silicon dioxide (SiO2)	15.40
Aluminum oxide (Al2O3)	13.74
Sulfur trioxide (SO3)	12.52
Iron oxide (FesO3)	2.38
Magnesium oxide (MgO)	1.26
Total alkalis (as Na2O)	0.56
Loss on ignition	2.84
Insoluble residue	0.78
Specific gravity	2.98

4.4. TEST EQUIPMENT AND PROCEDURES

4.4.1. Mixing for Compressive Strength, Calorimetry, and Miniature Slump

4.4.1.1 Pre-blending. Prior to mixing of the paste batches, the dry constituents of the mixture were pre-blended. This was performed by transferring no more than 1200 grams of the materials into a 4x8 in. (100x200 mm) plastic cylinder mold in similar proportions as used in the mixture. The cap was then placed on the cylinder and the cylinder was held horizontally with one hand on each end. The cylinder was then shaken 25 cycles using a six in. (150 mm) throw. This procedure is included in all of the test procedures in Appendix A.

4.4.1.2 Combined Test Method Mixing. The paste batches for semi-adiabatic calorimetry, compressive strength, and miniature slump testing were mixed using the

same procedure and equipment. The paste for all three test methods was typically mixed in a single batch. As noted by Cost (2009), the use of equipment and methods other than those given in ASTM C 305 (ASTM, 2006a) can successfully shorten mixing times to as little as sixty seconds, which may be necessary when batches for multiple test methods are made simultaneously. The choice of test method and equipment can render significantly different test results. In order to mix the materials adequately and within the time requirements of the tests being performed, a handheld kitchen mixer was used. The batches were mixed using a 250-watt Black and Decker Model MX217 hand mixer with egg beater-style paddles, shown in **Figure 4.2**, below.

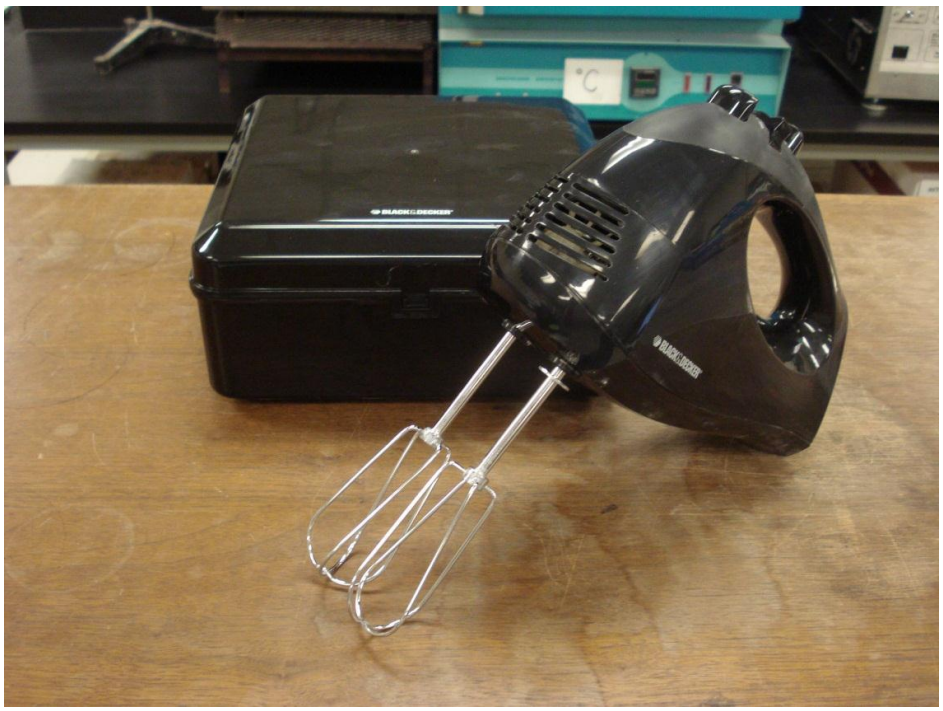

Figure 4.2 – Black and Decker hand mixer

The mixer had six speed settings along with a “Power Boost” option that would increase the mixing speed when pushed. The rotational speeds were determined in the

following manner. An adjustable rate strobe light was used to determine the rotational speeds for the various settings on the handheld mixer. To do this, a piece of white tape was attached to a fin of one paddle and a piece of orange tape was placed on the other paddle. The mixer was then started and the strobe light was adjusted to flash at different rates until the tape on the paddles appeared to stop moving. It was also noted that each fin appeared to stop when the proper rate was set on the light. This rate was read in RPMs off of the dial used to adjust the flashing rate. The rates determined were between 390 and 700 RPM, which is a reasonable result for this appliance. Judgment had to be used to make sure that higher or lower speeds were not taken to be the actual speed of the blender, since the stopped-movement appearance can occur at higher or lower flashing rates on the strobe light that would be unreasonable for this type of device. The rotational speeds for the various settings are given below in **Table 4.6**.

Table 4.6 – Hand Mixer Rotational Speeds

Speed Setting	Rotational Speed (RPM)
1	390
2	440
3	490
4	540
5	600
6	670
Power Boost	700

The paste was mixed in a stainless steel mixing bowl from a Hobart Model A-200 mixer, which had a capacity of 20 quarts (19 l). Temperature measurements of the paste, after mixing, were made using an analog thermometer with a probe length of five in. (125

mm). Other equipment included a stopwatch for timing of the mixing procedure and a ladle to transport the paste mixture from the mixing bowl. **Figure 4.3**, below, shows the mixing bowl, thermometer, and other equipment used during mixing.

Figure 4.3 – Equipment used in the Combined Mixing Procedure

In this study, the initial mixing of the paste batch was performed in ninety seconds, which allowed the first miniature slump test to be performed at two minutes after mixing began. The initial mixing consisted of adding the water to the cementitious materials, allowing the cement to absorb the water for ten seconds, mixing for 20 seconds at Speed 2 (440 rpm), and then mixing for 60 seconds at Speed 6 (670 rpm). As noted by Kantro (1980), brief setting of the paste mixture can be avoided by remixing the paste. This was done in this study by remixing the paste for thirty seconds at Speed 2 prior to each miniature slump test. The calorimeter specimens were prepared and inserted into the calorimeter after the 5-minute miniature slump test, which allowed for early data

collection, and the cube specimens were molded after the 15-minute miniature slump test, so that molding began within 2 minutes and 30 seconds after remixing. In **Table 4.7**, on the following page, the complete sequence of testing can be seen.

It was critical to adhere to the schedule to reduce variability in test results. In some cases, not all of the tests were performed using a single batch of paste. For these cases, the same mixing and remixing sequences were followed with the tests being performed at their respective times in the combined mixing procedure.

Table 4.7 – Combined Mixing Procedure Sequence

Elapsed Time (mm:ss)	Action
0:00	Add water to mixing bowl with cementitious materials Record Time (Start Time)
0:10	Start mixing at Speed 2 (440 RPM)
0:30	Start mixing at Speed 6 (670 RPM)
1:30	Stop Mixing Record Temperature of Paste Prepare mini-slump test
2:00	Lift mini-slump cone
4:00	Remix paste at Speed 2
4:30	Prepare mini-slump test
5:00	Lift mini-slump cone Prepare calorimeter specimens Insert calorimeter specimens in F-Cal 4000
10:00	Close and latch the lid of the F-Cal 4000
13:00	Remix paste at Speed 2
13:30	Prepare mini-slump test
15:00	Lift mini-slump cone Mold cement cubes
28:00	Remix paste at Speed 2
28:30	Prepare mini-slump test
30:00	Lift mini-slump cone
43:00	Remix paste at Speed 2
43:30	Prepare mini-slump test
45:00	Lift mini-slump cone
60:00	Measure and record mini-slump diameters

4.4.2. Cube Compressive Strength. Three replicate specimens per mixture were molded. Steel and plastic molds were used to mold the two-in. (50 mm) paste cubes. All of the cube molds were sealed with vacuum grease to prevent the paste from leaking. Excess vacuum grease was removed from the interior of the molds to avoid deforming the shape of the cubes. The vacuum grease was Dow Corning High-Vacuum Grease. In **Figure 4.4** is shown the cube molding equipment. The molding of the specimens followed the filling, tamping, and leveling procedures outlined in ASTM C 109 with a deviation of the time at which molding began (ASTM, 2008a). ASTM C 109 states that specimen molding should begin within two minutes and thirty seconds after completion of the original mixing of the batch. In this study, molding started after completion of the 15-minute miniature slump test, which would mean that molding started approximately fourteen minutes after completion of the initial mixing. However, this molding time was within two minutes and thirty seconds after completion of the remixing for the 15-minute miniature slump test. Also, it was noted that the paste at this time was sufficiently fluid to allow for complete consolidation. Following the completion of the molding procedures, the specimens (still in the molds) were placed in the moist room which had a relative humidity maintained at 95% or greater. There was concern about breakage of some of the weaker specimens, so three days of curing was allowed before stripping. The paste cubes were removed from the molds and placed in buckets of water saturated with hydrated lime. The buckets had a capacity of five gal (19 l) and were placed back in the moist room.

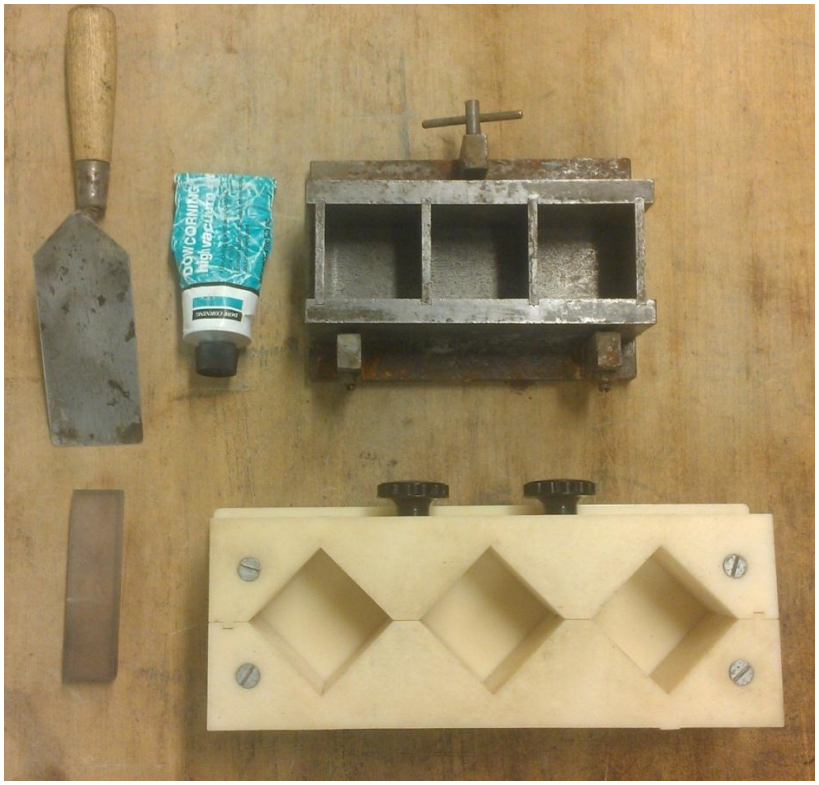

Figure 4.4 – Cube molding equipment

The two-in. (50 mm) cube specimens were tested for compressive strength on a hydraulic, Tinius-Olsen tension/compression machine with a capacity of 200,000 lbs (90,800 kg). The Tinius-Olsen is controlled using a desktop computer with MTestW software. It is important to match the loading platen size to the specimen size. Two loading platens were used to apply the load to the two loading faces of the cube specimens. The lower, square loading platen was about 12 in. tall and had a diagonal dimension of 3.5 in. (90 mm). It was attached to a larger, circular loading platen, typically used for cylinder testing, which rested on the lower table of the Tinius-Olsen machine. The upper, circular loading platen was about six in. (150 mm) tall and was attached to the upper crosshead of the Tinius-Olsen machine. The loading block of the upper platen was spherically seated and had a diameter of 3.5 in. (90 mm). **Figure 4.5**

shows the Tinius-Olsen machine with the loading platens and the computer used to control the machine.

Other equipment included digital calipers for measuring the dimensions of the specimen and sand paper to smooth the loading faces of the specimen. The sand paper had a grit size of 60.

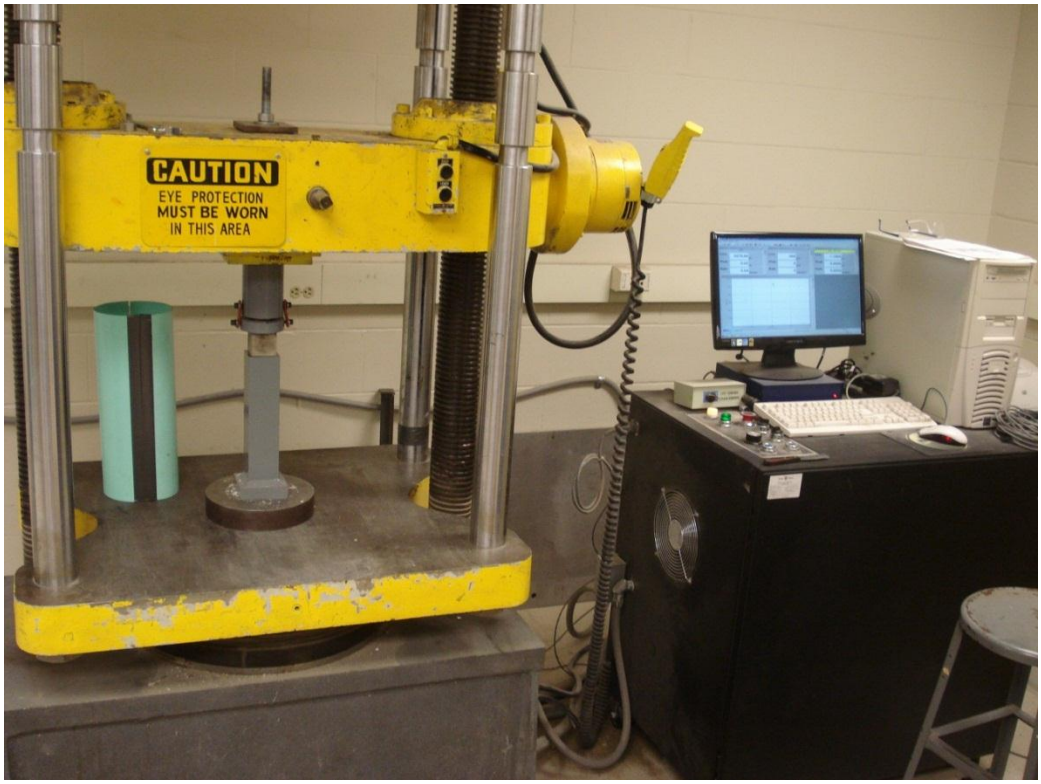

Figure 4.5 – Tinius-Olsen load frame and computer

The compressive strengths of the cubes were tested at a load rate of 200 lbs/sec (91 kg/sec), which is within the range allowed by ASTM C 109. Prior to loading the specimens, the molded faces of the cubes that were to be loaded were sanded to provide flat loading surfaces. The cubes and the loading platens were cleaned of any debris prior to the start of loading.

4.4.3. Semi-adiabatic Calorimetry. Semi-adiabatic calorimetry was performed on the paste mixtures using an F-Cal 4000 calorimeter with CalCommander v1.3 Software Suite from Calmetrix, Inc. Temperature measurements were taken of hydrating paste specimens over time. The F-Cal 4000, shown in **Figure 4.6**, consists of four receptacles in an insulated box with thermistors at the bottom of each receptacle. The thermistors, along with a USB port, are connected to a single data logger. The receptacles are sized to hold standard 4x8 in. (100x150 mm) plastic cylinder molds.

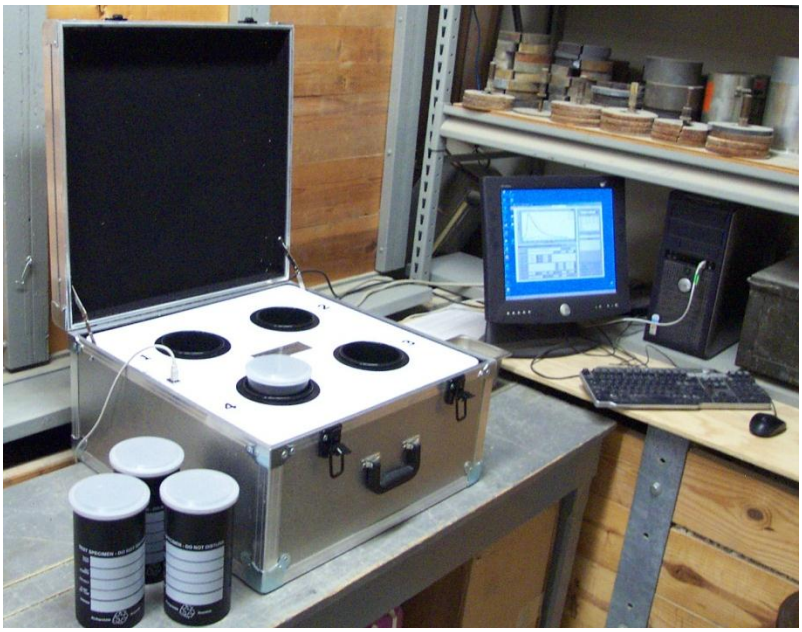

Figure 4.6 – F-Cal 4000, computer, and cylinder molds

Three specimens were inserted into the F-Cal 4000 for each mixture, with one receptacle containing the inert specimen. It was decided that three specimens should be used for each mixture, instead of testing multiple mixtures simultaneously, so that the results for a given specimen would not be affected by the temperature rise of the other specimens in the box with different compositions. The inert specimen consisted of high-

silica sand and deionized water with a water-to-sand ratio equal to the water-to-cementitious materials ratio of 0.40 and mass similar to the paste specimens. The use of a water and sand combination is intended to better simulate the thermal conductivity of the paste specimens, when compared to a dry sand inert specimen (T. Cost, personal communication, April 10, 2012). The mass of the inert specimen was 1250.0 grams and the masses of the paste specimens were 1250.0 grams with a tolerance of 10.0 grams. This mass is recommended in the F-Cal 4000/8000 User Manual and fills approximately one-third of the cylinder's volume. As noted in a draft ASTM standard for evaluating hydration using thermal measurements (ASTM, 2011a), the "masses of all specimens that will be compared with each other shall not differ by more than 5%". A tolerance of 10.0 grams was chosen since it was within this range, was easily accomplished, and could lessen the variability between specimens when compared to specimens differing in mass by 5%.

Prior to loading the specimens in the calorimeter, the cylinders were tapped ten times with an open hand to remove entrapped air from the paste. The cylinders were then capped and placed in the calorimeter. Logging typically continued for 48 hours after the start of the initial mixing. However, the logging time was shortened for mixtures that obtained the peak hydration curve in less than 48 hours and lengthened for mixtures that experience significant delays in hydration.

Once logging in the F-Cal 4000 was complete, the data was retrieved using the CalCommander software. The calorimeter was connected to a desktop computer with a USB cable. From the software, the data for each logging channel was exported as a separate Text Document (.txt) file. These were then imported into Microsoft Excel 2010

and the Signal-to-Noise ratio (S/N) was calculated for each of the three specimens. The Signal is the difference between the highest and lowest temperatures recorded for the sample being tested. The Noise is the difference between the highest and lowest temperatures recorded for the inert specimen. **Figure 4.7**, below, shows an example of the temperature versus time curves resulting from the raw data for a typical hydrating cement paste sample and corresponding inert specimen. The Signal and Noise quantities are indicated in the figure.

Cost (2009) noted that the curve generated for the inert specimen should be subtracted from the curve for the hydrating specimen, so that the resulting data represents only the heat evolution of the sample and not variances in the ambient temperature. Cost designated this quantity as ΔT, which is shown below in **Figure 4.8**. In this study, the curves for the three specimens were averaged to result in a single hydration curve for each paste mixture. The curve for the inert specimen was then subtracted from this averaged curve to result in a corrected average hydration curve.

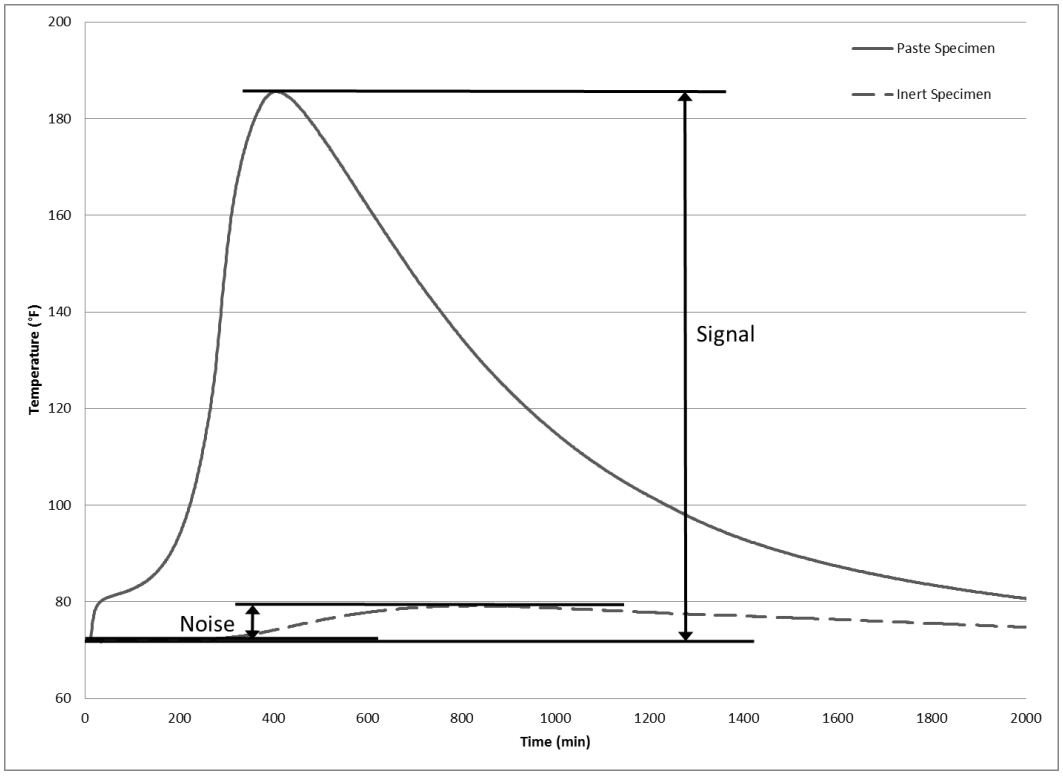

Figure 4.7. Examples of signal and noise quantities

This curve was then used to calculate predicted setting times using the Fractions Method and Derivatives Method, as discussed by Sandberg and Liberman (2007). For the Fractions Method, the main hydration response rise (M) is calculated, which is the difference between the peak temperature of the main hydration curve and the lowest temperature during the dormant period, and then two percentage values of the main hydration response rise are chosen to represent the initial and final set times. For this study, 20% of the main response was chosen for initial set and 50% was chosen for final set. A representation of the calculated values for the Fractions Method is shown below in **Figure 4.9**. For the Derivatives Method, initial set is taken as the time when the maximum second derivative of the main hydration curve occurs and final set is taken as the time when the maximum first derivative of the main hydration curve occurs.

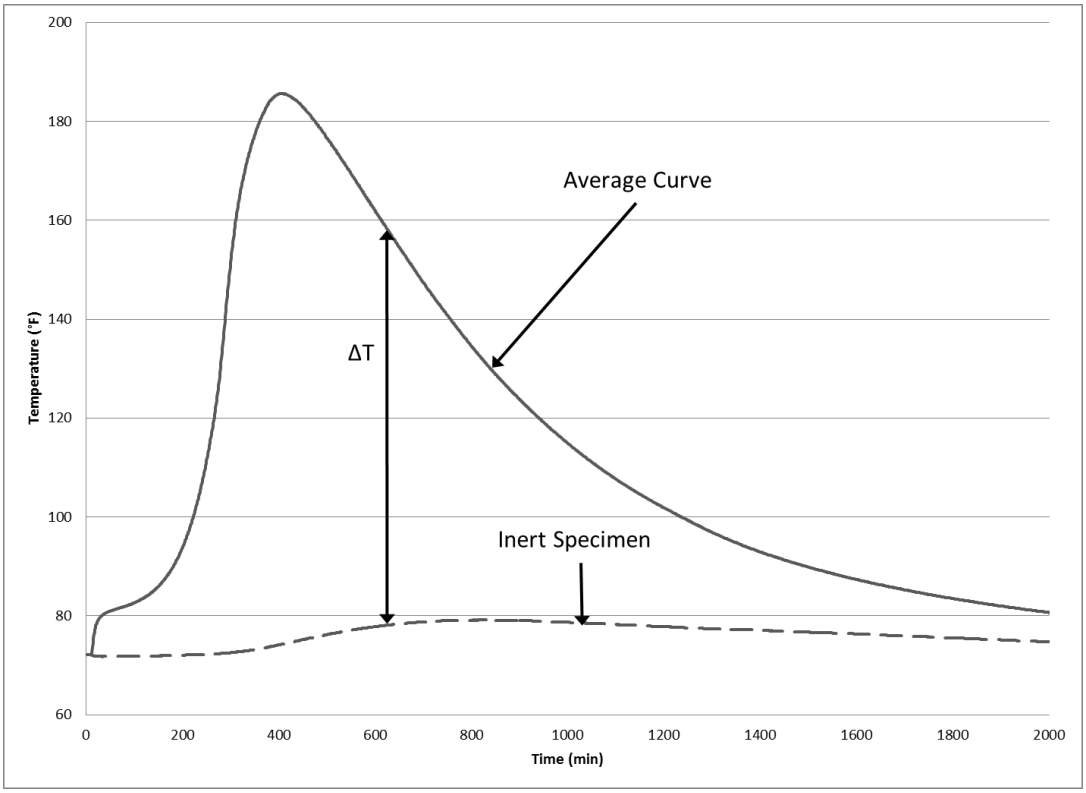

Figure 4.8. Representation of the ΔT quantity

The complete semi-adiabatic calorimetry procedure, including data reduction, is titled "Using the F-Cal 4000 & CalCommander Software for Testing Cement Paste" and is included in Appendix B.

After acquiring the F-Cal 4000, a verification of the internal connections was performed, as suggested in the F-Cal 4000/8000 User Manual, to ensure that the connections had not been damaged during shipping. This was done by filling four cylinders with water at 110°F (43.3 C) and inserting them into the F-Cal 4000. After 30 minutes, the temperature reading was checked for each of the sensors to ensure that no two sensors differed by more than 2°F (1.1 C).

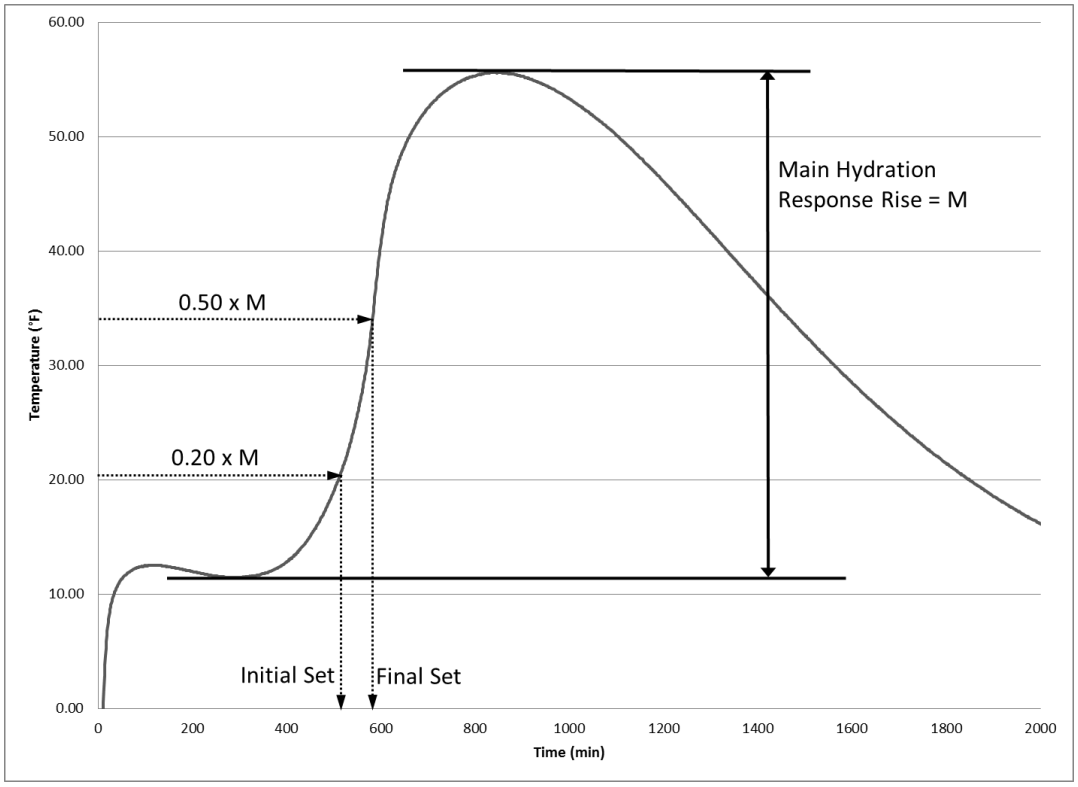

Figure 4.9. Example of setting time prediction by the fractions method

4.4.4. Miniature Slump. Two identical miniature slump cones were fabricated from Plexiglas with the dimensions given by Kantro (1980). The inside of the cones had dimensions in the same proportion as those specified for a standard slump cone as given in ASTM C 143 (0.75 in.(19 mm) top diameter, 1.5 in. (38 mm) bottom diameter, and 2.25 in. (57 mm) height)(ASTM, 2010a).

Figure 4.10, shows the two cones used in this study, along with other equipment used for performing this test, which included a Plexiglas board, plastic discs, and a spatula.

Figure 4.10 – Miniature slump cones and equipment

The paste for the miniature slump test was mixed according to the combined mixing procedure previously discussed. The test was performed at 2, 5, 15, 30, and 45 minutes, as was done by Bhattacharja and Tang (2001). The tests at 2 and 5 minutes were performed 30 seconds after the end of mixing or remixing. The tests at 15, 30, and 45 minutes were performed one minute and thirty seconds after the end of remixing to allow for a longer period to fill the cone, which was needed for stiffer mixtures.

The cones were placed on thin plastic discs, as suggested by Bhattacharja and Tang (2001), to prevent leaking from the bottom of the cone. The discs had diameters of two inches and were cut from Zip-Lock sandwich bags.

Previous research (Kantro, 1980; Bhattacharja and Tang, 2001), discussed the use of a planimeter for measuring the area of the miniature slump pats. To do this, tracings of the pats were made on paper and measured after the pats had hardened and were removed. An alternative method uses multiple diameter measurements to obtain an average diameter from which the area is calculated. While the planimeter method gives somewhat more accurate results, time constraints and concerns about variability

introduced by the paper led to the use of diameter measurements for area determination. In this study, this involved taking four diameter measurements, separated by rotations of 45 degrees, to obtain an average diameter from which the area was calculated.

The diameter measurements were taken at 60 minutes after the start of mixing. This time was chosen to allow the later miniature slump tests time to stabilize without allowing sufficient time for the results of the earlier tests to be affected by shrinkage from hydration and drying.

The complete test procedure, which was adapted from procedures given by Kantro (1980) and Bhattacharja & Tang (2001), is titled “Miniature Slump Cone” and is included in Appendix C.

4.4.5. Normal Consistency and Vicat Time of Setting. The Vicat apparatus described in ASTM C 191 and ASTM C 187 was used for both the Vicat setting time and normal consistency tests (ASTM, 2008b, 2010b). In **Figure 4.11** is shown the apparatus.

The paste was mixed using a Hobart Model N50 mixer, bowl, and paddle, which conform to the requirements of ASTM C 305 (ASTM, 2006a). The mixer has three speeds and moves the paddle in both planetary and revolving motions. **Figure 4.12**, below, shows the mixer and bowl scraper.

The paste for the normal consistency test was mixed according the Procedure for Mixing Pastes given in ASTM C 305 with one deviation. In this study, the bowl and paddle were wetted before mixing commenced to provide a more constant surface condition of these items when multiple tests were run in succession. Care was taken to ensure that excess water was not present, which would affect the normal consistency

results. Following the mixing procedure, normal consistency was determined according to ASTM C 187.

Figure 4.11 – Vicat apparatus with ring and glass plate

The paste from the normal consistency test was used to determine the time of setting by the Vicat method according to ASTM C 191 with one deviation. The specimen was kept in the moist room between penetration measurements and was covered with a plastic sheet while in the moist room to prevent damage to the surface of the specimen from dripping water. Similar modifications to ASTM C 191 have been made by other researchers (Bentz and Ferraris, 2010) to prevent evaporation from the surface of the specimen during the test.

Figure 4.12 – Hobart mixer with bowl scraper

For specimens that experienced initial set prior to the first penetration reading at 30 minutes, a penetration of 1.57 in. (40 mm) was assumed at time zero. This made possible the interpolation of initial set at a penetration of 0.98 in. (25 mm), as described in ASTM C 191.

4.5. RESULTS AND DISCUSSION

4.5.1. Screening Study

4.5.1.1. General. The purpose of the Screening Study was to make a first pass through all five cements and all five fly ashes to find the most reactive and the least reactive combination. The two selected pairings would then be the subject to the Main Effects Study, where the effects of powder additives would be explored. Historically,

early strength is one of the properties of most concern for HVFA, and as fly ash content increases, early strength is anticipated to be more problematic. Therefore, "reactivity" was defined as one day compressive strengths at 70% fly ash replacement without any powder additives or WR/HRWR. The other paste tests were also performed (miniature slump, Vicat setting time, and 28 day compressive strengths) for additional information.

4.5.1.2. Compressive Strength. One and 28 day cube compressive strengths are tabulated in Appendix F. Of 480 cubes cast and tested, there were eight outliers, according to the procedure of ASTM E178. The results were discarded.

The effects of fly ash replacement level on each combination are shown in **Figures 4.13-4.17**.

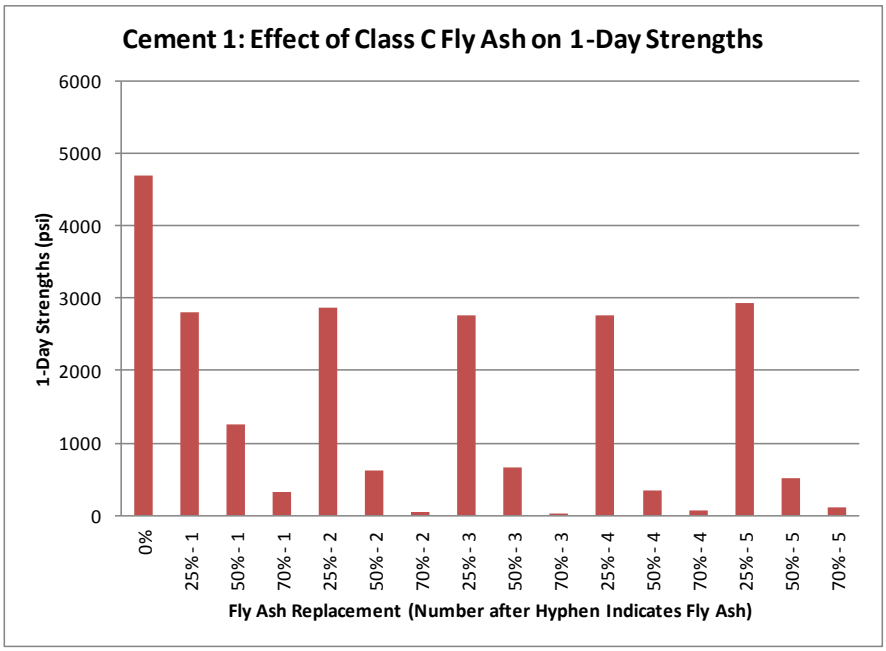

Figure 4.13 – Effect of Fly Ash Replacement Level on One Day Strengths of Cement 1 in Combination with Each Fly Ash

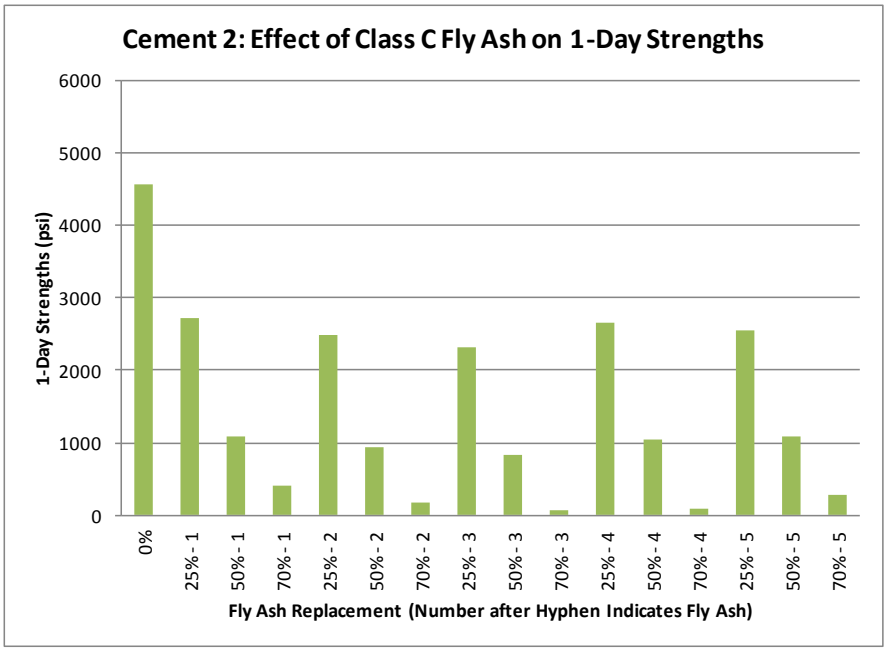

Figure 4.14 – Effect of Fly Ash Replacement Level on One Day Strengths of Cement 2 in Combination with Each Fly Ash

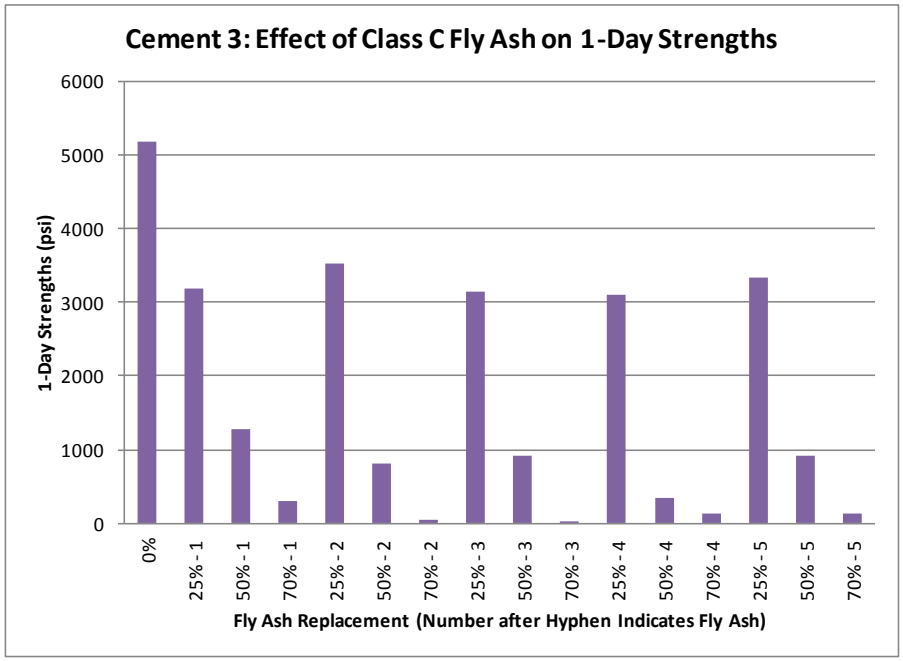

Figure 4.15 – Effect of Fly Ash Replacement Level on One Day Strengths of Cement 3 in Combination with Each Fly Ash

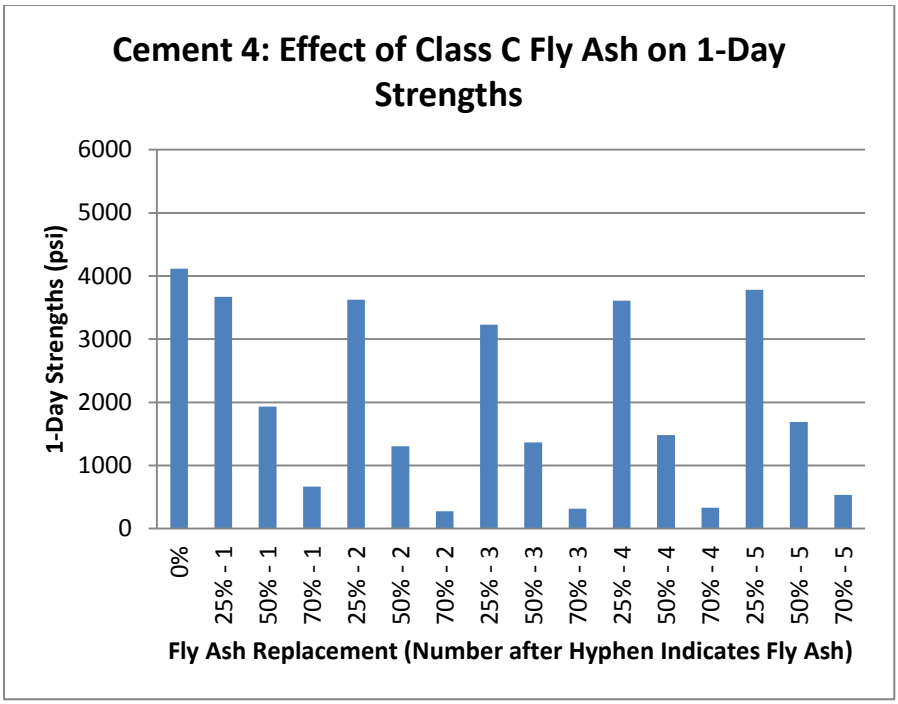

Figure 4.16 – Effect of Fly Ash Replacement Level on One Day Strengths of Cement 4 in Combination with Each Fly Ash

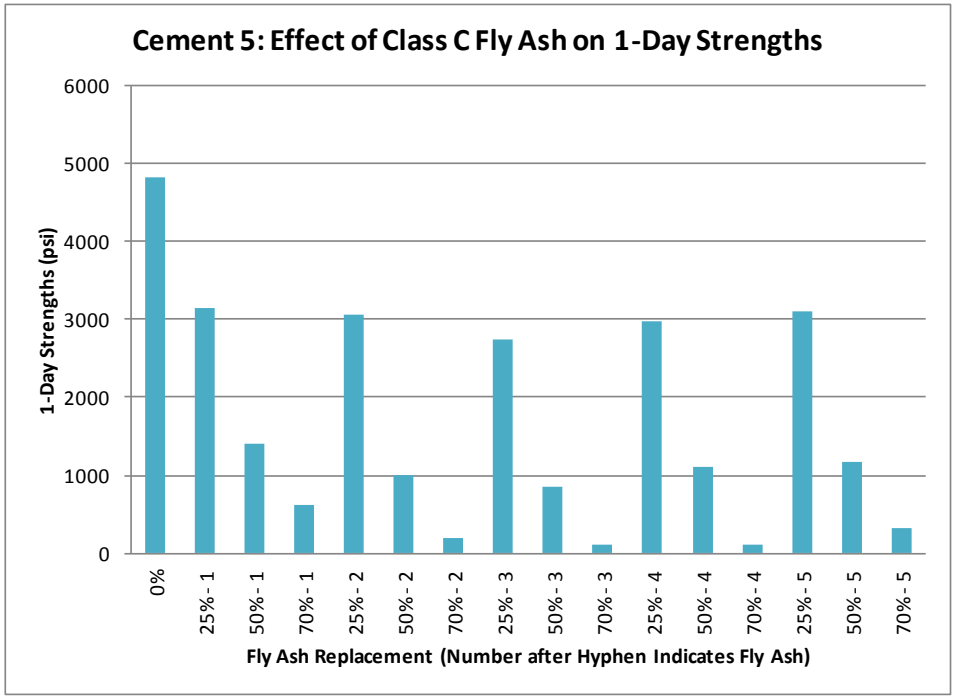

Figure 4.17 – Effect of Fly Ash Replacement Level on One Day Strengths of Cement 5 in Combination with Each Fly Ash

The general trend is as expected: as fly ash replacement level increases from 25% through 70%, one day strengths decreased. The specific combination of cement and fly ash sources also impacted the strengths. The combination of greatest one day strength at 70% replacement was Cement 4 with Fly Ash 1 (designated "4-1"). The lowest reactivity combination was Cement 1 with Fly Ash 3 (designated "1-3"). Fly Ash 3 was the lowest performer in almost every 70% combination. These two combinations were carried forward into the Main Effects Study. A value of 1000 psi (6.9 MPa) one day strength for concrete has been suggested as a minimum for acceptance (Cost and Knight, 2007). In this study, 1200 psi (8.3 MPa) paste strength corresponded to 1000 psi concrete strength. Of the 25 combinations, 12 exceeded 1200 psi.

The 28 day strengths of the different combinations are shown in **Figures 4.18-4.22.**

The general trend is as expected: as fly ash replacement level increases from 25% through 70%, 28 day strengths decreased. The specific combination of cement and fly ash sources also impacted the strengths. Fly ash 3 was the lowest performer in almost every 70% combination, although at 25 and 50%, other fly ashes exhibited lower strengths. The range of strengths for various replacement levels were: cement alone: 11,260-12,210 psi (77.7-84.2 MPa); at 25% fly ash: 5860-12,080 psi (40.4-83.3 MPa); at 50% fly ash: 4160-8800 psi (28.7-60.7 MPa); and 70% fly ash: 2350-6040 psi (16.2-41.6 MPa). So, the specific combination of cementitious materials at various ages is important to strength. In terms of pozzolanic action, only one combination at 25% fly ash level exceeded the straight OPC mixture, although seven combinations approached the zero fly ash controls within 1000 psi (6.9 MPa).

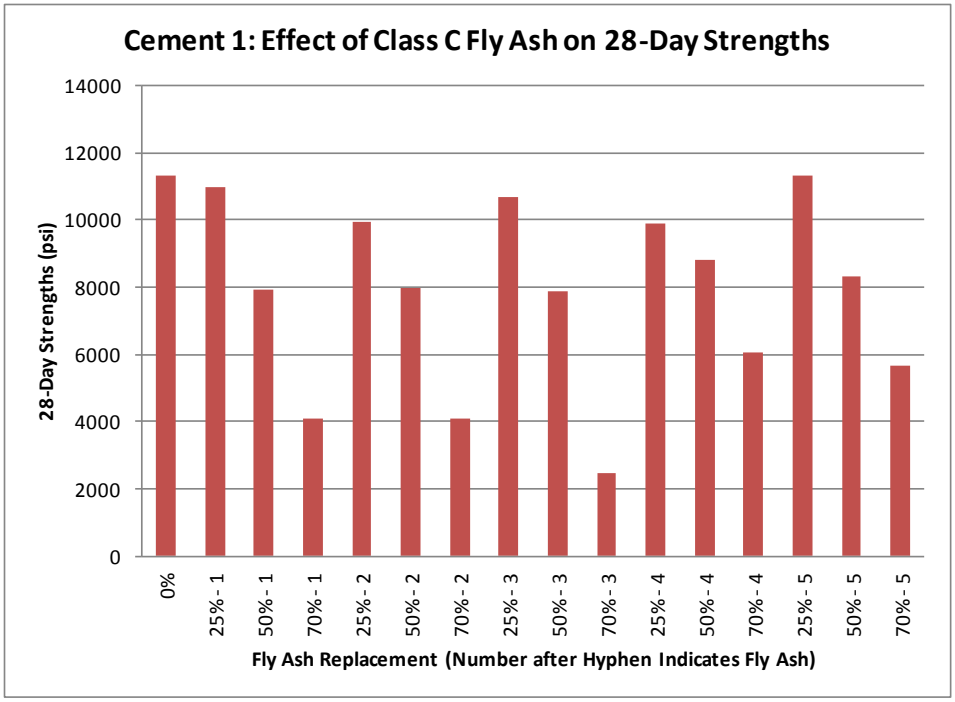

Figure 4.18 – Effect of Fly Ash Replacement Level on 28 Day Strengths of Cement 1 in Combination with Each Fly Ash

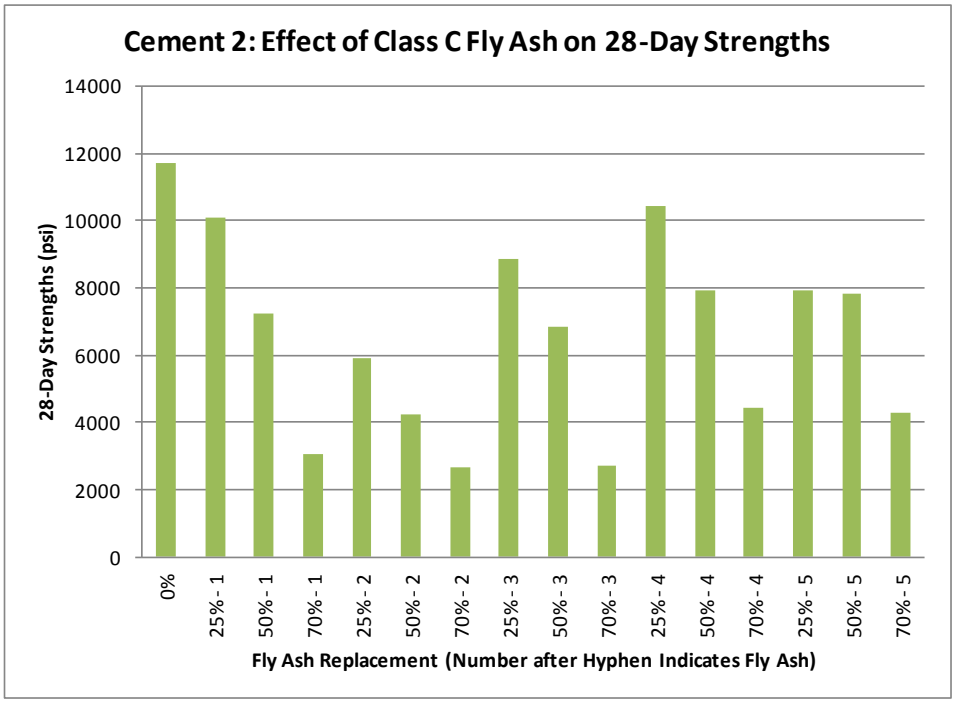

Figure 4.19 – Effect of Fly Ash Replacement Level on 28 Day Strengths of Cement 2 in Combination with Each Fly Ash

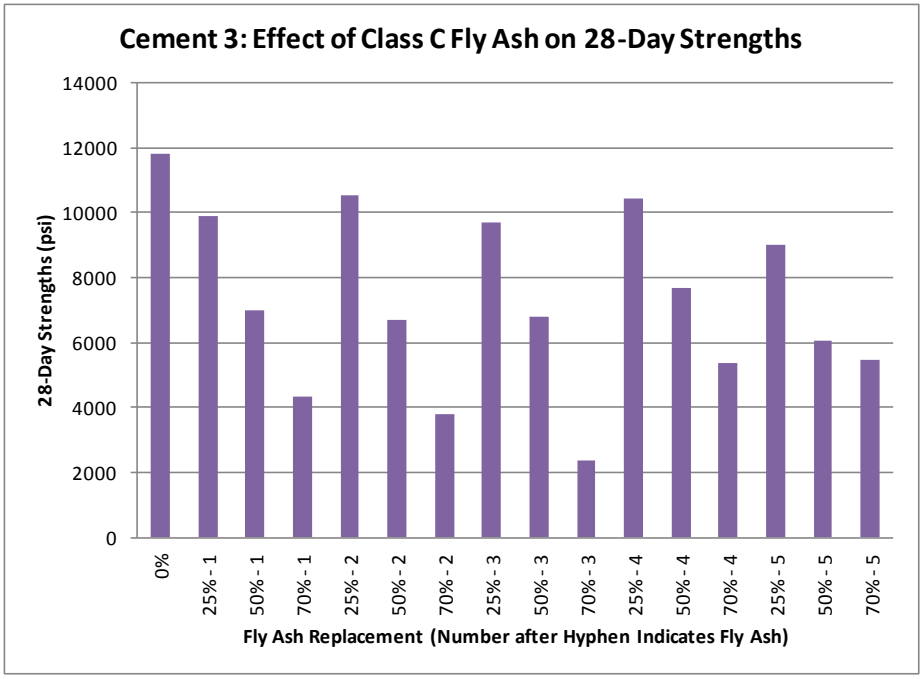

Figure 4.20 – Effect of Fly Ash Replacement Level on 28 Day Strengths of Cement 3 in Combination with Each Fly Ash

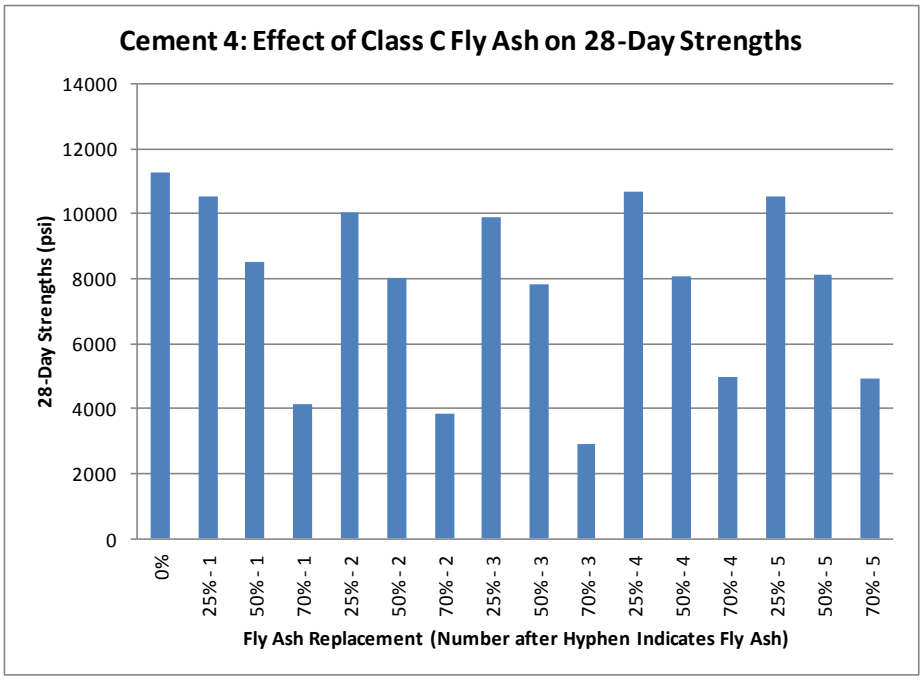

Figure 4.21 – Effect of Fly Ash Replacement Level on 28 Day Strengths of Cement 4 in Combination with Each Fly Ash

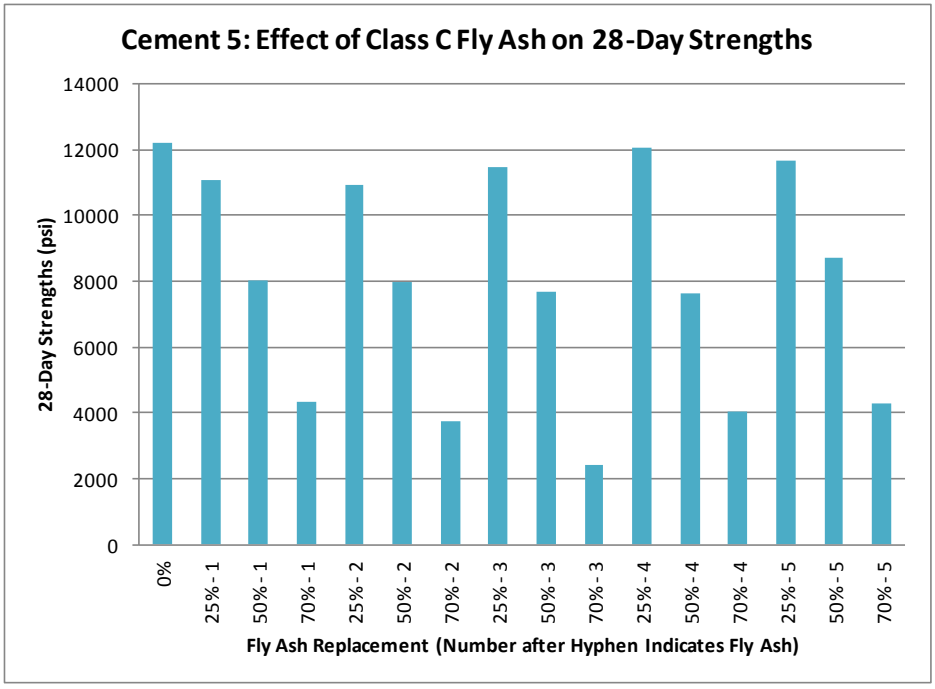

Figure 4.22 – Effect of Fly Ash Replacement Level on 28 Day Strengths of Cement 5 in Combination with Each Fly Ash

Various total oxide contents of each blend were calculated based on the individual cement and fly ash oxide analyses and their proportions (percentages) in the blend. For the combined Screening and Main Effects data, early strength is correlated to the total calcium oxide (CaO) (R= 0. 949), total aluminates (R= -0.872), and total equivalent alkalis (R= -0.898) in the OPC-fly ash system. These relationships are shown in **Figures 4.23-4.25**. Calcium ions are necessary for forming the main strength-producing hydration product, calcium silicate hydrate (C-S-H). High aluminate content systems react rapidly with calcium, thus reducing the calcium available to the silicate hydration reaction, lowering strengths. Likewise, high total equivalent alkalis increase the rate of reaction between the aluminates and the calcium.

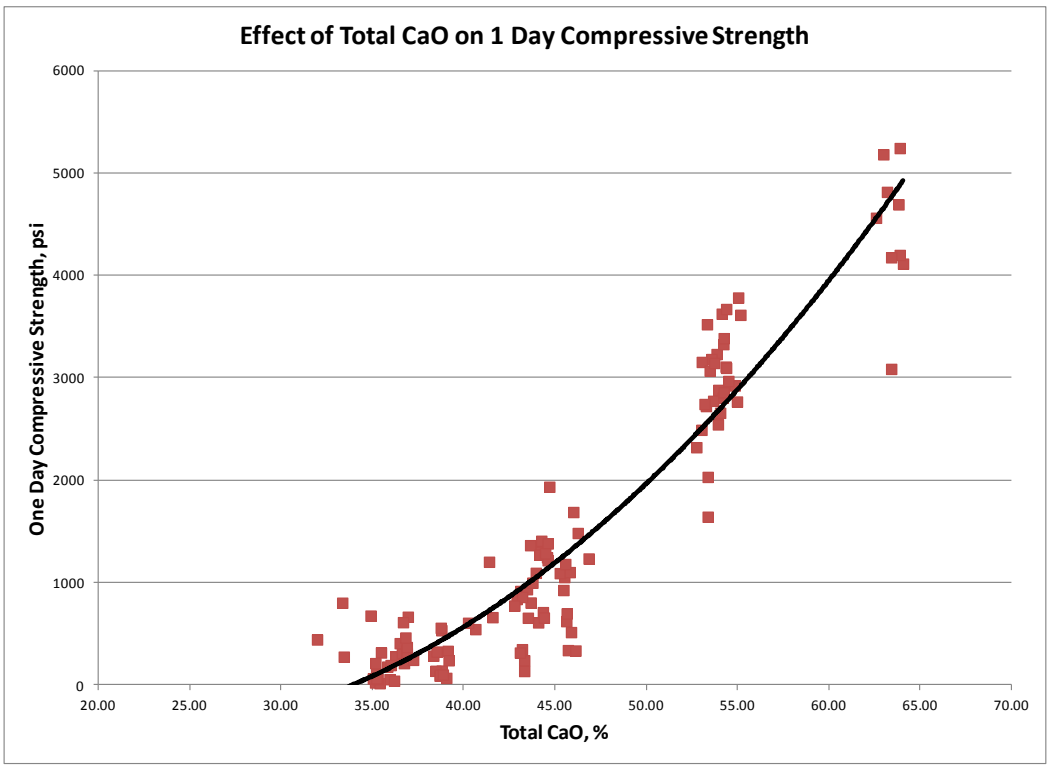

Figure 4.23 – Effect of Total CaO on One Day Compressive Strengths

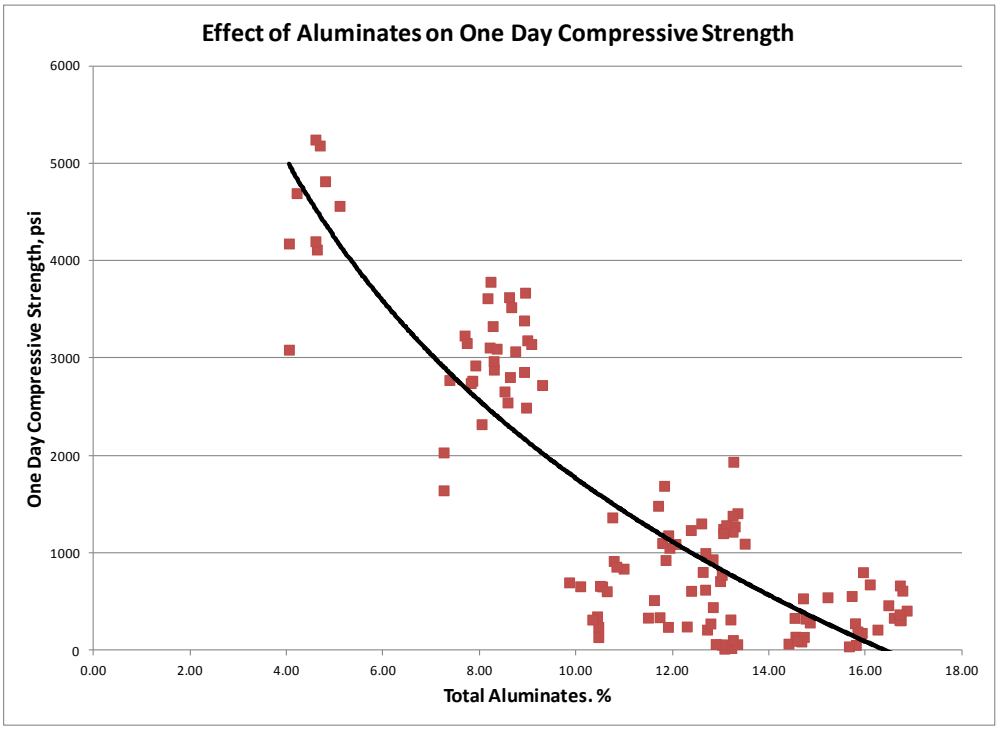

Figure 4.24 – Effect of Total Aluminates on One Day Compressive Strengths

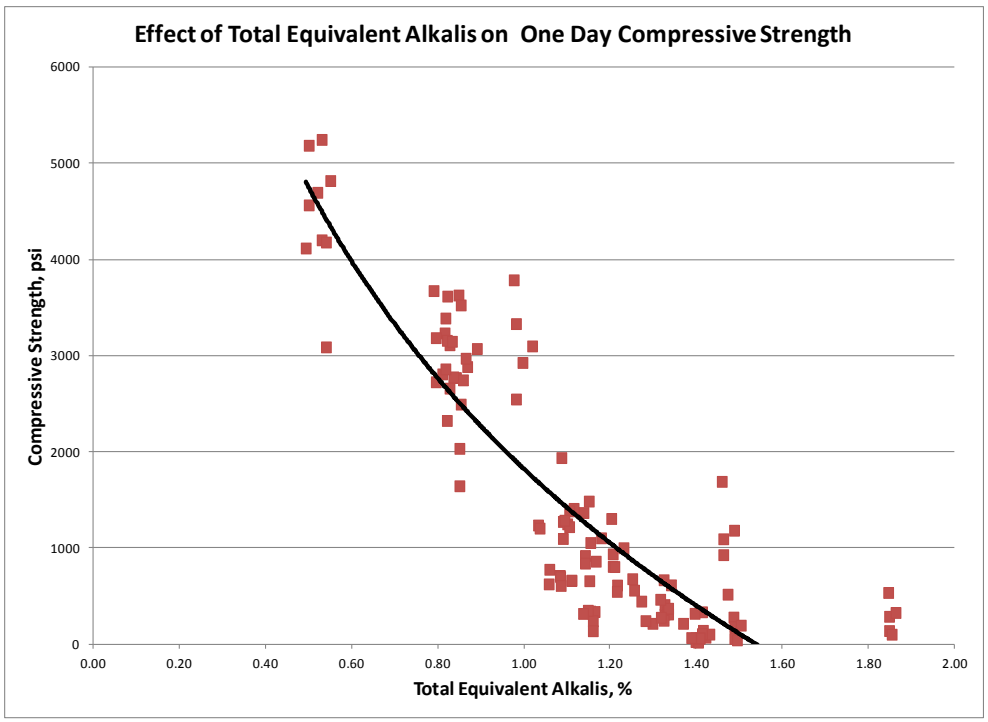

Figure 4.25 – Effect of Total Equivalent Alkalis on One Day Compressive Strengths

In a later section, the relationship of early compressive strength, calorimeter curves, and the oxide analyses will be explored.

The compressive strength results are tabulated in Appendix F.

4.5.1.3. Calorimetry. All 80 mixtures were subjected to semi-adiabatic calorimetry testing. The Signal/Noise ratio of each replicate was used to assess the occurrence of outliers. There were none in the screening study dataset. A typical set of results is shown in **Figure 4.26**.

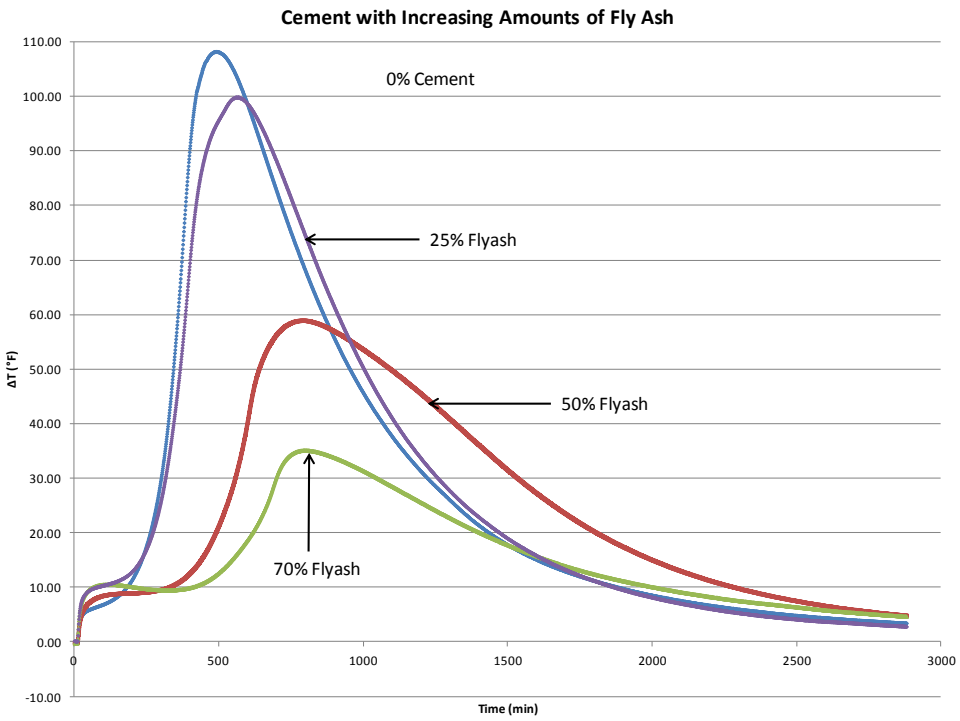

Figure 4.26 – Typical Calorimeter Curves

As shown, the expectations are that with increasing fly ash replacement, the peak of the temperature curve becomes lower, and occurs later because of the slower reaction of the fly ash compared to straight OPC. The peak temperature in this study is termed "NetTMax" and is shown in **Figure 4.27**.

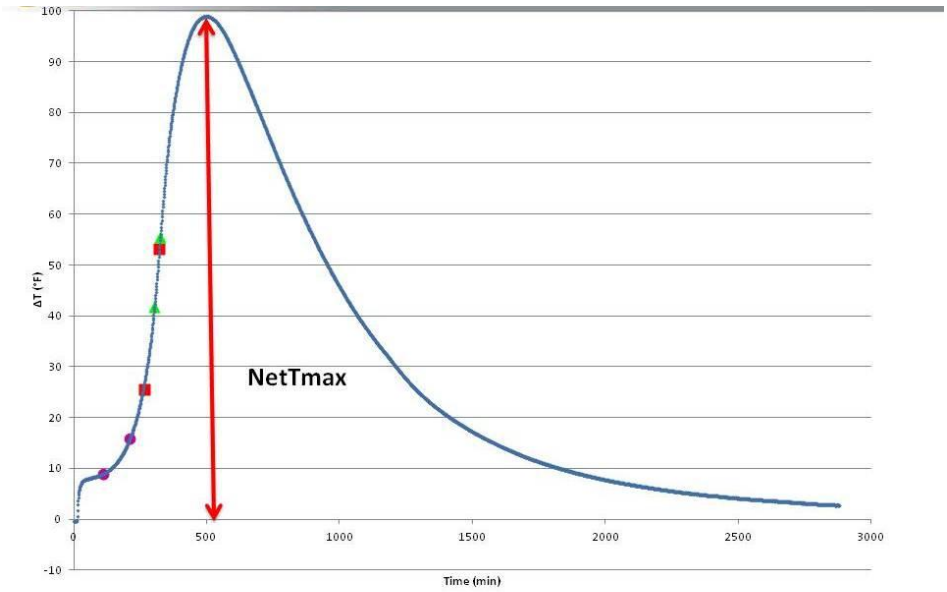

Figure 4.27 – Illustration of net peak temperature, NetTMax

A higher peak is associated with greater reactivity, especially at early ages (the reaction is typically during the first day of hydration). A correlation between NetTMax and one day compressive strength is shown in **Figure 4.28.** The correlation constant R is quite high (0.976). The data represents both the Screening Study and the Main Effects mixtures. In an earlier section, it was shown that one day compressive strengths were highly correlated to total calcium oxide, total aluminate, and total equivalent alkali contents. The same trends are in evidence for these oxides and NetTMax: total calcium oxide (R= 0.926), total aluminates (R= -0. 865), and total equivalent alkalis (R= -0.873).

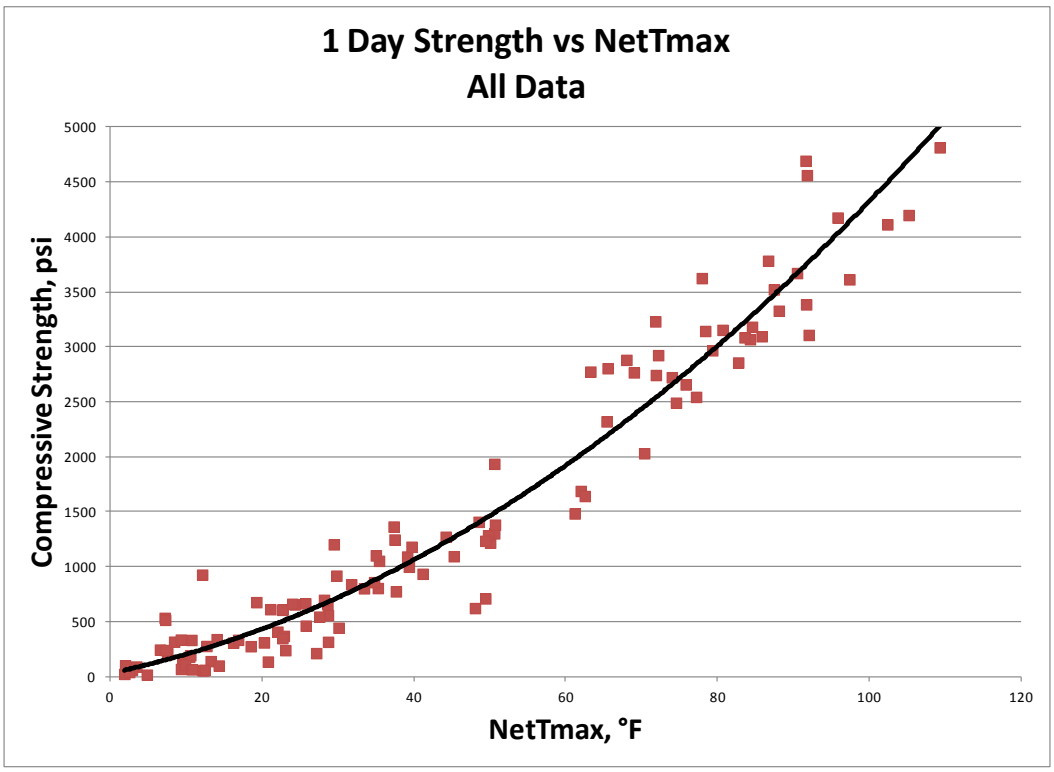

Figure 4.28 – Relationship of Calorimeter Peak Temperature NetTMax and One Day Compressive Strength

NetTMax also has a significant relationship with 28 day strength, although not as strong (R= 0.873), as shown in **Figure 4.29** (Screening and Main Effects data combined)**.**

The calorimeter results are tabulated in Appendix F.

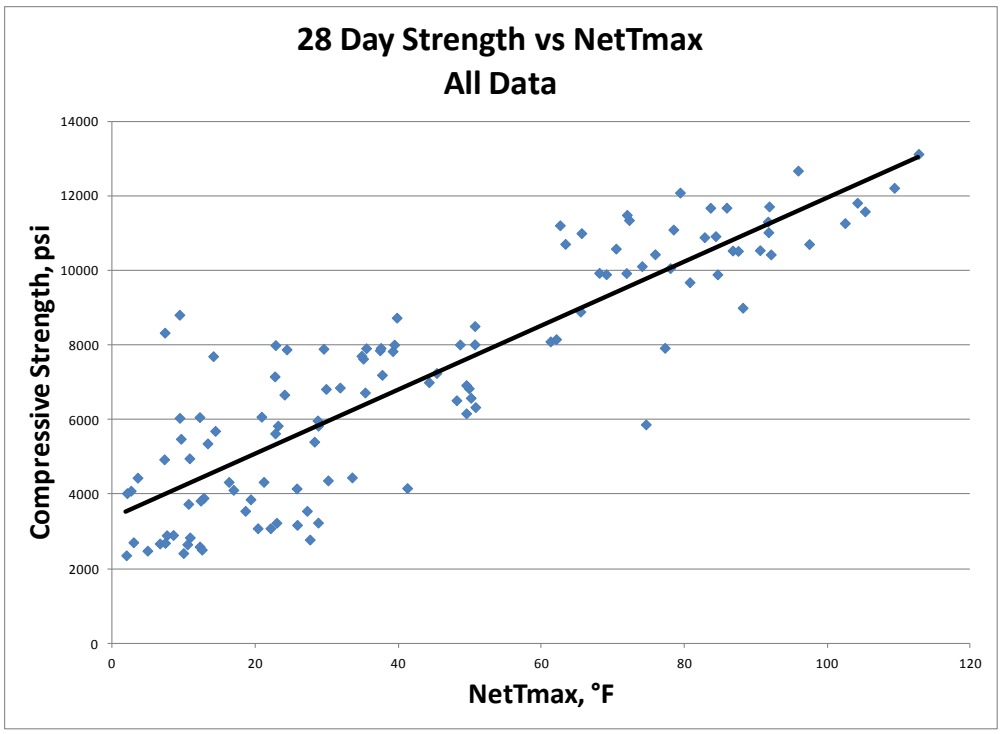

Figure 4.29 – Relationship of Calorimeter Peak Temperature NetTMax and 28 Day Compressive Strength

The calorimeter data was also examined in regard to prediction of setting time. This will be discussed in a later section.

Additionally, the calorimeter curves sometimes indicated abnormal behavior. This also will be discussed in a later section.

4.5.1.4. Miniature Slump. The miniature slump test is a measure of fluidity, and more importantly, a measure of early stiffening tendencies. The test interval spans the first 45 minutes of the life of the paste from the moment water contacts the cementitious materials through 45 minutes.

The effect on fluidity is as expected: as fly ash content increases, the mixture becomes more fluid, most likely because of the lubricating effect of the spherical nature of the fly ash particles. As shown in **Figure 4.30**, the 2 min. reading substantially

increases as the fly ash content varies from zero to 70%. The effect is also in evidence at readings 5 and 15, but has died off between the 30 minute and the 45 min. time intervals. The OPC line is essentially flat through the whole process, which is expected because the cement hydration is in the usual dormant period.

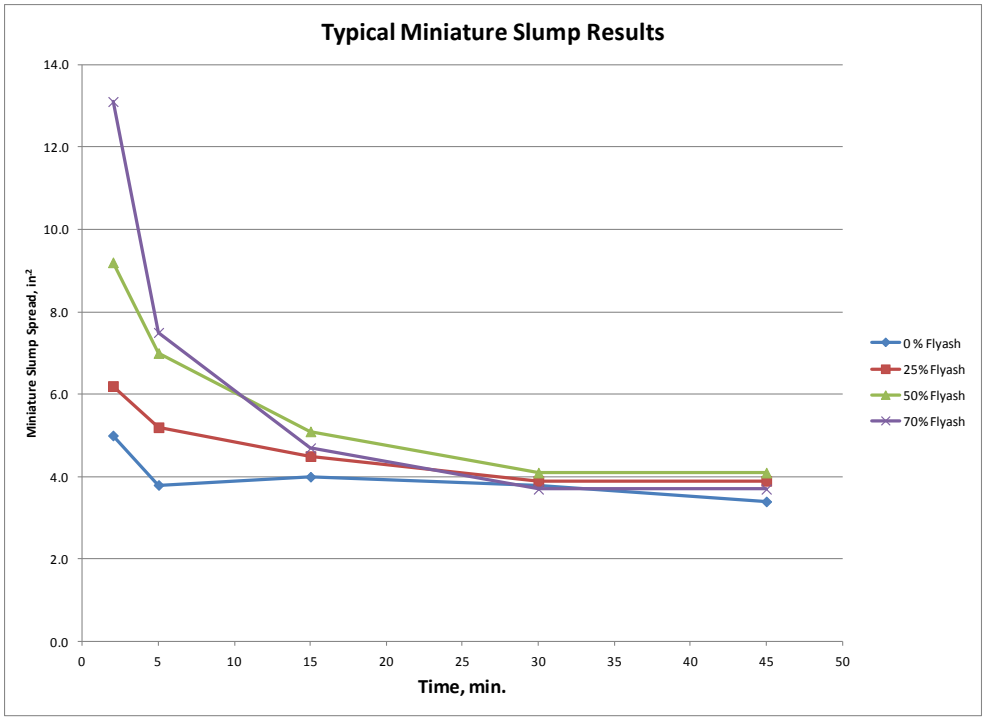

Figure 4.30 – Effect of Fly Ash Content on Miniature Slump Spread

It should be remembered that the paste was remixed immediately prior to each reading. This action should destroy any false setting effects due to an excess of gypsum precipitating out. In regard to the evaluation of early stiffening, several methods were examined. One was to examine the slope of the line between the 5 and 15 minute readings. A steeper slope would indicate a more rapid loss in slump. A second method as reported by Roberts and Taylor (Roberts and Taylor, 2007) was to calculate the ratio of the 30 min. spread to the 5 min. spread. As the ratio diminished, the paste would be

stiffening more rapidly. A correlation comparison with other indications of early reactivity such as initial set and 50%NetTMax time indicated that the ratio method resulted in a somewhat better correlation than the slope method. Roberts and Taylor recommend a minimum value of 0.85—below this, early stiffening is significant. However, they also warn that pastes are more sensitive to incompatibilities than concrete, so paste systems that indicate potential problems may behave normally in concrete.

In an attempt to explain the occurrence of early stiffening, correlations were performed with various total (OPC and fly ash) oxide amounts and ratios. The greatest correlations were with total equivalent alkali content (R = 0.859), shown in **Figure 4.31**, and total aluminate content (R= 0.739), which is shown in **Figure 4.32**. As total equivalent alkali content increases (greater fly ash content), more fly ash is activated, and the AR 5-30 ratio decreases, indicating an increase in stiffening. Likewise, as total aluminate content increases (because of an increase in fly ash content), the aluminate/gypsum balance is tilted toward more aluminates being free to react with water, thus causing a faster reaction.

An advantage of the miniature slump test as a diagnostic tool is its relatively quick time of obtaining results: 45 minutes as opposed to up to 10 hrs for Vicat setting time and up to three days for the calorimeter curve. Also, the equipment is simpler and the operator skill level is less demanding.

The miniature slump results are tabulated in Appendix F.

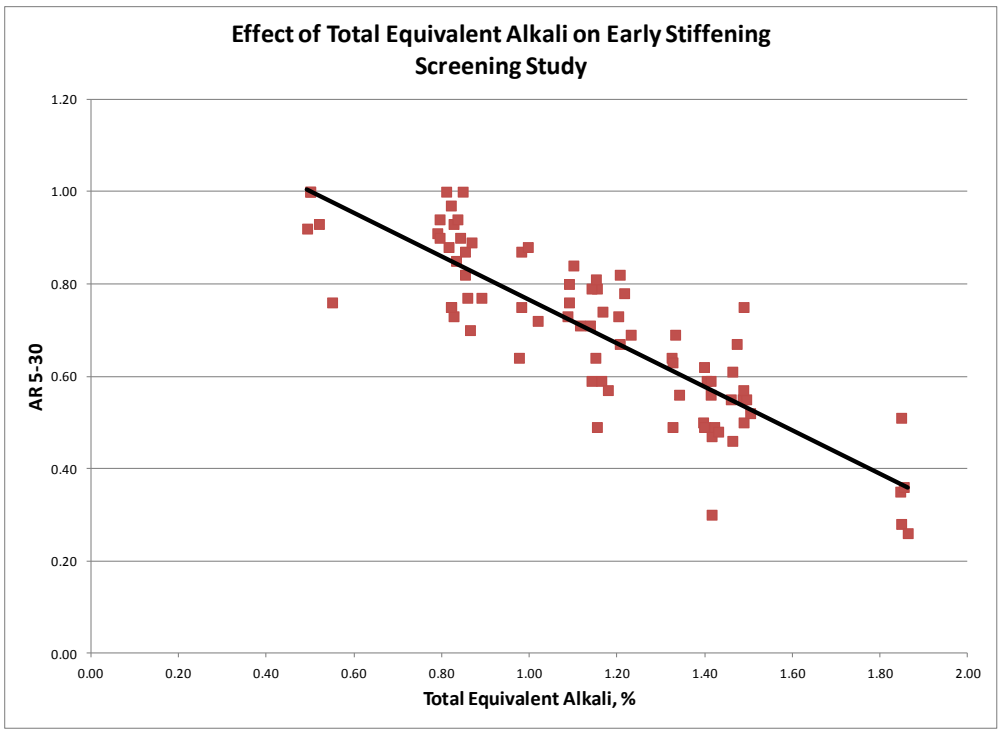

Figure 4.31 – Effect of Total Equivalent Alkali Content on Early Stiffening

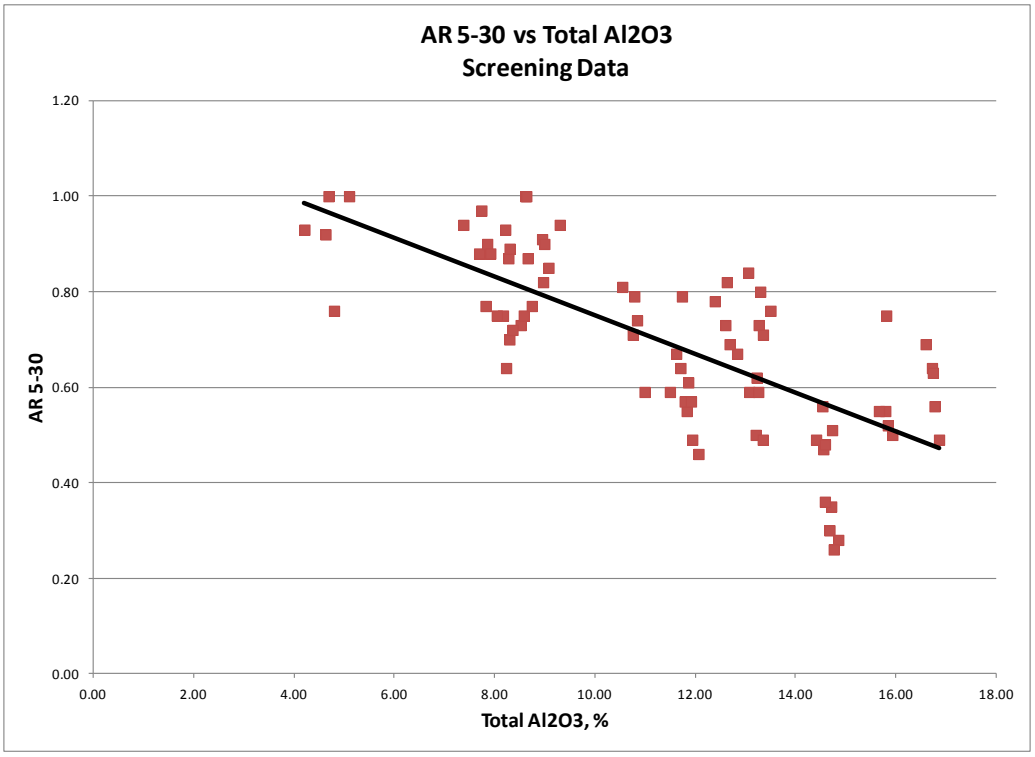

Figure 4.32 –Effect of Total Aluminate Content on Early Stiffening

4.5.1.5. Vicat Setting Time. Initial and final setting times of the pastes were determined by the Vicat method. Increasing levels of fly ash affect initial setting time. In 10 of the 25 combinations of OPC and fly ash sources (typical 1-4), there was a retarding effect at 25 and 50% fly ash levels as would be expected due to the slower reaction rates of fly ash compared to OPC. However, at 70% fly ash, there was acceleration, most likely due to the lack of gypsum and surplus of aluminate, causing a faster reaction. In nine of the combinations (typical 1-2), there was the expected retarding effect at 25% fly ash, but at 50 and 70%, there was an acceleration effect. In six combinations (typical 2-4), all levels of fly ash exhibited an accelerating effect. All three typical curve shapes are shown in **Figure 4.33**.

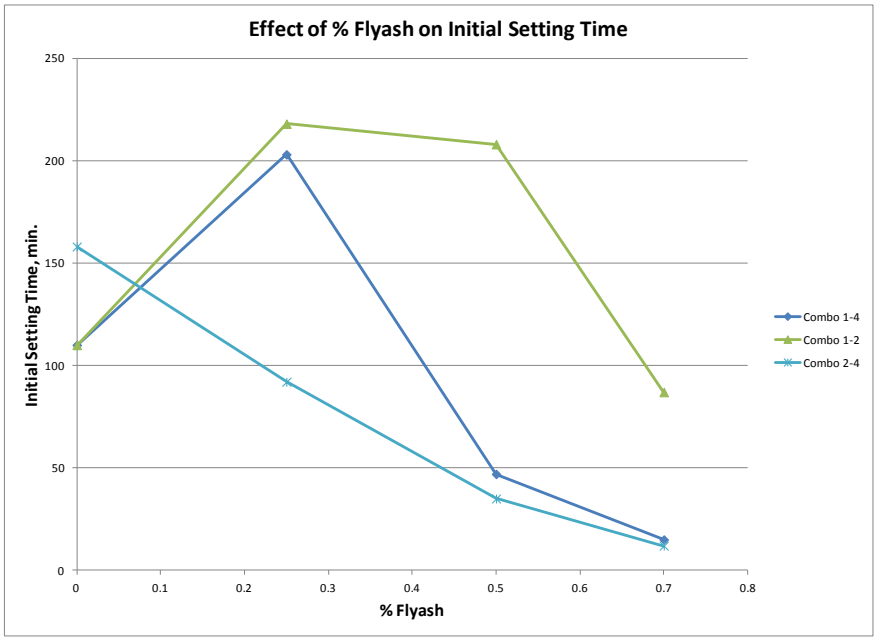

Figure 4.33 – Effect of Fly Ash level on Initial Setting Time

Although there were many OPC-fly ash blends that violated the recommended minimum initial setting time for straight OPC's of 45 min., there were only five blends

that exceeded the final setting time maximum limit of 8 hrs (480 min.). Four were at the 50% fly ash level and one was at 70%. The setting time results are tabulated in Appendix F.

The performance of the Vicat setting time test is lengthy and subjective. It has been postulated that setting time characteristics could be approximated by certain time intervals associated with the calorimeter curve such as at inflection points (second and first derivatives) and more arbitrarily at the 20 and 50% time intervals associated with the time that the peak temperature occurs, as shown in **Figure 4.34.**

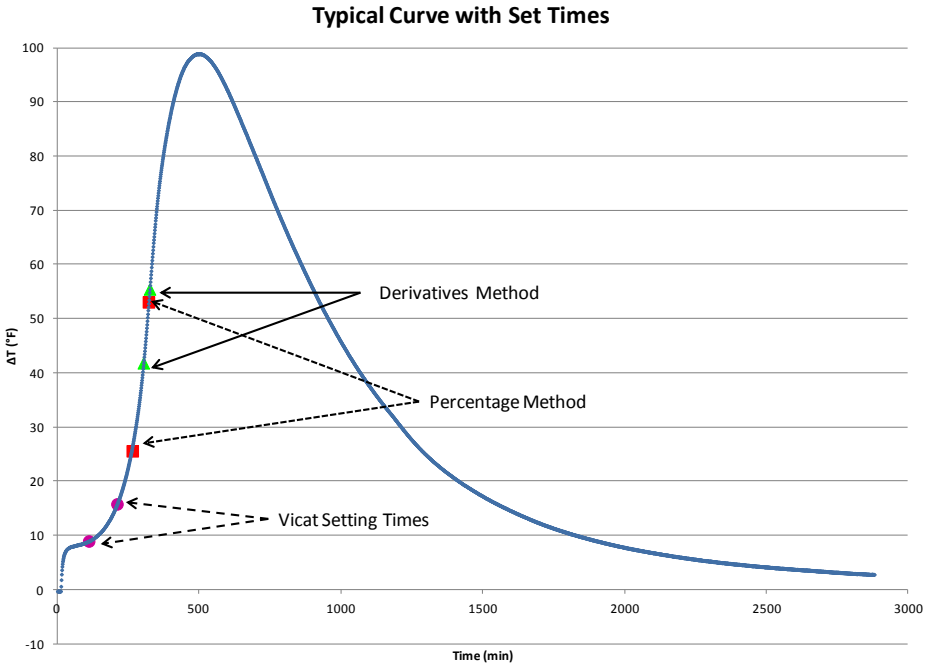

Figure 4.34 – Various Methods to Determine Setting Times

Initial set time and the following parameters had poor correlations: second derivative, first derivative, 20% NetTMax, and 50%NetTMax. However, initial set time and AR 5-30 had a fairly good correlation (0.781), as shown in **Figure 4.35.**

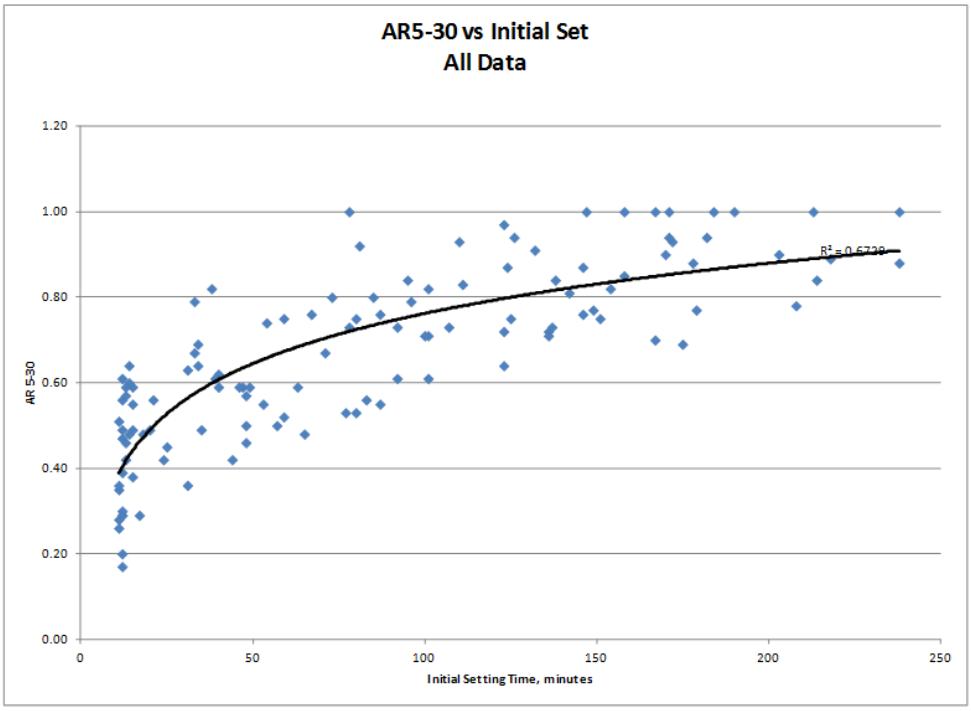

Figure 4.35 – Relationship of Early Stiffening and Initial Setting Time

Calorimeter curve characteristics, coupled with strength development, early stiffening, and setting time data, were examined in order to attempt to explain paste hydration behavior, especially potential incompatibilities among paste constituents. Seven different curve types were identified in this study and are shown in **Figures 4.36-4.42**. As explained earlier, the blend specimen temperature has been corrected for the inert specimen temperature.

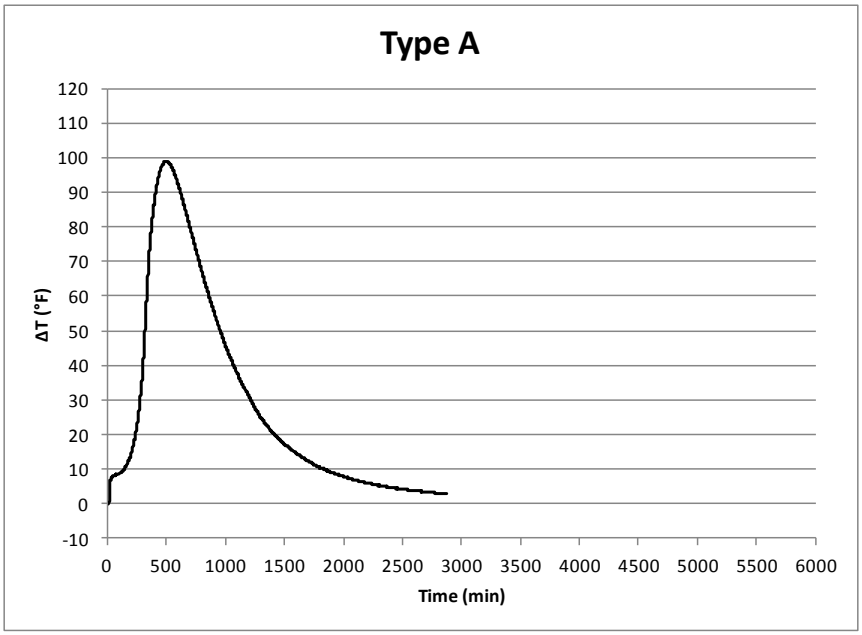

Figure 4.36 – Normally-shaped Type A Calorimeter Curve

The Type A curve is characterized by having a normal dormant period followed by a single tall hydration peak occurring at an average of 475 min. (OPC), 720 min. (25% fly ash), and 820 min. (50% fly ash), with no plateaus or shoulders. When water and cement come into contact, the aluminates go into solution rapidly, followed by the sulfate. The presence of the sulfate lowers the solubility of the aluminates, plus ettringite forms around the particles, both actions slowing hydration of the aluminate. A dormant period ensues until the pore solution is critically saturated with calcium ions, thus causing the silicates to react rapidly, releasing heat with a consequent rise in temperature and gain in strength. Type A curves had the greatest strengths, greatest CaO contents, lowest total equivalent alkalis, lowest total aluminates, and lowest total aluminate/total sulfate ratios. Type A curves were always exhibited by OPC and 25% fly ash mixtures, along with some of the 50% fly ash mixtures. Early stiffening was either not a problem or only

marginal (average AR 5-30 = 0.82). The silicate hydration and the aluminate reaction (sulfate depletion) probably occurred relatively simultaneously.

Type B curves, shown in **Figure 4.37**, exhibited smaller magnitude in peak heights and longer times-to-peak heights. The very short peak height curves were from both 50% and 70% fly ash mixtures, with peak heights occurring later than Type A curves, and times of around 860 min. Type B curves exhibited lower CaO contents, greater total equivalent alkalis, greater total aluminates, and greater total aluminate/total sulfate ratios than Types A, C, and D mixtures. B curves generally occurred sooner than C and D curves (all 50% fly ash). The lower magnitude heights and delayed times were to be expected from higher fly ash contents due to slower reactions and less calcium ions available for reacting with the silicates producing calcium silicate hydrates. Early stiffening (AR5-30= 0.60) was an issue.

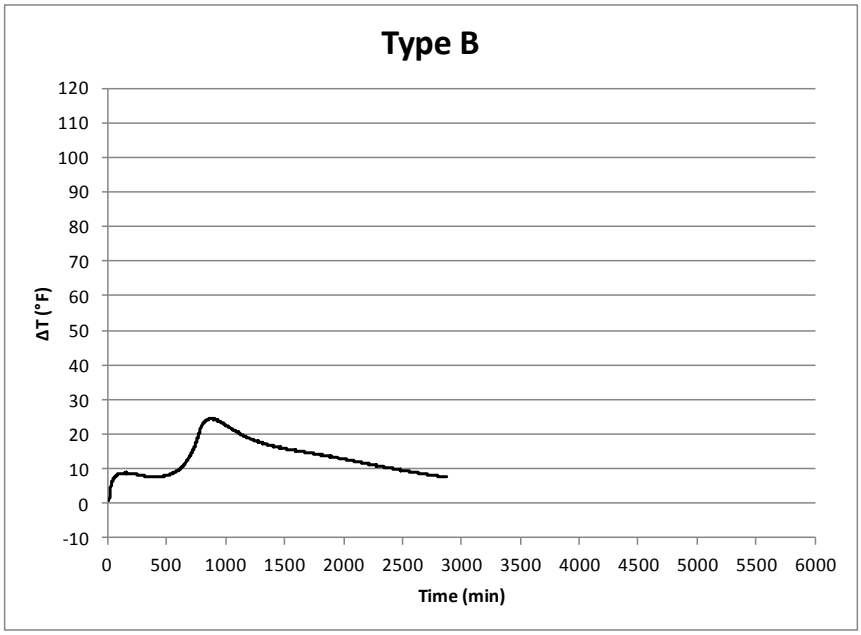

Figure 4.37 – Normally-shaped, Lower Magnitude Type B Calorimeter Curve

Type C curves were always associated with 50% fly ash mixtures and typically had somewhat greater peak heights and were broader in nature than Type B curves, which was to be expected (e.g. peak heights between Types A and B). However, peak times occurred later than Type B's. Type C is shown in **Figure 4.38.** Compared to Type A curves, C curve mixtures had less CaO, greater equivalent alkali and aluminate contents, and greater aluminate/sulfate ratios. Early stiffening was either not a problem or only marginal (average AR 5-30 = 0.80).

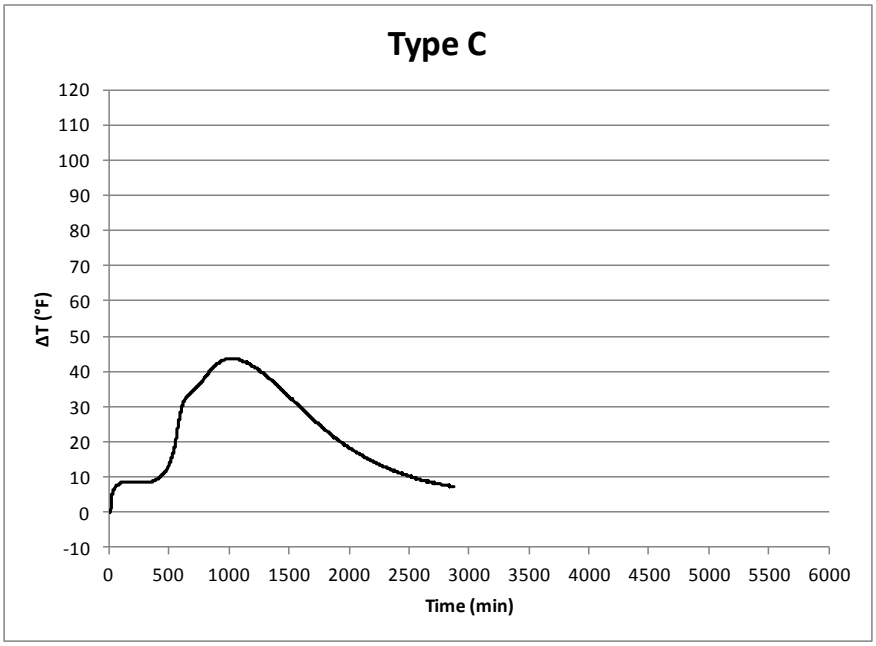

Figure 4.38 – Normally-shaped, Lower Magnitude, Broader Type C Calorimeter Curve

Type D curves (**Figure 4.39**) were always from 50% fly ash mixtures, but involved a double peak. The second peak, thought to be the silicate reaction, was taller than the first (aluminate reaction), and occurred after the first peak. The first peak occurred around 625 min. on the average, (sometimes called a "delayed" aluminate peak,

meaning delayed from the normal position of being very early in the reaction) (Cost and Knight, 2007) while the second peak was at about 1700 min. The second peak usually occurred much later than Types A, B, and C curves, and was lower in magnitude than A and C curves. Type D curve mixtures had moderate CaO contents, moderate equivalent alkali contents, and moderate aluminate/sulfate ratios, but high aluminate contents. Early stiffening (AR5-30= 0.62) was an issue.

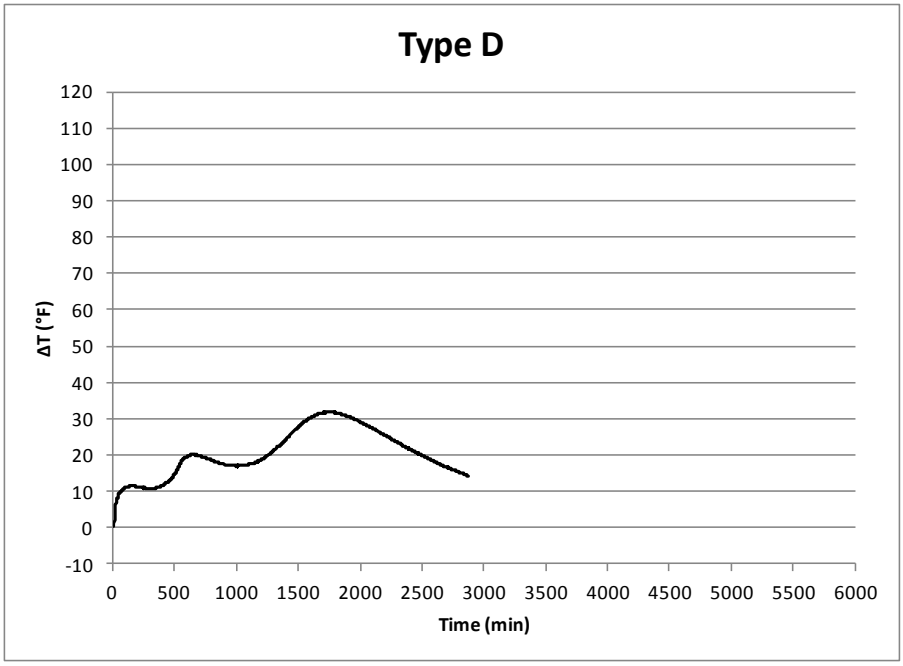

Figure 4.39 – Double Peak, Delayed Second Peak Type D Curve.

Type E curves (**Figure 4.40**) were of fairly low peak height magnitude but quite broad in nature, or were a combination of two consecutive peaks but of equal height, resulting in a long time of occurrence. Type E curves resulted from 70% fly ash mixtures. The curves were accelerated compared to curves A through D. E curve mixtures were low in CaO, and high in equivalent alkali, aluminate, and aluminate/sulfate. Early

stiffening (AR5-30= 0.47) was more of an issue than A through D and as bad as Types F and G.

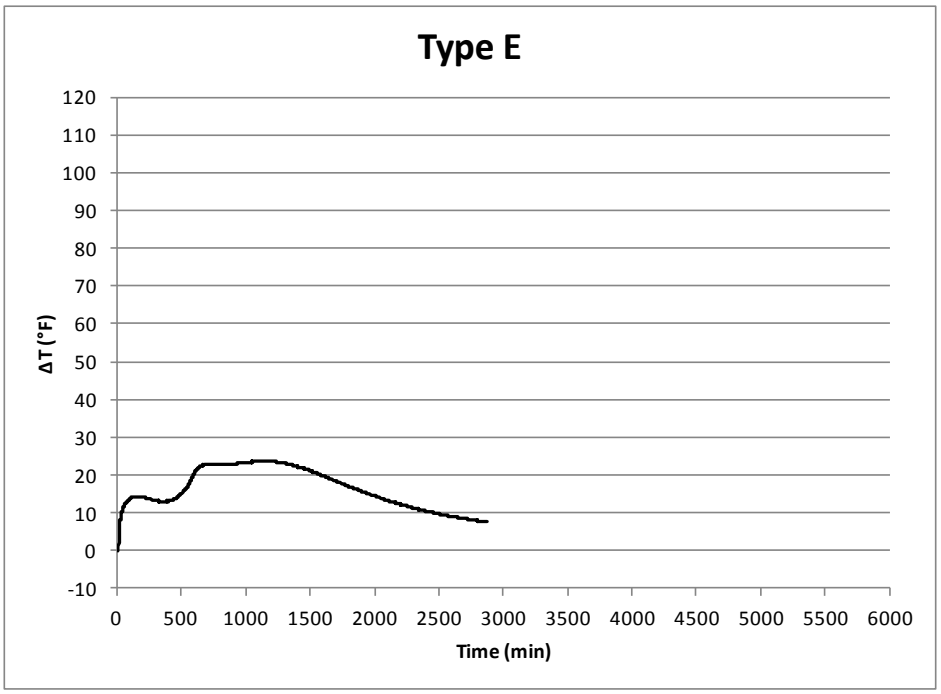

Figure 4.40 – Type E Curve Exhibiting Delayed, Broad or Equal Double Peaks

Type F curves (**Figure 4.41**) were drastically different than Types A through E in that they developed very short magnitude peak heights (thought to be "delayed" initial aluminate reactions) occurring at an average of 245 min., with no silicate peak. All Type F curves were from 70% fly ash mixtures. F mixtures had the lowest one day strengths, low CaO contents, and were high in total equivalent alkali, aluminate, and aluminate/sulfate. Calcium ions are necessary for forming the main strength-producing hydration product, calcium silicate hydrate (C-S-H). High aluminate content systems react rapidly with calcium, thus reducing the calcium available to the silicate hydration reaction, lowering strengths. Likewise, high total equivalent alkalis increase the rate of

reaction between the aluminates and the calcium. Apparently, the system was so low in available calcium ions after the initial aluminate reaction that the silicate reaction could not happen. Early stiffening (AR5-30= 0.49) was more of an issue than A through D mixtures.

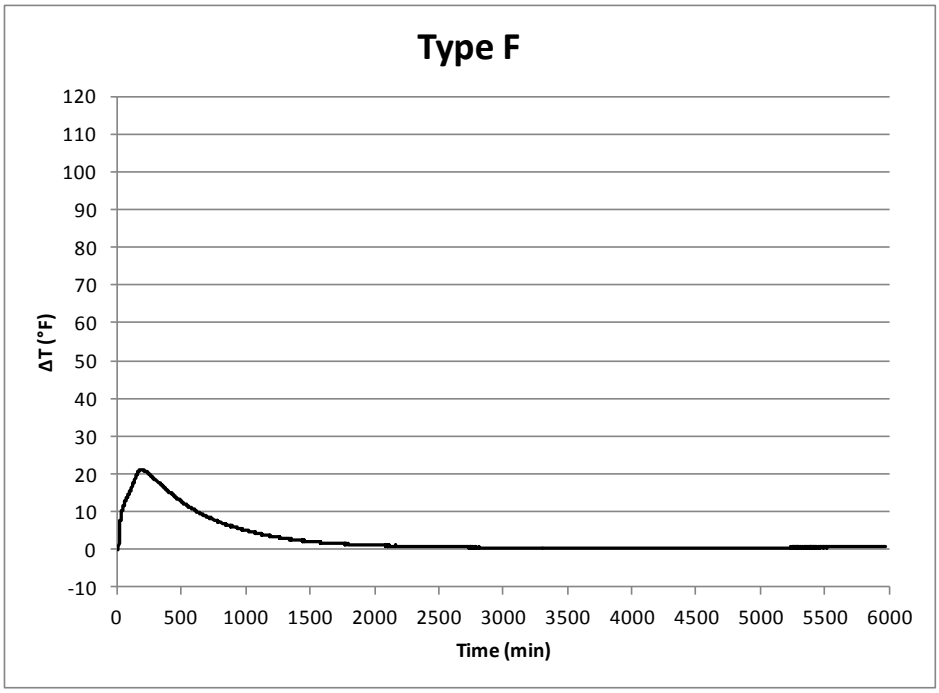

Figure 4.41 – Type F Curve Exhibiting Accelerated Time to Peak Height

Finally, Type G Curves (**Figure 4.42**) were similar to Type F curves with a first peak (average 370 min.), thought to be the "delayed" initial aluminate reaction, but with a very delayed second peak (average around 4020 min.), and thought to be the silicate reaction. Some of the mixtures labeled Type F may have been actually Type G, but early in the study the time in the calorimeter was prematurely terminated, thus missing a potential second curve. All Type G curves were from 70% fly ash mixtures.

An overlay plot of all seven typical curve types is shown in **Figure 4.43**.

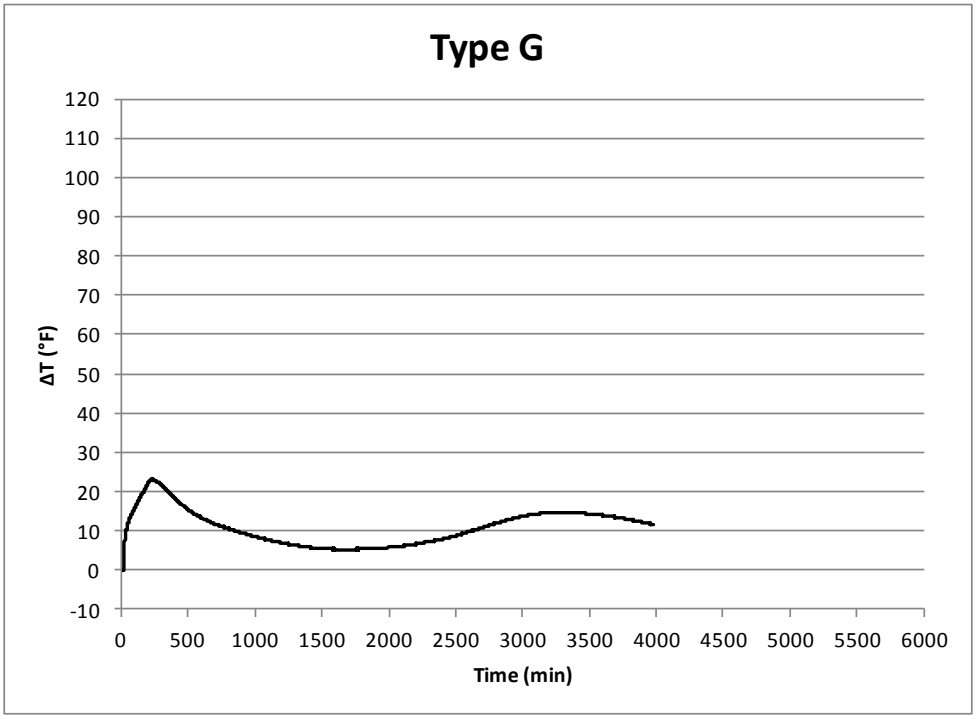

Figure 4.42 – Type G Curve Exhibiting Accelerated Time to Peak Height with Delayed Second Peak.

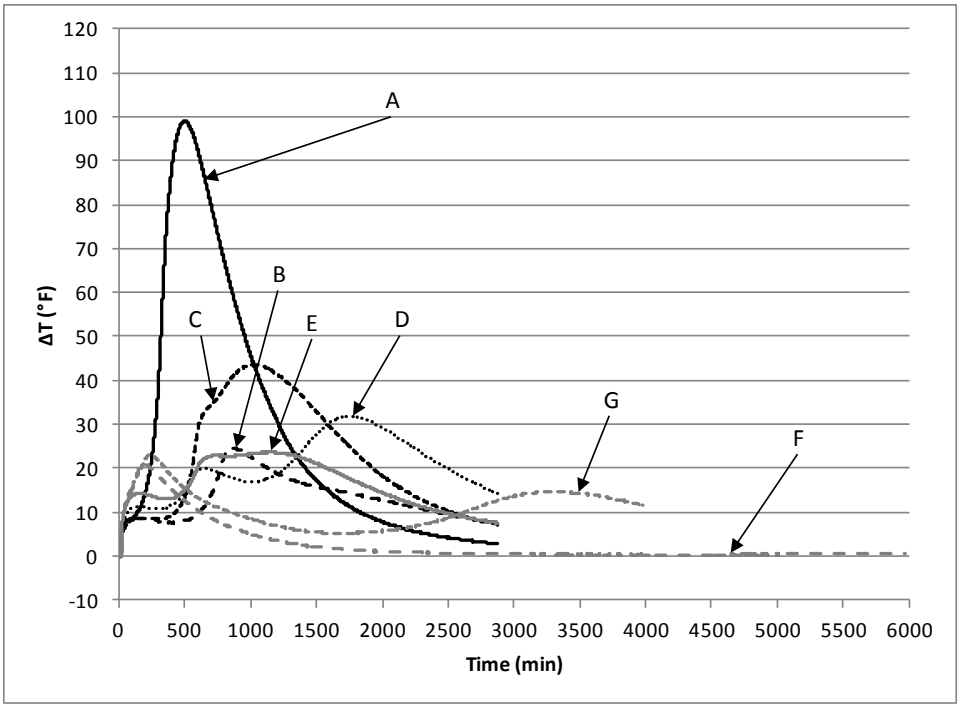

Figure 4.43 – All curve types (typical)

Thus, Types A, B, and C curves exhibited the expected peak height shortening and delay as expected from increased fly ash contents. Types F and G curves showed an unusual acceleration of the peak (along with the expected short peak heights) from some 70% fly ash mixtures. Early stiffening and flash setting were characteristics of these two curve types, indicating a possible incompatibility between the particular cement and the fly ash at the proportions in the mixture. The D and E types were unusual in that they too exhibited early stiffening and flash setting but had delayed silicate reaction curve occurrence times. All Screening Study mixture calorimetry curves are in Appendix D.

4.5.2 Main Effects Study

4.5.2.1. Mixture Designs. Once the least and most reactive combinations of cement plus fly ash were determined, the Main Effects portion of the paste study began, using combinations 4-1 and 1-3. In order, WR/HRWR dosage, gypsum content, and finally lime or RSC contents were explored, all at zero, 50% and 70% fly ash replacement levels. As in the Screening Study, the *w/cm* and total cementitious materials content was kept constant.

First, WR/HRWR dosage was chosen. As previously mentioned, recognizing that mixtures of the relatively low *w/cm* would encounter workability issues for the straight OPC mixtures, it was decided to use a water reducer (WR). Although a traditional Type A may have been less problematic, a WR was chosen that was advertised as being able to function as both an A and as an F high range water reducer (HRWR). Because it has been shown that WR will affect setting time (usually retard), and may cause early stiffening because of an interaction with a particular sources of cement and fly ash, it was decided to explore the effect of several levels of WR. Three dosage levels were selected: zero,

low, and high. “Low” was defined as the dosage necessary to achieve the required design slump of the concrete control mix. The “high” level was selected at an arbitrarily greater value compared to the low dosage. In an on-going parallel HVFA study, some work with concrete mixtures had been completed. From that, WR dosage between 2 and 3 fl oz/cwt was necessary to achieve a 5 in. slump. Thus, the WR dosage was selected as 2.75 fl oz/cwt.

Next, gypsum level was selected, based on previous studies by Bentz (2010), who used 2% gypsum by TCM mass. In the present study, for most mixtures, 4% by mass of fly ash was used. This translates into a range of 1.91 to 2.63% by TCM mass for the mixtures in this study, as shown earlier in **Table 4.1**. Additionally, the effect of 4% gypsum was compared to 2% (both by mass of fly ash).

Lime content was chosen in a similar manner. Bentz used 5 % lime by TCM mass. In the present study, 10% lime by weight of fly ash (4.67-6.54% by TCM mass) was studied. Additionally, the effect of 10% lime was compared to five %, both by mass of fly ash (5% ~2.39-3.38% by TCM mass).

Finally, RSC content was chosen. Bentz used 10% RSC by TCM mass. In the present study, 20% RSC by weight of fly ash (8.93-12.28% by TCM mass) was studied. Additionally, the effect of 20% RSC was compared to 10%, both by mass of fly ash (10% ~4.67-6.54% by TCM mass).

As stated earlier, at the low level of WR and at 4 % gypsum, the level of lime (5 and 10 %) and RSC (10 and 20%) was varied for fly ash levels of zero, 50, and 70%.This partial factorial experimental design resulted in 48 mixtures. An additional 16 mixture experiment with no gypsum was also conducted (eight with lime, eight with RSC at 50

and 70% fly ash). The test methods were the same as in the screening study: miniature slump, Vicat setting time, calorimetry, and compressive strength. However, the compressive strength testing was expanded to include more ages: 1, 3, 7, 28, and 56 days. From all this, 10 concrete mixtures were selected for Phase II with the optimum WR/HRWR, gypsum, lime, and RSC levels at zero, 50, and 70% fly ash levels.

4.5.2.2. Effect of Fly Ash. The effect of increasing fly ash content was evaluated in terms of calorimeter curve peak height and time, miniature slump early stiffening, early and later compressive strengths, and setting time.

As expected, strength at early ages was decreased as fly ash content increased. In most cases, strength of the fly ash mixtures were not fully equivalent to OPC mixtures as late as 56 days. This is shown in **Figures 4.44** and **4.45**. The effect of WR/HRWR is also shown: at up to seven days, WR has little effect, but at later ages, strength is increased somewhat. It should be noted that for combination 1-3 at 70% fly ash, strengths at ages up to 7 days was very low, indicating little activity.

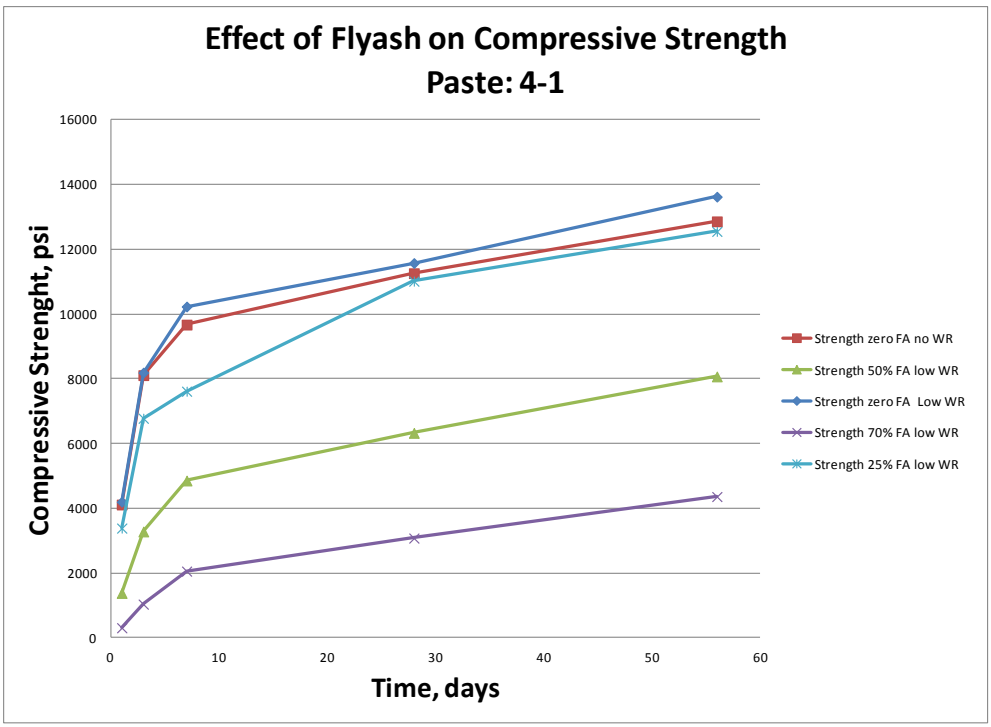

Figure 4.44 – Effect of Fly Ash Content and WR/HRWR on Compressive Strength, Combination 4-1

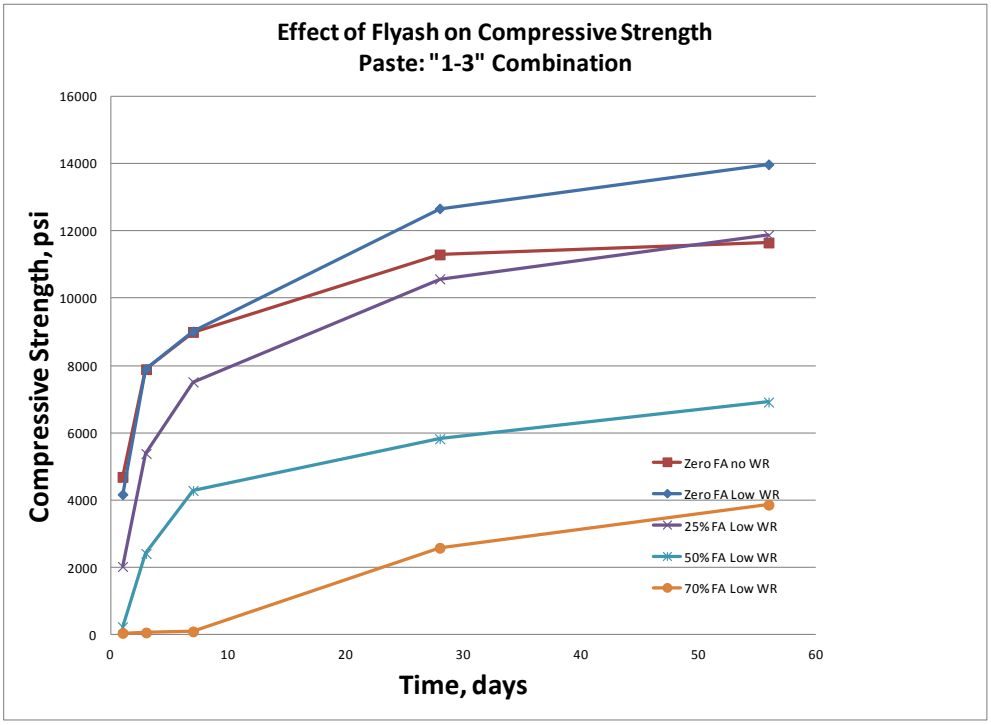

Figure 4.45 – Effect of Fly Ash Content and WR/HRWR on Compressive Strength, Combination 1-3

The effect of fly ash content and presence of WR/HRWR on reaction time as represented by the 50% NetTMax time of occurrence is shown in **Figure 4.46**. The admixture served to retard the curve position. In the case of the 4-1 combination, increasing fly ash content increasingly retarded the reaction. As for the 1-3 combination, 25% and 50% retarded increasingly. However, the 70% replacement level, the reaction was greatly accelerated, as seen in the Screening Study, indicating some kind of incompatibility.

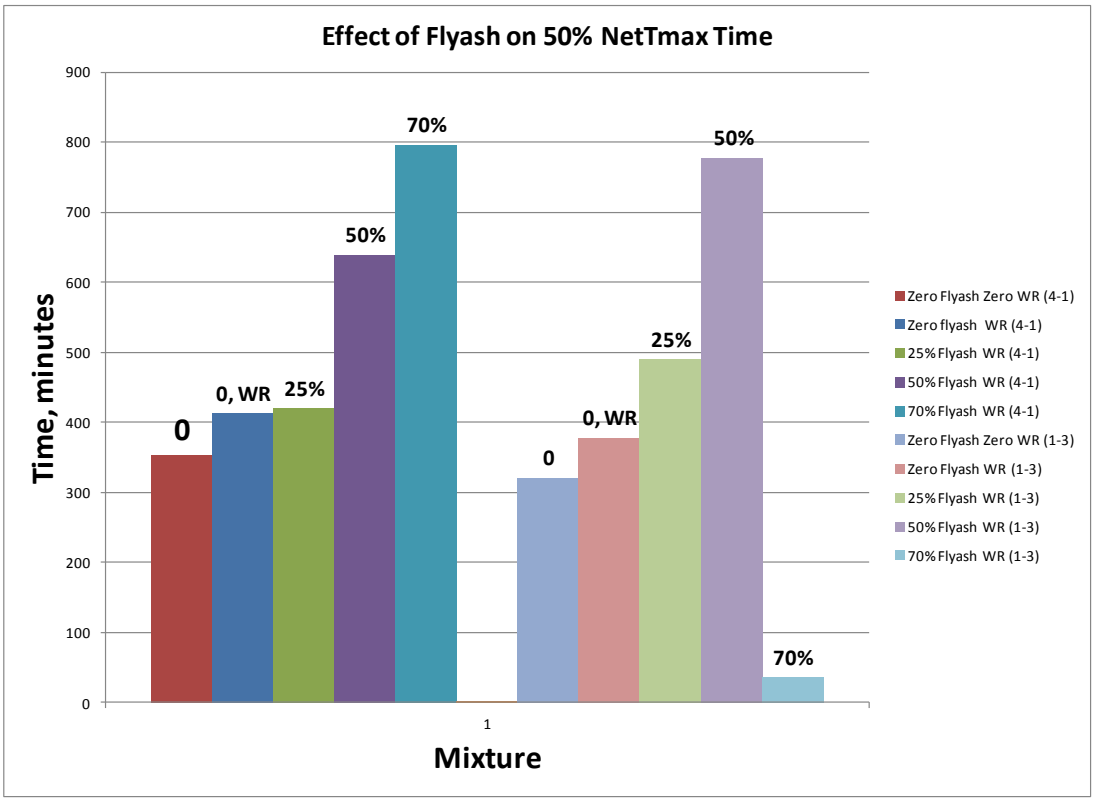

Figure 4.46 – Effect of Fly Ash Content and WR/HRWR on 50%NetTMax Time for Zero, 25, 50 and 70% Fly Ash Mixtures

The effect of fly ash on setting time is shown in **Figure 4.47.** For both cementitious combinations, 25% fly ash mixtures were retarded. For the 4-1 mixture, the

50% fly ash mixture also was retarded, but the 1-3 combination was accelerated. The 70% fly ash level accelerated setting time for both combinations, and was below the 45 min. threshold.

Only one mixture exceeded the ASTM C150 final setting time maximum limit of 480 min.: the 1-3 70% fly ash (525 min.).

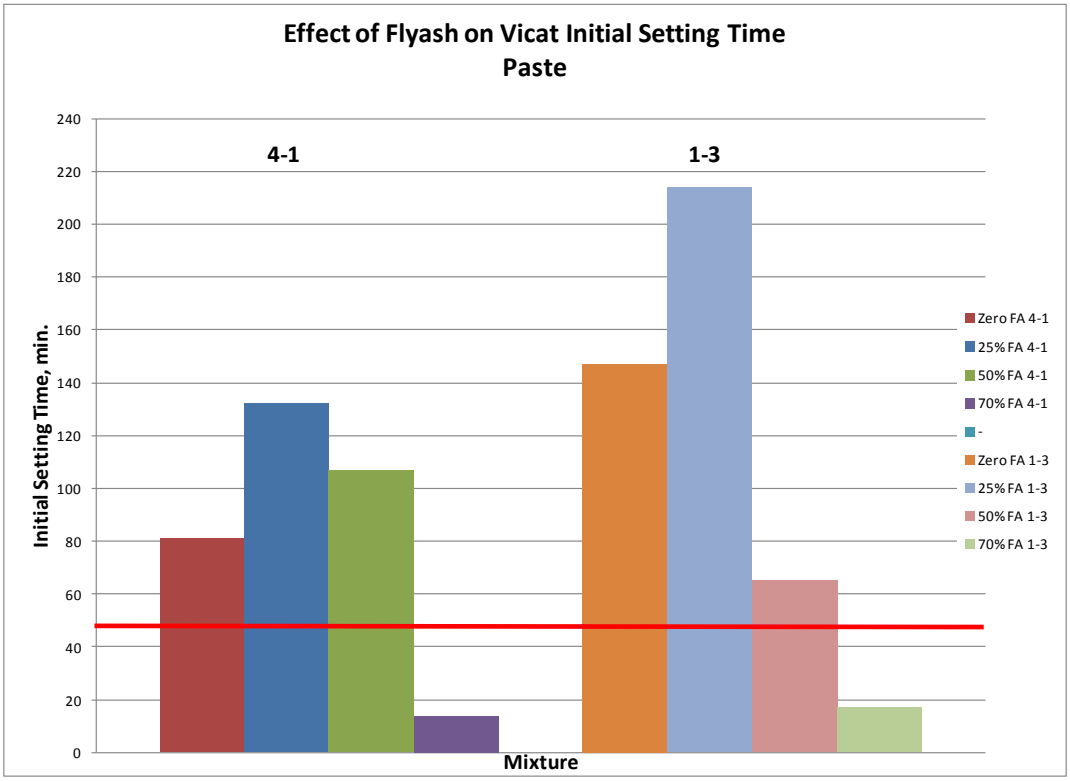

Figure 4.47 – Effect of Fly Ash Content on Initial Setting Time for Zero, 25, 50, and 70% Fly Ash Contents

The effect of fly ash on early stiffening is shown in **Figure 4.48.** Although increasing fly ash content increases fluidity (not shown), the fly ash causes an increase in early stiffening tendencies. The zero and 25% fly ash mixtures do not, but the 50% and especially the 70% fly ash mixtures fall below the threshold of 0.85.

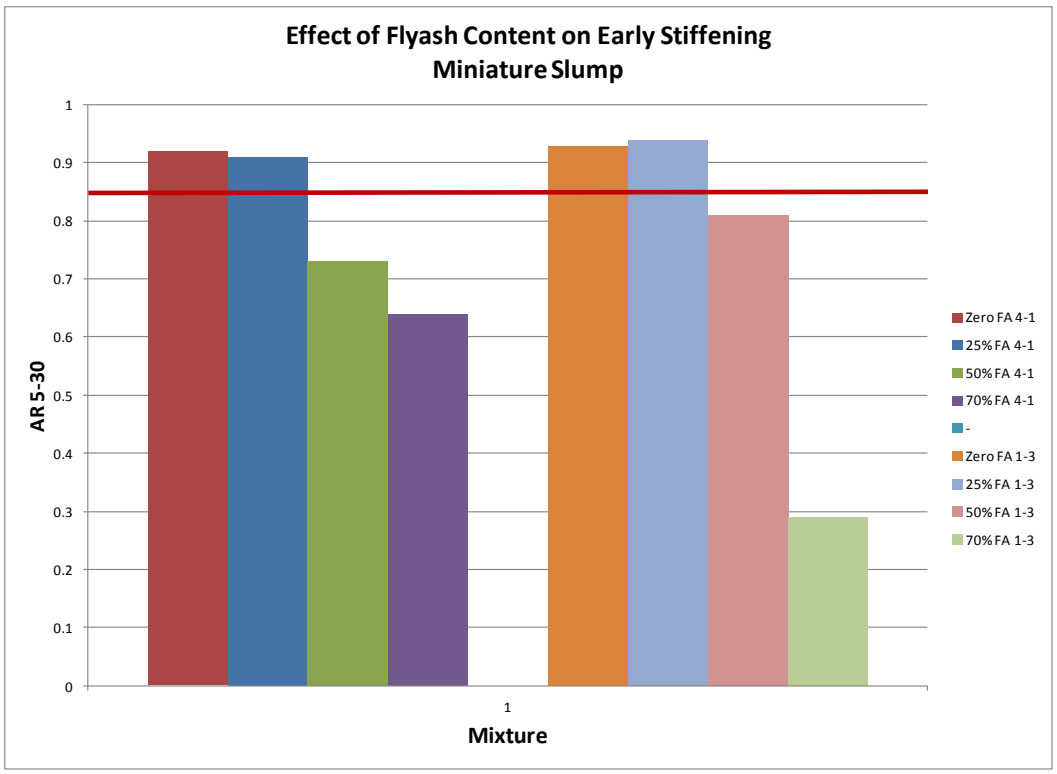

Figure 4.48 – Effect of Fly Ash Content on Early Stiffening for Zero, 25, 50 and 70% Fly Ash Mixtures

4.5.2.3. Effect of WR/HRWR. The effect of the WR/HRWR on compressive strength and 50%NetTMax time has been presented.

In **Figure 4.49** is shown a typical set of calorimeter curves with zero, low, and high dosages superimposed. In all cases, increasing dosage of WR/HRWR retarded the curves. All Main Effect study curves are in Appendix G.

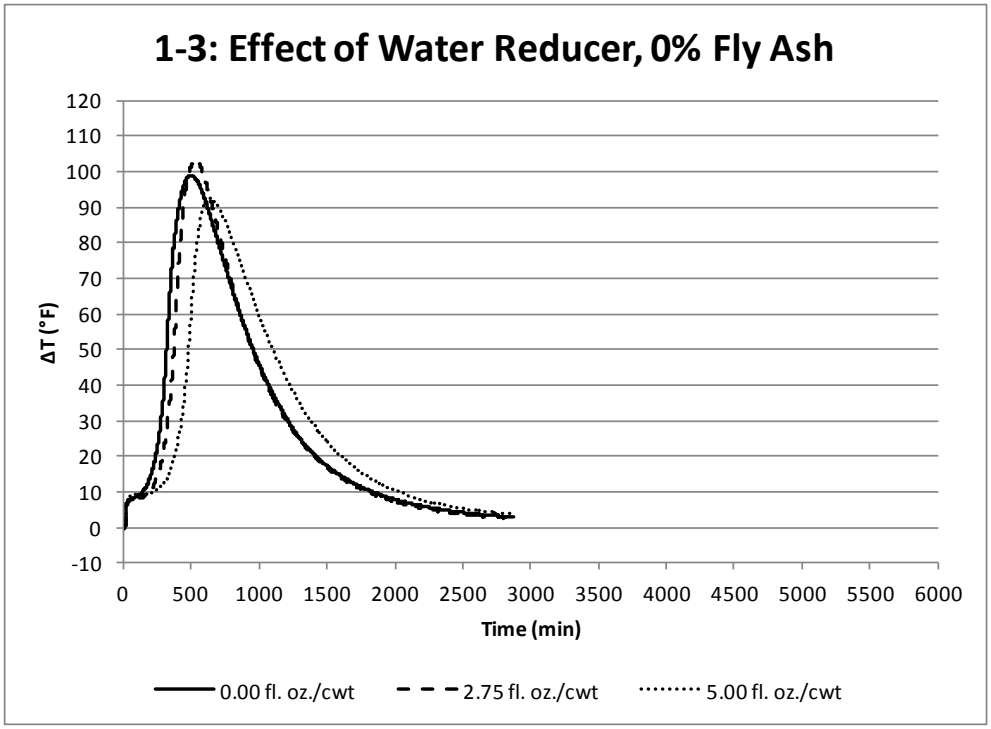

Figure 4.49 – Typical Effect of WR/HRWR Dosages on Calorimeter Curve Characteristics

The effect on initial setting time of zero and 50% fly ash mixtures is shown in **Figure 4.50**. For the 100% OPC mixtures, the WR/HRWR retarded initial setting time significantly. For the 50% fly ash mixtures, the effect was mixed. For the 4-1 combination, the low dosage (2.75 fl oz/cwt) retarded while the high dosage (5.0 fl oz/cwt) accelerated. For the 1-3 combination, both dosages accelerated.

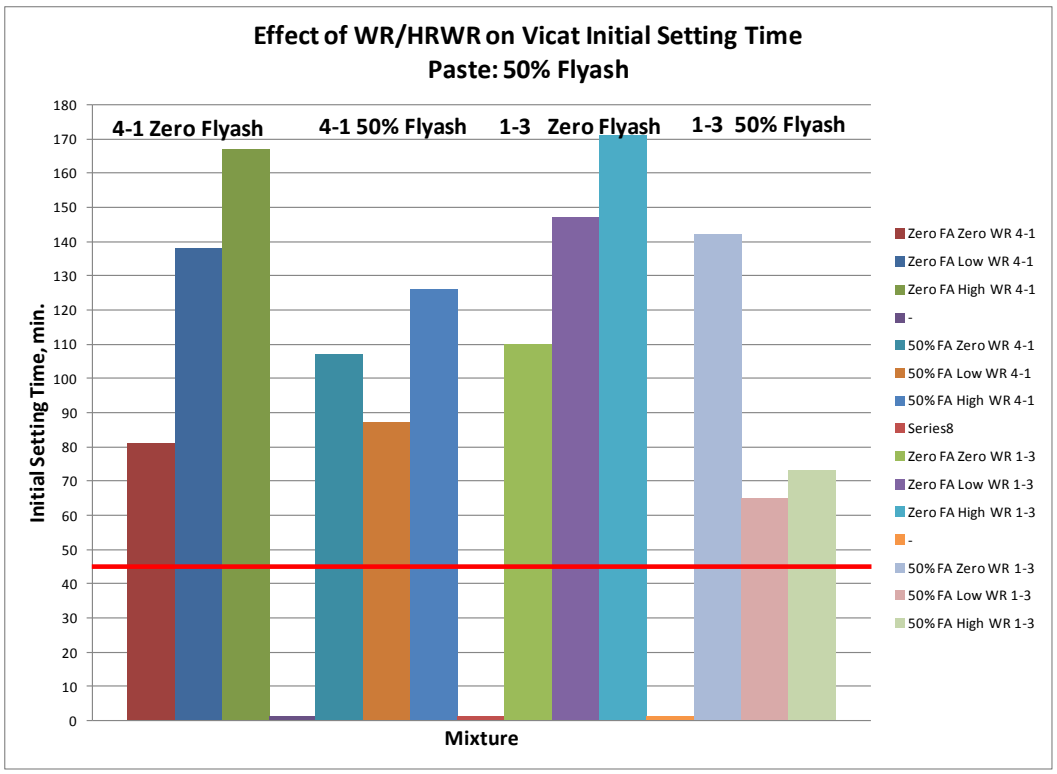

Figure 4.50 – Effect of WR/HRWR on Initial Setting Time, 50% Fly Ash Mixtures

The effect of WR/HRWR had opposite effects on the 70% fly ash mixtures, depending on combination of cementitious materials. The 4-1 combination shows retardation, while the 1-3 mixtures were accelerated, shown in **Figure 4.51**. Most mixtures set too quickly to meet the 45 min. minimum.

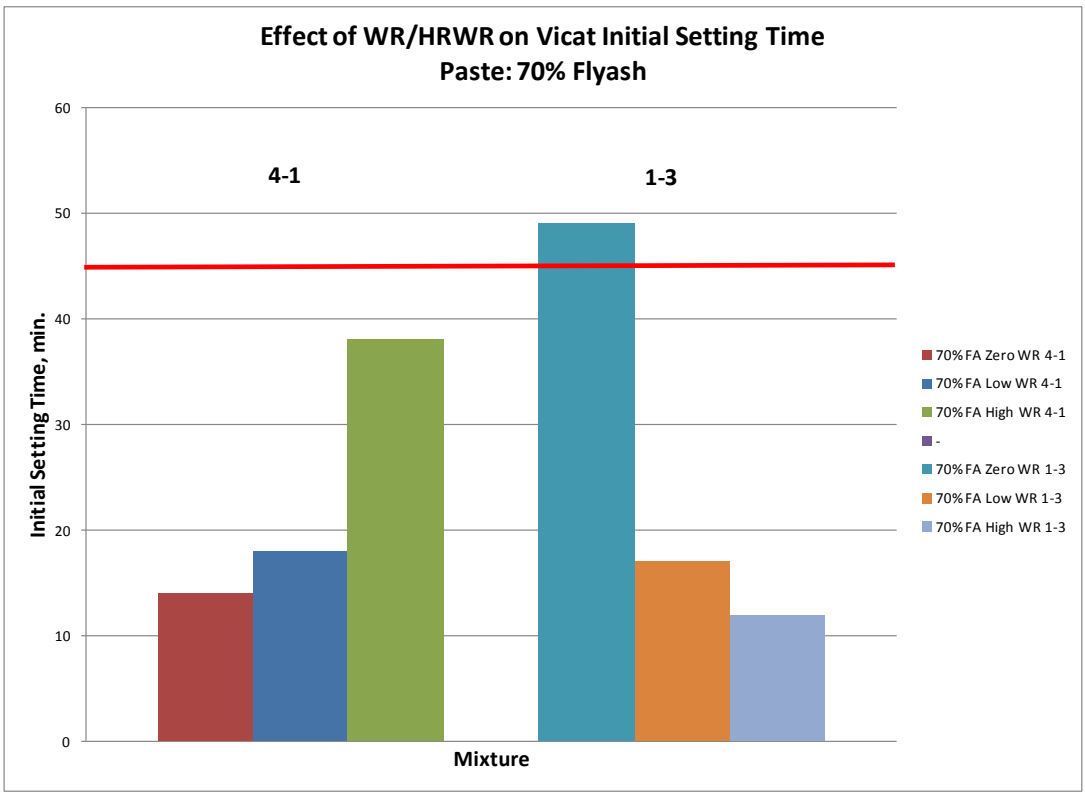

Figure 4.51 – Effect of WR/HRWR on Initial Setting Time, 70% Fly Ash Mixtures

The effect of WR/HRWR on early stiffening for combination 4-1 is shown in **Figure 4.52.** In general, the low dosage increased early stiffening tendencies while the high dosage did the opposite. The worst situation was 70% fly ash with the low WR/HRWR dosage. For the 1-3 combination (**Figure 4.53**), the low dosage generally made early stiffening worse. The high dosage alleviated or worsened the stiffening, depending on fly ash content.

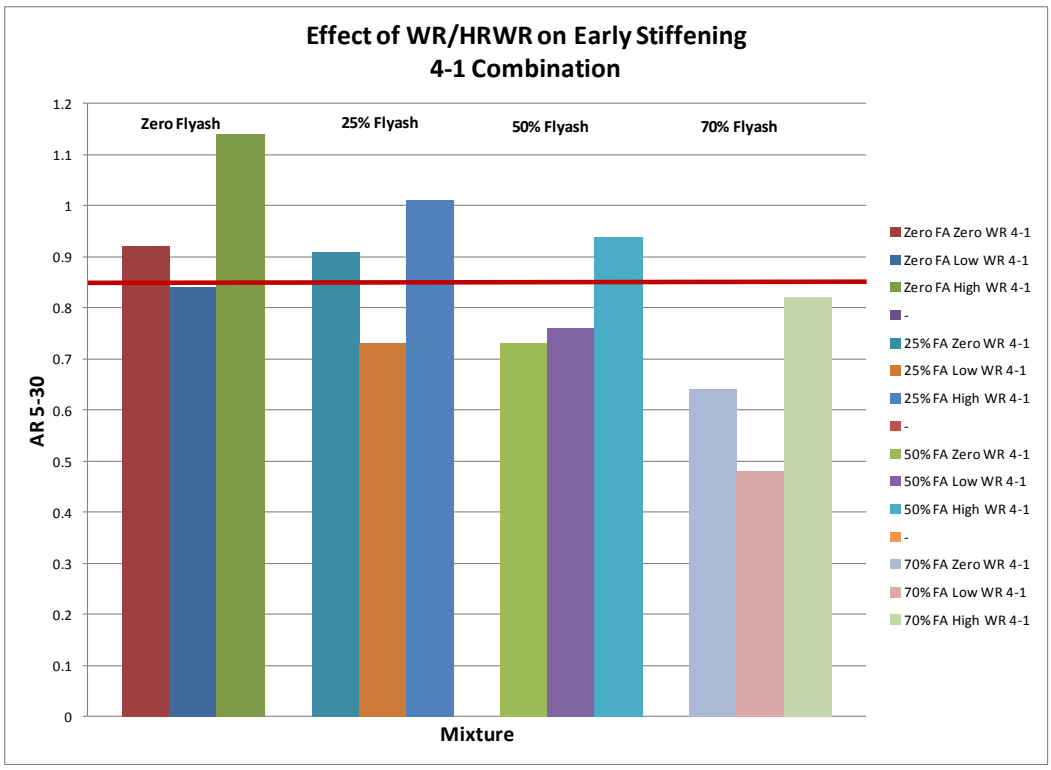

Figure 4.52 – Effect of WR/HRWR and Fly Ash Content on Early Stiffening for Zero, 25, 50 and 70% Fly Ash Mixtures (4-1 Combination)

Only three mixtures exceeded the ASTM C150 final setting time maximum limit of 480 min.: the 1-3 25% fly ash low WR (510 min.), the 1-3 25% fly ash high WR (555 min.), and the 1-3 50% fly ash high WR (510 min.).

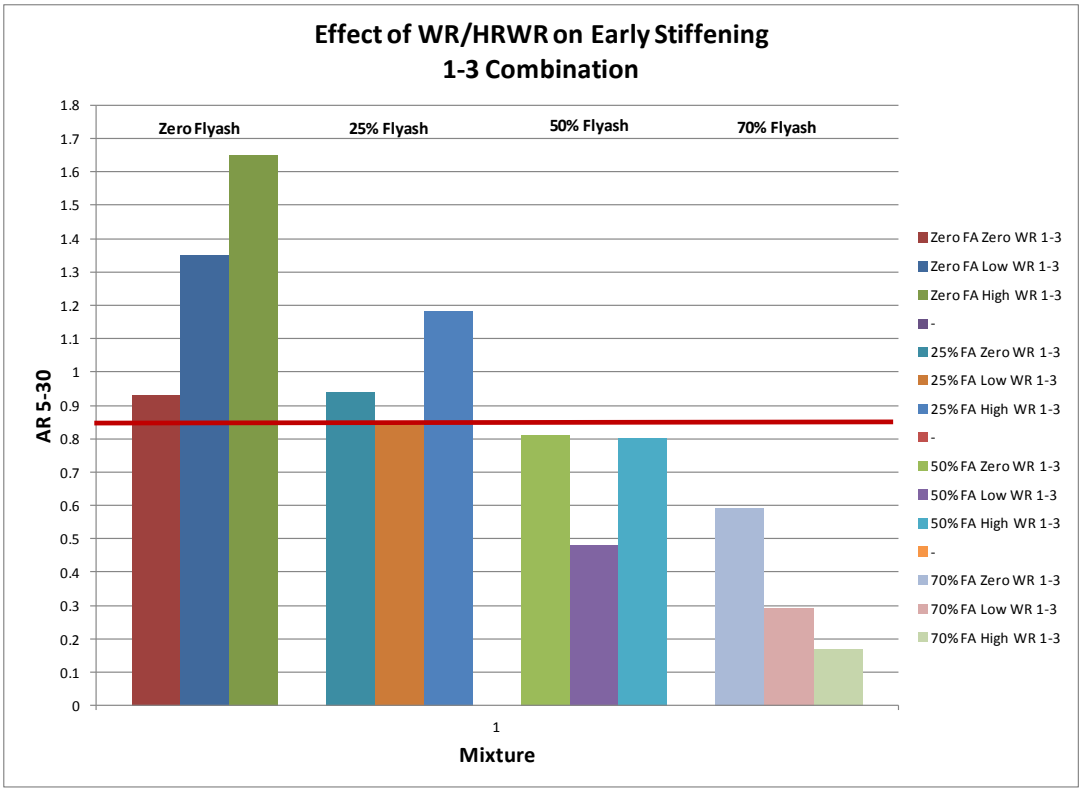

Figure 4.53 – Effect of WR/HRWR and Fly Ash Content on Early Stiffening for Zero, 25, 50 and 70% Fly Ash Mixtures (1-3 Combination)

All subsequent mixtures involving the effects of gypsum, lime, and RSC contained the low dosage (2.75 fl oz/cwt) of WR/HRWR because that is what the preliminary testing indicated would be the dosage for the concrete mixtures.

4.5.2.4. Effect of Gypsum. Initially, two levels of gypsum (2 and 4% by mass of fly ash) were examined at zero, 50, and 70% fly ash. The effect on reaction curve position is indicated by the effect on 50%NetTMax time, as shown in **Figure 4.54,** for the 50% fly ash content mixtures. As can be seen, for the 4-1 combination of OPC and fly ash, gypsum retarded the reaction and the effect increased with increasing gypsum content. For the 1-3 combination, the effect of gypsum accelerated the curve; however, the 2% content accelerated the reaction more than the 4% content. Also shown is the

50%NetTMax time for the zero fly ash mixtures. **Figure 4.55** shows the calorimeter curves for the 4-1 blend. As gypsum level increases, the curves shift increasingly rightward (delayed).

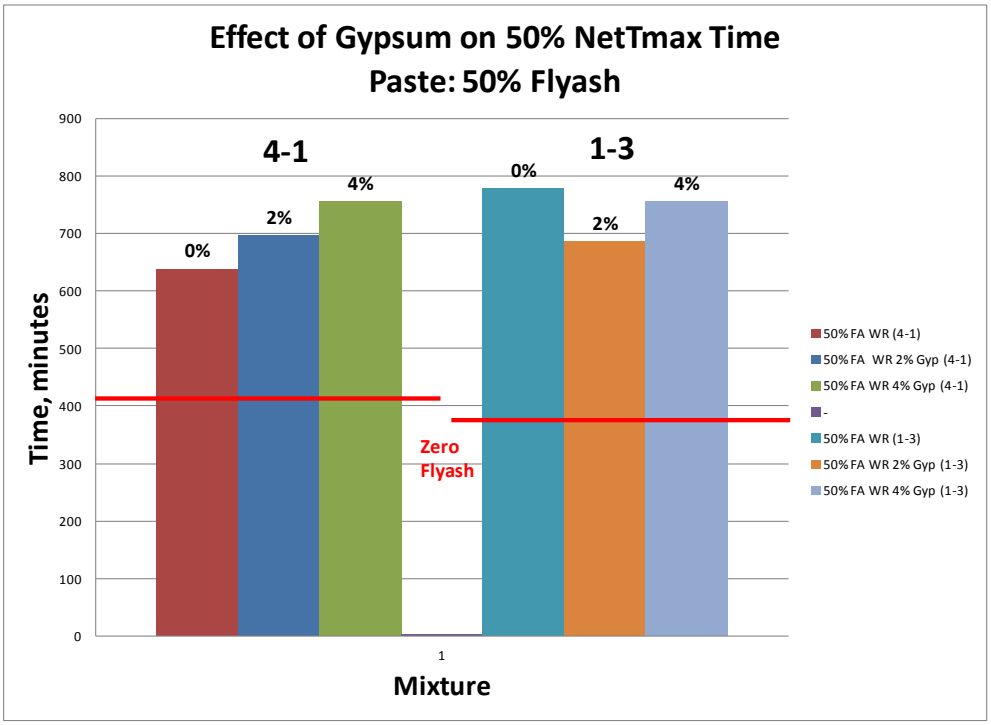

Figure 4.54 - Effect of Gypsum Content on 50%NetTMax Time for 50% Fly Ash Mixtures

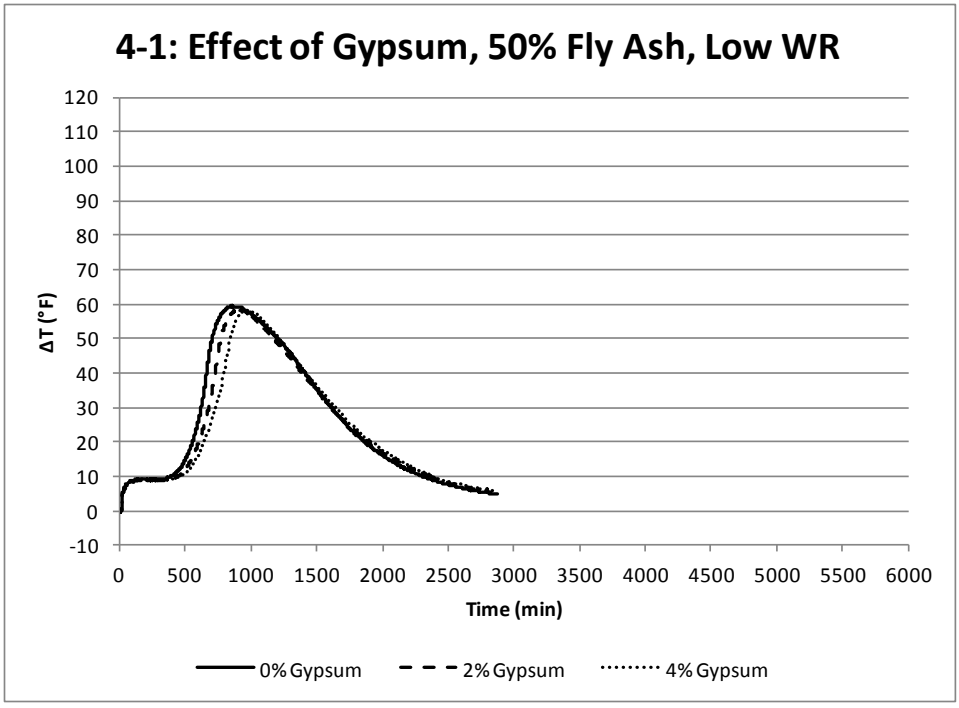

Figure 4.55– Typical Effect of Gypsum Content on Calorimeter Curve Characteristic

Figure 4.56 shows the same relationships for the 70% fly ash mixtures. The 4-1 combination at 70% fly ash acted in the same manner as at 50% fly ash: gypsum retarded the reaction and the effect increased with increasing gypsum content. The effect was more pronounced at 70% fly ash. For the 1-3 combination, the zero gypsum curve was greatly accelerated; the presence of gypsum appears to be negligible.

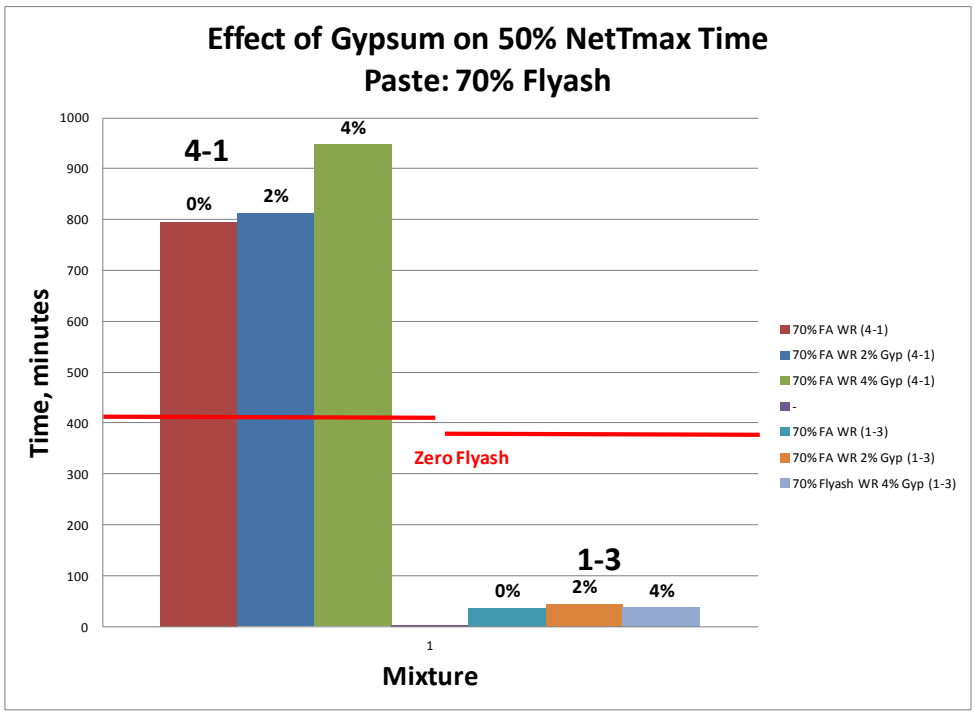

Figure 4.56 - Effect of Gypsum Content on 50%NetTMax Time, 70% Fly Ash Mixtures

The effect of gypsum on one day compressive strengths for the 50% fly ash mixtures is shown in **Figure 4.57.** As can be seen, 2% gypsum reduced the strength somewhat and the effect was greater with 4% gypsum for combination 4-1. For the 1-3 combination, gypsum increased strength marginally, with 2% slightly more than 4%.

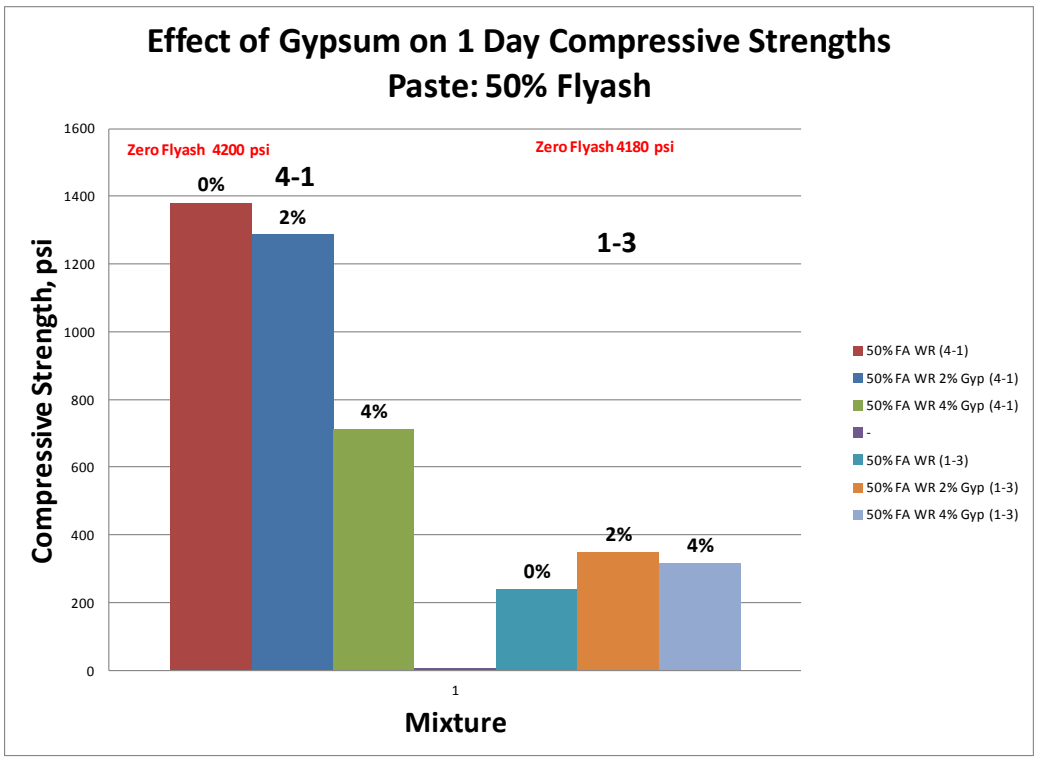

Figure 4.57 - Effect of Gypsum Content on One Day Compressive Strength for 50% Fly Ash Mixtures

For the 70% fly ash mixtures, the effect of gypsum was somewhat different, as shown in **Figure 4.58.** For the 4-1 combination, 2% gypsum increased strength while 4% decreased it. For the 1-3 combination, 2% gypsum had little effect while 4% increased strength. It is interesting to examine a calorimeter curve for the 1-3 70% mixture. As shown in **Figure 4.59**, the zero gypsum curve is of the F type which essentially has no silicate reaction curve. But, upon gypsum addition, some activity is spurred on as evidenced by the secondary peaks.

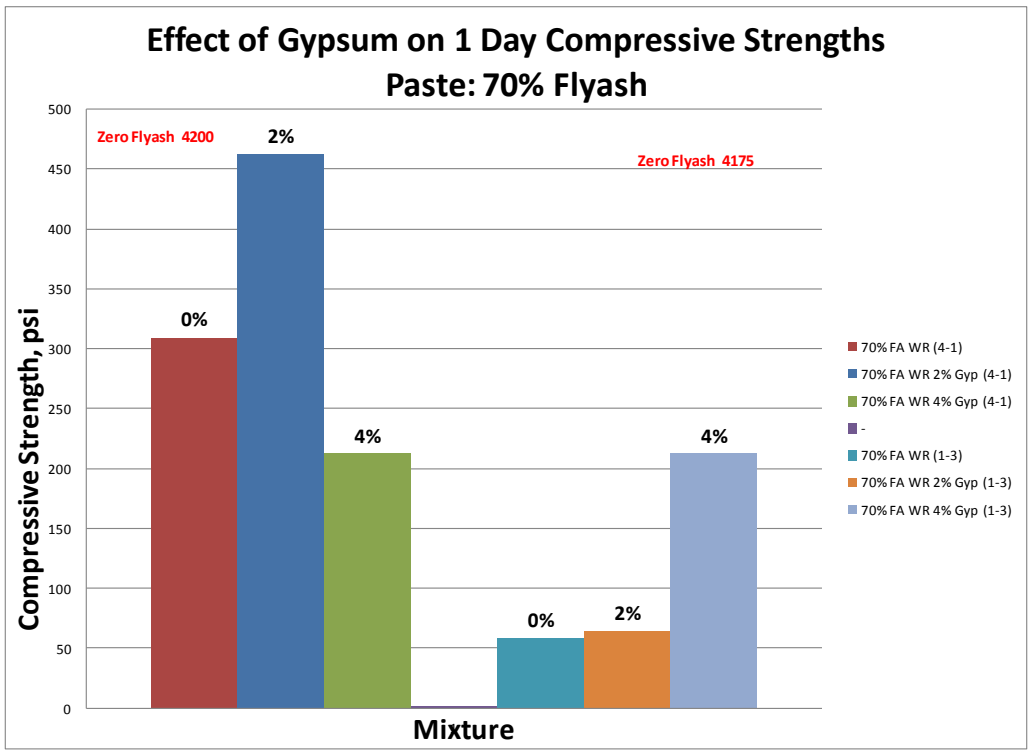

Figure 4.58 - Effect of Gypsum Content on One Day Compressive Strength for 70% Fly Ash Mixtures

At 56 days, **Figure 4.60** shows the effect of gypsum. The effect is negligible to marginal for all of the mixtures.

Finally, the effect of gypsum on 56 day strength for the 70% fly ash mixtures is shown in **Figure 4.61.** For most mixtures, the addition of gypsum reduced strength only marginally; however, at 2% for the 4-1 combination, the reduction was more significant.

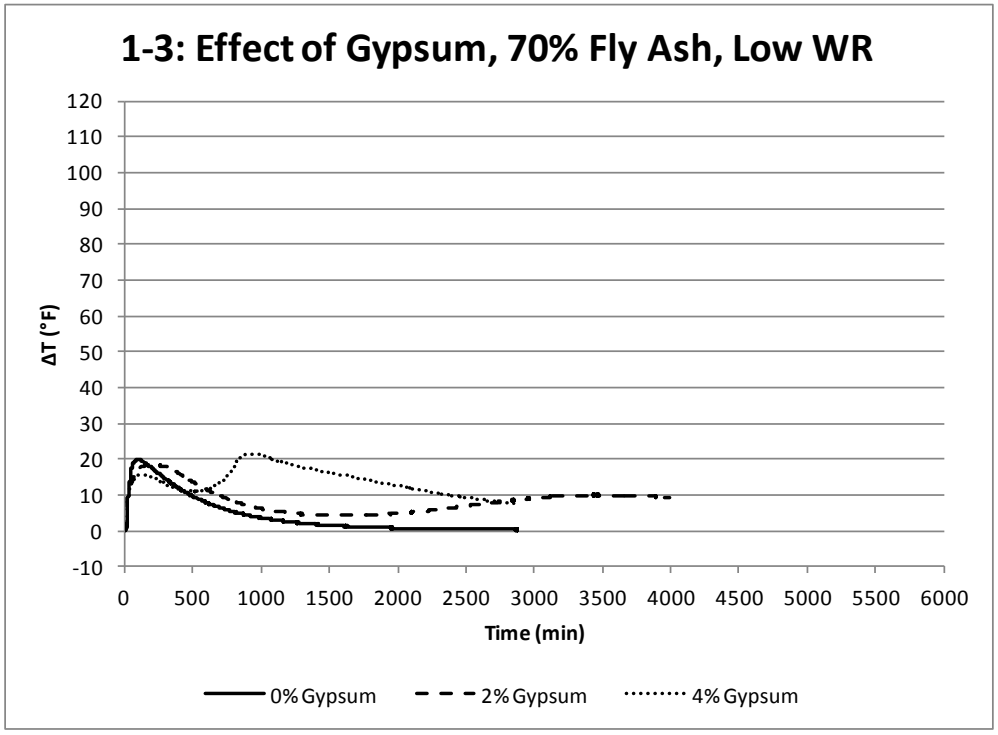

Figure 4.59– Typical Effect of Gypsum Content on Calorimeter Curve Characteristics

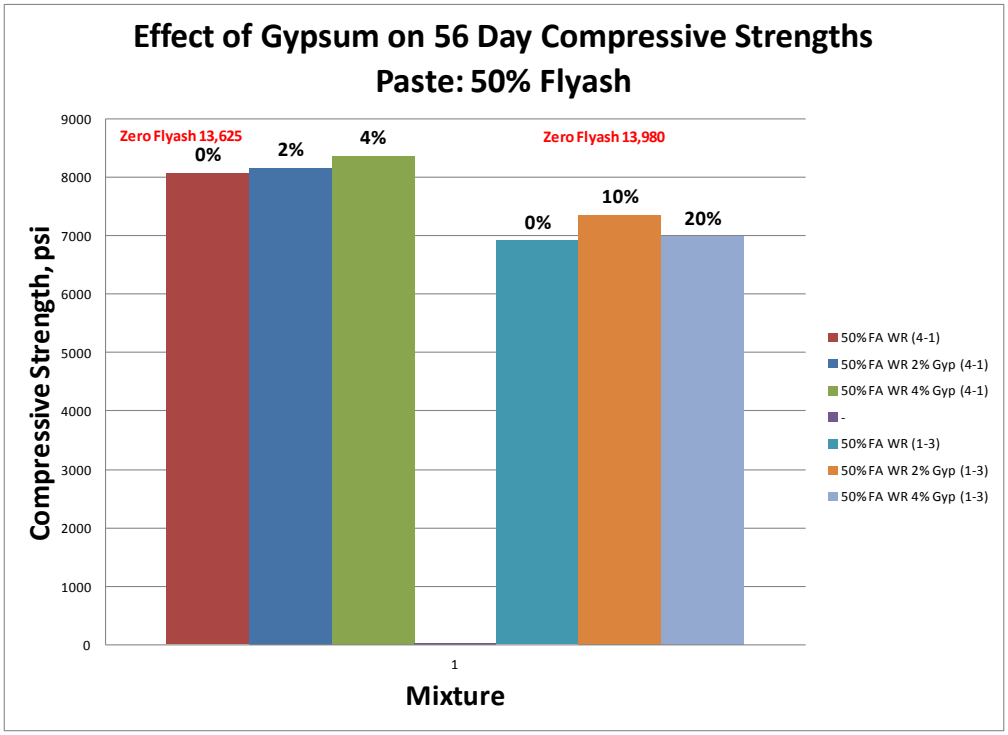

Figure 4.60 - Effect of Gypsum Content on 56 Day Compressive Strength for 50% Fly Ash Mixtures

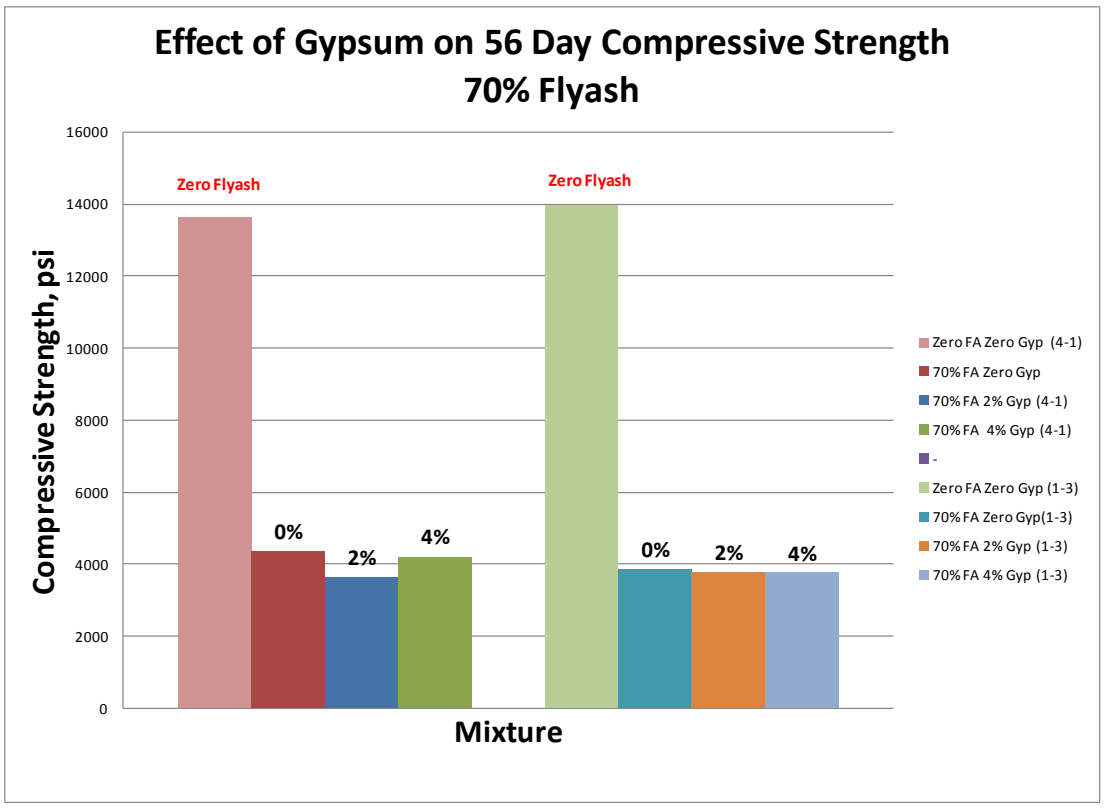

Figure 4.61 - Effect of Gypsum Content on 56 Day Compressive Strength for 70% Fly Ash Mixtures

The effect of gypsum on initial setting time (Vicat) for the 50% fly ash mixtures is shown in **Figure 4.62**. As can be seen, fly ash by itself accelerated the setting time significantly. When introduced, the gypsum retarded the set. In the case of the 4-1 combination, the setting time was essentially restored to the zero fly ash time, with 2% gypsum slightly more effective than the 4% level. For the 1-3 combination, the gypsum at both 2 and 4% levels only marginally retarded the setting time-it was still quite early. For the 70% fly ash mixtures (**Figure 4.63**), which were badly accelerated, in most cases the gypsum retarded the setting time (which is a good thing), but only to a small degree (10 minutes or less). As a point of reference, the ASTM C150 and C1157 minimum threshold

of 45 min. is shown. All 50% mixtures were greater than the minimum. However, only the 2% gypsum 4-1 mixture met the minimum. All the rest set up too quickly.

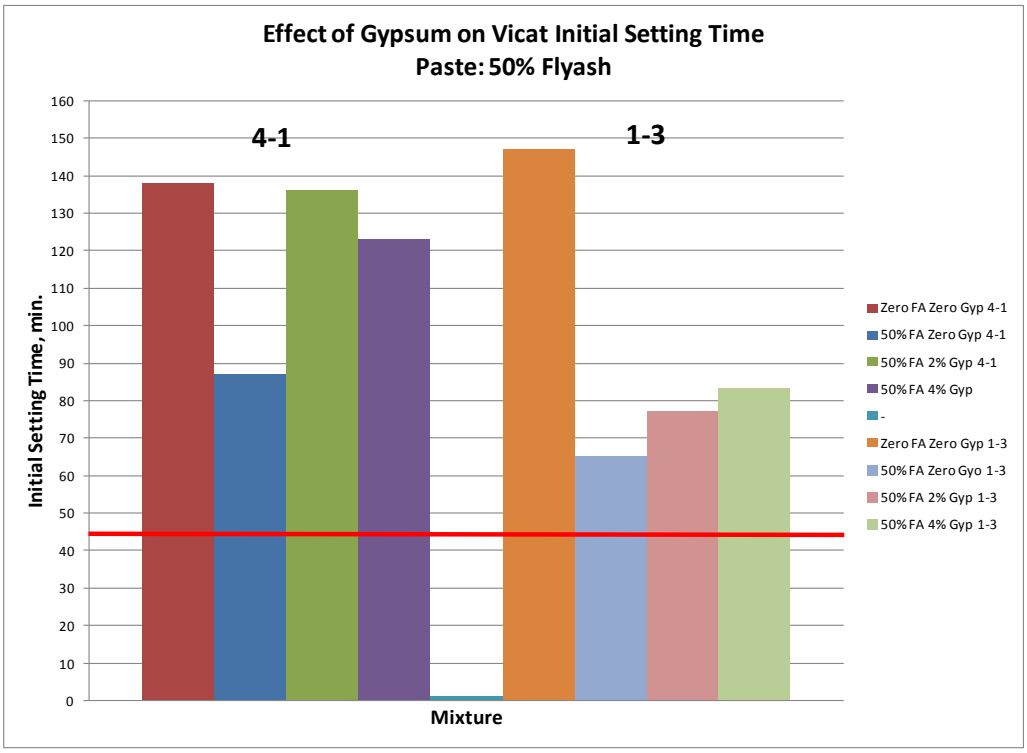

Figure 4.62 - Effect of Gypsum Content on Vicat Initial Setting Time for 50% Fly Ash Mixtures

Only three mixtures exceeded the ASTM C150 final setting time maximum limit of 480 min.: the 1-3 50% fly ash 2% gypsum (570 min.), the 4-1 50% fly ash 4% gypsum (540 min.), and the 1-3 50% fly ash 4% gypsum (675 min.).

Figure 4.64 depicts the effect of gypsum on early stiffening. In three of the four mixtures with fly ash, gypsum improved early stiffening tendencies. However, none of the effects of gypsum was more than marginal. All mixtures (with fly ash) were prone to early stiffening to some degree.

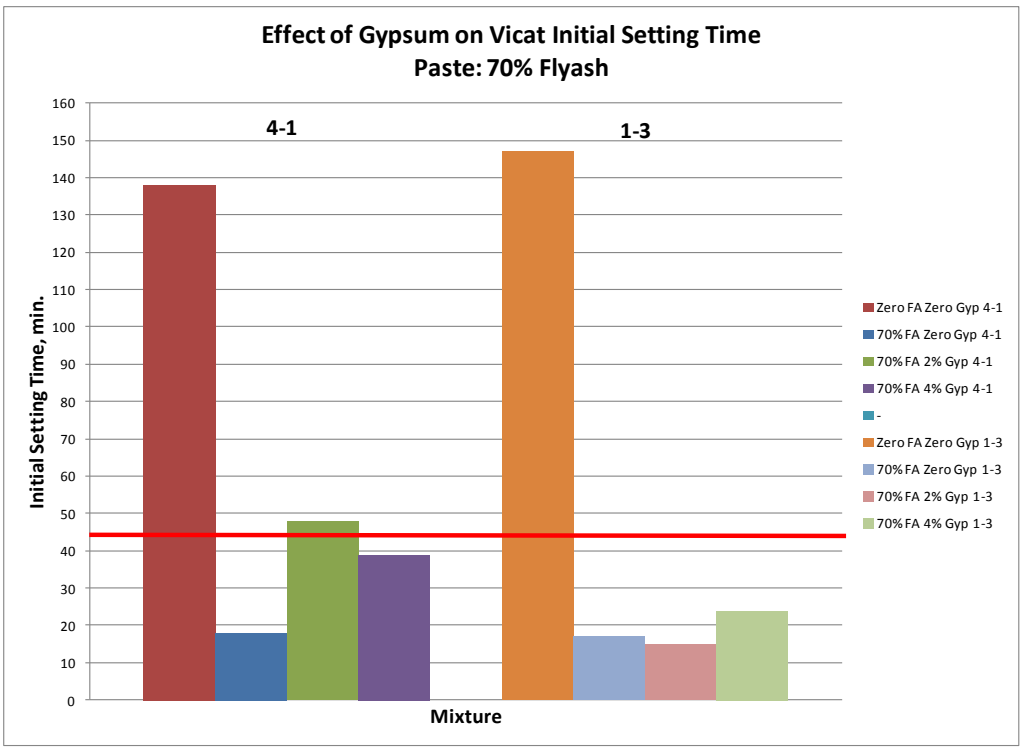

Figure 4.63 - Effect of Gypsum Content on Vicat Initial Setting Time for 70% Fly Ash Mixtures

4.5.2.5. Effect of Lime. A limited amount of testing was performed to examine the effect of lime by itself. **Figure 4.65** shows a comparison of compressive strength to that of OPC mixtures, all with the low dosage of WR/HRWR, for the 4-1 combination. Likewise, **Figure 4.66** depicts the 1-3 combination. The 5% lime improved strength somewhat for the 50% and 70% fly ash 4-1 mixture at later strengths; at other ages and fly ash contents there was no improvement, or even small decreases. The 10% lime strength generally was slightly lower than the 5% lime. For the 1-3 combination, there was little or no improvement for the 50% and 70% mixtures, but both lime percentages increased strength at 56 days for both the 50 and 70% fly ash mixtures. Also, both lime contents improved the seven day strengths of the 70% mixtures.

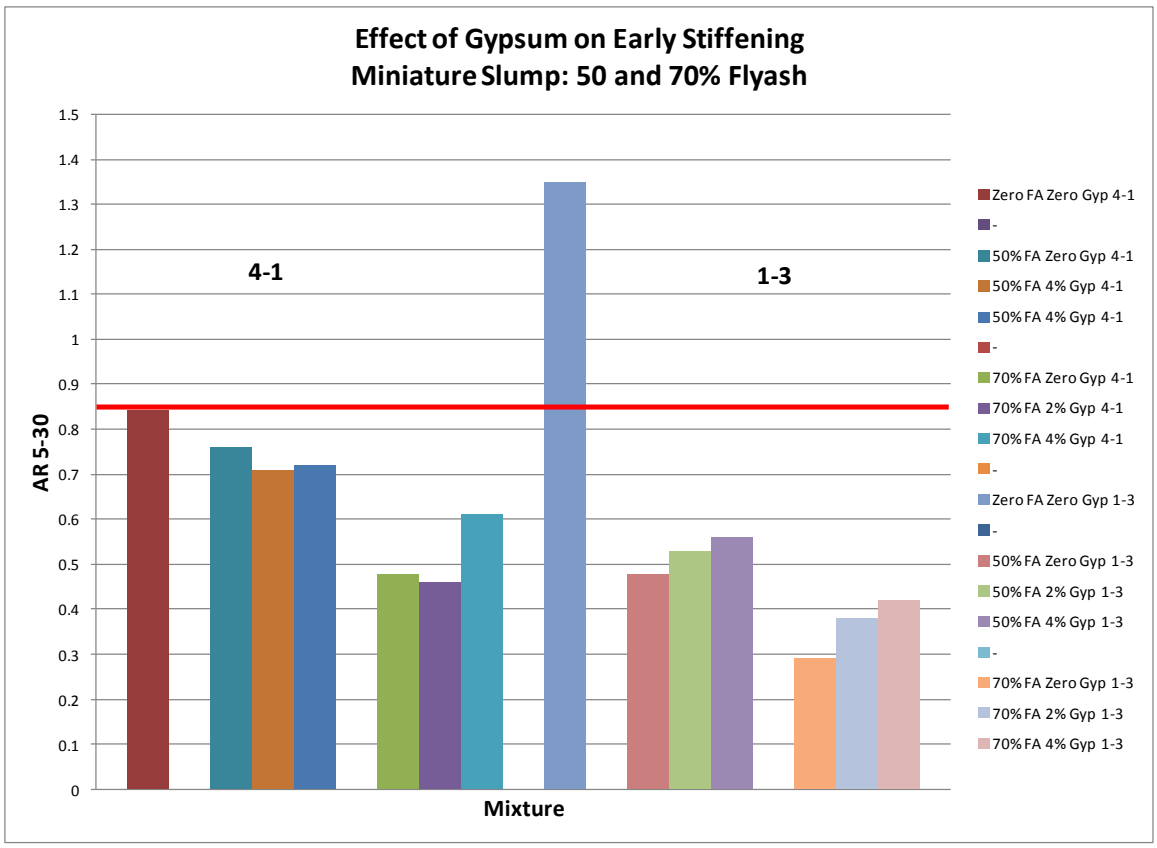

Figure 4.64 – Effect of Gypsum and Fly Ash Content on Early Stiffening for Zero, 50, and 70% Fly Ash Mixtures

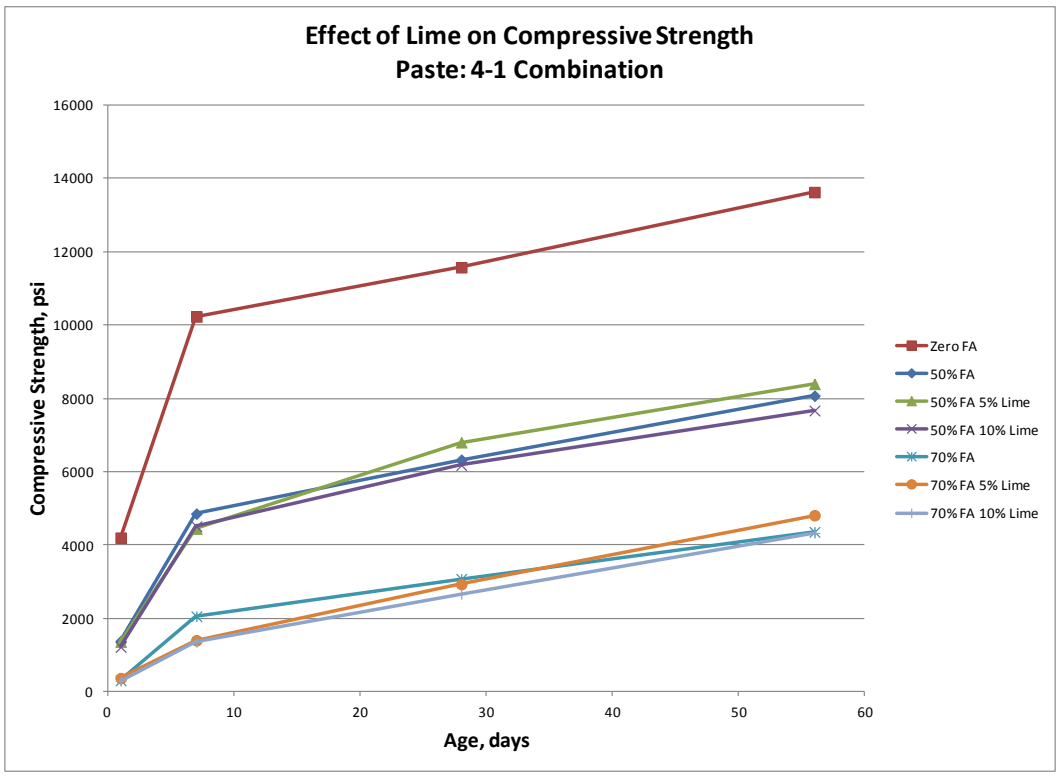

Figure 4.65 – Effect of Lime on Compressive Strength, 4-1 Combination

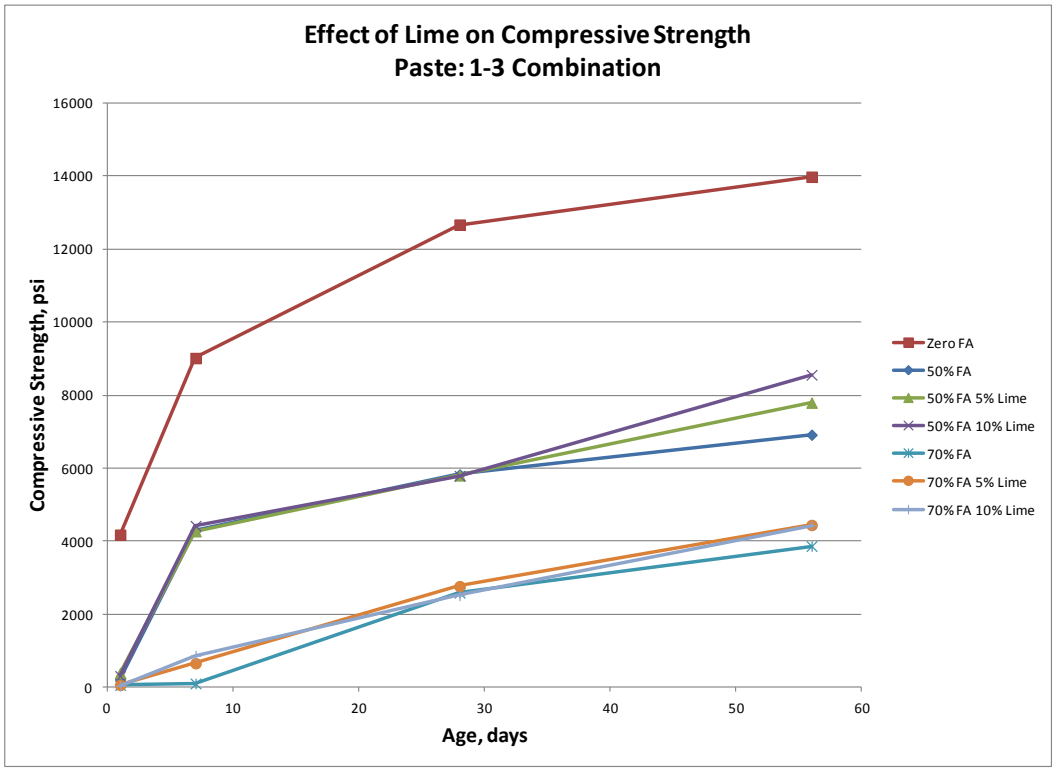

Figure 4.66 – Effect of Lime on Compressive Strength, 1-3 Combination

4.5.2.6. Effect of RSC. A limited amount of testing was performed to examine the effect of RSC by itself. **Figure 4.67** shows a comparison of compressive strength to that of OPC mixtures, all with the low dosage of WR/HRWR, for the 4-1 combination. Likewise, **Figure 4.68** depicts the 1-3 combination. RSC improved strengths for both cementitious combinations at ages of seven days and later, but only marginally at one day. Both RSC levels improved 56 day strengths somewhat, with the 20% RSC level faring better.

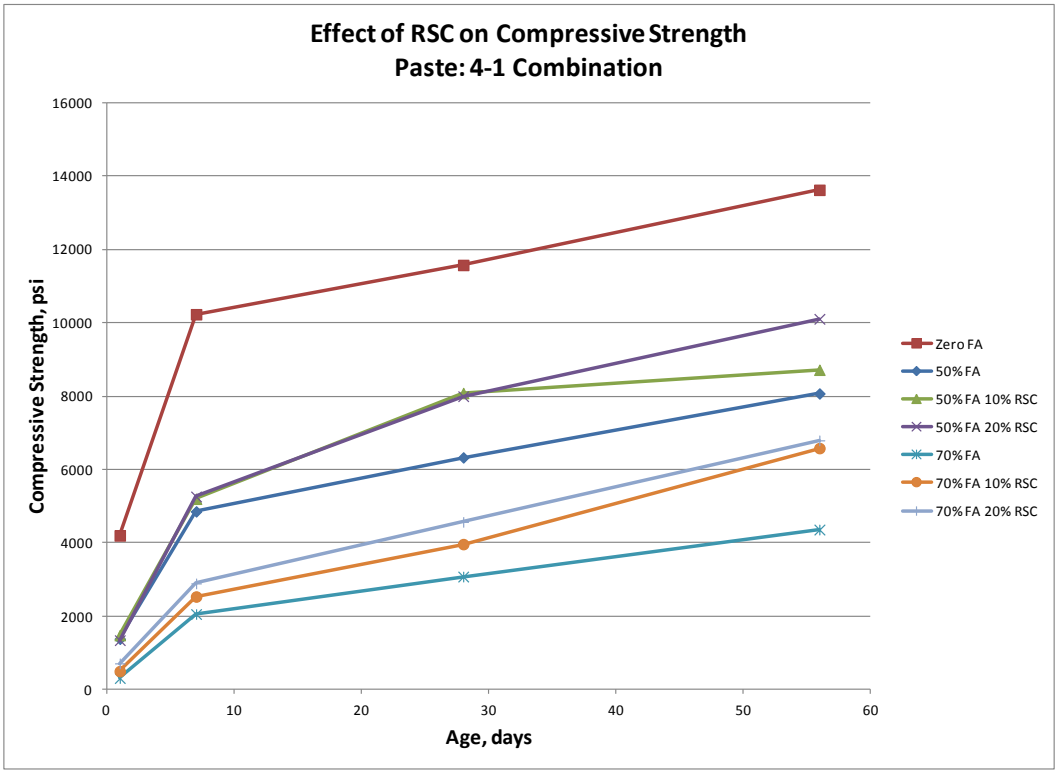

Figure 4.67 – Effect of RSC on Compressive Strength, 4-1 Combination

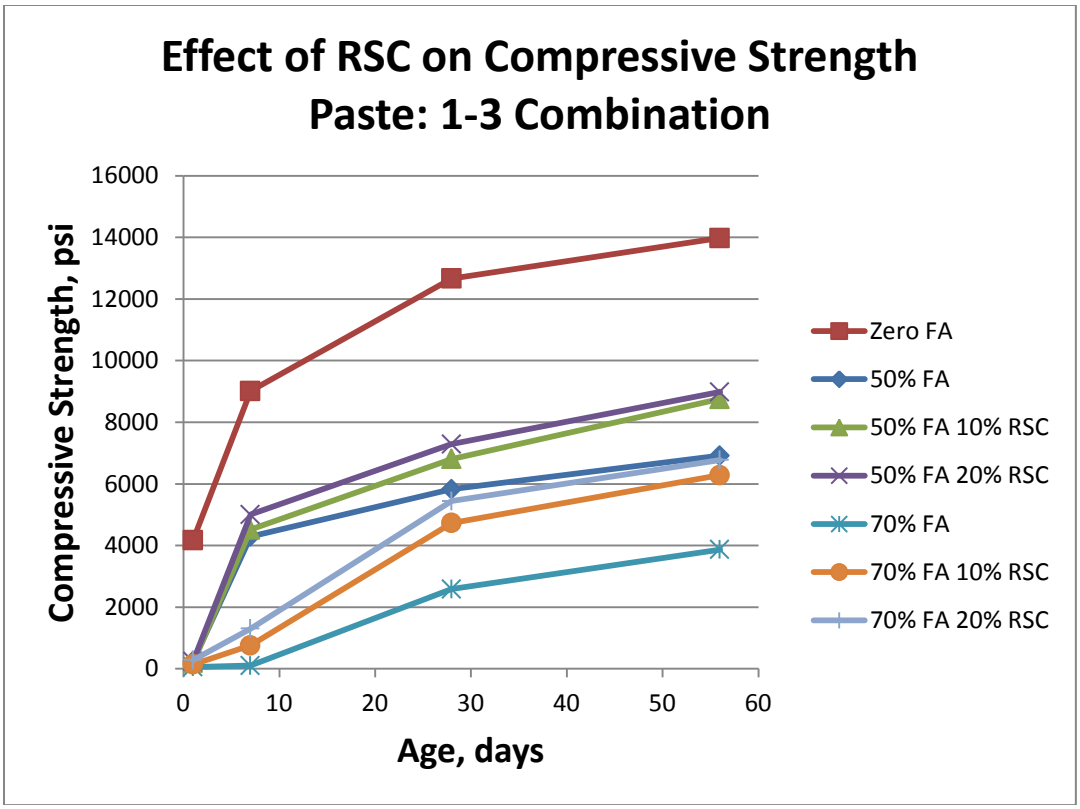

Figure 4.68 – Effect of RSC on Compressive Strength, 1-3 Combination

4.5.2.7. Effect of Gypsum-Lime. At the 4% gypsum level, two levels of lime were explored: 5 and 10%. **Figures 4.69** and **4.70** show the results of the effect of 50 and 70% fly ash contents, respectively, on one day strengths. The results are mixed: for the 50% fly ash 4-1 blend, gypsum-lime reduced strengths at both the 5 and 10% levels of lime. However, for the 50% fly ash mixtures 1-3 blend and both combinations at 70% fly ash, the gypsum-lime increased strengths. Dosage made little difference.

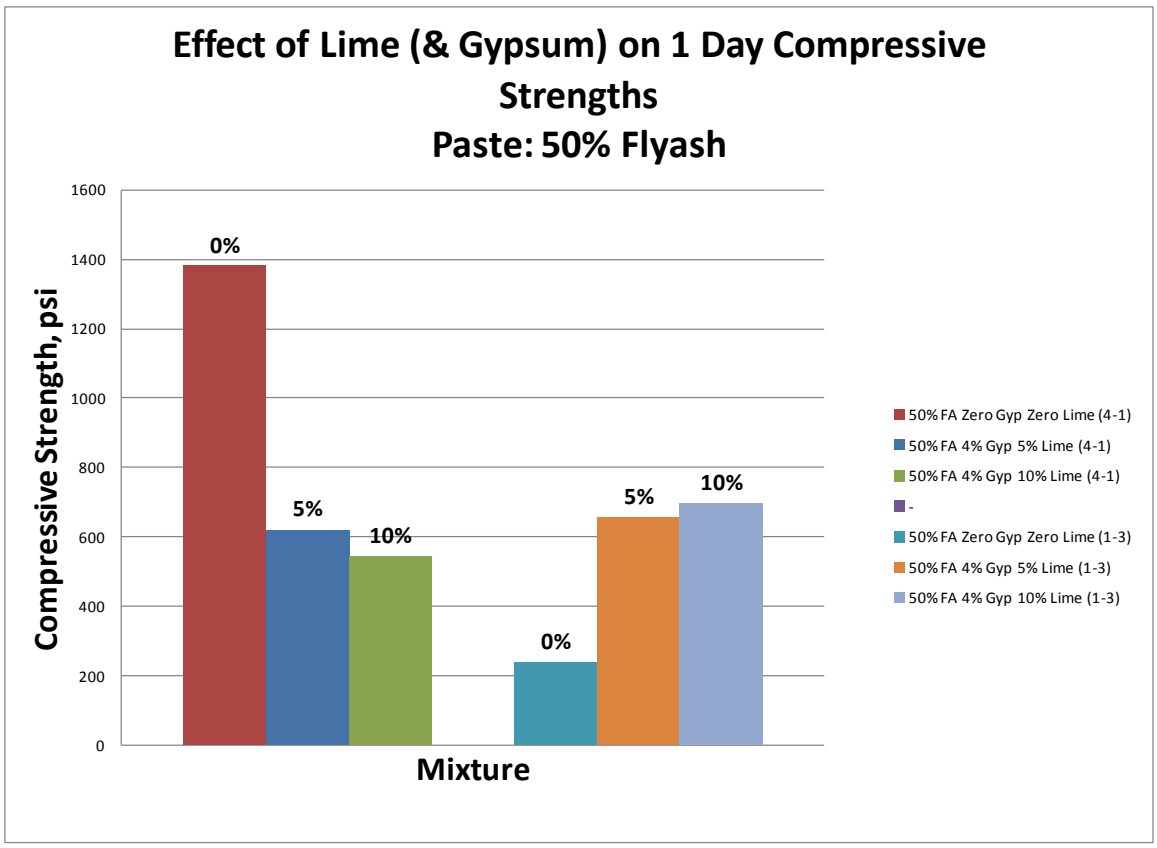

Figure 4.69 – Effect of Gypsum-Lime on One Day Compressive Strength for 50% Fly Ash Mixtures

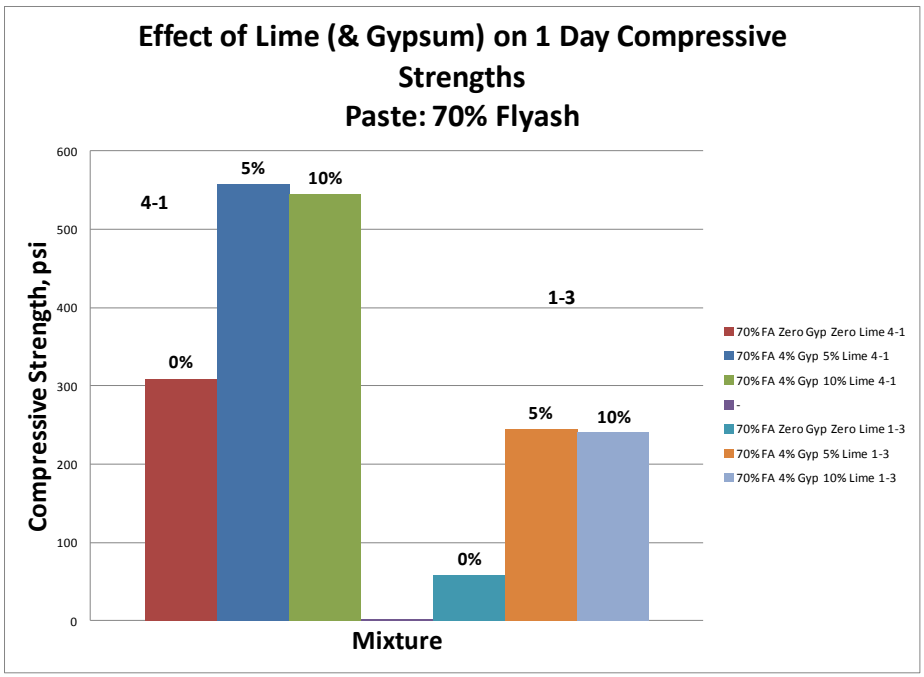

Figure 4.70 – Effect of Gypsum-Lime on One Day Compressive Strength for 70% Fly Ash Mixtures

At 56 days, **Figures 4.71** and **4.72** indicate that gypsum-lime reduced strengths. Again, dosage made little difference.

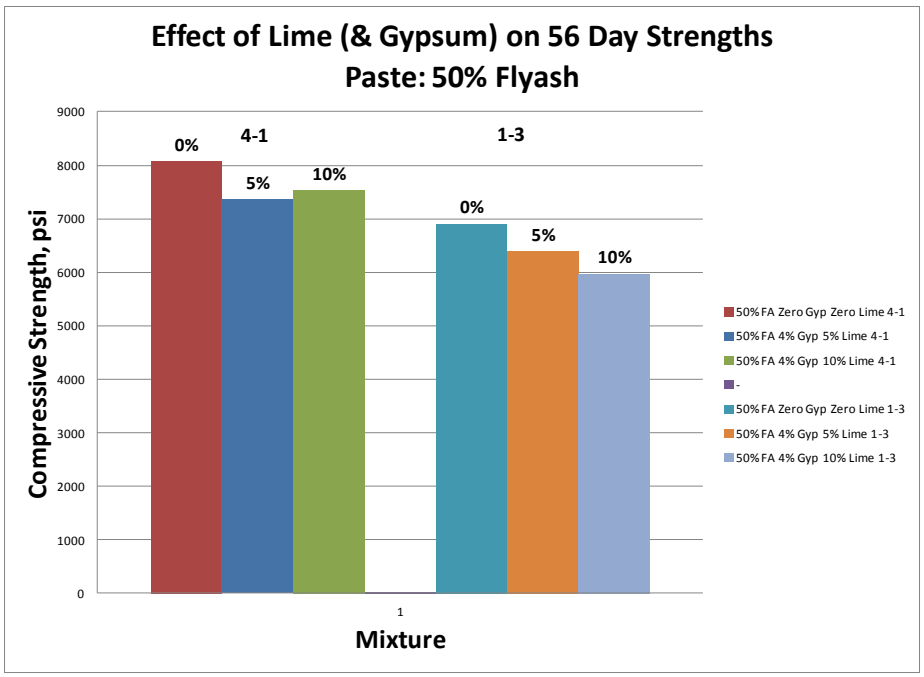

Figure 4.71 – Effect of Gypsum-Lime on 56 Day Compressive Strength for 50% Fly Ash Mixtures

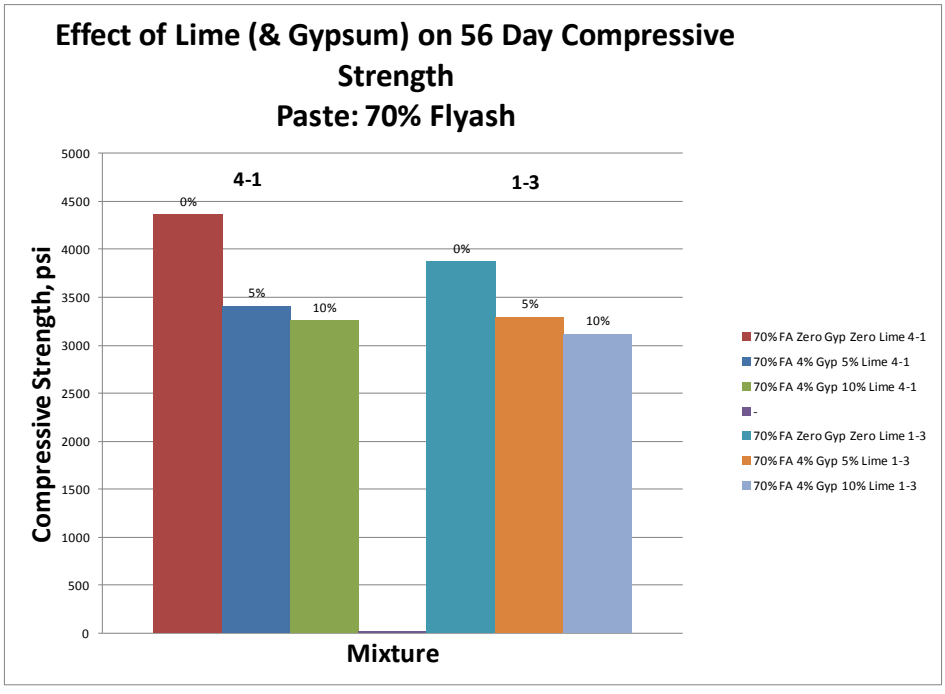

Figure 4.72 – Effect of Gypsum-Lime on 56 Day Compressive Strength for 70% Fly Ash Mixtures

The effect of 4% gypsum-lime (5 and 10%) on calorimetry (50%NetTMax time) results is shown in **Figures 4.73** and **4.74** for 50% and 70% fly ash, respectively.

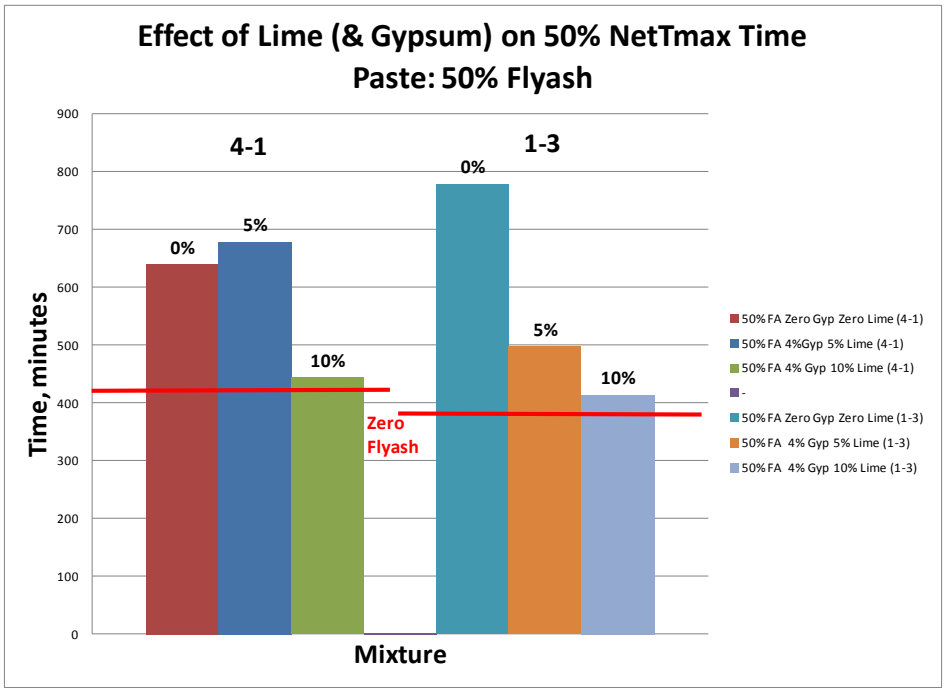

Figure 4.73 – Effect of Gypsum-Lime on 50%NetTMax Time for 50% Fly Ash Mixtures

In general, it appears that the curves are accelerated (50%NetTMax time decreases) quite significantly for the combination 4-1 at both the 50% and 70% fly ash contents, and for the 1-3 mixture at 50% fly ash. The optimum lime content is 10%.

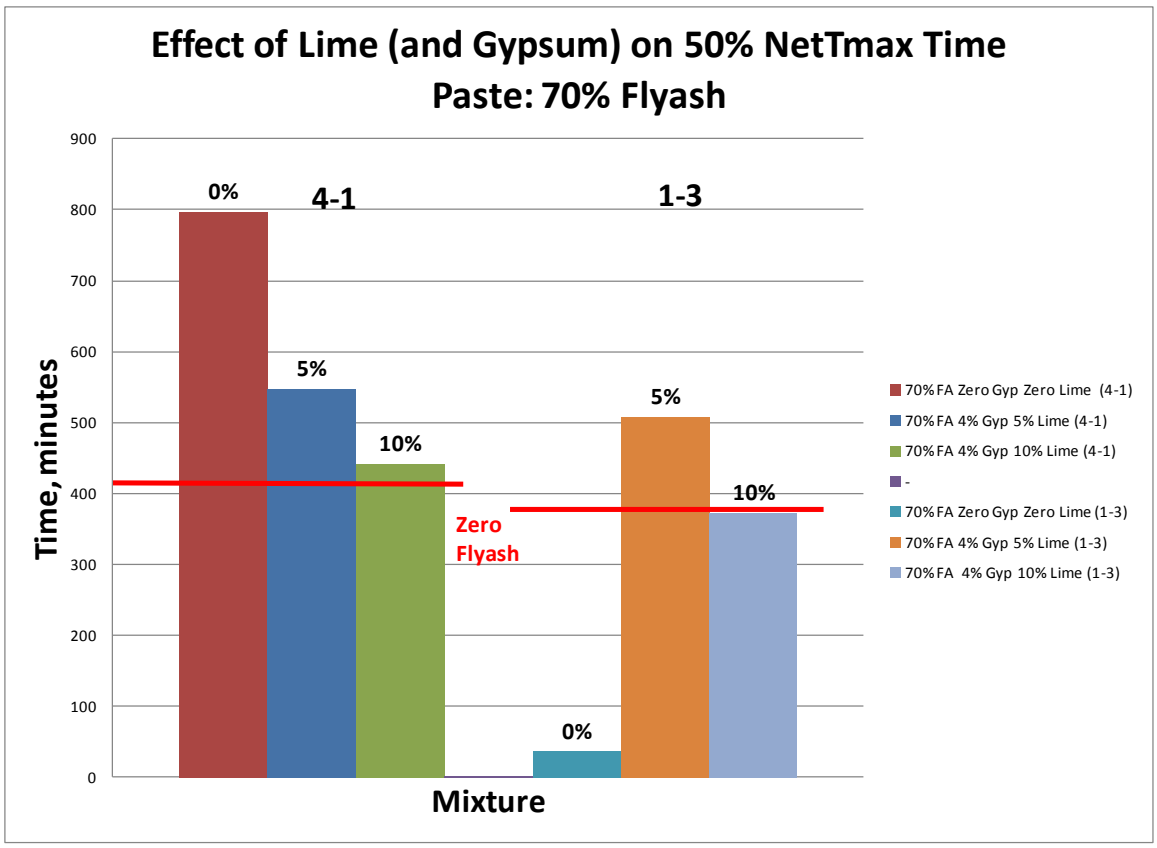

Figure 4.74 – Effect of Gypsum-Lime on 50%NetTMax Time for 70% Fly Ash Mixtures

A typical calorimeter set of curves showing all three levels of lime (zero, 5, and 10%) is depicted in **Figure 4.75**. It can be seen that the curves are shifted to the left with increasing amounts of lime, indicating an acceleration of the reactions.

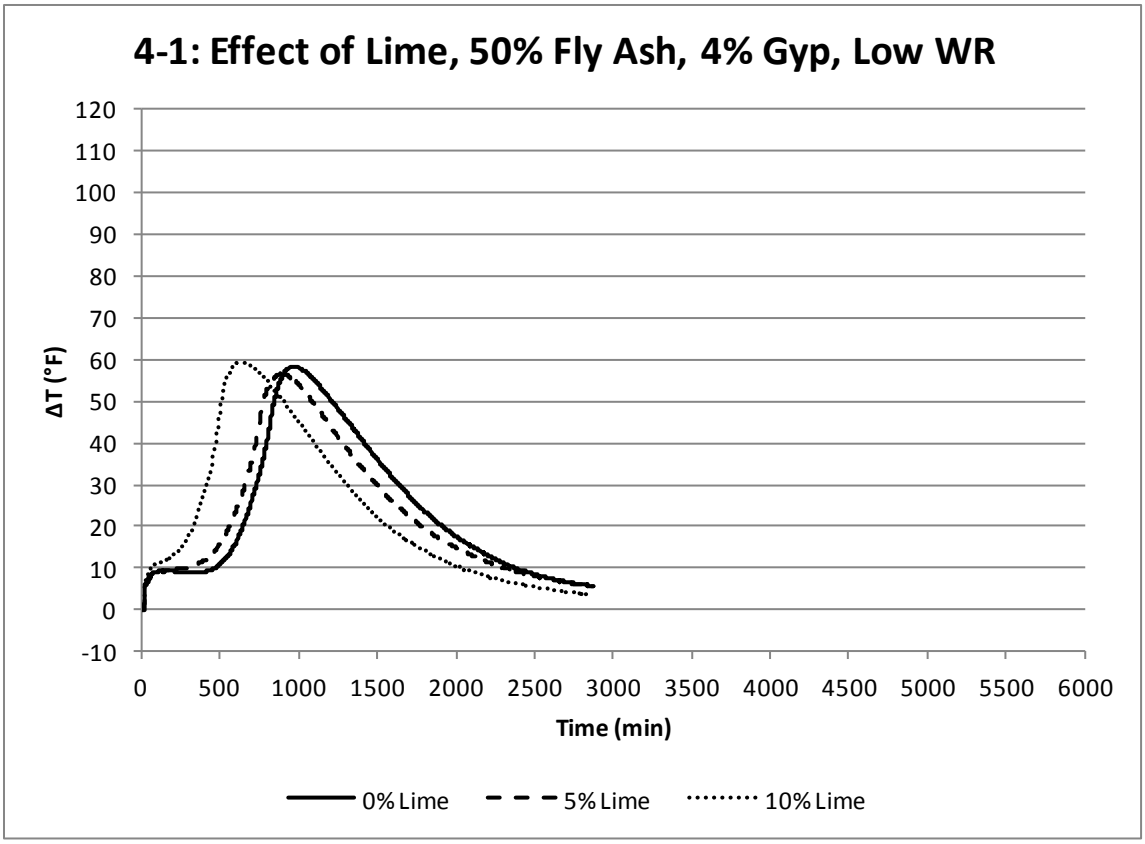

Figure 4.75– Typical Effect of Gypsum-Lime Content on Calorimeter Curve Characteristics

Referring back to **Figure 4.74**, for the 70% fly ash 1-3 blend, which is greatly accelerated without powder additives, the addition of gypsum-lime appears to retard the 50%NetTMax time to at or greater than the zero fly ash time. However, upon inspection of the calorimeter curves **(Figure 4.76**), the curves with the powder additives appear to shift to the left, as in all the other calorimeter curves with this treatment. This apparent non-agreement between the bar chart and the calorimeter curves points out the possibility of pulling off a single value (e.g. 50% NetTMax time) from oddly-shaped curves, where the data point may happen to be on the secondary curve.

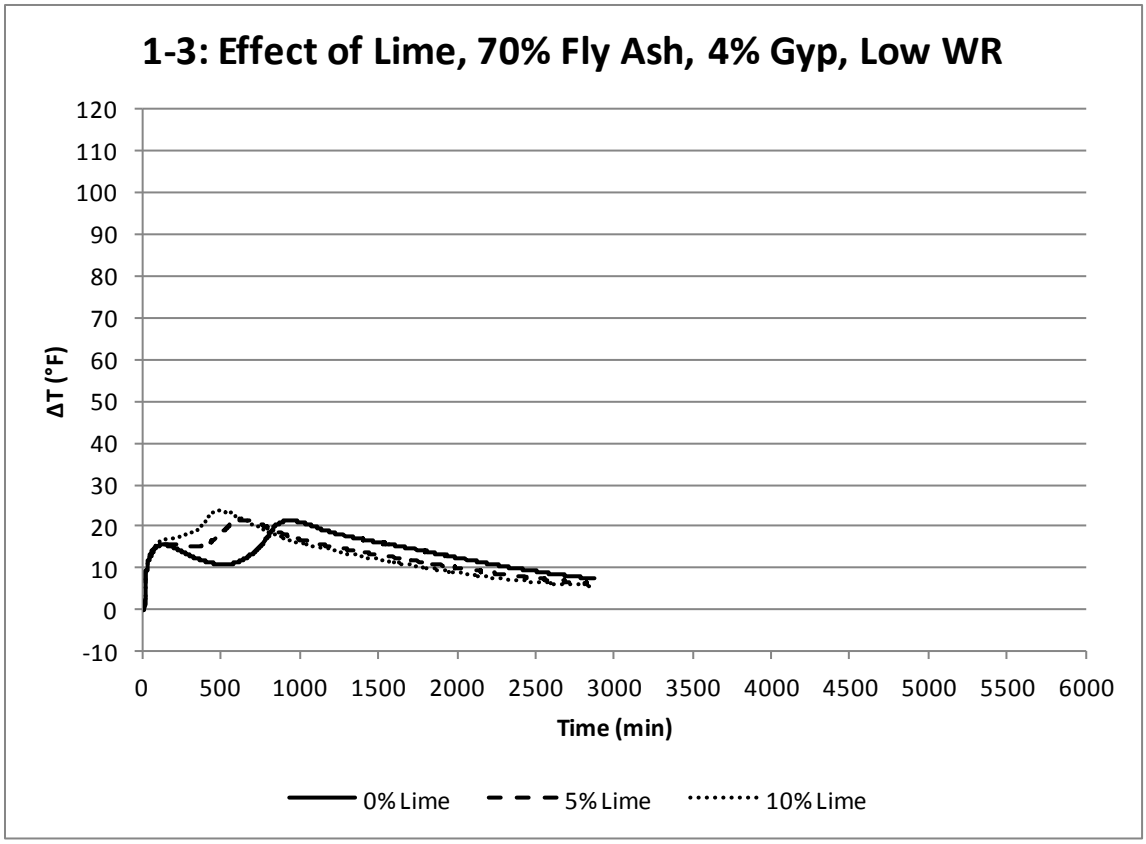

Figure 4.76– Gypsum-Lime Content Calorimeter Curve Showing Dilemma of Picking the 50%NetTMax Point

The effect of gypsum-lime on initial setting time is shown in Figures 4.77 and **4.78** for the 50 and 70% fly ash content mixtures, respectively. In the case of the 4-1 blend at 50% and 70 % fly ash, the gypsum-lime retarded the set, with no consistency between lime contents. However, for the 3-1 blends, the results were mixed, with retardation, acceleration, and no change. However, magnitudes were small.

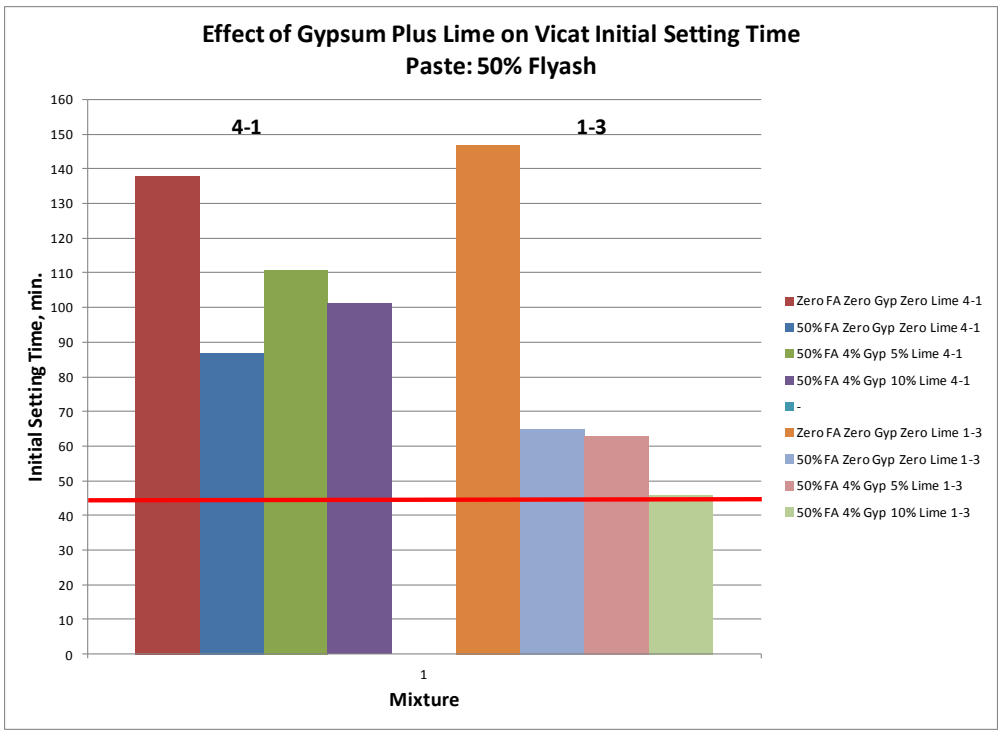

Figure 4.77 – Effect of Gypsum-Lime on Initial Setting Time, 50% Fly Ash

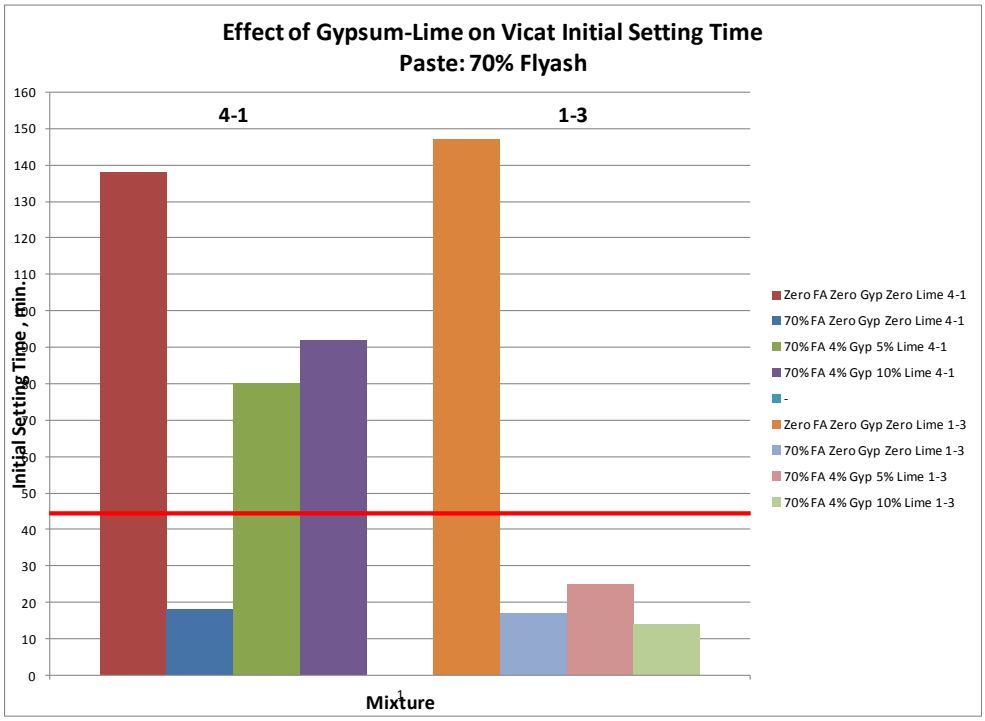

Figure 4.78 – Effect of Gypsum-Lime on Initial Setting Time, 70% Fly Ash

The effect of gypsum-lime on early stiffening is shown in **Figure 4.79**. In almost all cases, addition of the powder additives improved (increased AR 5-30) early stiffening behavior.

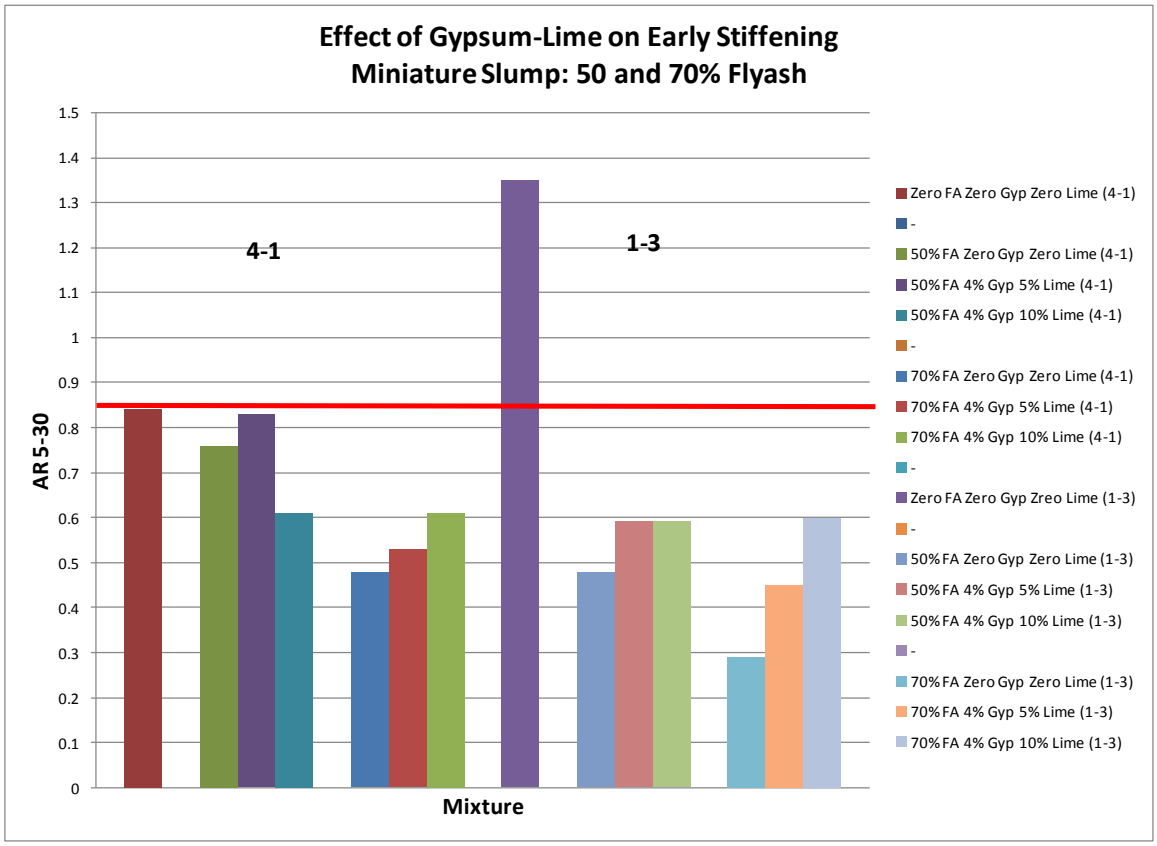

Figure 4.79 – Effect of Gypsum-Lime on Early Stiffening, 50 and 70% Fly Ash Contents

4.5.2.8. Effect of Gypsum-RSC. The effect of gypsum-RSC addition at 10 and 20% levels on one day compressive strength is shown in **Figure 4.80** and **4.81**. For the 1-3 blend, powder additives increased early strength both at 50 and 70% fly ash, with mixed results in terms of which dosage (10 or 20% RSC) is better. For the 4-1 blend, at 70% fly ash, both levels of powder additives improved strength, with 20% RSC being superior. However, the additives lowered strength at 50% fly ash.

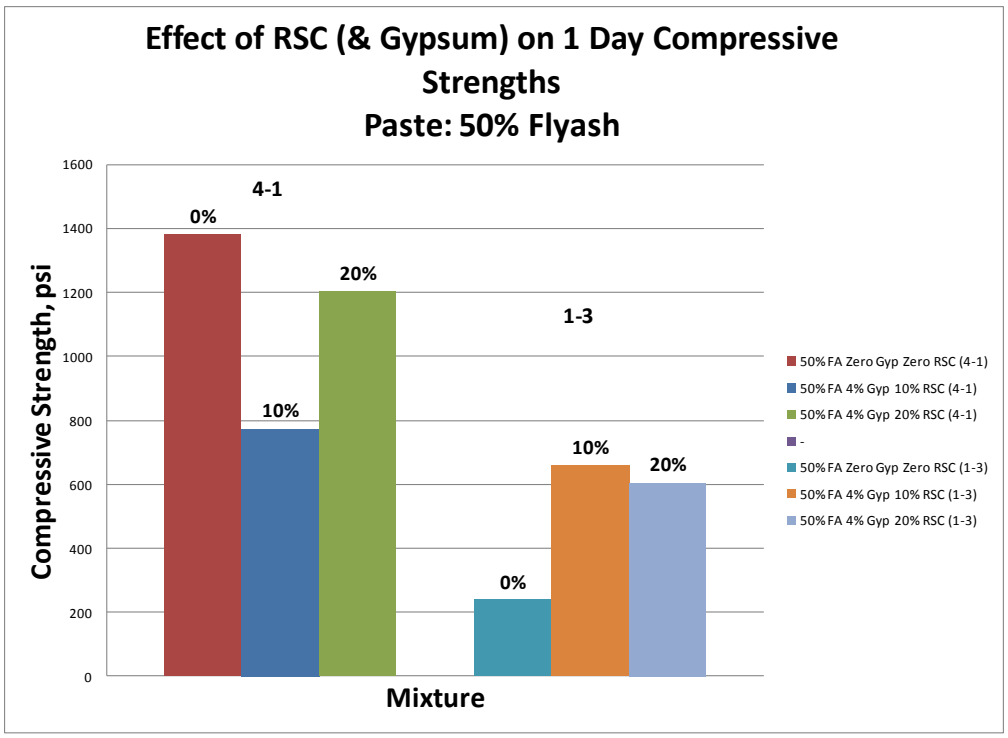

Figure 4.80 – Effect of Gypsum-RSC on One Day Compressive Strength, 50% Fly Ash

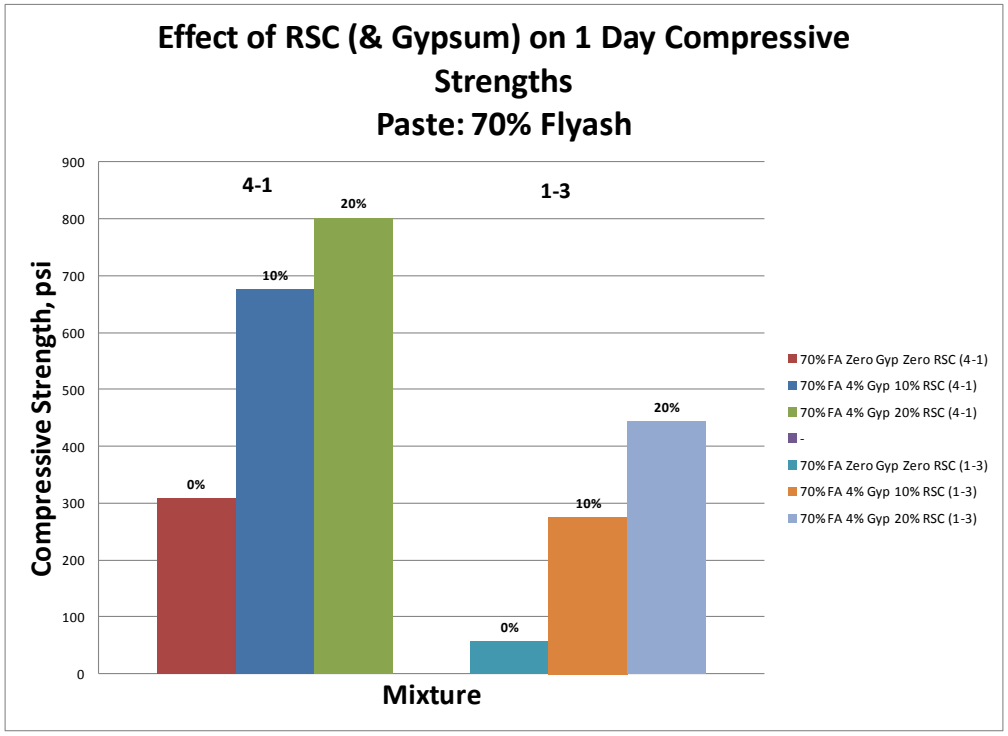

Figure 4.81 – Effect of Gypsum-RSC on One Day Compressive Strength, 70% Fly Ash

In regard to 56 day strengths, **Figures 4.82** and **4.83** depict the effects of the gypsum-RSC on both 50 and 70% mixtures. In every case, gypsum-RSC increased strength, with 20% being superior to 10%. In one case the improvement was only marginal, and in the others it was inconsistent as to which RSC level was more efficient.

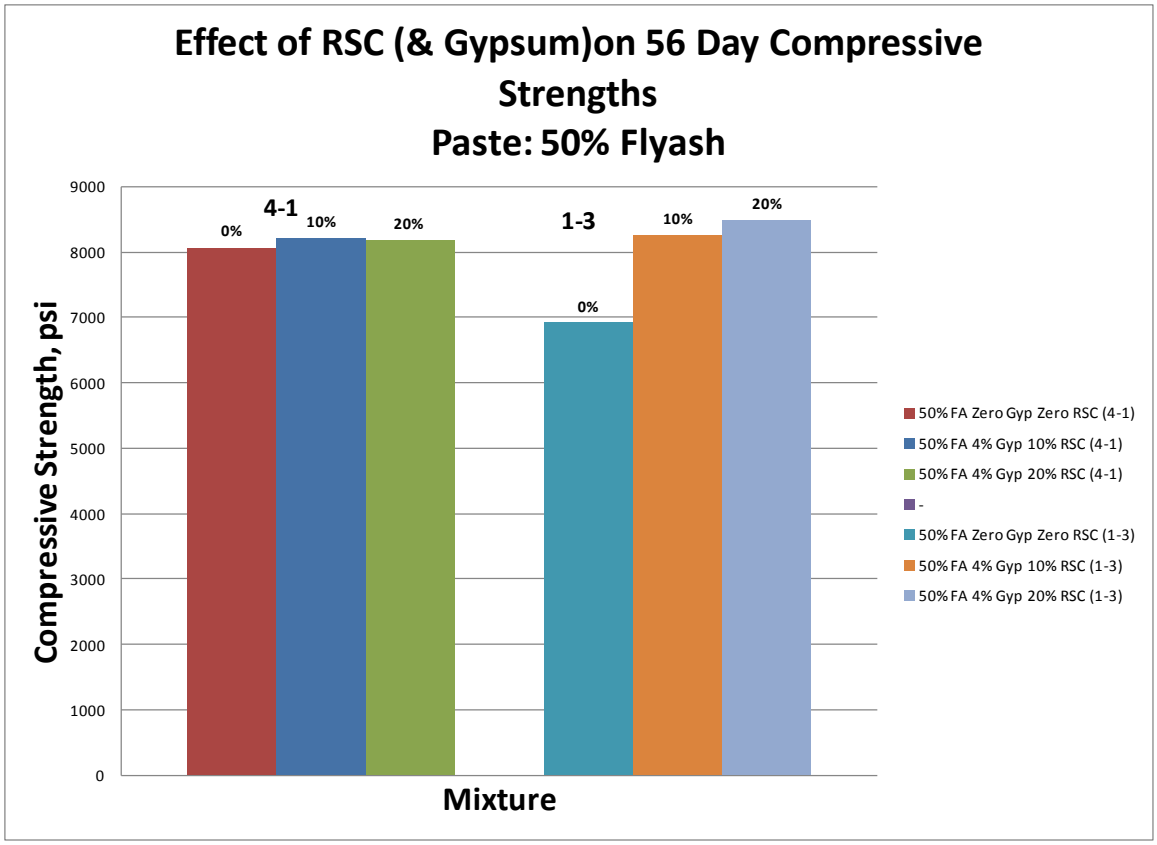

Figure 4.82 – Effect of Gypsum-RSC on 56 Day Compressive Strength, 50% Fly Ash

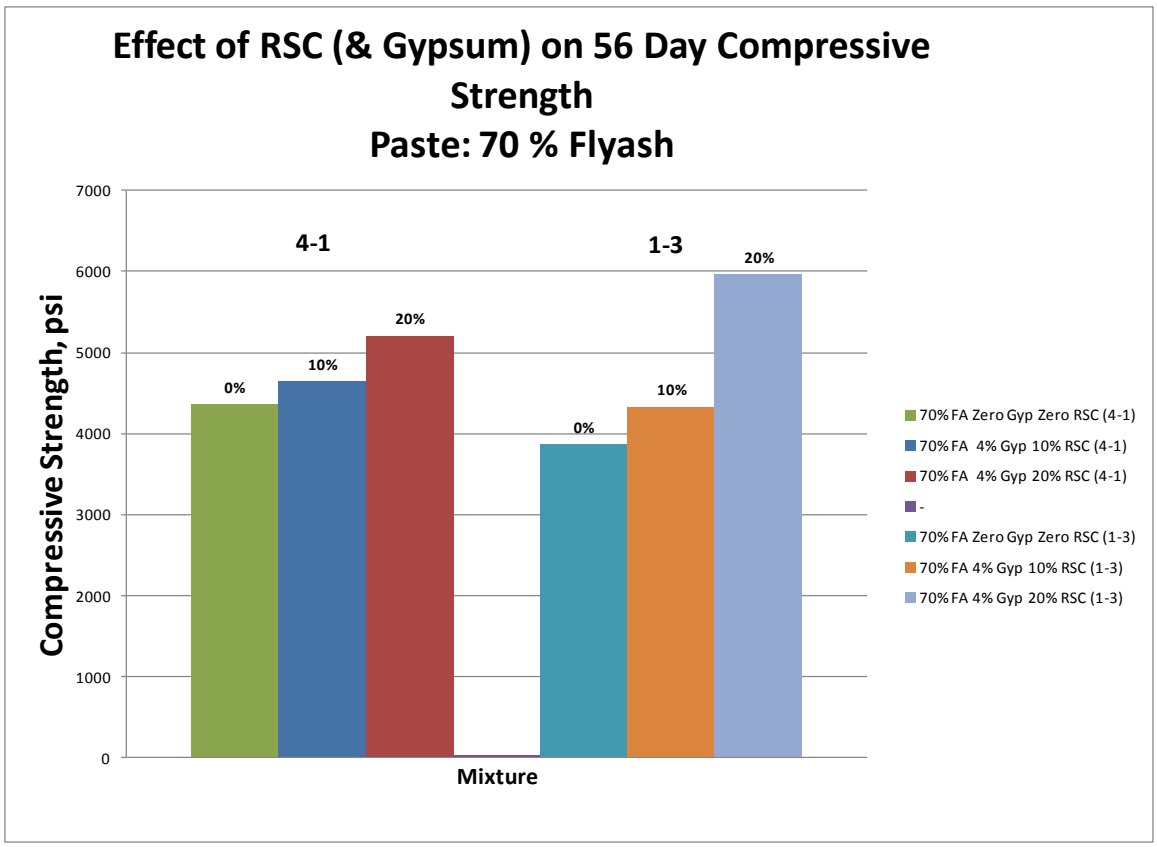

Figure 4.83 – Effect of Gypsum-RSC on 56 Day Compressive Strength, 70% Fly Ash

The effect of gypsum-RSC on calorimeter results (50%NetTMax time) is shown in **Figures 4.84** and **4.85**. For the 4-1 blend at 50 and 70% fly ash and the 1-3 blend at 50% fly ash, addition of gypsum-RSC reduced 50%NetTMax times. The 10% level times approached the zero fly ash times, but the 20% level accelerated the reaction excessively. This can be seen in **Figure 4.86**. For the 1-3 blend 70% fly ash mixture, even without the gypsum-RSC, the mixture reacted too quickly, and the powder admixtures did not change that.

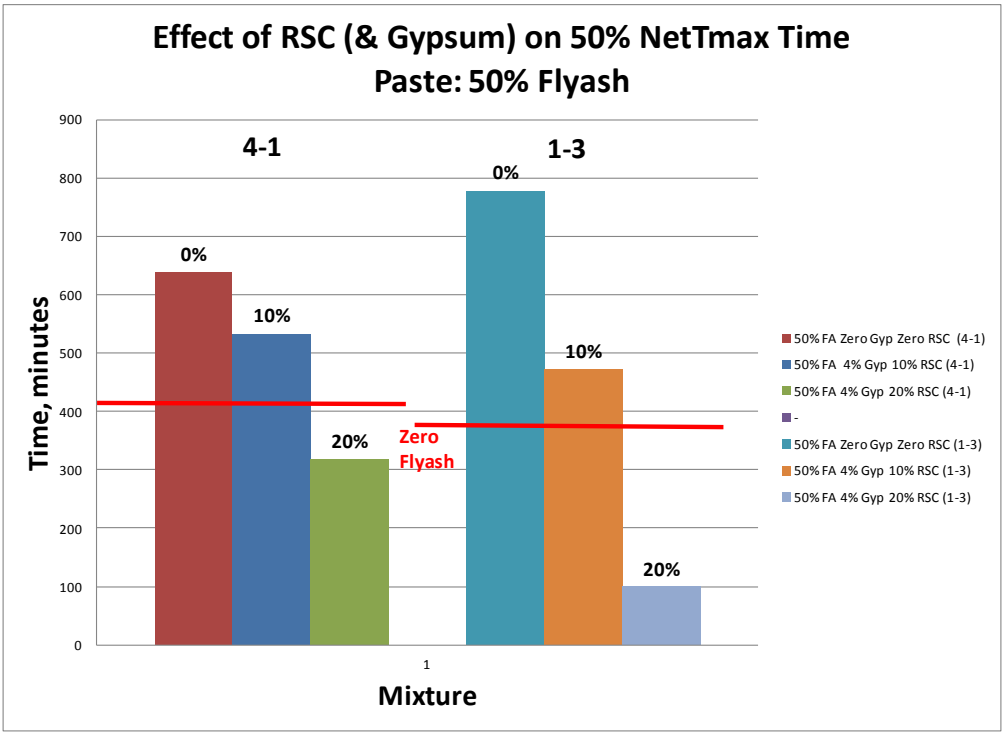

Figure 4.84 – Effect of Gypsum-RSC on 50%NetTMax Time for 50% Fly Ash Mixtures

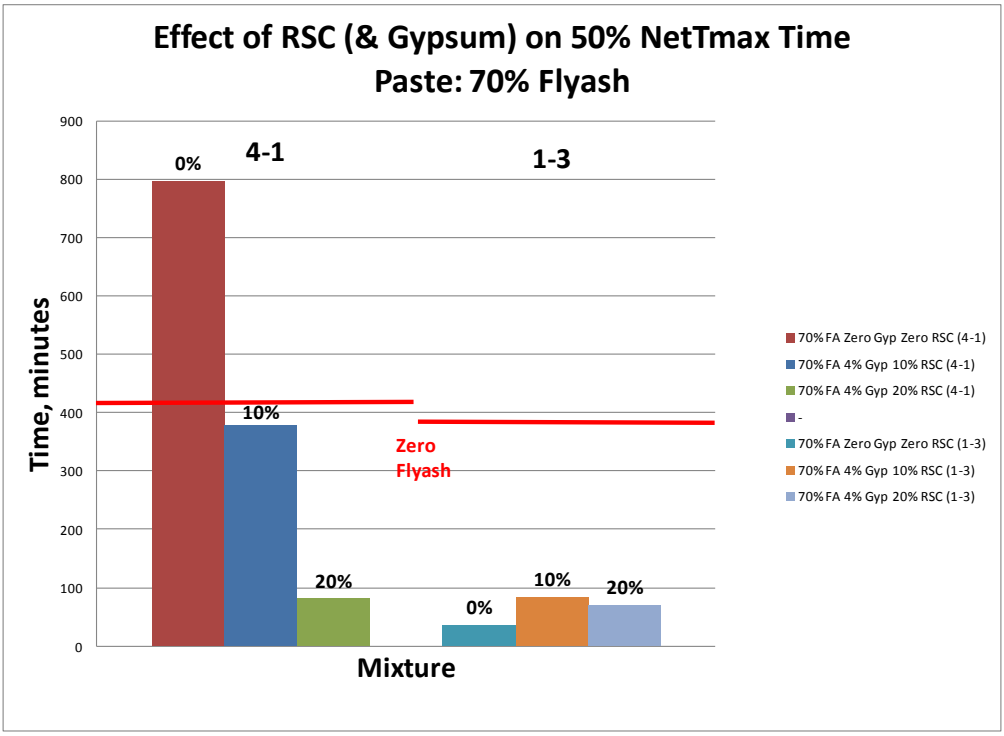

Figure 4.85 – Effect of Gypsum-RSC on 50%NetTMax Time for 70% Fly Ash Mixtures

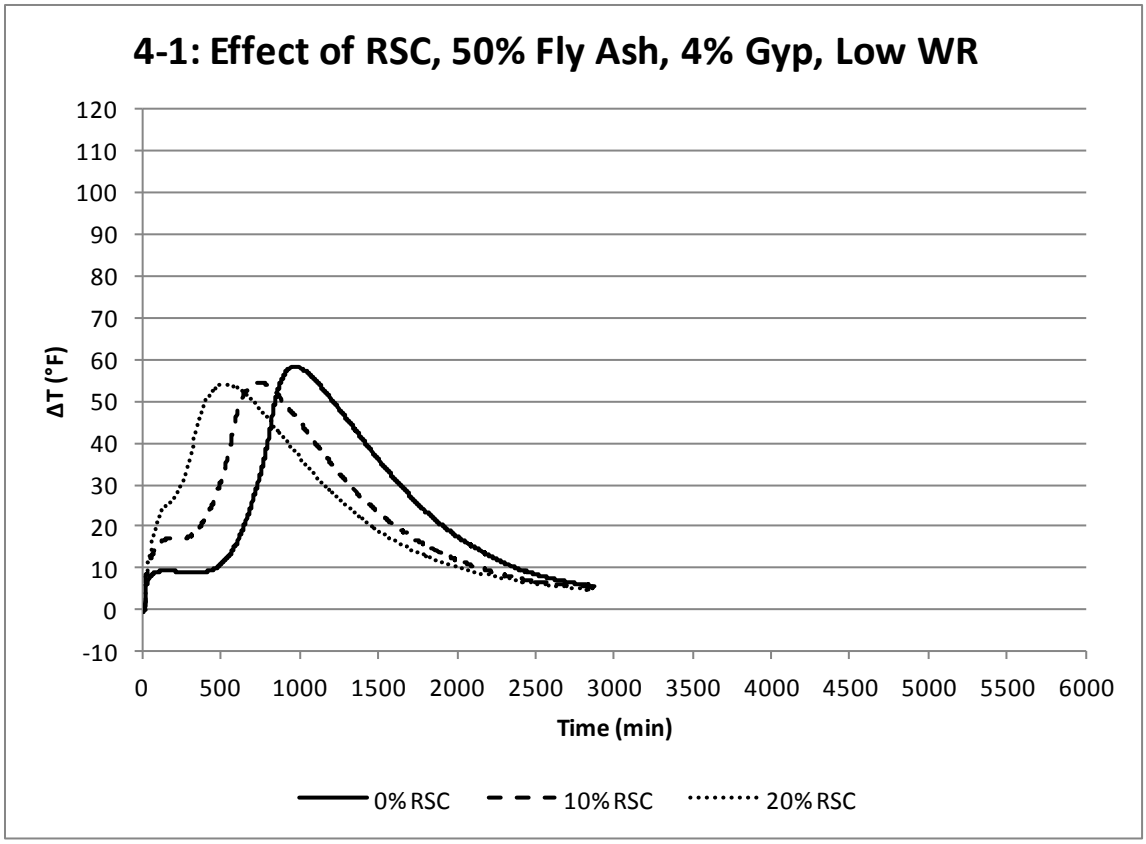

Figure 4.86– Typical Effect of Gypsum-RSC Content on Calorimeter Curve Characteristics

The effect of gypsum-RSC on initial setting time is seen in **Figure 4.87** and **4.88** for 50 and 70% fly ash contents, respectively. In 3 of the 4 cases, the mixtures were accelerated. The 1-3 blend 70% fly ash mixture was retarded somewhat.

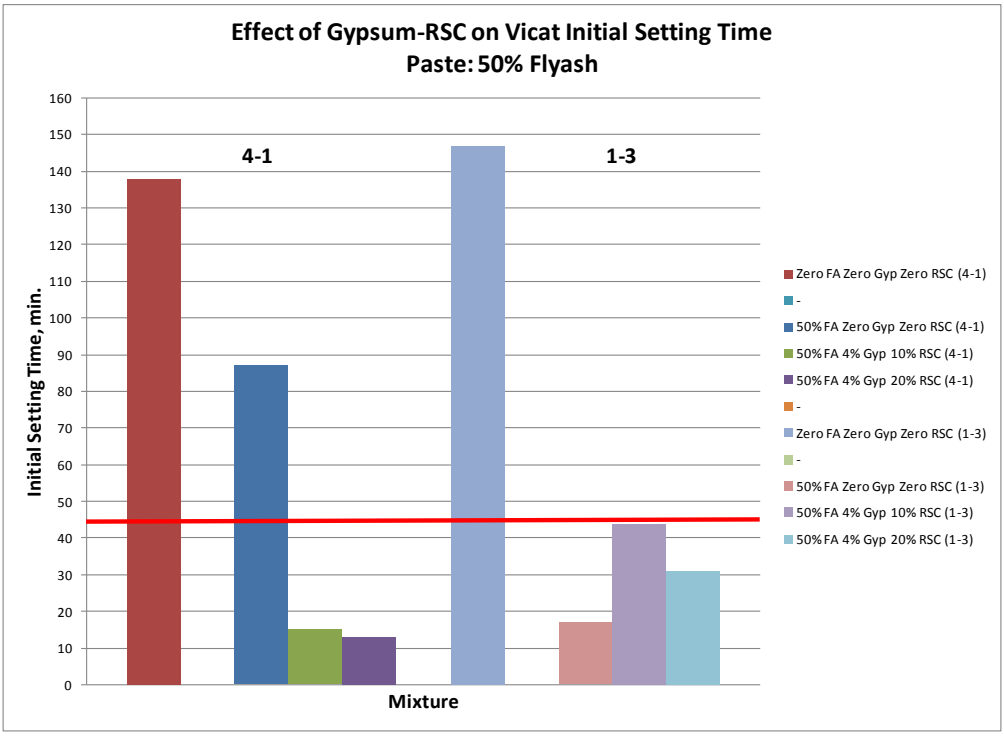

Figure 4.87 – Effect of Gypsum-RSC on Initial Setting Time, 50% Fly Ash Content

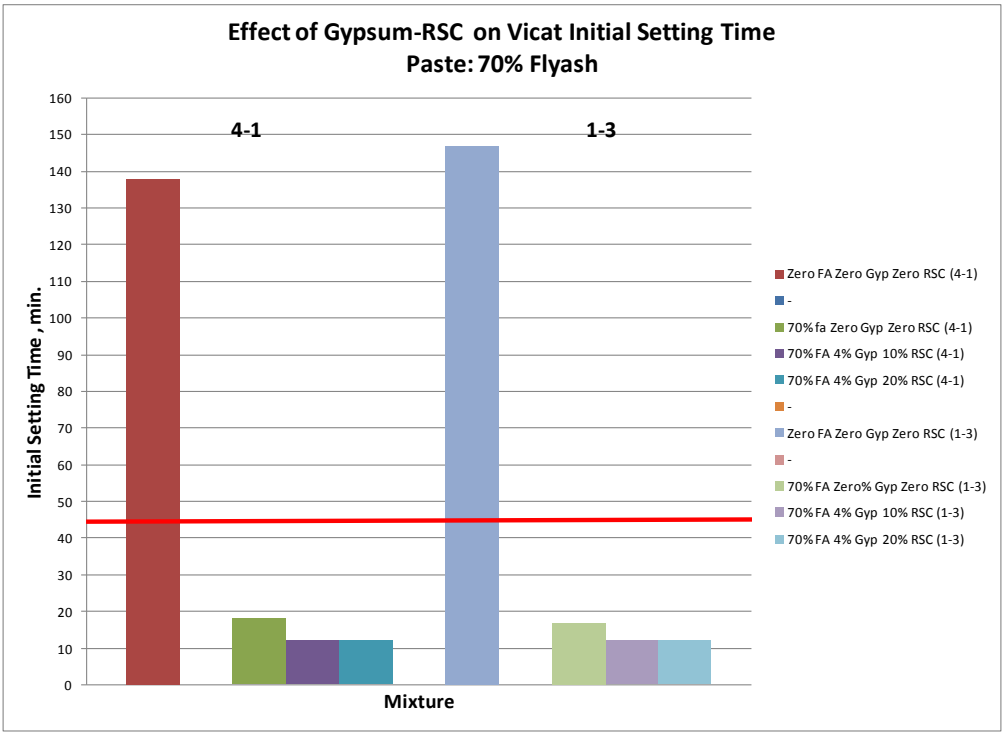

Figure 4.88 – Effect of Gypsum-RSC on Initial Setting Time, 70% Fly Ash Content

The effect of gypsum-RSC on early stiffening can be seen in **Figure 4.89**. Generally, as RSC level increased from 10 to 20%, early stiffening potential increased.

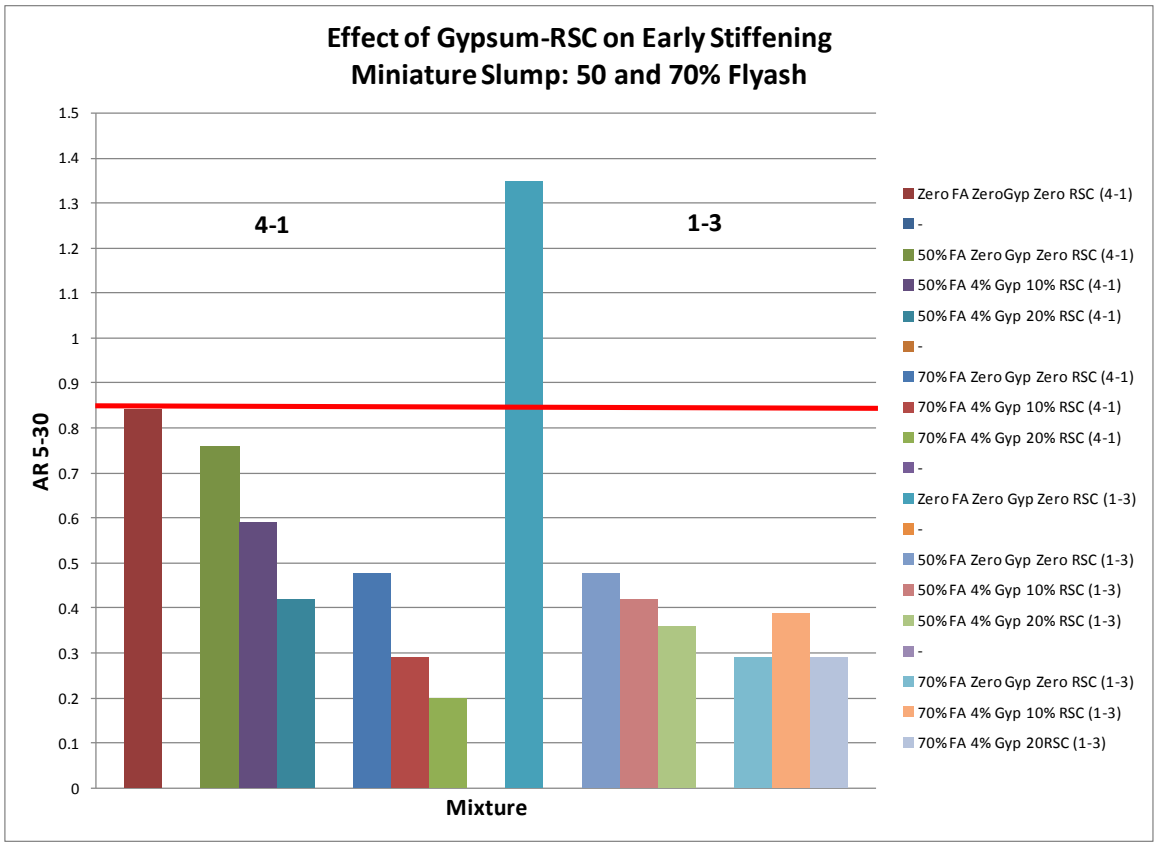

Figure 4.89 – Effect of Gypsum-RSC on Early Stiffening, 50 and 70% Fly Ash Contents

All Main Effects test results are tabulated in Appendix G.

4.5.2.9. Maximum Sulfur Trioxide Limit. The maximum sulfur trioxide (SO_3) limit for OPC and Class C fly ash is 3.0% and 5.0%, respectively for both current ASTM and the AASHTO specifications. In the mixtures in the Main Effects study, sources of SO_3 were OPC, fly ash, gypsum, and RSC. The combined SO_3 contents for the various mixtures (not including straight OPC base mixtures) ranged between 3.0 and 5.0 with one exception: the 1-3 blend at 70% fly ash, 4% gypsum, and 20% RSC. At a typical

maximum specification limit of 25% fly ash with OPC and fly ash at their maximum allowable SO_3 limits, the highest calculated combined SO_3 would be 3.5%. Thus, it is recommended that if a calculation of a given blend of materials shows a high combined SO_3 content, physical testing be conducted to assure that excessive expansion will not occur, especially if the concrete is going to be in a high sulfate service environment.

4.6. PASTE STUDY CONCLUSIONS

4.6.1. Background. In the Screening Study, 25 combinations of five Type I/II portland cements and five Class C fly ashes in paste form with no chemical or powder additives were tested by semi-adiabatic calorimetry, Vicat setting time, miniature slump, and compressive strength at one and 28 days. The two most reactive and least reactive combinations (defined by one day strengths) were further evaluated in the Main Effects Study.

In the Main Effects Study, the effects of two levels each of WR/HRWR, gypsum, lime, RSC, and gypsum-lime, and gypsum-RSC were determined. Except for the WR/HRWR experiment, all other mixtures contained the low (2.75 fl oz/cwt) dosage. Except for the gypsum level experiment, all other mixtures contained 4% gypsum by mass of fly ash. The lime levels were 5 and 10% and the RSC levels were 10 and 20%, both by mass of fly ash. Based on both the Screening Study and Main Effects Study, the following conclusions were drawn.

4.6.2. Fly Ash Replacement. In terms of the constituents (oxide content, etc) of the blends, as fly ash increased, CaO was reduced and aluminates, alkalis, and the aluminate/sulfate ratio increased. The total amount of the important oxides was a function

of the amounts present in the OPC, the individual fly ash, and the fly ash content of the blend.

In terms of when reactions occurred relative to straight OPC as characterized by calorimeter curve position, whether the curve was retarded or accelerated and the magnitude of reaction rate and peak height depended on the total chemistry of the blend. At high levels of CaO and low levels of aluminate, alkali, and aluminate/sulfate, as fly ash increased, the curves were increasingly delayed and the peaks were shorter. As the CaO dropped and the aluminate, alkali, and aluminate/sulfate increased to more moderate levels, the curves became shorter and broader, sometimes exhibiting two peaks. When the CaO was low and the aluminate, alkali, and aluminate/sulfate were high, the curves reversed and occurred earlier than straight OPC curves. The position of the curve was reflected in setting times, early strength achieved, and tendency for early stiffening. Thus, it is difficult to make general statements about what to expect with certain levels of fly ash in terms of physical properties without information on oxide contents, fineness, and glass content.

Fly ash reduced one day strengths at all levels of replacement. Fly ash usually reduced 56 day strengths at all levels of replacement, with one exception at 25%.

Fly ash effects on initial setting time were mixed. At 25%, retardation usually occurred. At 50%, both retardation and acceleration occurred. At 70%, many times acceleration occurred.

4.6.3. WR/HRWR. At the 0.40 *w/cm*, the use of WR/HRWR was necessary to restore workability. The effect of WR/HRWR generally was to slow down reactions and their outcomes. Calorimeter curves were usually delayed and one day strengths were

lower. However, the effect on setting times and early stiffening were mixed. Many times the setting time was accelerated, but sometimes retarded. Likewise, early stiffening was usually an issue, and but sometimes not. Beyond one day, strengths were usually increased. Overall, there was no clear advantage between the two dosage levels.

4.6.4. Gypsum. Gypsum addition generally usually delayed the calorimeter curves or was negligible. The higher dosage made a more pronounced effect. Setting time usually was retarded. Because in all four cases the setting time had been accelerated by the high fly ash substitution, retarding by gypsum was a positive benefit. Early stiffening tendencies were either improved or were negligibly affected. One day strengths were down, or negligibly affected, and 56 day strengths were not much affected. Overall, there was no clear advantage to either the 2 or 4% gypsum levels.

4.6.5. Lime. One day strengths were negligibly impacted, some severely low 7 day strengths were improved, and late strengths were negligibly impacted. The 5 % level of lime had a slight edge over the 10% level.

4.6.6. Rapid Set Cement. At all ages and fly ash contents at seven days and later, the addition of RSC significantly increased compressive strengths. At one day, strengths were increased, but marginally so. The 20% level usually was superior to the 10% level.

4.6.7. Gypsum-Lime. In three of the four cases, the gypsum-lime addition improved one day strengths, with little difference between the 5 and 10% levels. However, all 56 day strengths were lowered, with 10% level usually the worst by a small amount. The calorimeter curves were shifted to earlier times, with the 10% level earlier than the 5% level. The 10% lime mixture positions were almost restored back to where

the zero fly ash curves were. Initial setting times had been accelerated by the replacement of fly ash. Upon addition of gypsum-lime, the 4-1 blend was retarded at both levels of fly ash, approaching the zero fly ash values (an improvement), but there was little effect on the 1-3 blend setting times. The tendency to early stiffen was alleviated somewhat by gypsum-lime in every blend but one, with the 10% level usually better.

4.6.8. Gypsum-Rapid Set Cement. In all cases of gypsum-RSC addition, the calorimeter curves were accelerated. In three of the four cases, the gypsum-lime addition improved one day strengths, with a moderate advantage with the 20% RSC level. In all cases, the 56 day strengths were improved, some quite significantly. In regard to initial setting time, all four blends had been accelerated by the fly ash replacement, three of the four severely so. Unfortunately, addition of gypsum-RSC made it worse in one blend, was negligible in two others, and helped (retarded) somewhat in the fourth blend. Also, in almost all mixtures, the early stiffening tendencies were significantly worsened. It should be noted that the combined SO3 content in some of these mixtures is somewhat high.

4.6.9. Summary. To improve early strengths, lime, RSC, or gypsum by themselves were not particularly helpful. However, gypsum and lime together were effective, but lowered later strengths. Gypsum-RSC improved strengths at all ages. Gypsum by itself helped restore (retarded) the fly ash-accelerated HVFA calorimeter curve positions, as did gypsum-RSC. Gypsum-lime restored the curves almost to the zero fly ash positions. Early stiffening tendencies were alleviated by gypsum and gypsum-lime, but made worse by gypsum-RSC.

The dosages chosen for the concrete study were 4% (vs. 2%) gypsum because it controlled the fly ash-accelerated reactions best, 10% (vs. 5%) lime because in

combination with the 4% gypsum, it controlled the accelerated reactions best, and 20% (vs. 10%) RSC because it improved one day strengths best.

High calculated combined SO3 level mixtures should be checked via expansion testing for possible issues, especially if the concrete is going to be in a high sulfate service environment.

5. PHASE II – CONCRETE STUDY

5.1. EXPERIMENTAL DESIGN

5.1.1. Variables. The objective of the concrete properties study was to scale up the most promising powder additive combinations from paste to concrete and evaluate the mixtures in terms of plastic and hardened properties. Thus the mixture matrix included OPC-fly ash blends at two levels ("4-1" and "1-3) and fly ash at three levels (zero, 50 and 70%). WR dosage (nominal 2.75 fl oz/cwt), gypsum content (4%), lime content (10%), and RSC content (20%) were held constant.

5.1.2. Test Methods. Plastic concrete properties of interest were slump, air content, unit weight, concrete setting time, and water content (and *w/cm*). Hardened concrete properties were compressive strength, flexural strength (modulus of rupture = MOR), splitting tensile strength, modulus of elasticity (MOE), shrinkage, abrasion resistance, freeze-thaw resistance, permeability (rapid chloride penetration = RCP), and salt scaling resistance.

5.1.3. Mixture Designs. Because of concerns about possible salt scaling issues for pavements (PCCP), bridge decks (B-2 and MB-2), and barrier walls (B-1), it was decided to target the MoDOT structural mixture design (B). However, the mixture was designed to also meet the more stringent PCCP specification as a point of interest. After consulting MoDOT mixture design personnel for typical mixture designs that are approved by MoDOT, the design parameters were chosen.

Cement content and *w/cm* were chosen to not only meet specifications for mixtures B and PCCP, but to also be in line with typical approved mixtures. Choice of fly ash contents were carried forward from the paste study (50 and 70%).

In regard to slump, being locked into a certain water content by the fixed *w/cm* and fixed cementitious content rendered a stiff mixture (~1 in.) which would be practical for a slip-formed pavement mixture but not a structural mixture. The upper limit on fly ash was 70%; at this level, previous experience with the project materials indicated that the slump would be about 5 in. So, the mixture was locked in at 5 in. slump. To achieve a slump of 5 in. for the less-than-70% fly ash mixtures (zero and 50%), necessitated the use of admixtures: a combination of the required air entraining agent plus a WR.

It was anticipated that with a *w/cm* of 0.40, a WR, and a high quality coarse aggregate, would produce at least 4000 psi at 28 days for the base mixture (actual design was for 5170 psi (35.6 MPa)). Air content was the minimum required. Sand content was chosen at 40% which was typical for both mixture types. Choice of a coarse aggregate gradation was a D which would meet the 501 specification for the B concrete mixture, is used commonly for PCCP mixtures, and is readily available. A comparison of MoDOT 501 and 1005 (MoDOT, 2011) specifications, typical mixtures, and values used in this study are shown in **Table 5.1.**

The five mixture design proportions are given in **Table 5.2**. These were used for both the blends of OPC and fly ash, as the specific gravities of both cements were the same and both fly ashes were (surprisingly) the same.

Table 5.1 - Mixture Design Requirements, Typical Values, and Final Choices

	501 B	Typical B	501 PCCP	Typical PCCP	Choice
OPC, min., lbs/cy	525	535	535	564	564
Fly ash, at 25% max., lbs/cy	131	---	134	---	varied
w/cm, max.	0.51	0.45	0.50	0.40	0.40
Air content, min., %	5.0	6.0	5.0	6.0	5.0
Slump, max., in.	4	---	---	1.5	5
Comp. strength, min., psi	3000	---	4000	>4000	----
Sand, %	---	40	---	40	40
CA abs., max. , %	3.5	---	3.5	---	1.4
CA gradation	D or E	---	---	---	D
FA DRUW, lbs/cf	109	---	109	---	111.4

Table 5.2 - Proportions of Five Concrete Mixtures

Material	Unit	Base Zero Fly Ash	Lime 50% Fly Ash	Lime 70% Fly Ash	RSC 50% Fly Ash	RSC 70% Fly Ash
OPC	lbs	564	264	154	252	145
Fly ash	lbs	0	264	360	252	338
Gypsum	lbs	0	11	14	10	14
Lime	lbs	0	26	36	0	0
RSC	lbs	0	0	0	50	68
Water	lbs	226	226	226	226	226
CA, ssd	lbs	1877	1877	1877	1877	1877
FA,ssd	lbs	1249	1195	1175	1202	1186
Air (4-1)	fl oz/cwt	4.7	2.1	2.1	1.9	1.9
WR (4-1)	fl oz/cwt	5.3	2.8	1.9	3.6	2.8
Air (1-3)	fl oz/cwt	8.1	6.5	7.3	6.5	7.3
WR (1-3)	fl oz/cwt	5.0	4.0	4.9	5.3	6.2

5.2. REPLICATE SPECIMENS

For all plastic concrete tests only one specimen was tested. For the hardened concrete tests, usually three replicate specimens were tested. Two replicate cylinders were made for the RCP procedure, but each cylinder yielded two slices, thus totaling four replicate test values. There were two replicate shrinkage test specimens cast.

5.3. MATERIALS

5.3.1. General. The cement, fly ash, gypsum, lime, RSC, and WR/HRWR used in the concrete study were the same as were used in the paste study. Additional materials used in the concrete study are tap water, coarse aggregate, fine aggregate, and an air entraining agent. Cementitious material specific gravities are shown in **Table 5.3**.

Table 5.3 Cementitious Materials Specific Gravities

Cement 1	Cement 4	Fly Ash 1	Fly Ash 3	Gyp	Lime	RSC
3.15	3.15	2.686	2.685	2.00	2.34	2.98

5.3.2. Air Entrainment. The air entraining agent used was BASF MB AEA 90.

5.3.3. Aggregate. The coarse aggregate was St. Louis Limestone Formation, Ledges 1-7, Gradation D from Bluff City Minerals at Alton, Illinois. The fine aggregate was Missouri River sand. Aggregate properties are shown in **Table 5.4**.

5.4. TESTING EQUIPMENT AND PROCEDURES

5.4.1. Aggregate.

5.4.1.1. Specific Gravity and Absorption. Specific gravity of the coarse and fine aggregates was determined in accordance with ASTM C 127 and C 128, respectively (ASTM, 2012a; ASTM, 2012b).

5.4.1.2. Gradation. Sieve analyses coarse and fine aggregates was determined in accordance with ASTM C 136 and C117 (ASTM 2006b; ASTM, 2004).

5.4.2. Plastic Concrete.

5.4.2.1. Mixing. In order to assure uniform moisture contents in the aggregate used to mix fresh concrete, an aggregate preparation schedule was developed. First,

roughly 25 lbs (11 kg) of Jefferson City dolomite were tumbled in the concrete mixer for five minutes in order to clean the drum out and loosen any hardened concrete on the fins or in the drum. This aggregate was disposed of after tumbling. The drum mixer was a six cu. ft. (0.17 m^3) capacity, variable speed mixer, pictured below in **Figure 5.1.**

Table 5.4 - Aggregate Characteristics

Test	Unit	CA	FA
Specific grav., ssd		2.66	2.64
Absorption	%	1.4	0.7
DRUW	lbs/cf	97.0	111.4
FM			2.73
NMS	in.	3/4	
Gradation	% passing		
1	in.	100	
¾	in.	92	
½	in.	53	
3/8	in.	26	100
#4		6	98.5
#8		4	92
#16			79
#30		3	50
#50			9
#100		3	1
#200		2.6	0.2

To prepare the aggregate for mixing, the coarse and fine aggregate were both weighed, exceeding the estimated amount needed for a given batch by roughly 50 to 100 lbs. (23 to 46 kg). Coarse aggregate was mixed first, and then fine aggregate. Both aggregates were mixed at a speed of “9” in the concrete drum for five minutes. Upon completion of the mixing time, each aggregate was discharged into a separate mortar box, mixed with a square pointed shovel, and then tightly covered with plastic sheeting.

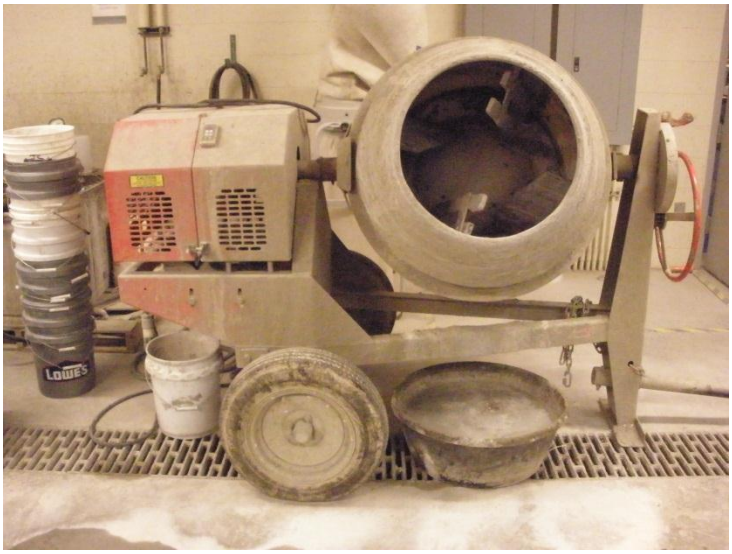

Figure 5.1- Six Cubic Foot Variable Speed Mixer

Three hours prior to mixing, the plastic sheet was momentarily removed in order to take moisture content samples. A shovel was used to mix the aggregate again, taking a moisture content sample from each aggregate bin. The plastic sheet was then replaced until it was time to batch out aggregates for the mix. Aggregate was dried for three hours in a forced air drying oven at 235 F (113 C). Immediately prior to concrete mixing, the moisture content samples were removed from the drying oven, weighed, and used to determine the necessary moisture content adjustments to be made to aggregate and batch water.

The mixing procedure used was a modified version of ASTM C 192 (ASTM, 2007). Prior to mixing fresh concrete, the mixer was "buttered" by adding several pounds of cementitious materials matching the mix design to the drum, adding water, and allowing this fluid to mix in the drum for at least five minutes, coating all surfaces of the inside of the drum. This fluid was discharged and wasted just prior to the beginning of fresh concrete mixing.

Batch water was separated into two buckets, one containing two thirds of the total batch water plus the total amount of air entraining agent, the other containing one third of the water, plus the water reducer. This procedure was recommended by the admixture technical representative to assist in loosening the very stiff mixture so that the Type A/F HRWR would have a chance of working properly. Next, the total amount of coarse aggregate was added to the drum, and the mixer was started on a speed setting of "12". The bucket of water containing air entrainment agent was then added, taking care to flush any fines on the sides of the mixer back into the aggregate. The sand was then added, and the mixer was run until the aggregates appeared well blended. Cement and the remaining water containing water reducer were then metered in so that the mix appeared uniform. After completion of addition of the mix constituents, the concrete was mixed at a speed setting of "15" for three minutes, subjected to a rest period of three minutes, and then remixed for a period of two minutes before discharging. Notably, the mixer was not covered during the three minute rest period as dictated in ASTM C 192.

Due to the large number of specimens combined with the limited capacity of the mixer, three batches were made for each mixture. The test methods assigned to each batch were chosen because of the potential for trying to correlate properties within the batch. Thus, one batch was for strength (compressive, flexural, and splitting) and modulus, the second for durability (freeze-thaw, rapid chloride penetration, salt scaling, and abrasion), and the third for shrinkage and setting time.

5.4.2.2. Temperature. Temperature of the concrete mixes was measured with an analog thermometer with a 5 in. (127 mm) probe length, and a resolution of one degree. Temperature of fresh concrete was conducted in accordance with ASTM C 1064 (ASTM,

2011b). The temperature of the batch was taken in a wheelbarrow immediately after discharge of the concrete from the drum.

5.4.2.3 Unit Weight. Air content of the concrete mixes was measured by means of a Type B pressure meter, and unit weight was measured in the air content bowl. Unit weight of fresh concrete was conducted in accordance with ASTM C 138 (ASTM 2012c). The same measure and concrete sample were used for the air content test immediately after determining the unit weight.

5.4.2.4. Slump. The slump of fresh concrete was determined in accordance with ASTM C 143 (ASTM, 2010a).

5.4.2.5. Air Content. The air content of fresh concrete was determined in accordance with ASTM C 231, using a type B pressure meter (ASTM, 2010c). This test was run upon the same measure and concrete sample used previously to determine unit weight. This often meant cleaning the rim of the bowl a second time after transporting it to a scale and back.

5.4.2.6. Water Content. A 1250 watt microwave from Panasonic was used to determine the microwave water content of fresh concrete. The sample was wrapped in a fiberglass cloth sheet approximately 20 in. x 20 in. (508 mm x 508 mm), and placed in a microwave-safe baking dish. A 1 in. (25 mm) wide metal scraper and a 2in. (25 mm) diameter ceramic pestle were used to break up the concrete sample. The microwave water content equipment is pictured below in **Figure 5.2**.

Figure 5.2 - Microwave Water Content Station

Microwave water content of fresh concrete was determined in accordance with AASHTO 318 (AASHTO, 2007). During the study, initially the sample was taken from the batch sometime after it had been discharged and during the time that the other tests specimen preparation had commenced. It was observed that after some time in the wheelbarrow, some batches would segregate, leading to areas of variable water contents in the batch. Sampling of this led to variable tested water contents. The results led to a refinement of the sampling/testing procedure. Ultimately, the sample for microwave water content was taken halfway through discharge of the drum and weighed immediately. The test was then conducted after the other fresh concrete tests had been completed.

In addition to determining the water content by the microwave method, it was also calculated based upon the amount of water actually batched. Using either of these two values, the *w/cm* can be calculated.

5.4.2.7. Setting Time of Concrete. The concrete time of set test was performed using an Acme penetrometer from Humboldt. The concrete sample was passed over a #4 sieve, and collected in a 6 in. (150 mm) diameter cylinder mold, cut to a 6 in. (150 mm) depth. Needles of varying diameter (1", ½", ¼", 1/10", 1/20", and 1/40") are attached to a loading arm, and the load required to penetrate the concrete is recorded upon a dial gauge on the penetrometer. The concrete time of set equipment is pictured below in **Figure 5.3**. Concrete time of set was conducted in accordance with ASTM C 403 (ASTM, 2008c). Samples were wet sieved over a #4 sieve after fresh concrete testing was completed, and remixed by hand after a suitable amount of concrete had been sieved for the test.

Figure 5.3 - Concrete Time of Set Equipment

5.4.2.8. Curing Equipment. With the exception of freeze-thaw prisms, concrete specimens were cured in a moist cure room at Missouri S&T. The moist cure room mists

water over the specimens in such a manner as to maintain at least 95% relative humidity at all times. Freeze-thaw prisms were cured in a saturated limewater bath, as were flexural strength beams for the final 24 hrs. before testing.

5.4.3. Hardened Concrete.

5.4.3.1. Compressive Strength. Four in. (100 mm) diameter concrete cylinders for compressive strength were cast in accordance with ASTM C 192 (ASTM, 2007). Placement consisted of two lifts, each being consolidated with 25 roddings with a 3/8 in. (9.5 mm) tamping rod, and 10 taps. Three replicate specimens were cast from each mixture, demolded after 24 hrs., moist-cured under standard curing conditions, and then tested at 28 days. Compressive strength of the 4x8 in. (100 mm x 200 mm) concrete cylinders was determined in accordance with ASTM C 39 (ASTM, 2012d). A 400,000 lb (181,600 kg) load frame from Forney was used in determining the compressive strength. Cylinders were capped with sulfur in accordance with ASTM 617 prior to testing. Cylinder diameter measurements were taken using calipers.

5.4.3.2. Modulus of Rupture. .Concrete beams were cast in accordance with ASTM C 192. Placement consisted of two layers, each layer rodded 72 times, tapped 12 times, and then spaded around the edges. Three replicate specimens were cast from each mixture, demolded after 24 hrs., moist-cured under standard curing conditions, and then tested at 28 days. Beams were cured in saturated limewater for the last 24 hours of curing prior to testing. Flexural strength of the concrete beams was determined in accordance with ASTM C 78 (ASTM, 2010d). A 200,000 lb. (90,800 kg) universal Tinius Olsen load frame was used in determining the flexural strength. An alignment jig constructed at Missouri S&T was used to ensure that the beam testing apparatus was aligned properly

with the top load being applied at third points. The flexural strength specimens were tested on a Test Mark third point loading beam testing apparatus. The testing apparatus is pictured in **Figure 5.4**.

Figure 5.4 - Beam Testing Apparatus

5.4.3.3. Splitting Tensile Strength. Splitting tensile strength was determined on 6 in. (150 mm) diameter cylinders, cast in accordance with ASTM C 192. Placement consisted of three layers, each being consolidated with 25 roddings with a 5/8 in. (16 mm) tamping rod, and 10 taps. Three replicate specimens were cast from each mixture, demolded after 24 hrs., moist-cured under standard curing conditions, and then tested at 28 days. Splitting tensile strength was determined in accordance with ASTM C 496 using a 400,000 lb (181,600 kg) Forney compression load frame (ASTM, 2011c). A marking jig pictured below in **Figure 5.5** was used to mark diametral lines upon the specimens. The testing jig pictured in **Figure 5.6** was used to center and load the specimens. The testing jig was not available at the start of testing; therefore early testing was conducted

by manually centering the specimen below the crosshead, and using a piece of steel stock as a supplementary bearing block.

Figure 5.5 - Cylinder Marking Jig

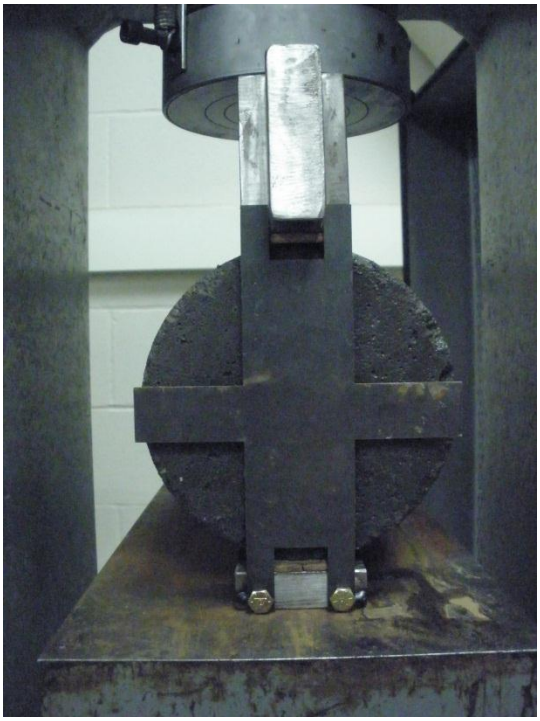

Figure 5.6 - Splitting Tensile Testing Jig

5.4.3.4. Modulus of Elasticity. Modulus of elasticity was determined on 6 in. (150 mm) diameter cylinders, cast in accordance with ASTM C 192. Placement consisted of three layers, each being consolidated with 25 roddings with a 5/8 in. (16 mm) tamping rod, and 10 taps. Three replicate specimens were cast from each mixture, demolded after 24 hrs., moist-cured under standard curing conditions, and then tested at 28 days. Modulus of elasticity was determined in accordance with ASTM C 469 (ASTM, 2010e). A 200,000 lb. (90,800 kg) Tinius Olsen universal load frame from was used. Each cylinder was secured in a yoke, which held an LVDT to measure axial compression during the test. Prior to testing, the concrete cylinders were sulfur capped to ensure planeness of loading surfaces.

5.4.3.5. Abrasion Resistance. Specimens for abrasion resistance were cast in one lift, consolidated with 96 roddings with a 5/8 in. (16 mm) diameter tamping rod, followed by 10 taps with a rubber mallet, and finally spaded around the edges. The specimens were 3.5 x 6 x 16 in. (89 x 150 x 406 mm). Two specimens were cast from each mixture, screeded with an aluminum float, demolded after 24 hrs., moist-cured under standard curing conditions, and then tested at 28 and 56 days. After the moist curing time, the specimens were surface dried using a towel. Abrasion testing was conducted in accordance with ASTM C 944 (ASTM, 2005a); however, the test was conducted at 300 rotations per minute instead of 200 rotations per minute, due to limitations of the drill press. A specialized abrasion head, constructed at Missouri S&T was used to abrade the concrete, and a weight was hung from the arm of the drill press, corresponding to a 44 lb. double load as noted in ASTM C 944. The abrasion testing equipment is pictured below in **Figure 5.7**.

Figure 5.7 - Abrasion Testing Equipment

The initial weight of each specimen slab was determined. A two min. abrasive action was applied to the specimen surface, the dust removed, and weight determined. Depth of wear was also determined at eight points at both the innermost and outermost abraded rings on the specimen using a digital caliper. This procedure was repeated twice more on the same spot, and the results averaged. Then, the whole procedure was repeated on two additional spots, for a total of three replicate tests. A typical tested specimen is shown in **Figure 5.8**. The abrasion resistance test procedure is included in Appendix H.

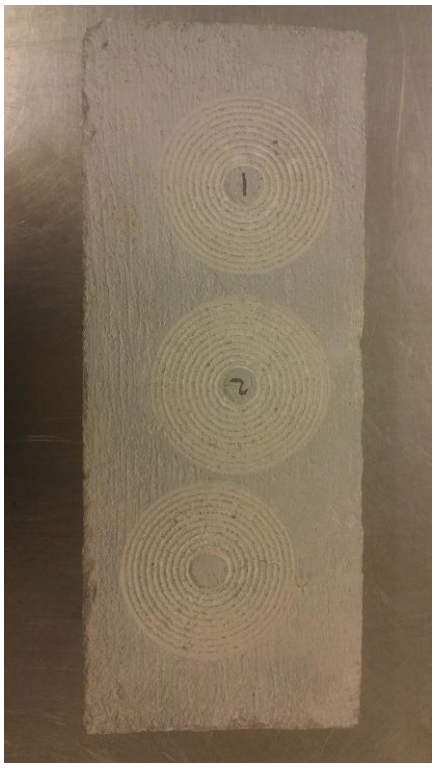

Figure 5.8 – Example of Abrasion Test Specimen

5.4.3.6. Drying Shrinkage. Two replicate specimens used to determine linear shrinkage of concrete were cast in 4 in. (100 mm) inner diameter PVC molds, each 24 in. (610 mm) long. Concrete was placed in two layers in the molds, and consolidated by vibration. The next day, specimens were demolded by use of a Dremel tool with a cutting head. DEMEC points were attached with a metal and concrete epoxy, and initial readings were taken as soon as was feasible. Linear shrinkage of concrete was determined in a modified version of ASTM C 157, using a cylindrical specimen with DEMEC points attached (ASTM, 2008d). DEMEC points were attached with a metal and concrete epoxy 24 hours after casting. A DEMEC gauge was used in order to measure shrinkage of the specimens. The specimens and DEMEC gauge are pictured below in **Figure 5.9**.

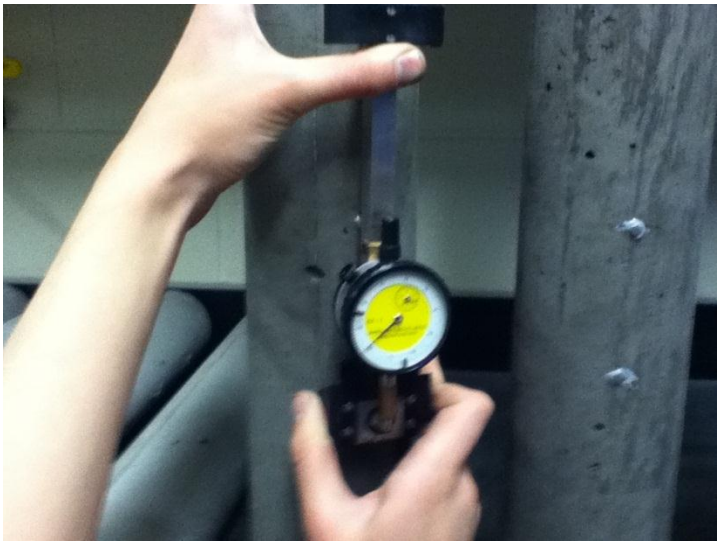

Figure 5.9 - DEMEC Gauge and Specimen

Initially, readings were taken daily, with increasing periods of time between readings as the rate of shrinkage of the specimens decreased. Data was then adjusted for the reference bar; the shrinkage was calculated in microstrain and plotted. The drying shrinkage test procedure is included in Appendix I.

5.4.3.7. Freeze-Thaw Durability. Freeze-thaw resistance, in terms of a Durability Factor, was determined in accordance with ASTM C 666 Method B (ASTM, 2008e). Durability factor (DF) is a relative measure, adjusting the relative dynamic modulus for the number of cycles that the specimen has undergone, relative to the total number of cycles it should undergo. Concrete prisms measuring 4.5 in. (114 mm) deep, 3.5 in. (89 mm) wide, and 16 in. (406 mm) long were cast with gauge studs at either end to Specimens were cast in two layers, and consolidated by means of 28 roddings, 10 tappings, and spading around the perimeter of the specimens. Three specimens were cast from each mixture. After demolding, freeze-thaw prisms were cured in a saturated limewater tank until the date of testing. The prisms were transported to MoDOT's

Central Testing Laboratory between 14 and 21 days of age, and were tested there at age 35 days. Testing was conducted according to ASTM C 666 Method B.

5.4.3.8. Salt Scaling. Three replicate specimens for salt scaling resistance were cast in molds 12 x 12 x 4 in. deep (300 x 300 x 100 mm) in one lift and rodded 72 times. Initially, specimens were cast at a full 4 in. (100 mm) depth with a broomed finish, and a 1 in. (25 mm) high, 1 in. (25 mm) wide mortar dam was built atop the finished surface with the aid of an angle iron backer. After consultation with technicians from MoDOT, however, the casting procedure was revised. The molds for scaling resistance specimens were under filled, and the concrete surface finished approximately an in. (25 mm) below the top surface of the mold. This surface was broomed, and a 1 in. (25 mm) high, 1 in. (25 mm) wide mortar dam was built atop the finished surface against the steel mold.

Scaling specimens were cured in the moist cure room for 14 days, after which they were subjected to a 14 day drying period prior to testing. Between 14 days and 21 days, the scaling specimens were transported to MoDOT central testing laboratories for testing in accordance with ASTM C 672 (ASTM, 2003). The mold and finished specimen are shown in **Figures 5.10** and **5.11.**

5.4.3.9. Rapid Chloride Penetration. Two replicate concrete cylinders 4 in. (100 mm) in diameter were cast for use in the rapid chloride permeability test. These cylinders were placed and consolidated in the same manner that the compressive strength cylinders were. Concrete was placed in two lifts, and each lift was rodded 25 times with a 3/8” diameter tamping rod before being tapped 10 times. Samples were transported to MoDOT Central Testing Laboratory between 14 and 21 days of age for testing according to ASTM C 1202 (ASTM, 2012e).

Figure 5.10 – Salt Scaling Mold

Figure 5.11 – Salt Scaling Specimen

5.5. RESULTS AND DISCUSSION

5.5.1. Plastic Concrete Test Results.

5.5.1.1. Slump. Glenium 7500 water reducer was used in all 10 concrete mixes in order to adjust the slump to 5±1 inches. In **Table 5.2** was shown the dosages used for each mix. For the 4-1 combination, as would be expected (Bouzoubaa, et al., 2007), less

water reducer was required to achieve a 5 in. (27 mm) slump as the amount of fly ash in the mix increased. Mixes with rapid set cement as an activator required more water reducer than did those with calcium hydroxide as an activator. The rapid hydration of rapid set cement led to a more rapid rate of slump loss than calcium hydroxide, and the dosage of rapid set cement was 20% by weight of fly ash, or twice that of the dosage used for calcium hydroxide.

For the 1-3 combination, the trend is not as clear. Mixes using rapid set cement as an activator required higher dosages of water reducer than those using calcium hydroxide for the same reasons outlined before. However, increasing fly ash content in these mixes led to an increase in the required dosage of water reducer. Rapid slump loss was noticed during mixing for fly ash mixes in the 1-3 combination, so it is possible that rapid aluminate reactions due to the fly ash meant that a higher dosage of water reducer was necessary in order to achieve a target slump. There were 35 batches made in the concrete study; the average slump was 5.1 in., with a range of 4 to 7 in.

5.5.1.2. Air Content. BASF's MB-AE-90 air entrainment admixture was used in all 10 concrete mixes in order to adjust the air content to 5±0.75%. In **Table 5.2** was shown the required dosages in oz/cwt to achieve this air content. For the 4-1 combination, the required dosage of air entrainment agent was lower at higher percentages of fly ash replacement. This is likely tied to the increased workability seen with these mixes, therefore requiring a lower dosage to entrain the same amount of air. Very little difference was noted in air entrainment dosages between those mixes utilizing calcium hydroxide as an activator and those utilizing rapid set cement as an activator.

For the 1-3 combination, again, no difference was noted in air entrainment dosages between those utilizing calcium hydroxide and those utilizing rapid set cement as activators. As in the case of the water reducer, fly ash mixes initially required less air entrainment agent to achieve a given air content, though the required dosage increased as the fly ash content increased from 50% to 70%. Again, this is partially due to the more rapid rate of slump loss. Additionally, the fly ash used in the 1-3 combination had a much greater Loss-on-Ignition (LOI) and was darker in color than that used in the 4-1 combination, indicating higher carbon content. Fly ash mixes with higher carbon content typically require more air entrainment admixture to achieve a given air content. For the 35 concrete batches, the average air content was 5.2% with no batches outside the target range of 4.0 to 6.0 %.

5.5.1.3. Microwave Water Content. Although great care was taken to correct the water content of each concrete batch for moisture content of the aggregate, it was decided to begin checking the water content by the microwave method, AASHTO T318 (AASHTO, 2002). Using the water content and knowing the cement content, the *w/cm* can be calculated. The average difference in *w/cm* in the concrete study was only 0.006, however, there was a fair amount of scatter in the results. As mentioned previously, as experience was gained, the sampling method was refined. Part of the reason for the scatter in results may have been due to the timing and location of the sampling. It was observed that waiting to sample from the completed batch sometime after mixing resulted in samples of varying consistency. From this limited experience, it is felt that the microwave method may be a practical tool for field checking of *w/cm* from ready mix

operations. The method is used routinely by such agencies as the New York and New Jersey Port Authority.

5.5.1.4. Time of Set. Time of set was determined on each of the 10 concrete mixtures tested for this project. **Figure 5.12** below details the initial and final set times determined for the 4-1 combination.

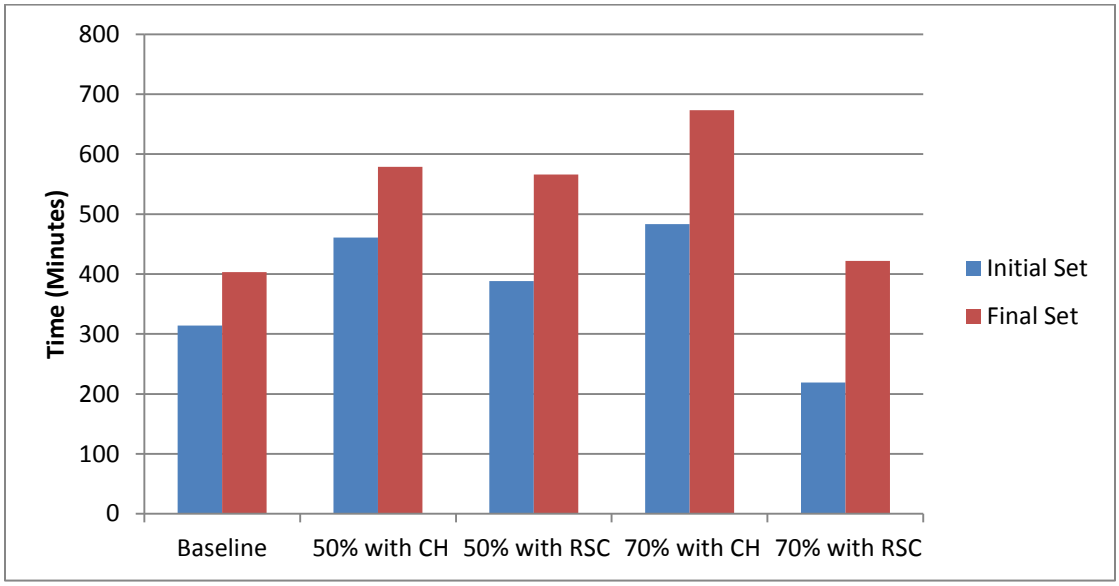

Figure 5.12 - Initial and Final Set Times for the 4-1 Combination

The addition of gypsum-lime to fly ash mixtures caused both the initial and final set to increase for mixes incorporating calcium hydroxide as an activator. The effect was more pronounced at the 70% fly ash replacement rate. Mixes incorporating rapid set cement as an activator fared better than their calcium hydroxide counterparts in reducing the lengthened time of set due to fly ash substitution. Notably, at 70% replacement of cement with fly ash, the rapid set cement mixture brought the time of set down considerably more than at 50% replacement of cement with fly ash. This discrepency is likely due to the fact that since activator levels are determined as a percentage of fly ash,

more rapid set cement is present in the 70% fly ash mixture than the 50% fly ash mix, resulting in a decreased time of set.

The results of time of set tests on combination 1-3 are pictured below in **Figure 5.13**. Results on the 1-3 combination are very similar to those found for the 4-1 combination. At 50% fly ash replacement the rapid set cement mixture responds in a similar way to the calcium hydroxide mix, whereas at 70% fly ash replacement, the rapid set cement mixture exhibits a marked decrease in set time from the calcium hydroxide mixture. The setting time results are tabulated in Appendix J.

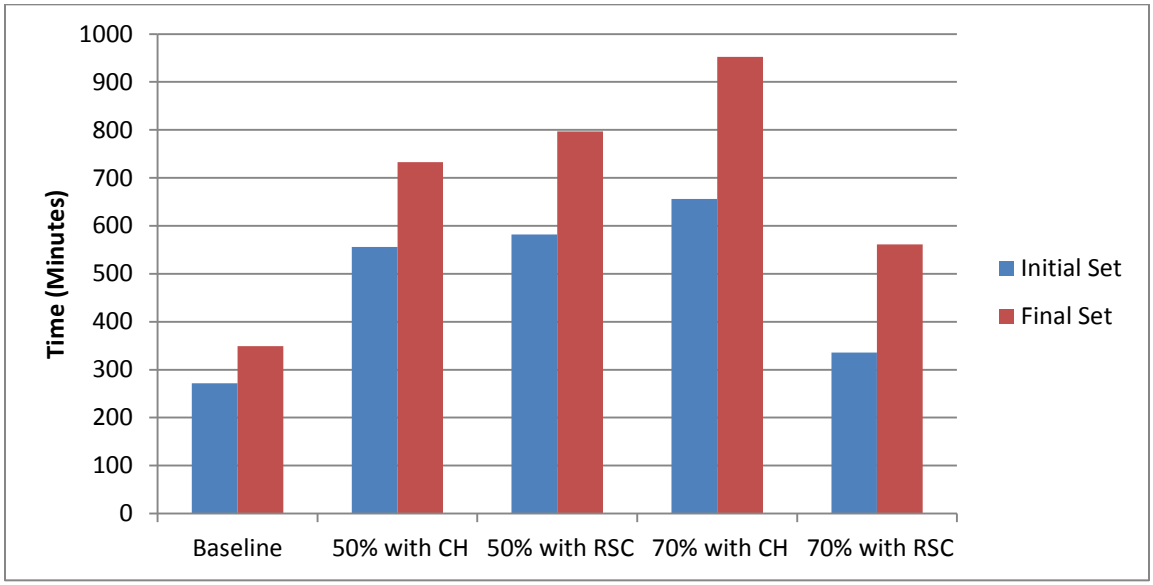

Figure 5.13 - Initial and Final Set Times for the 1-3 Combination

In most cases, powder additives retarded concrete setting time. This is in contrast to the results of the paste study where in all cases the additives followed the acceleration of the fly ash replacement for these particular cementitious blends. In the case of the 1-3 mixtures, the WR/HRWR dosage was greater than that used in the paste study. Whether this had an effect is unclear.

5.5.2. Hardened Concrete Test Results.

5.5.2.1. Compressive Strength. An outlier analysis was performed in accordance with ASTM E178—there were two outlier test results, which were discarded. Results from the 4-1 combination are presented in **Figure 5.14**, below. All fly ash mixtures, regardless of replacement percentage, suffered in terms of short term strength gain compared to the baseline mixture. However, both 4-1 blends at 50% fly ash with either lime or RSC met or exceeded the 1000 psi (6.9 MPa) minimum threshold. By seven days of age, however, the 50% fly ash mixtures had begun to exhibit more reasonable strengths, exceeding 3000 psi (20.7 MPa)(the MoDOT structural B mixture min. 28 day strength). In fact, they reached 2750 psi (19.0 MPa) (a typical form removal minimum) in 5 to 6 days. They continued to gain strength, approximating the baseline mixture strengths by 28 days (exceeding 4000 psi (27.6 MPa) which is the PCCP mixture 28 day min.) and at 56 days exceeding baseline strengths, topping 5000 psi (34.5 MPa). Mixtures with 70% fly ash replacement exhibited greatly lowered strengths when compared to baseline mixtures, or even their 50% fly ash replacement counterparts at all ages, although they almost achieved 3000 psi (20.7 MPa) at 28 days and 3500 psi (24.1 MPa) at 56 days. The difference in strength due to activator selection was small at most ages, though mixtures using rapid set cement were always somewhat stronger than mixtures using calcium hydroxide as an activator. In comparison to the paste study results, the trends in strength for concrete followed the trends shown for paste, although the RSC‘s superiority was more pronounced in the paste results.

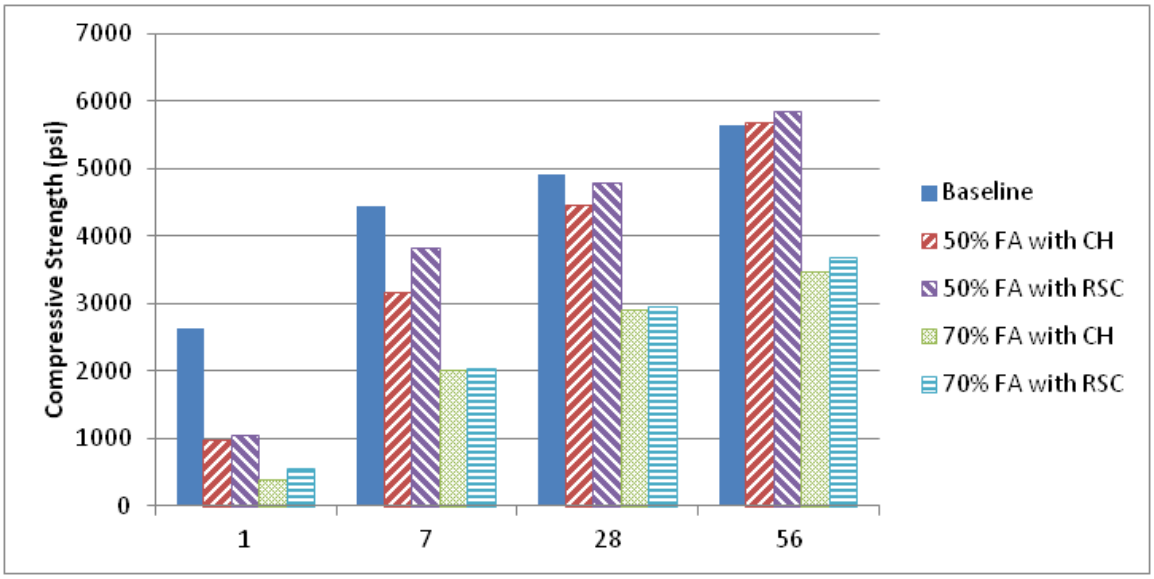

Figure 5.14 - Compressive Strengths for Combination 4-1

Results from the 1-3 combination are presented in Figure 5.15, below. All fly ash mixes for this combination exhibited lower strengths than the baseline concrete mixture at all ages. For the 50% fly ash replacement level, mixtures using calcium hydroxide as an activator showed slightly greater strengths than mixtures using rapid set cement as an activator. The 70% fly ash mixes displayed lower strengths than the 50% fly ash mixtures, as expected. None of the fly ash mixtures reached 1000 psi (6.9 MPa) at one day. The 50% fly ash mixtures reached 2750 psi (19.0 MPa)(a typical form removal minimum) in 5 to 6 days, exceeded 4000 psi (27.6 MPa) at 28 days, and were equal to or greater than 5000 psi (34.5 MPa) at 56 days. The 70% fly ash mixture with 20% RSC exceeded 3000 psi (20.7 MPa) at 28 days, and both activated 70% fly ash mixtures exceeded 3000 psi (20.7 MPa) at 56 days. In comparison to the paste study results, the trends in strength for concrete followed the trends shown for paste for lime, but RSC showed superior strengths at one and 56 days in the paste results.

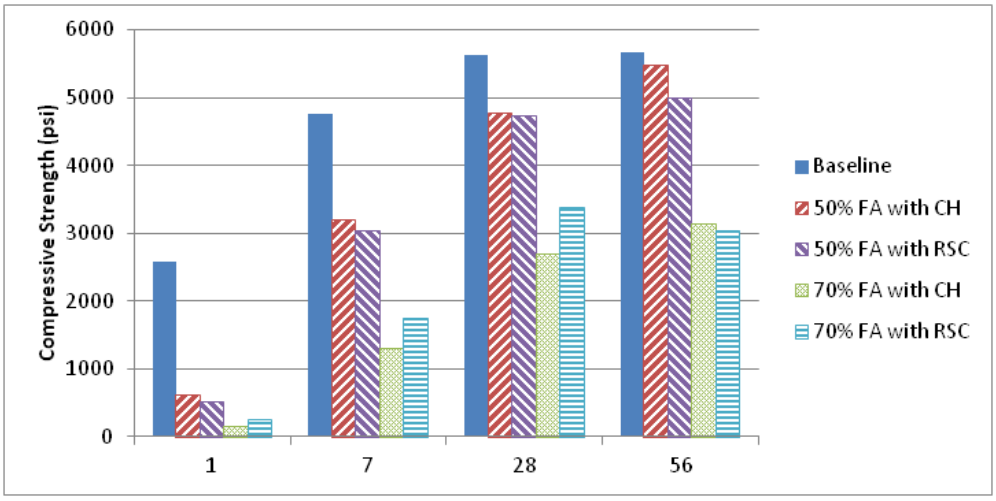

Figure 5.15 - Compressive Strengths for Combination 1-3

The compressive strength results are tabulated in Appendix J.

5.5.2.2. Flexural Strength (MOR). An outlier analysis was performed: there were no outlier test results. Results from the 4-1 combination are presented below in **Figure 5.16**. At 50% replacement of cement with fly ash with both activators, the 28 day flexural strengths were close to the base mixture and were at nearly 700 psi (4.8 MPa). At the 70% replacement level, there was a notable loss in flexural strength, more so with the calcium hydroxide mixture than the rapid set cement mixture.

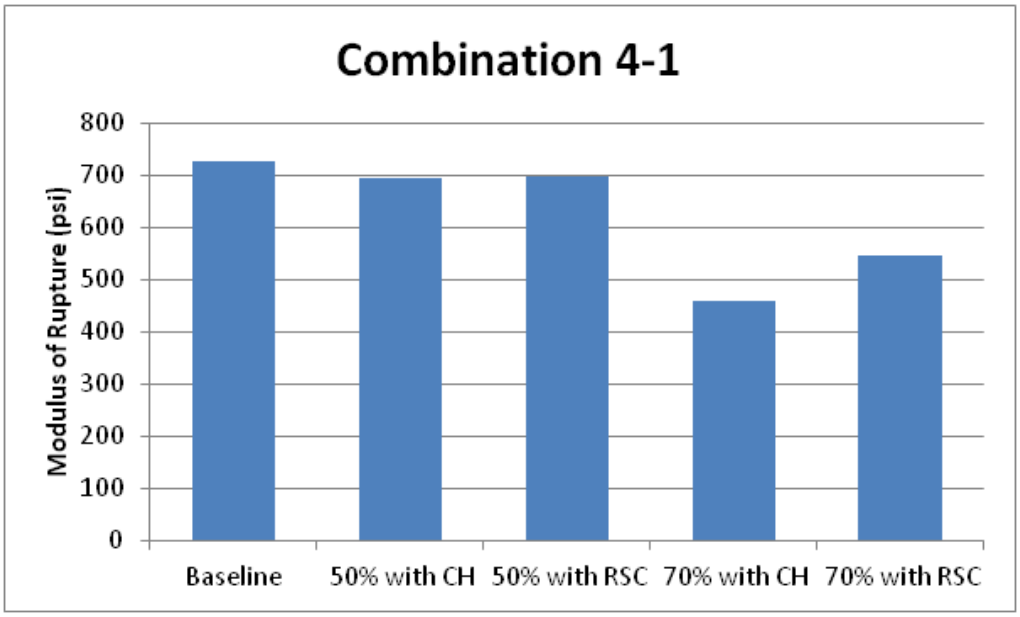

Figure 5.16 - Flexural Strength of Combination 4-1

Results from the 1-3 combination are presented below in **Figure 5.17**. At 50% replacement of cement with fly ash, calcium hydroxide and rapid set cement mixtures performed similarly, though a greater loss of strength was observed here than with combination 4-1. At 70%, another drop in strength is seen, with the rapid set cement mixture providing a greater flexural strength than the calcium hydroxide mixture. The flexural strength results are tabulated in Appendix J.

The loss of flexural strength moving from 50% fly ash replacement to 70% fly ash replacement is consistent with work by Naik, et al (1995), showing that as Class C fly ash content increases, the flexural strength suffers. It is possible, however, if the flexural strength testing had been conducted at later ages, that higher volume fly ash mixtures may have exhibited greater flexural strength in the longer term.

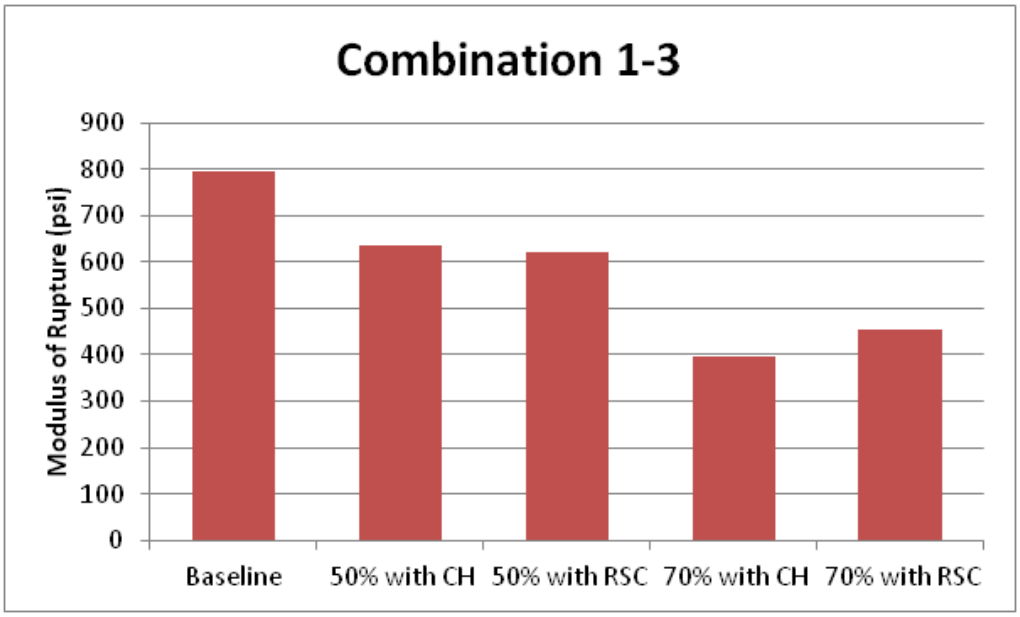

Figure 5.17 - Flexural Strength of Combination 1-3

5.5.2.3. Splitting Tensile Strength. An outlier analysis was performed which revealed that there was one outlier test result, which were discarded. Results from the 4-1 combination are shown below in **Figure 5.18**. At 50% fly ash substitution, splitting tensile strength results were greater than the baseline mixture, while at higher levels of fly ash substitution, the splitting tensile strength was reduced. Results from the 1-3 combination are shown in **Figure 5.19**. The 50% fly ash replacement mixes show a small loss in splitting tensile strength, with a larger loss present at 70% fly ash replacement. In both 4-1 and 1-3 combinations, rapid set cement appears to be a more effective activator at 70% replacement.

The drop in splitting tensile strength from 50% fly ash replacement to 70% fly ash replacement falls in line with previous research showing a lowered splitting tensile strength with increased Class C fly ash content (Naik, et al, 1995). The majority of the splitting tensile strengths at 28 days fall within 8.9% to 10.7% of the compressive

strength at 28 days, with one mix exhibiting a splitting tensile strength 12.8% of the compressive strength. Previous research has shown that splitting tensile strengths are expected to fall within 8% to 10% of the compressive strength of concrete, and this appears to be fairly true (Rivest, et al, 2004). The splitting tensile strength results are tabulated in Appendix J.

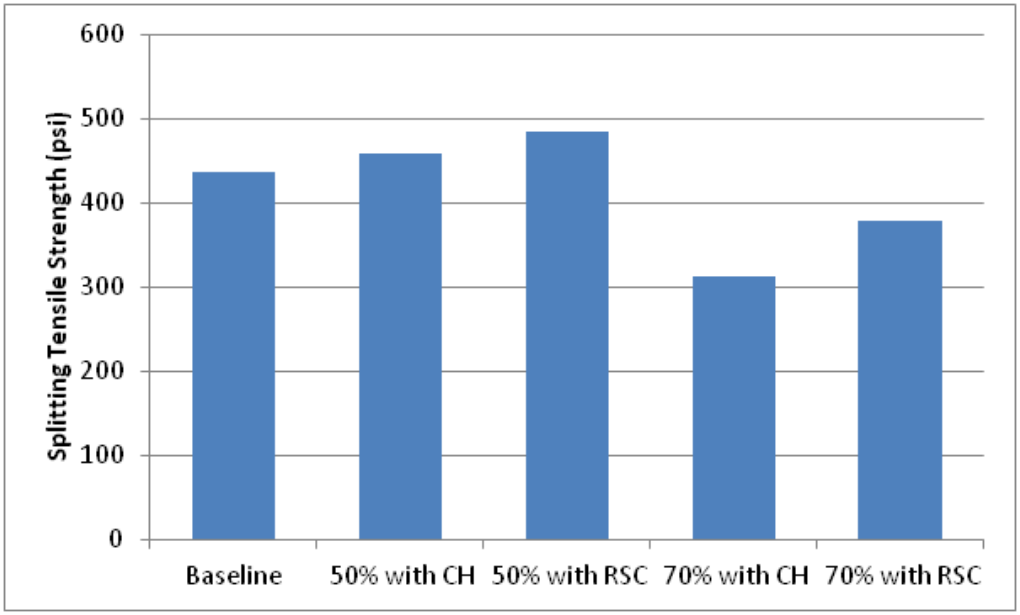

Figure 5.18 - Splitting Tensile Strength of Combination 4-1

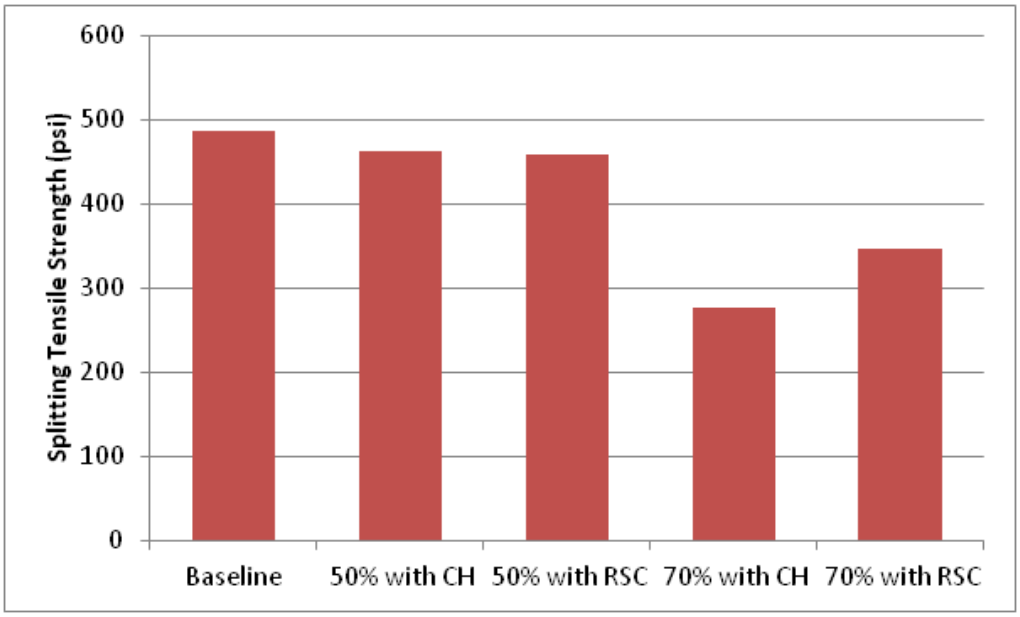

Figure 5.19 - Splitting Tensile Strength of Combination 1-3

5.5.2.4. Modulus of Elasticity. No outliers were found in the MOE dataset. Results from the 4-1 combination are shown in **Figure 5.20**, and from the 1-3 combination in **Figure 5.21**. In both the 4-1 and 1-3 combinations, the 50% fly ash mixes show a similar or slightly increased modulus of elasticity, indicating a stiffer concrete. At 70% replacement of cement with fly ash, all concrete mixtures exhibit a lower modulus of elasticity, with those 70% fly ash mixtures using rapid set cement as an activator suffering the smallest loss in modulus.

It has been suggested that the increased modulus of elasticity of the high volume fly ash concretes could be due to unreacted particles acting as fine aggregates to contribute to the rigidity of the concrete (Rivest, et al, 2004). This could likely explain why even the 70% fly ash concrete mixtures exhibited a modulus of elasticity around 4 million psi, despite a drastically lowered compressive strength. The modulus of elasticity results are tabulated in Appendix J.

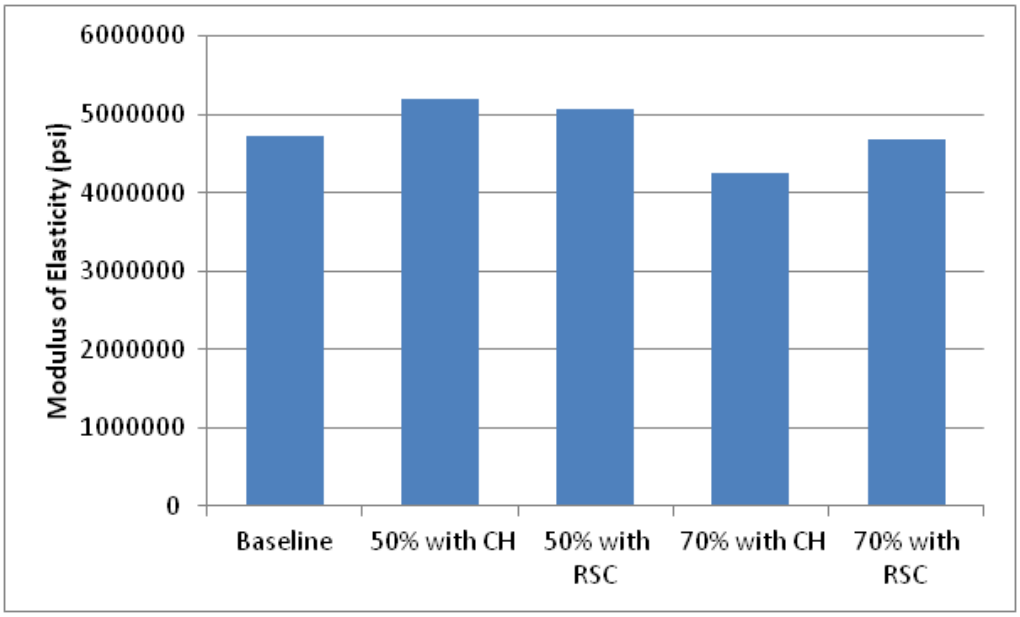

Figure 5.20 - Combination 4-1 Modulus of Elasticity

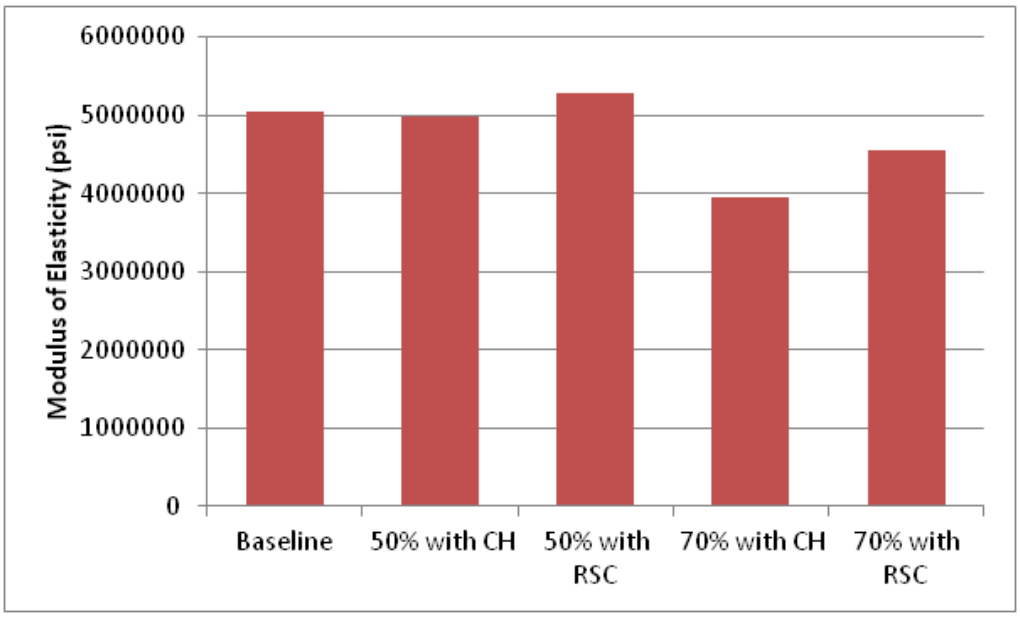

Figure 5.21 - Combination 1-3 Modulus of Elasticity

5.5.2.5. Abrasion Resistance. Outlier analyses of abrasion data showed one mass test and one depth of wear test result to be outliers—these were discarded. Abrasion resistance was measured in both mass loss and depth of wear of the abrasion specimens

in three replicates. **Figure 5.22** shows a strong correlation between the two measured methods of abrasion resistance.

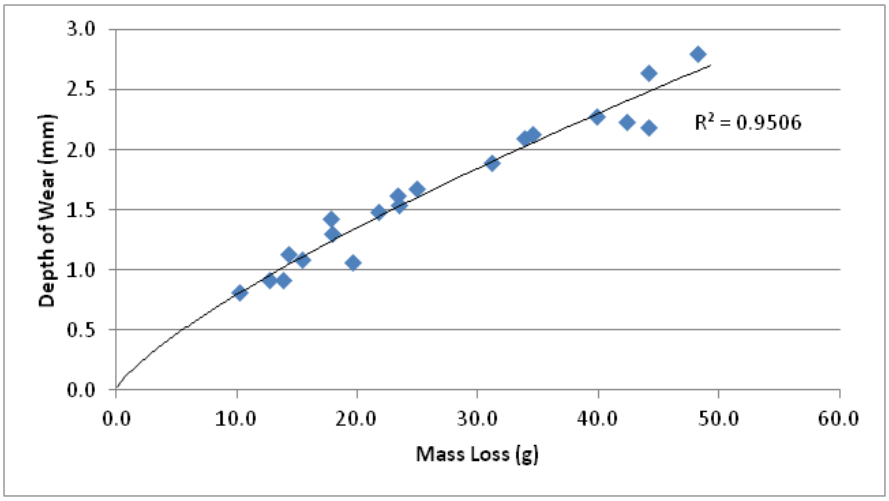

Figure 5.22 - Mass Loss/Depth of Wear Correlation

In all cases, HVFA concrete mixes showed less resistance to abrasion than their baseline counterparts. Between 28 days and 56 days of age, the HVFA concrete mixes did gain some abrasion resistance, though in every case they still fared more poorly than their baseline counterparts. For combinations 4-1, the 50% fly ash mix using calcium hydroxide as an activator came closest to matching the performance of the baseline concrete, while for 1-3 the RSC activator did better. Mass loss for each mix at 28 and 56 days is plotted in **Figure 5.23** for combination 4-1, and in **Figure 5.24** for combination 1-3. Some scatter is evident in the baseline mixture data, as made apparent by 56 day abrasion tests of the baseline mixes being quite similar or higher than 28 day abrasion tests despite having higher compressive strengths at 56 days. The abrasion results are tabulated in Appendix J.

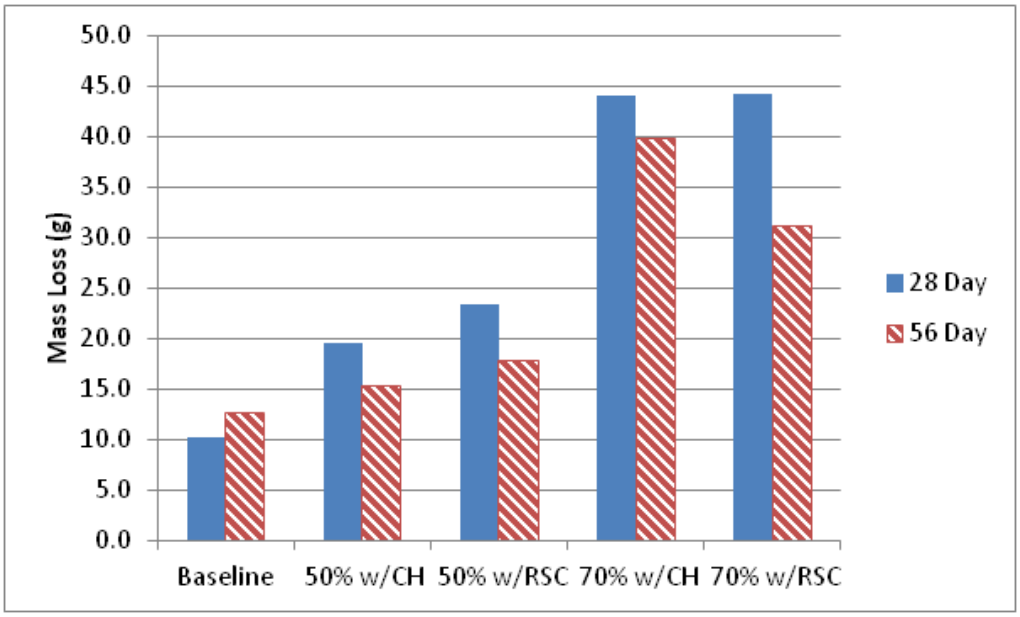

Figure 5.23 - Abrasion Resistance Mass Loss for 4-1

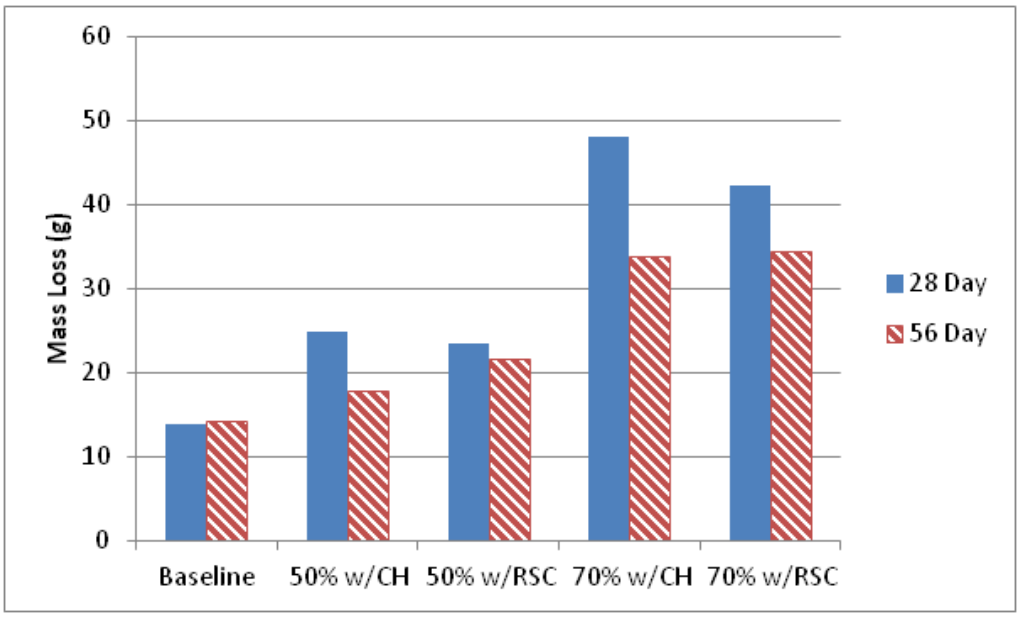

Figure 5.24 - Abrasion Resistance Mass Loss for 1-3

Figures 5.25 and **5.26** detail the depth of wear for each mix and show similar results as the mass loss data. This data seems in agreement with research by Naik, Singh, and Ramme on abrasion resistance of high volume Class C fly ash concretes: they noted

that replacement of cement with fly ash at low dosages (20% to 50%) fly ash seems to not greatly influence abrasion resistance of the concrete, while higher cement replacements show lowered resistance to abrasion. They also reported a gain in resistance with time. The authors also noted the significant effect of varying fly ash sources on abrasion resistance (Naik, et al, 2002).

Overall, the loss of abrasion resistance with increasing fly ash replacements is expected because of a similar effect on compressive strength, which correlates highly with abrasion resistance. This correlation between compressive strength and mass loss is illustrated in **Figure 5.27**, and between compressive strength and depth of wear in **Figure 5.28.**

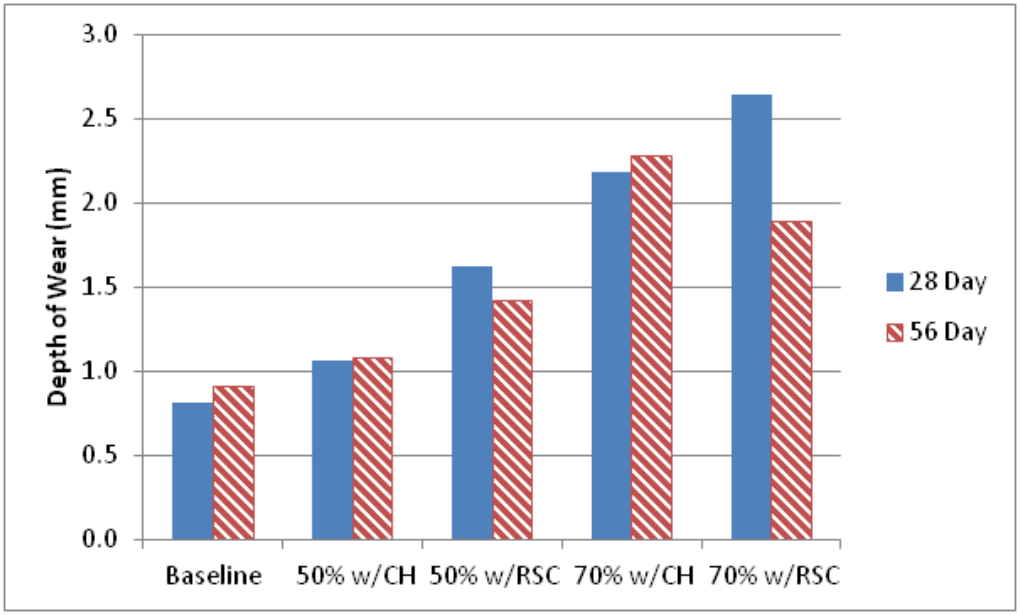

Figure 5.25 - Abrasion Resistance Depth of Wear for 4-1

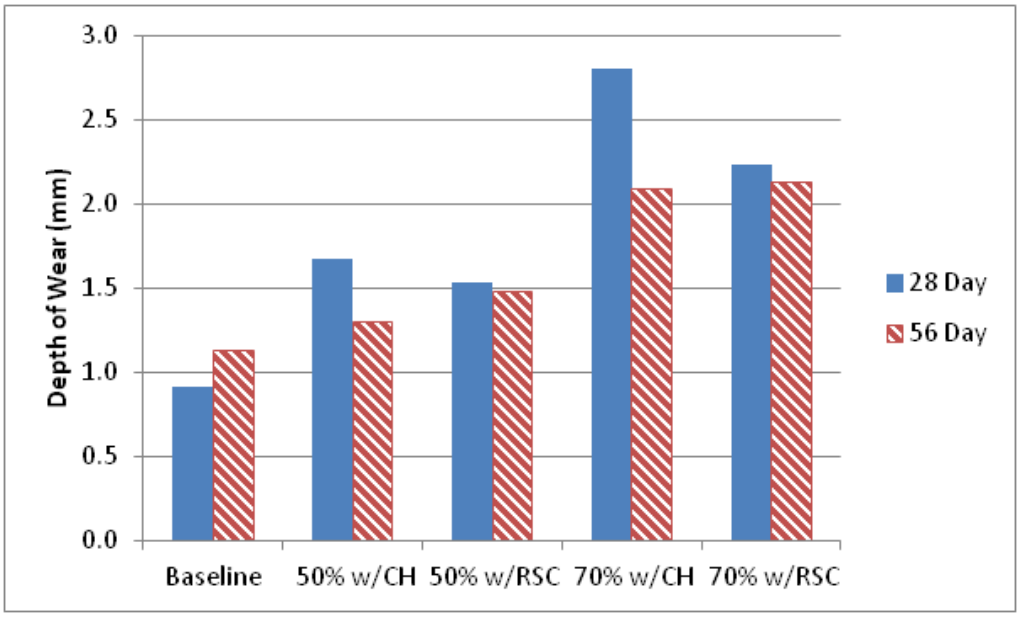

Figure 5.26 - Abrasion Resistance Depth of Wear for 1-3

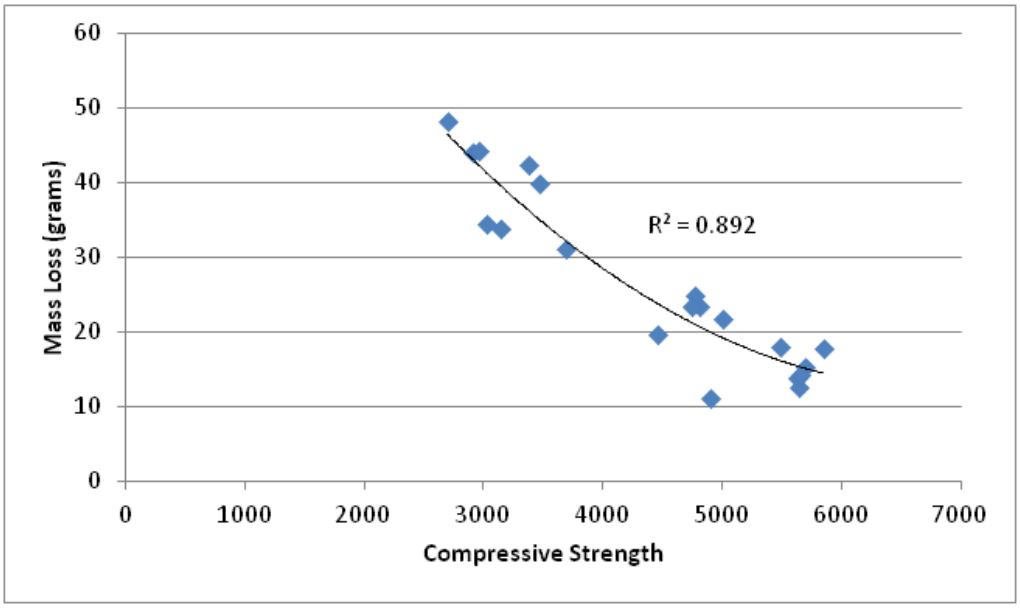

Figure 5.27 - Mass Loss versus Compressive Strength

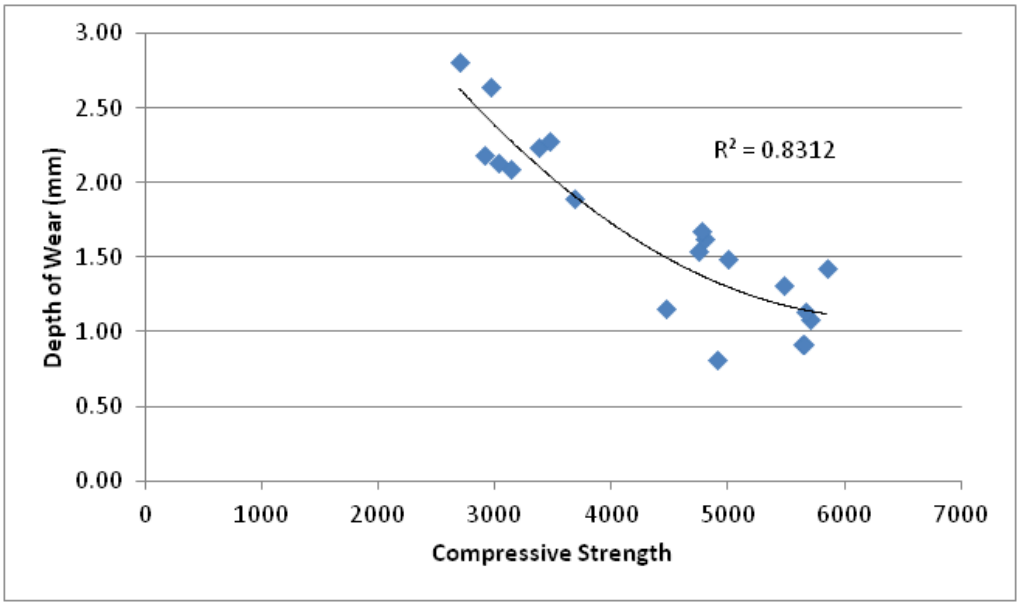

Figure 5.28 - Depth of Wear versus Compressive Strength

5.5.2.6. Drying Shrinkage. Linear shrinkage was measured on cylindrical specimens with two lines of DEMEC points applied at 180 degrees from each other. **Figure 5.29** below shows the shrinkage curves for combination 4-1, and **Figure 5.30** shows the shrinkage curves for combination 1-3. In all cases, fly ash mixes plotted below the baseline mix, meaning that these mixes incurred less shrinkage. The slopes of the lines parallel the baseline curve closely, making it unlikely that the fly ash mixes will cross the baseline curve and incur greater shrinkage. This lower shrinkage could be due to the decreased amount of water reducer needed in fly ash mixes, though this explanation is unlikely to explain the reduced shrinkage in combination 1-3, due to the need for increased water reducer dosages from the baseline in some cases. The lower shrinkage of high volume fly ash concrete mixes falls in line with results from Rivest, et al, suggesting that unhydrated cementitious material within the high volume fly ash mixes may be acting as aggregate and restraining the specimens from shrinkage. While

Rivest et al. used a lower *w/cm* for fly ash concretes and attributed the lower water content to decreased shrinkage of the HVFA mixes, it is clear that other factors are at work (Rivest, et al, 2004).

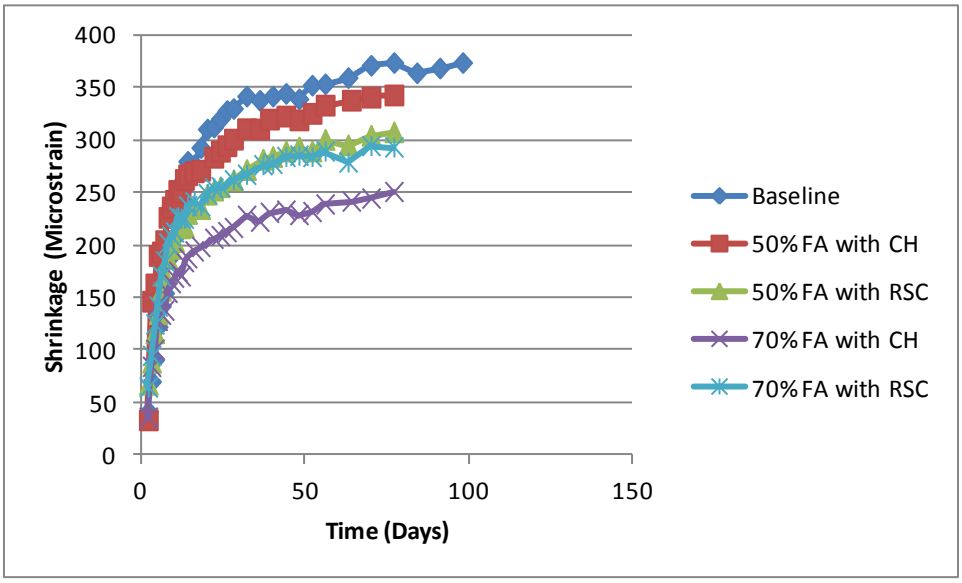

Figure 5.29 - Shrinkage Curves for Combination 4-1

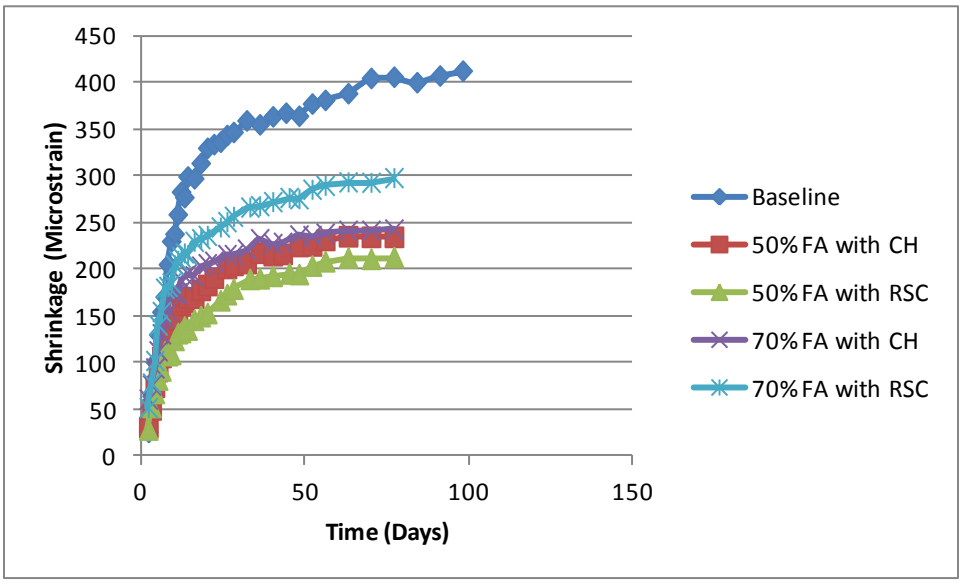

Figure 5.30 - Shrinkage Curves for Combination 1-3

5.5.2.7. Rapid Chloride Permeability. Outlier analyses of RCP test result to be an outlier—this was discarded. The rapid chloride permeability (RCP) test is a direct measure of electrical conductivity rather than an actual permeability test. However, this test shows good correlation with more intensive chloride ponding tests. This test was conducted on two cylinders for each concrete mix at 28 days of age. Two slices were taken of each cylinder, for a total of four measurements of charge passed. These four measurements were subject to an ASTM E 178 outlier analysis, and only one outlier was found. Permeability classes for each mix were determined in accordance with Table X1.1 from ASTM C 1202.

Figure 5.31 below shows the RCP test results for the most reactive combination, 4-1. At 50% replacement of cement with fly ash, both calcium hydroxide and rapid set cement mixes exhibited greatly decreased permeability, with an adjusted charge passed of less than half of that exhibited by the baseline mix. At 70% replacement, however, both calcium hydroxide and rapid set cement mixes proved to be more permeable than the baseline mix. It is important to note, however, that this test was conducted at 28 days, and as the 70% fly ash mixes approach 100% hydration, they may exhibit a more impermeable microstructure. In both cases, rapid set cement mixes had a more drastic effect on the permeability than calcium hydroxide.

Figure 5.32 shows the results of the RCP test on the least reactive combination, 1-3. Results for this combination are less clear cut, with 50% fly ash mixes exhibiting somewhat similar permeability to the baseline mix. The 50% fly ash mix utilizing rapid set cement as an activator decreased the permeability from the baseline mix by a slight amount, while the mix utilizing calcium hydroxide was more permeable than the baseline

mix. At 70%, both mixes exhibited high permeability, with the mix utilizing calcium hydroxide as an activator passing too high a charge to finish the test. Therefore, as the test could not run for the full 6 hours, no data for this test is provided. The compressive strength results are tabulated in Appendix J.

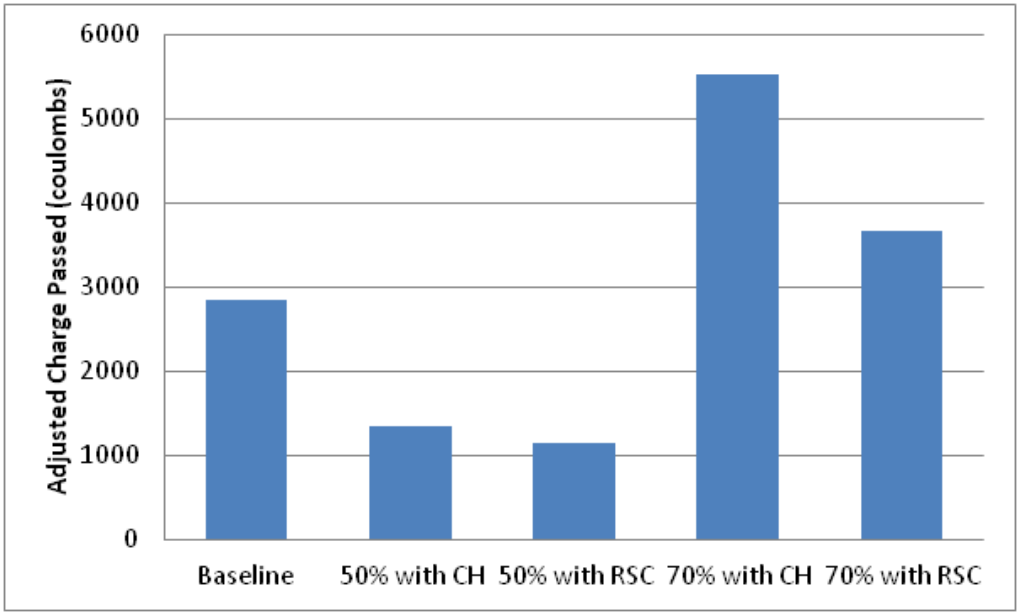

Figure 5.31 - Rapid Chloride Permeability Results for 4-1 Mixes

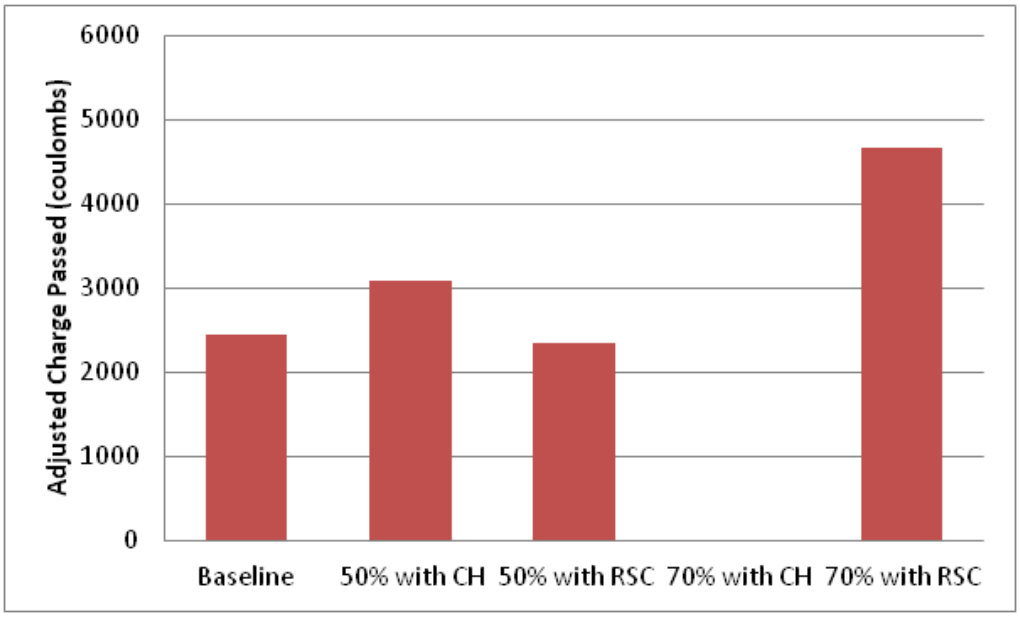

Figure 5.32 - Rapid Chloride Permeability Results for 1-3 Mixes

Previous research shows fly ash mixtures at 58% replacement exhibiting fairly low charges passed, with values falling off drastically at 91 days and 1 year (Bilodeau, et al. 1994; Gu, et al., 1999; Bouzoubaa et al., 2007). In the present study, the most reactive mix combination (4-1) shows similarly decreased chloride ion permeability at 50% fly ash content. Possible reasons for the higher charge passed at 70% for the 4-1 combination and for both 50% and 70% fly ash replacement of the 1-3 mix could be due to the test being conducted at the relatively early age of 28 days, when pozzolanic activity of the fly ash may not contribute significantly until 56 or 90 days of age, and therefore unreacted fly ash particles act as filler rather than hydration products, increasing the porosity of the paste microstructure.

5.5.2.8. Freeze-thaw Resistance. Three replicate beams were cast and tested for each mixture freeze-thaw resistance at 35 days of age; no outliers were found. Freeze-thaw resistance was measured by means of the durability factor (DF) in accordance with

ASTM C666, Method B. Freeze-thaw results for combinations 4-1 and 1-3 may be seen in **Figure 5.33** and **Figure 5.34** below. All fly ash mixtures had DF's greater than 90. The data suggests that the inclusion of fly ash, regardless of which powder activator is used in the mix, significantly improves the durability factor from that of the baseline mix, with 70% fly ash mixes in some cases showing a higher durability factor than those containing 50% fly ash. The freeze-thaw results are tabulated in Appendix J.

While their concretes were not air entrained, this increased durability of high volume fly ash concretes seems to be in line with previous work showing that higher volume fly ash concretes resist freezing and thawing more than their cement-only counterparts (Galeota, et al, 1995), and it shows high durability factors for fly ash mixes, in line with other research which showed high volume fly ash mixes being able to withstand severe freezing and thawing conditions, exhibiting high DF's (≥96) (Bilodeau, et al, 1994).

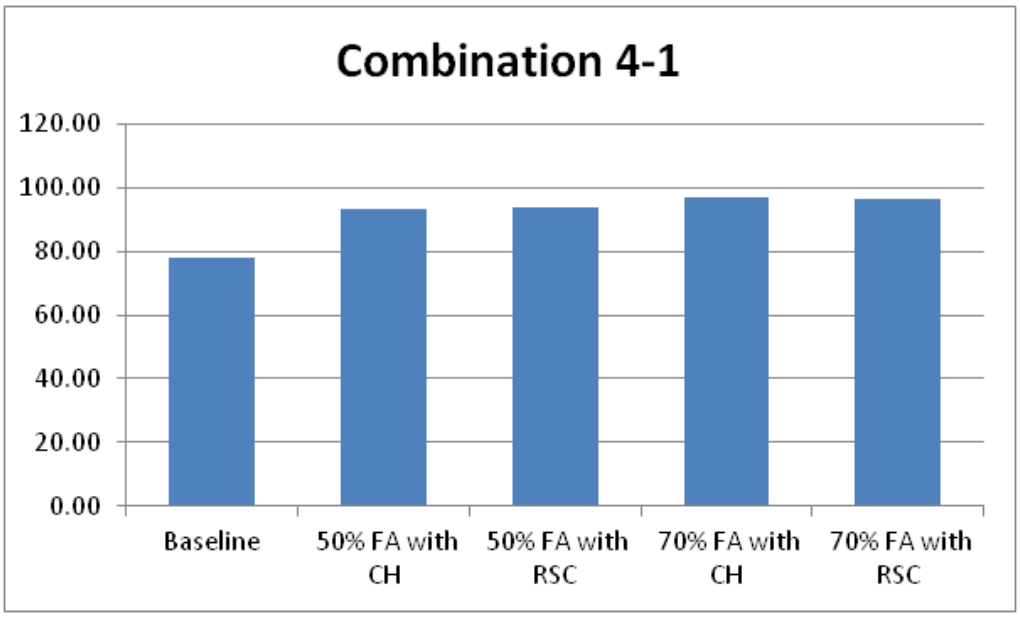

Figure 5.33 - Durability Factors of 4-1 Combinations

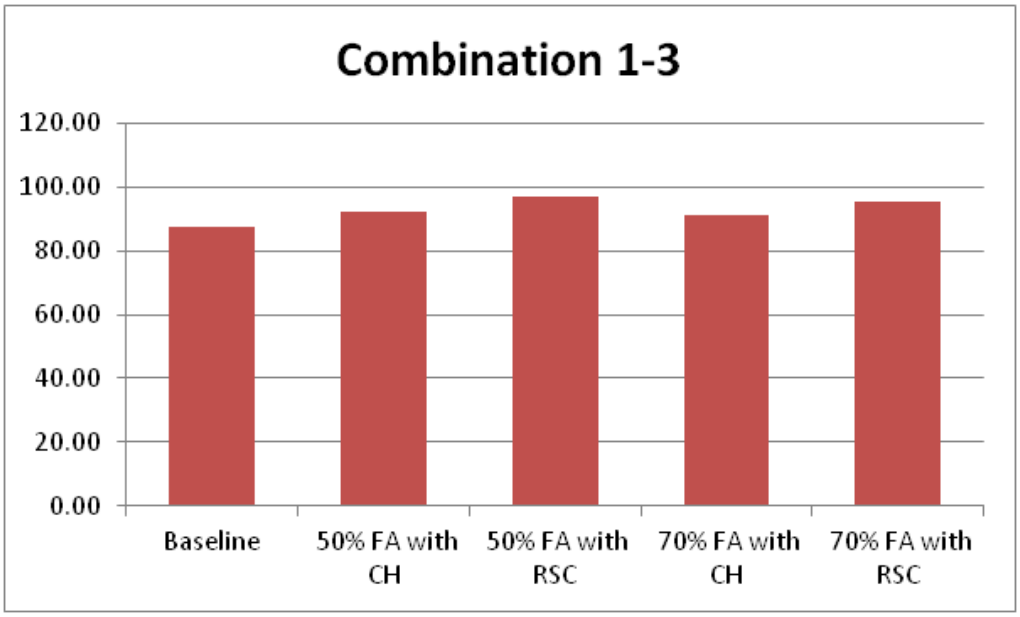

Figure 5.34 - Durability Factors of 1-3 Combinations

5.5.2.9. Salt Scaling Resistance. Three replicates of each mixture were tested for scaling resistance. Specimens were visually rated every five cycles, and rankings typically matched across all three replicate specimens. Small variations in finishing procedure may have led to differing rankings between specimens although most tests showed no variation between replicates. The results are shown in **Figure 5.35**. The baseline mixtures performed adequately (Scaling Scale ≤ 2), showing only very slight scaling (blend 4-1 rated 1 and blend 1-3 rated 2). This suggests that the molding and finishing procedures were adequate. Most fly ash mixtures showed severe scaling (rating = 5), defined by ASTM C 672 as coarse aggregate being visible over the entire surface of the specimen. Two mixtures (blend 1-3) fared slightly better: the 50% fly ash with RSC had a rating of 4, and the 70% fly ash with RSC was a 3. The mixtures containing 70% replacement of cement with fly ash show a much more rapid scaling than those containing 50%, albeit with the same end result. This tendency toward severe scaling

seems to mirror previous findings where eight different fly ashes with both high calcium contents and low calcium contents (corresponding to Class C and Class F) were examined. At 58% fly ash replacement, all 16 of the mixes showed severe scaling after 50 cycles according to ASTM C 672 (Bilodeau, et al., 1994). Results are tabulated in Appendix J.

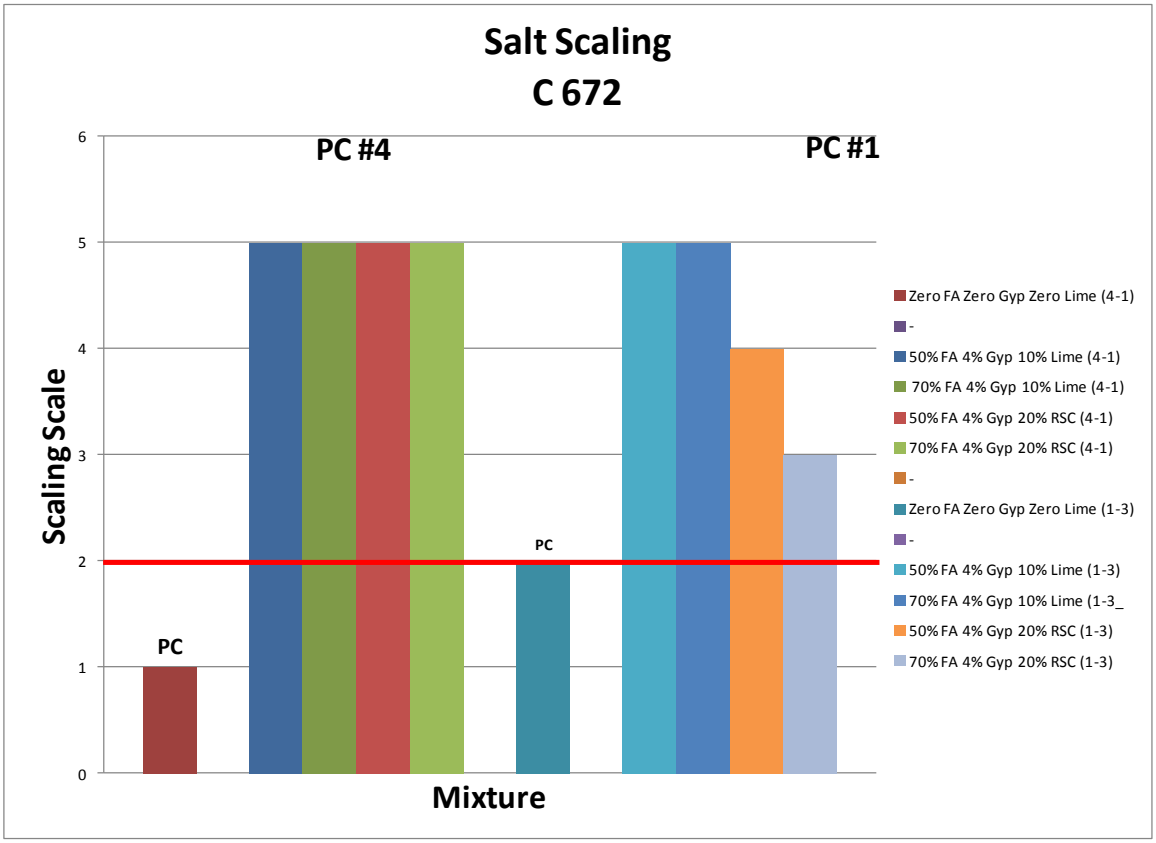

Figure 5.35 – Salt Scaling Results

6. SUMMARY AND CONCLUSIONS

In the Paste Screening Study, 25 combinations of five Type I/II portland cements and five Class C fly ashes in paste form with no chemical or powder additives were tested by semi-adiabatic calorimetry, Vicat setting time, miniature slump, and compressive strength at one and 28 days at room temperature. The two most reactive and least reactive combinations (defined by one day strengths) were further evaluated in the Main Effects Study.

In the Paste Main Effects Study, the effects of two levels each of WR/HRWR, gypsum, lime, RSC, and gypsum-lime, and gypsum-RSC were determined. Except for the WR/HRWR experiment, all other mixtures contained the low (2.75 fl oz/cwt) dosage. Except for the gypsum level experiment, all other mixtures contained 4% gypsum by mass of fly ash. The lime levels were 5 and 10% and the RSC levels were 10 and 20%, both by mass of fly ash.

The objective of the Concrete Properties Study was to scale up the most promising powder additive combinations from paste to concrete and evaluate the mixtures in terms of plastic and hardened properties. Thus the mixture matrix included OPC-fly ash blends at two levels (“4-1” and “1-3) and fly ash at three levels (zero, 50 and 70%). WR dosage (nominal 2.75 fl oz/cwt), gypsum content (4%), lime content (10%), and RSC content (20%) were held constant. The following are conclusions reached from the study of HVFA.

6.1. FLUIDITY

Increasing fly ash contents increased fluidity as evidenced by a greater spread of paste in the miniature slump test, and by decreasing required dosages of WR/HRWR to maintain fluidity in the concrete slump test. One exception to this was the 1-3 blend which required additional WR/HRWR. In all cases, the mixtures containing RSC need more WR/HRWR than their lime counterparts.

6.2. AIR ENTRAINMENT

As fly ash content increased, the required dosage to maintain 5% air decreased.

6.3. MICROWAVE WATER CONTENT

Within the confines of a limited use in this study, the microwave water content test method appears to have potential for field checking of the water content (and hence w/cm) of plastic concrete in the field.

6.4. REACTION TIME

Reaction time was evaluated by a combination of tests: semi-adiabatic calorimetry, Vicat setting time, and miniature slump early stiffening. Whether a given mixture behaved normally or was accelerated or retarded was a function of many variables, including the characteristics of the OPC and fly ash in conjunction with each other, type and level of powder additives used, dosage of WR/HRWR, and the type of test method used for evaluation.

At the 0.40 w/cm, the use of WR/HRWR was necessary to restore workability. The effect of WR/HRWR generally was to slow down reactions and their outcomes. Calorimeter curves were usually delayed and one day strengths were lower. However, the effect on setting times and early stiffening were mixed. Many times the setting time was accelerated, but sometimes retarded. Likewise, early stiffening was usually an issue, and but sometimes not. Beyond one day, strengths were usually increased. Overall, there was no clear advantage between the two dosage levels.

Fly ash effects on initial setting time were mixed. At 25%, retardation usually occurred. At 50%, both retardation and acceleration occurred. At 70%, many times acceleration occurred.

Gypsum addition generally usually delayed the calorimeter curves or was negligible. The higher dosage made a more pronounced effect. Setting time usually was retarded. Because in all four cases the setting time had been accelerated by the high fly ash substitution, retarding by gypsum was a positive benefit. Early stiffening tendencies were either improved or were negligibly affected.

The calorimeter curves were shifted to earlier times, with the 10% level earlier than the 5% level. The 10% lime mixture positions were almost restored back to where the zero fly ash curves were. Initial setting times had been accelerated by the replacement of fly ash. Upon addition of gypsum-lime, the 4-1 blend was retarded at both levels of fly ash, approaching the zero fly ash values (an improvement), but there was little effect on the 1-3 blend setting times. The tendency to early stiffen was alleviated somewhat by gypsum-lime in every blend but one, with the 10% level usually better.

In all cases of gypsum-RSC addition, the calorimeter curves were accelerated. In regard to initial setting time, all four blends had been accelerated by the fly ash replacement, three of the four severely so. Unfortunately, addition of gypsum-RSC made it worse in one blend, was negligible in two others, and helped (retarded) somewhat in the fourth blend. Also, in almost all mixtures, the early stiffening tendencies were significantly worsened. It should be noted that the combined SO3 content in some of these mixtures is somewhat high.

6.5 COMPRESSIVE STRENGTH

An increase in fly ash content decreased strength at all ages (one to 56 days). One day compressive strengths were greatly reduced by 50 fly ash replacement and even more so with 70% fly ash, even with the use of powder additives. In the paste study, one day compressive strengths were not enhanced much by gypsum, lime, or RSC by themselves, but gypsum-lime and gypsum-RSC did improve early strengths. In the concrete study, where gypsum was always present, the trend in strength loss was the same as in the paste. Effects of lime vs. RSC were not much different. That said, 12 combinations at 50% fly ash in the Screening Study met the 1200 psi (8.3 MPa) one day strength min. threshold with no powder additions, and in the concrete study, both 4-1 blends with lime or RSC met the 1000 psi (6.9 MPa) threshold. For concrete, all the 50% fly ash mixtures had reached 3000 psi (20.7 MPa) by day 7, with little advantage to lime vs. RSC. By day 28, all 50% mixtures had caught up with the OPC mixtures, and by 56 days, had exceeded the OPC strengths. The 70% mixtures lagged: however, they reached 3000 psi (20.7 MPa) by 28 days and about 3500 psi (24.1 MPa) at 56 days. For the most part, there was

no clear advantage of lime compared to RSC. Which one gave a little more strength depended on the specific blend and fly ash level.

6.6. FLEXURAL STRENGTH

All tests were conducted at 28 days. Depending on the blend, the 50% fly ash mixtures were about the same strength as the OPC mixture, or somewhat below, although the weakest was still greater than 600 psi (4.1 MPa). At the 70% fly ash level, strengths dropped below the 50% fly ash level. Only one mixture achieved 550 psi (3.8 MPa).

6.7. SPLITTING TENSILE STRENGTH

At the 50% fly ash level, the splitting tensile strengths either slightly exceeded or were a bit below the OPC strengths. 70% fly ash level mixtures were weaker than 50% fly ash mixtures.

6.8. MODULUS OF ELASTICITY

As a general rule, the 50% fly ash MOE values were close to, and in some cases slightly greater than the OPC strengths. As expected, the 70 % mixtures were lower in MOE.

6.9. ABRASION RESISTANCE

Abrasion resistance was measured in terms of both mass loss and depth of wear. As expected, as fly ash level increased, abrasion resistance decreased significantly. Results were mixed and not greatly different between lime and RSC. The abrasion

resistance at 56 days was greater than at 28 days, but with only the 50% mixtures approaching the OPC levels of resistance.

6.10. DRYING SHRINKAGE

At the time of writing, the drying specimens were 80 to 100 days old. The fly ash mixtures had lower shrinkage values than OPC mixtures. In the 4-1 blend case, the 70% fly ash level mixtures had the lowest shrinkage, while the case of 1-3 blend, the 50% fly ash level mixtures were lower.

6.11. RAPID CHLORIDE PERMEABILITY

RCP specimens were tested at 28 days. In three of the four of the cases, at 50% fly ash, RCP was lower in the fly ash specimens than the OPC mixtures. However, all mixtures at 70% fly ash had the greatest permeabilities, with RSC mixtures having lower values than lime mixtures.

6.12. FREEZE-THAW RESISTANCE

Both 4-1 and 1-3 blends exhibited higher durability factors than their respective OPC counterparts. Fly ash DF’s were 93 or more.

6.13. SALT SCALING

OPC mixture specimens achieved scaling scores of 1 and 2 indicating adequate scaling resistance. All fly ash mixtures fared worse, with the 70% mixtures deteriorating more rapidly. Most fly ash mixtures reach a maximum level of 5; at the time of writing,

two mixtures are at 40 cycles and are already at scores of 3 and 4. However, several studies of actual pavements and sidewalks subjected to numerous freeze-thaw cycles and deicers have shown very good resistance to scaling, suggesting that the scaling test method is too severe (Bouzoubaa, et al.2001; Naik et al., 2003).

6.14. BOTTOM LINE

6.14.1 Compressive strength. At the 50% fly ash level, one day strengths were low no matter what powder additive was used, but 1000 psi (MPa) was reached in a number of OPC-fly ash blends, with and without powder additions. Good strengths can be achieved at 3 days. At the 70% fly ash level, concrete is weaker, but reasonable strengths can be reached at 28 days.

6.14.2. Abrasion Resistance. At 50% fly ash, resistance is somewhat lower. At 70% the effect is much worse.

6.14.3. Drying Shrinkage. It appears that HVFA mixtures shrink less than their OPC counterparts.

6.14.4. Rapid Chloride Permeability. In a comparison to OPC mixtures, RCP is lower for 50% fly ash mixtures, but 70% fly ash mixtures are more permeable.

6.14.5. Freeze-Thaw Resistance. All HVFA mixtures had greater DF's than the OPC mixtures.

6.14.6. Salt Scaling. All fly ash mixtures did poorly in regard to salt scaling.

6.14.7. Reaction Time. Reaction time (calorimeter curve time, setting time, stiffening time) varied as a function of characteristics of the OPC and fly ash in

conjunction with each other, type and level of powder additives used, dosage of WR/HRWR, and the type of test method used for evaluation.

7. RECOMMENDATIONS

HVFA concrete at a 50% cement replacement level has been shown to be feasible under certain circumstances and applications, while use of a replacement at 70% level would be more restricted. In regard to 50% fly ash mixtures, it appears that although one day strengths may be low, certain blends of OPC and fly ash can reach minimum required strengths. Reasonable three day and later strengths can be achieved through use of certain powder activators, such as a combination of gypsum and lime or gypsum and rapid set cement. Delayed setting times may be problematic, thus construction operations would be impacted, especially during cool weather. However, certain blends of cement-fly ash-water reducers may actually accelerate hydration to the point of flash setting. Durability seems satisfactory in regard to permeability and freeze-thaw resistance. At this stage of development, use of HVFA for pavements, bridge decks, and other exterior slabs is not recommended because of salt scaling potential and possibly issues of excessive wear. The subject of plastic shrinkage cracking was not explored in this research project, but slabs with HVFA concrete may be prone to this problem.

Before HVFA is contemplated for use in a given project, it is absolutely imperative that the specific cement, fly ash, and admixtures be checked for incompatibilities through use of semi-adiabatic calorimetry, miniature slump, Vicat setting time, and the strength-type-of-interest at early, middle, and late ages, all at the temperature that will prevail during construction. Elevated temperatures are known to create additional incompatibilities with the cement, fly ash, and admixtures. Additionally, if the sulfate level will be adjusted (increased) through use of gypsum, RSC, or other source of sulfate, the mixture should be checked for excessive expansion characteristics.

REFERENCES

AASHTO. (2002). "Water content of freshly mixed concrete using microwave oven drying." *AASHTO T 318-02*, American Association of State Highway and Transportation Officials, Washington, D. C.

ACI. (1991). "Standard Practice for Selecting Proportions for Normal, Heavyweight, and Mass Concrete," *ACI 211.1-91*, American Concrete Institute, Farmington, MI.

ASTM. (2003). "Standard test method for scaling resistance of concrete surfaces exposed to deicing chemicals." *ASTM C 672/C 672M – 03*, ASTM International, West Conshohocken, PA.

ASTM. (2004). "Standard test method for materials finer than no. 200 sieve in mineral aggregates by washing." *ASTM C 117 – 12*, ASTM International, West Conshohocken, PA.

ASTM. (2005a). "Standard test method for heat of hydration of hydraulic cement." *ASTM C 186 – 05*, ASTM International, West Conshohocken, PA

ASTM. (2005b). "Standard test method for abrasion resistance of concrete or mortar surfaces by the rotating-cutter method." *ASTM C 944/C 944M – 99*, ASTM International, West Conshohocken, PA.

ASTM. (2006a). "Standard practice for mechanical mixing of hydraulic cement pastes and mortars of plastic consistency." *ASTM C 305 – 06*, ASTM International, West Conshohocken, PA.

ASTM. (2006b). "Standard test method for sieve analysis of fine and coarse aggregates." *ASTM C 136 – 06*, ASTM International, West Conshohocken, PA.

ASTM. (2007). "Standard practice for making and curing concrete test specimens in the laboratory." *ASTM C 192/C 192M – 07*, ASTM International, West Conshohocken, PA.

ASTM. (2008a). "Standard test method for compressive strength of hydraulic cement mortars (using 2-in. or [50-mm] cube specimens." *ASTM C 109/C 109M – 08*, ASTM International, West Conshohocken, PA.

ASTM. (2008b). "Standard test method for time of setting of hydraulic cement by Vicat needle." *ASTM C 191 – 08*, ASTM International, West Conshohocken, PA.

ASTM. (2008c). "Standard test method for time of setting of concrete mixtures by penetration resistance." *ASTM C 403/C 403M – 08*, ASTM International, West Conshohocken, PA.

ASTM. (2008d). "Standard test method for length change of hardened hydraulic-cement mortar and concrete." *ASTM C 157/C 157 M – 03*, ASTM International, West Conshohocken, PA.

ASTM. (2008e). "Standard test method for resistance of concrete to rapid freezing and thawing." *ASTM C 666/C 666M – 03*, ASTM International, West Conshohocken, PA.

ASTM. (2009). "Standard practice for measuring the hydration kinetics of hydraulic cementitious mixtures using isothermal calorimetry." *ASTM C 1679 – 09*, ASTM International, West Conshohocken, PA.

ASTM. (2010a). "Standard test methods for slump of hydraulic cement concrete." *ASTM C 143/C 143M – 10a*, ASTM International, West Conshohocken, PA.

ASTM. (2010b). "Standard test method for normal consistency of hydraulic cement." *ASTM C 187 – 10*, ASTM International, West Conshohocken, PA.

ASTM. (2010c). "Standard test method for air content of freshly mixed concrete by the pressure method." *ASTM C 231/C 231M – 10*, ASTM International, West Conshohocken, PA.

ASTM. (2010d). "Standard test method for flexural strength of concrete (using simple beam with third-point loading)." *ASTM C 78/C 78M – 10*, ASTM International, West Conshohocken, PA.

ASTM. (2010e). "Standard test method for static modulus of elasticity and Poisson's ratio of concrete in compression." *ASTM C 469/C 469M – 10*, ASTM International, West Conshohocken, PA.

ASTM. (2011a). "Standard practice for evaluating hydration of hydraulic cementitious mixtures using thermal measurements (draft)." *ASTM WK23967*, ASTM International, West Conshohocken, PA.

ASTM. (2011b). "Standard test method for splitting tensile strength of cylindrical concrete specimens." *ASTM C 496/C 496M – 11*, ASTM International, West Conshohocken, PA.

ASTM. (2011c). "Standard test method for temperature of freshly mixed hydraulic-cement concrete." *ASTM C 1064/C 1064M – 11*, ASTM International, West Conshohocken, PA.

ASTM. (2012a). "Standard test method for density, relative density (specific gravity), and absorption of coarse aggregate." *ASTM C 127 – 12*, ASTM International, West Conshohocken, PA.

ASTM. (2012b). “Standard test method for density, relative density (specific gravity), and absorption of fine aggregate.” *ASTM C 128 – 12*, ASTM International, West Conshohocken, PA.

ASTM. (2012c). “Standard test method for density (unit weight), yield, and air content (gravimetric) of concrete.” *ASTM C 138/C 138M – 12*, ASTM International, West Conshohocken, PA.

ASTM. (2012d). “Standard test method for compressive strength of cylindrical concrete specimens.” *ASTM C 39/C 39M – 12*, ASTM International, West Conshohocken, PA.

ASTM. (2012e). “Standard test method for electrical indication of concrete’s ability to resist chloride ion penetration.” *ASTM C 1202 – 12*, ASTM International, West Conshohocken, PA.

Bentz, D. P. (2010). “Powder additions to mitigate retardation in high-volume fly ash mixtures.” *ACI Materials Journal*, 107(5), 508-514.

Bentz, D. P. and Ferraris, C. F. (2010). “Rheology and setting of high volume fly ash mixtures.” *Cement & Concrete Composites*, 32, 265-270.

Bentz, D. P., Chiara, F. F., De La Varga, I., Peltz, M. A., & Winpigler, J. A. (2010). "Mixture Proportioning Options for Improving High Volume Fly Ash Concretes." *International Journal of Pavement Research and Technology, 3*(5), 234-240.

Bhattacharja, S. and Tang, F. J. (2001). “Rheology of cement paste in concrete with different mix designs and interlaboratory evaluation of the mini-slump cone test.” *PCA R&D Serial No. 2412*, Portland Cement Association, Skokie, IL.

Bilodeau, A., Sivasundaram, V., Painter, K. E., and Malhotra, V. M. (1994). “Durability of concrete incorporating high volumes of fly ash from sources in the U.S.” *ACI Materials Journal*, 91(1), 3-12.

Bouzoubaa, N., Bilodeau, A., Sivasundaram, V., & Chakraborty, A. (2007). "Mechanical Properties and Durability Characteristics of High Volume Fly Ash Concrete Made with Ordinary Portland Cement and Blended Portland Fly Ash Cement." *ACI Special Publication 242*, American Concrete Institute, Farmington Hills, MI, 303-320.

Bouzoubaa, N., Zhang, M. H., Malhotra, V. M., & Golden, D. M. (2001). "Mechanical Properties and Durability of Laboratory Produced High-Volume Fly Ash Blended Cements." *ACI Special Publication 199,* American Concrete Institute, Farmington Hills, MI, 55-82.

Calmetrix. (2010a). “Calcommander software v1.3 user manual.” Calmetrix, Inc.

Calmetrix. (2010b). “F-cal 4000/8000 user manual.” Calmetrix, Inc.

Cost, T. (2009). “Thermal measurements of hydrating concrete mixtures.” *NRMCA Publication 2PE004*, National Ready Mixed Concrete Association, Silver Spring, MD.

Cost, V. T. and Knight, G. (2007). “Use of thermal measurements to detect incompatibilities of common concrete materials.” *ACI Special Publication 241*, American Concrete Institute, Farmington Hills, MI, 39-58.

Detwiler, R. J., Bhatty, J. I., and Bhattacharja, S. (1996). “Supplementary cementing materials for use in blended cements.” *Research and Development Bulletin RD112T*, Portland Cement Association, Skokie, IL.

Cabrera, J. G., & Atis, C. D. (1999). "Design and Properties of High Volume Fly Ash High-Performance Concrete." *ACI Special Publication 186,* American Concrete Institute, Farmington Hills, MI, 21-31

Galeota, D., Giammatteo, M., and Marino, R. (1995). “Structural concrete incorporating high volume of fly ash.” *ACI Special Publication 153,* American Concrete Institute, Farmington Hills, MI, 25-42.

Gibbon, G. J., Ballim, Y., and Grieve, G. R. H. (1997). “A low-cost, computer-controlled adiabatic calorimeter for determining the heat of hydration of concrete.” *Journal of Testing and Evaluation*, 25(2), 261-266

Gu, P., Beaudoin, J. J., Zhang, M.-H., & Malhotra, V. (1999). "Performance of Steel Reinforcement in Portland Cement and High-Volume Fly Ash Concretes Exposed to Chloride Solution. " *ACI Materials Journal, 96*(5), 551-558.

Hübert, C., Wieker, W., & Heideman, D. (2001). "Investigations of Hydration Products in High-Volume Fly Ash Binders. " *ACI Special Publication 199,* American Concrete Institute, Farmington Hills, MI, 83-97

Jiang, L., Lin, B., & Cai, Y. (1999). "Studies on Hydration in High-Volume Fly Ash Concrete Binders." *ACI Materials Journal*, *96*(6), 703-706.

Kantro, D. L. (1980). “Influence of water-reducing admixtures on properties of cement paste – a miniature slump test.” *Cement, Concrete, and Aggregates*, 2(2), 95-102.

Lerch, W. (1946). “The influence of gypsum on the hydration and properties of portland cement pastes.” *Bulletin 12,* Portland Cement Association, Chicago, IL.

Marlay, K.M. (2011), “Hardened concrete properties and durability assessment of high volume fly ash concrete,” M.S. Thesis, Missouri Univ. of Science and Technology, Rolla, MO.

Mehta, P., & Montiero, P. J. (1993). *Concrete Microstructure, Properties, and Materials.* McGraw-Hill.

Mindess, S., Young, J. F., and Darwin, D. (2003). “Concrete.” Prentice Hall, Upper Saddle River, NJ.

MoDOT. (2011a), “Concrete, section 501, standard specifications.” Jefferson City, MO.

MoDOT. (2011b), “Aggregate for concrete, section 501, standard specifications.” Jefferson City, MO.

NCPTP. (2007), “Integrated materials and construction practices for concrete pavement: a state of the practice manual,” National Concrete Pavement Technology Center, FHWA No. HIF-07-004, Washington, D.C.

Nagi, M. and Whiting, D. (1994). “Determination of water content of fresh concrete using a microwave oven.” *Cement, Concrete, and Aggregates*, 16(2), 125-131.

Naik, T. R., Ramme, B. W., Kraus, R. N., & Siddique, R. (2003). "Long-Term Performance of High-Volume Fly Ash Concrete Pavements." *ACI Materials Journal, 100*(2), 150-155.

Naik, T. R., Ramme, B. W., and Tews, J. H. (1995). “Pavement construction with high-volume Class C and Class F fly ash concrete.” *ACI Materials Journal*, 92(2), 200-210.

Naik, T. R., Singh, S. S., and Ramme B. W. (2002). “Effect of source of fly ash on abrasion resistance of concrete.” *Journal of Materials in Civil Engineering*, 14(5), 417-426.

Rivest, M., Bouzoubaa, N., and Malhotra, V. (2004). “Strength development and temperature rise in high-volume fly ash and slag concretes in large experimental monoliths.” *ACI Special Publication 221*, American Concrete Institute, Farmington Hills, MI, 859-878.

Roberts, L. R. and Taylor, P. C. (2007). “Understanding cement-SCM-admixture interaction issues.” *Concrete International*, 29(1), 33-41.

Rosli, A., & Harnik, A. (1980). "Improving the Durability of Concrete to Freezing and Deicing Salts." *Durability of Building Materials and Components*, pp. 464-473.

Sandberg, J. P. and Liberman, S. (2007). “Monitoring and evaluation of cement hydration by semi-adiabatic field calorimetry.” *ACI Special Publication 241*, American Concrete Institute, Farmington Hills, MI, 13-23.

Wang, K. (2006). “Monitoring heat evolution of concrete mixtures.” *National Concrete Pavement Technology Center*

Wang, H. C., Qi, C., Farzam, H., & Turici, J. (2006). "Interaction of Materials Used in Concrete." *Concrete International, 28*(4), 47-52.

APPENDICES

APPENDIX A
Miniature Slump, Cement Cubes, and Calorimeter Combined Mixing Procedure
(6-19-2012)

Procedure

1. Refer to Miniature Slump, Cement Cubes, and Calorimeter procedures for preparations needed prior to mixing cement paste.
2. Add all cementitious materials to the mixing bowl and follow the time schedule below. Refer to Miniature Slump, Cement Cubes, and Calorimeter procedures for more detail.

Elapsed Time (mm:ss)	Action
0:00	Add water to mixing bowl with cementitious materials Record time (Start Time)
0:10	Start mixing at Speed 2 (440 RPM)
0:30	Start mixing at Speed 6 (670 RPM)
1:30	Stop mixing Record temperature of paste Prepare mini-slump test
2:00	Lift mini-slump cone
4:00	Remix paste at Speed 2
4:30	Prepare mini-slump test
5:00	Lift mini-slump cone Prepare calorimeter specimens Insert calorimeter specimens in F-Cal 4000
10:00	Close and latch the lid of the F-Cal 4000
13:00	Remix paste at Speed 2
13:30	Prepare mini-slump test
15:00	Lift mini-slump cone

	Mold cement cubes
28:00	Remix paste at Speed 2
28:30	Prepare mini-slump test
30:00	Lift mini-slump cone
43:00	Remix paste at Speed 2
43:30	Prepare mini-slump test
45:00	Lift mini-slump cone
60:00	Measure and record mini-slump diameters

APPENDIX B

Using the F-Cal 4000 & CalCommander Software for Testing Cement Paste

(Calmetrix F-Cal 4000/8000 User Manual, CalCommander Software v1.3 User Manual, and ASTM C 305)

(Revised 6-19-2012)

Equipment and Materials

1. F-Cal 4000, USB cable, and CalCommander Software v1.3.
2. Black and Decker 250-Watt Hand Mixer (Model MX217) with egg beater paddles
3. 20-quart Hobart mixing bowl
4. Plastic ladle
5. Hamilton 1-mL Adjustable Volume SoftGrip Pipette (readable to 0.01 mL)
6. 3-quart or larger white plastic bowl with spout
7. Metal spoon
8. Small stainless steel spatula
9. Four, clean 4”x8” plastic cylinder molds and caps per mix
10. Sper Scientific Humidity/Temperature Monitor (Model 800016)
11. Analog thermometer with 5-inch probe
12. High silica sand obtained from U.S. Silica, Pacific, MO
13. 12-kg Denver Instrument balance
14. Space heater
15. Microsoft Excel and TableCurve 2D software

Procedure

1. At least 1 hour before inserting the first specimen: connect the F-Cal to the computer using the USB cable, open the CalCommander program, click

on the “F-Cal Logger” tab at the top of the window, and click on “Start Logging” at the right side of the window.

2. To enter information about the mix: click “Read Configuration from Logger”, click on the tab in the bottom portion of the window which corresponds to the slot in which the specimen will be placed in the F-Cal; enter the Mix ID, Water/Cement Ratio, Cement Source, Cement Content (lbs/cy), and any SCMs (Type, Percent, and Source); and click “Update Configuration File” on the right side of the window. Also, make sure the Sensor Enabled box is checked.
3. Prepare a clean mold with a 1250 gram inert specimen. The inert specimen consists of high silica sand and deionized water. The proportion of water to oven-dried sand should reflect the proportion of water to cementitious materials used in the mixture being tested.
4. Verify that the air temperature is 23.0±3.0°C (68.0-78.8°F), mixing water temperature is 23.0±2°C (69.8-77.0°F), and that the relative humidity of the air is not less than 50%. Record these parameters.
5. To blend the dry constituents of the mix: Place about 1000 grams of the dry materials into a 4”x8” cylinder mold in the same proportions to be used in the paste mixture, hold the cylinder horizontally with one hand on each end of the cylinder, and then shake the cylinder 25 cycles using a 6” throw.
6. To dissolve admixtures into the mix water: Place all of the deionized water into the plastic bowl, use the 1-mL syringe to add the desired amount of admixture to the water, and use the small spatula to gently stir the water until all of the admixture is dissolved.
7. Add the pre-mixed cementitious materials to the mixing bowl, forming a donut shape.
8. Add all of the mix water to the mixing bowl, start the timer, and record the time (Start Time).
9. Wait 10 seconds to allow the cement to absorb the water.

10. Mix at Speed 2 (440 RPM) for 20 seconds. Rotate the bowl 90° every 5 seconds.
11. Mix at Speed 6 (670 RPM) for 60 seconds. Rotate the bowl 90° every 15 seconds and occasionally run the mixing paddles along the side of the bowl.
12. At the end of the initial mixing, record the temperature of the paste.
13. At 4 minutes, remix the paste at Speed 2 for 30 seconds.
14. After remixing, pour 1250 grams of paste into each of the three remaining 4”x8” cylinder molds. Tap each cylinder with an open hand 10 times to remove entrapped air.
15. Quickly cap the molds, ensure that the outsides of the molds are clear of paste or other debris, and place the molds into the appropriate slots in the F-Cal (including the mold with the control sand). This should be done within 10 minutes after the Start Time.
16. Enter the “Mix Date/Time” (noted in step #8) and “Mix Temperature” (noted in step #12) into the software under the mix information tabs and click “Update Configuration File”.
17. Disconnect the USB cable from the computer and F-Cal, close and latch the F-Cal lid, and leave the specimens for at least 48 hours. Note: shorter logging times may be used depending on the amount of information desired and prior knowledge of the materials being tested.
    (CAUTION: DO NOT MOVE THE F-CAL WHILE TESTING IS IN PROGRESS)
18. After 48 hours, open the F-Cal lid, reconnect the USB cable, open the CalCommander software, click the “F-Cal Logger” tab, and click “Read Data from Logger” at the right side of the window. If it is decided that logging should cease, click “Stop Logging”.
19. Save the log data by clicking “Read Data from Logger” and then selecting “Save Log Data to File”.
20. Remove the specimens from the F-Cal.

21. To export data: click on “F-Cal Reports” at the top of the CalCommander software window, click “Add Logs” in the bottom right corner of the screen, select the appropriate file(s), select “Accept” in the “Add F-Cal/AdiaCal Logs” window, select the tab corresponding to the channel from which data is needed, click on “Save Selected Log as Text File” in the bottom right corner of the screen, input desired file name, and click “Save”.
22. To import data into Microsoft Excel: Open Microsoft Excel, select “Data” at the top of the screen, go to “Import External Data”, click “Import Data...”, double-click on the desired text file, click the “Next >” button two times in the “Text Import Wizard” window, click “Finish”, and then select “OK” in the “Import Data” window.
23. Record the Signal-to-Noise Ratio for each specimen. The Signal is the difference between the highest and lowest temperatures recorded for the sample being tested. The Noise is the difference between the highest and lowest temperatures recorded for the inert specimen. To calculate the Signal-to-Noise Ratios:

    a. Import the data for each specimen into Excel.

    b. Determine the difference between the time logging began and the time water was added to the cementitious materials (Start Time). This will be used to determine the log time that corresponds to the Start Time.

    c. For each specimen log, find the maximum temperature by using the MAX function for the range of specimen temperatures starting with the log time that corresponds to the Start Time and ending at the end of the logging period. To find the minimum temperature, follow a similar procedure using the MIN function for the same range.

    d. Calculate the Signal for each specimen by subtracting the minimum specimen temperature from the maximum specimen temperature.

    e. Calculate the Noise by subtracting the minimum temperature of the inert specimen from the maximum temperature of the inert specimen.

f. Divide the Signal for each specimen by the Noise to determine the Signal-to-Noise ratio for each specimen.

24. To estimate set times using the Percentage Method:

a. Import the data for each specimen into Excel.

b. Determine the difference between the time logging began and the time water was added to the cementitious materials (Start Time). This will be used to determine the log time that corresponds to the Start Time.

c. Remove all log data prior to the log time corresponding to the Start Time.

d. Find the average temperature log for the specimens by averaging the temperatures of the three specimens at every minute for the duration of the logging.

e. Subtract the inert specimen temperature log from the average temperature log to determine the corrected average temperature log.

f. Plot the corrected average hydration curve by plotting the corrected average temperatures against time.

g. Visually examine the curve to determine a time window that encompasses the dormant period and the peak of the hydration curve. There will be an initial rise in the temperature near time zero that indicates the initial rise in temperature of the thermistors from the ambient temperature to the specimen temperature. This area should not be considered to be part of the dormant period.

h. Use the MAX and MIN functions, within the time range chosen above, to determine the maximum and minimum temperatures (ΔT_{max} and ΔT_{min}) of the hydration curve.

i. Using the values from Step 25.h., calculate the main hydration response rise ($M = \Delta T_{max} - \Delta T_{min}$), twenty percent of the main hydration response rise ($M_{20\%} = 0.2M$), and fifty percent of the main hydration response rise ($M_{50\%} = 0.5M$).

j. Initial Set is taken as the time when 20% of the main hydration response rise ($M_{20\%}+\Delta T_{min}$) occurs.

k. Final Set is taken as the time when 50% of the main hydration response rise ($M_{50\%}+\Delta T_{min}$) occurs.

25. To estimate set times using the Derivatives Method:

a. Copy and paste the time log and corrected average temperature log from Step 25, above, into a new Excel file.

b. In TableCurve 2D, click “Import” in the upper left corner of the window and “Open” the Excel file.

c. In the “Select Columns for X-Y Data Table” window, select “(1)Sheet1!A” for the X Column, select “(1)Sheet1!B” for the Y Column, and then select “OK”.

d. In the “Data Description and Variable Names” window, enter a title for the plot, enter titles for the axes, and select “OK”.

e. Select “Data” at the top of the window, choose “Section Data...”, select a time range from the dormant period to the peak of the main hydration curve, click the green checkmark box in the upper left corner, and select “Yes” in the “Update Data Table” window.

f. Select “Process” at the top of the window, choose “Curve-Fit All Equations”, and select “Graph Start” after fitting has ceased. The curve-fit automatically applied has the highest R-squared value and should not be changed.

g. On the left side of the screen, select “Numeric”. Look toward the bottom of the “Numeric Summary” screen to find the “1st Deriv max” and the “2nd Deriv max” with corresponding X-Values.

h. The time for Initial Set is the x-value corresponding to the maximum second derivative (2nd Deriv max).

i. The time for Final Set is the x-value corresponding to the maximum first derivative (1st Deriv max).

Calorimeter Data Sheet

High Volume Fly Ash Cement Paste Study

Date: _____

Technician: _____

Mix ID: _____

Cement: _____ % Fly Ash: _____ % Gypsum: _____ %

CH: _____ % RS Cem: _____ % Admix: _____ w/cm: _____

Cement Source: _____ Fly Ash Source: _____

Thermal Measurement Equip.: _____ Specimen Containers: _____

Material Type: _____

Inert Specimen Preparation	
Total Design Mass, $m_{i,T}$ (g):	
Proportion of Water to Sand, w/s [=w/cm]:	
Design Mass of Sand, $m_{i,S}$ (g) [=($m_{i,T}$)/(1+w/s)]:	
Design Mass of Water, $m_{i,W}$ (g) [=$m_{i,T}$ - $m_{i,S}$]:	
Actual Mass of Sand (g):	
Actual Mass of Water (g):	
Total Actual Mass of Inert Specimen (g):	

Mixing and Sample Preparation	
Air Temperature (°F):	
Water Temperature (°F):	
Relative Humidity (%):	
Start Time:	
Admix Addition Time:	
Paste Temp. at End of Mixing (°F):	
Sample 1 Mass (g):	
Sample 2 Mass (g):	
Sample 3 Mass (g):	

Signal-to-Noise Ratios (Raw Data)	
Inert Specimen	
Max. Temperature of Inert Specimen, $T_{i,max}$ (°F):	
Min. Temperature of Inert Specimen, $T_{i,min}$ (°F):	
Sample 1	
Max. Temperature of Sample, $T_{s,max}$ (°F):	
Min. Temperature of Sample, $T_{s,min}$ (°F):	
Signal-to-Noise Ratio [=($T_{s,max}$-$T_{s,min}$)/($T_{i,max}$-$T_{i,min}$)]:	
Sample 2	
Max. Temperature of Sample, $T_{s,max}$ (°F):	
Min. Temperature of Sample, $T_{s,min}$ (°F):	
Signal-to-Noise Ratio [=($T_{s,max}$-$T_{s,min}$)/($T_{i,max}$-$T_{i,min}$)]:	
Sample 3	
Max. Temperature of Sample, $T_{s,max}$ (°F):	
Min. Temperature of Sample, $T_{s,min}$ (°F):	
Signal-to-Noise Ratio [=($T_{s,max}$-$T_{s,min}$)/($T_{i,max}$-$T_{i,min}$)]:	

Thermal Setting Times (Corrected Average Data)	
Percentage Method	
Max. Temp. of Main Hydration Curve, ΔT_{max} (°F):	
Time when ΔT_{max} Occurs (min):	
Min. Temp. During Dormant Period, ΔT_{min} (°F):	
Main Hydration Response Rise, M (°F) [=ΔT_{max} - ΔT_{min}]:	
20% of Main Hydration Response Rise, $M_{20\%}$ (°F) [=0.2M]:	
$M_{20\%}$+ΔT_{min} (°F):	
Initial Set (min) [=Time when $M_{20\%}$+ΔT_{min} First Occurs]:	
50% of Main Hydration Response Rise, $M_{50\%}$ (°F) [=0.5M]:	
$M_{50\%}$+ΔT_{min} (°F):	
Final Set (min) [=Time when $M_{50\%}$+ΔT_{min} First Occurs]:	
Derivatives Method	
Maximum 2nd Derivative (from Tablecurve):	
Initial Set (min) [=Time when Max. 2nd Derivative Occurs]:	
Maximum 1st Derivative (from Tablecurve):	
Final Set (min) [=Time when Max. 1st Derivative Occurs]:	

Notes/Deviations: _____

APPENDIX C

Miniature Slump Cone
(Kantro (1980) and Bhattacharja & Tang (2001))
(Revised 6-19-2012)

Equipment

1. Black and Decker 250-Watt Hand Mixer (Model MX217) with egg beater paddles

2. 20-quart Hobart mixing bowl
3. Plastic ladle
4. Hamilton 1-mL Adjustable Volume SoftGrip Pipette, (readable to 0.01 mL)
5. 3-quart or larger white plastic bowl with spout
6. Metal spoon
7. Analog thermometer with 5-inch probe
8. Stopwatch
9. Small stainless steel spatula (0.625 in. wide and 4 in. long)

10. 2 mini-slump cones

11. Lucite sheet (0.2 inches thick). Label the area of the sheet where each test will be performed with the time the cone will be lifted (2, 5, 15, 30, 45 minutes)
12. Plastic wrap
13. 5 thin plastic discs (2 in. diameter) cut from Zip-lock bags
14. 12-kg Denver Instrument balance
15. Sper Scientific Humidity/Temperature Monitor (Model 800016)

Procedure

1. Place the 5 plastic discs on the board 8 inches apart on center and at least 3 inches away from any edge of the board.
2. Place each of the two mini-slump cones on a plastic disc.
3. Verify that the air temperature is 23.0±3.0°C (68.0-78.8°F), mixing water temperature is 23.0±2°C (69.8-77.0°F), and that the relative humidity of the air is not less than 50%. Record these parameters.
4. To blend the dry constituents of the mix: Place about 1000 grams of the dry materials into a plastic 4”x8” cylinder mold in the same proportions to

be used in the paste mixture, hold the cylinder horizontally with one hand on each end of the cylinder, and then shake the cylinder 25 cycles using a 6” throw.

5. To dissolve admixtures into the mix water: Place all of the deionized water into the plastic bowl, use the 1-mL syringe to add the desired amount of admixture to the water, and use the small spatula to gently stir the water until all of the admixture is dissolved.
6. Add all cementitious materials to the mixing bowl, forming a donut shape.
7. Add all of the water to the mixing bowl, start the timer, and record the time (Start Time).
8. Wait 10 seconds to allow the cement to absorb the water.
9. Mix at Speed 2 (440 RPM) for 20 seconds. Rotate the bowl 90° every 5 seconds.
10. Mix at Speed 6 (670 RPM) for 60 seconds. Rotate the bowl 90° every 15 seconds and occasionally run the mixing paddles along the side of the bowl.
11. Record the temperature of the paste.
12. At the completion of mixing (1.5 minutes after the Start Time), fill the first mini-slump cone until a slight hump is formed above the top of the cone.
13. Use the spatula with a rodding motion at a slight angle to remove entrapped air. The paste should be “rodded” 5 to 10 times.
14. If the paste is depressed below the top of the cone after removing the entrapped air, use paste spilled on the rim to fill the cone.
15. Use the spatula to strike off the top surface of the cone.
16. At 2 minutes after the Start Time, lift the cone within a few tenths of a second. The lifting motion should be rapid enough for the bottom of the cone to be free of the flowing paste, but slow enough to avoid imparting an upward momentum to the paste as it is flowing from the cone.
17. At 4 minutes after the Start Time, remix the paste remaining in the bowl at Speed 2 for 30 seconds.

18. Pour the paste into the second cone and remove entrapped air with the same procedure used above.
19. At 5 minutes after the Start Time, lift the cone.
20. Cover the remaining paste in the mixing bowl using plastic wrap.
21. At 13 minutes after the Start Time, uncover the paste and remix the paste at Speed 2 for 30 seconds.
22. Pour the paste into a clean, dry cone and remove entrapped air with the same procedure used above.
23. At 15 minutes after the Start Time, lift the cone.
24. Repeat the procedure in Steps 21-23 for slumps at 30 and 45 minutes after the Start Time. See the table, below, which summarizes the mixing, pausing, and testing times
25. At 1 hour after the Start Time, measure and record the diameter of each of the paste pats 4 times using digital calipers. The measurements should each be rotated 45°.
26. Calculate the average diameter of each pat and use the average diameter to calculate the area of the pat. Record this area in square inches.

Elapsed Time (mm:ss)	Action
0:00	Add water to mixing bowl with cementitious materials Record Time (Start Time)
0:10	Start mixing at Speed 2
0:30	Start mixing at Speed 6
1:30	Stop Mixing Record Temperature of Paste Prepare mini-slump test
2:00	Lift mini-slump cone
4:00	Remix paste at Speed 2
4:30	Prepare mini-slump test
5:00	Lift mini-slump cone
13:00	Remix paste at Speed 2
13:30	Prepare mini-slump test
15:00	Lift mini-slump cone
28:00	Remix paste at Speed 2
28:30	Prepare mini-slump test
30:00	Lift mini-slump cone
43:00	Remix paste at Speed 2
43:30	Prepare mini-slump test
45:00	Lift mini-slump cone
60:00	Measure and record mini-slump diameters

Miniature Slump Data Sheet

High Volume Fly Ash Cement Paste Study

Date: _____

Technician: _____

Mix ID: _____

Cement: _____ % **Fly Ash:** _____ % **Gypsum:** _____ %

CH: _____ % **RS Cem:** _____ % **Admix:** _____ **w/cm:** _____

Cement Source: _____ **Fly Ash Source:** _____

Air Temperature (°F): _____ **Water Temperature (°F):** _____ **Relative Humidity (%):** _____

Start Time: _____ **Paste Temperature at Completion of Mixing (°F):** _____

Test Time (min)	Diameter Measurements (in)				Average Diameter (in)	Area (in^2)
2						
5						
15						
30						
45						

Notes/Deviations: _____

_____

_____

APPENDIX D

THERMAL CURVE PLOTS FROM THE SCREENING STUDY

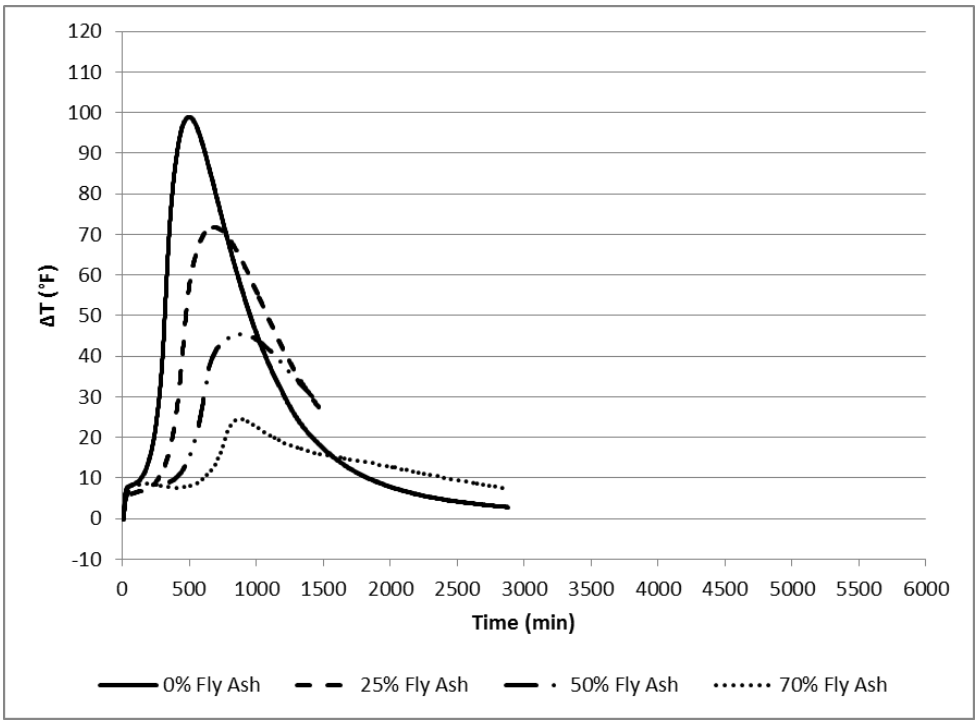

Figure D.1. Thermal Curve Plots for Combination 1-1

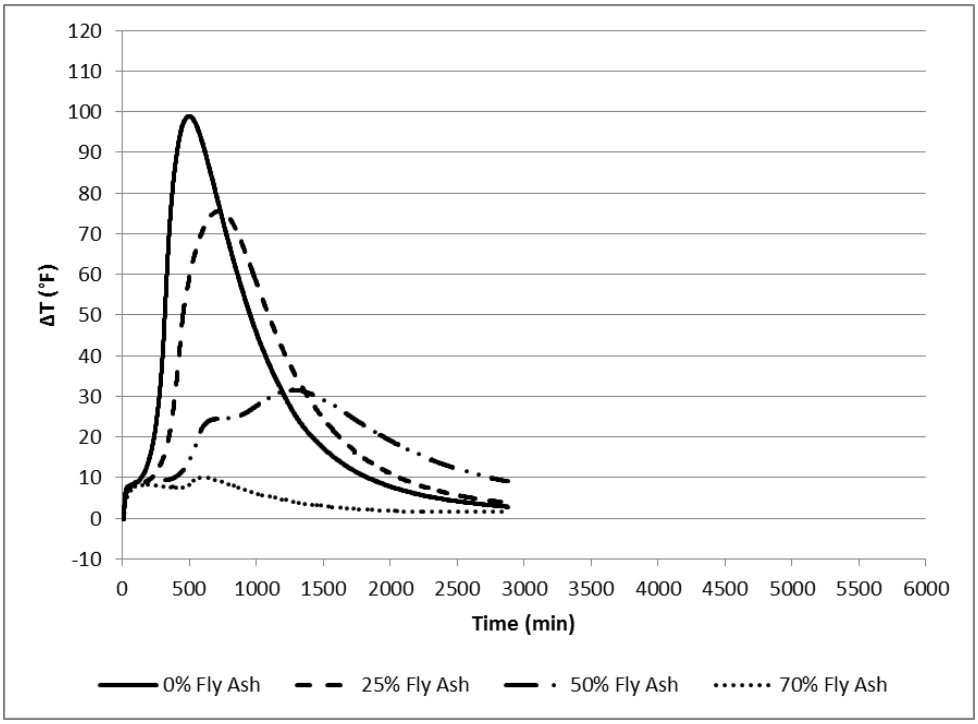

Figure D.2. Thermal Curve Plots for Combination 1-2

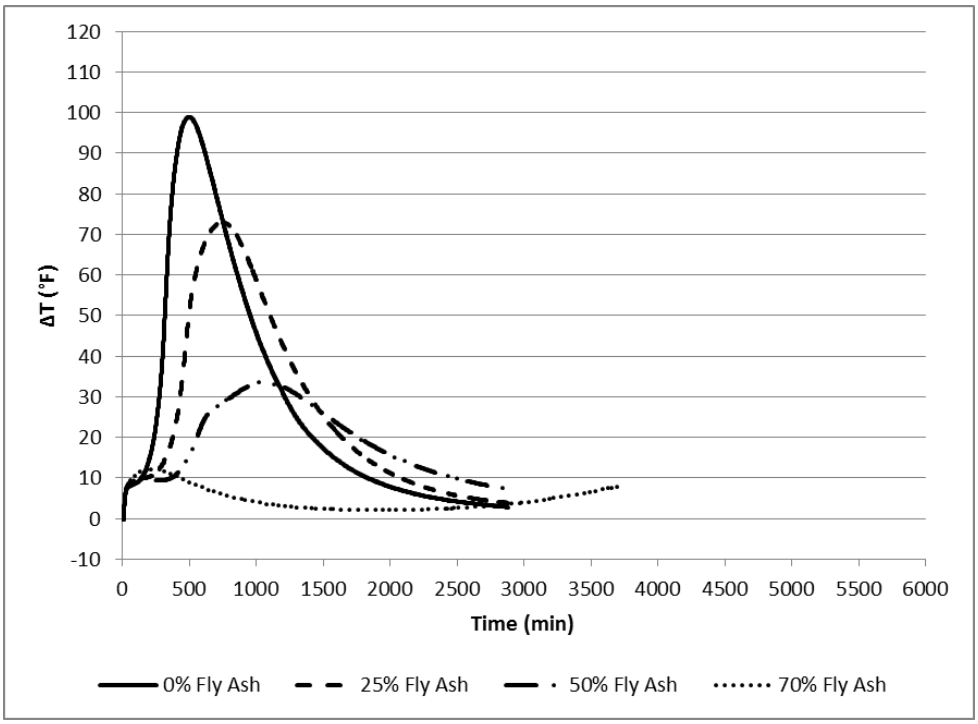

Figure D.3. Thermal Curve Plots for Combination 1-3

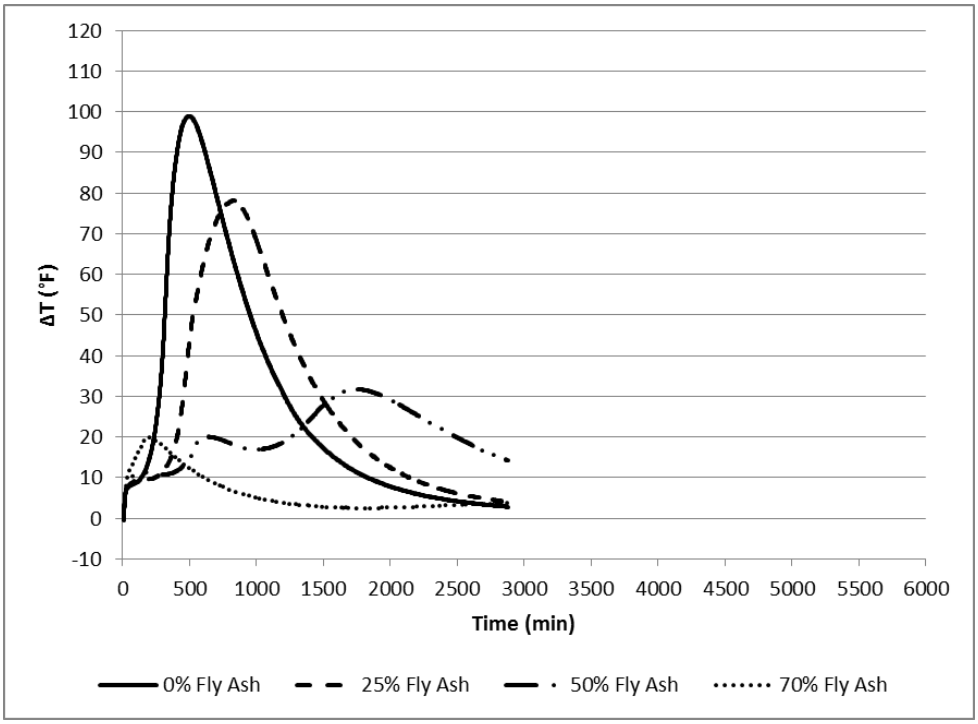

Figure D.4. Thermal Curve Plots for Combination 1-4

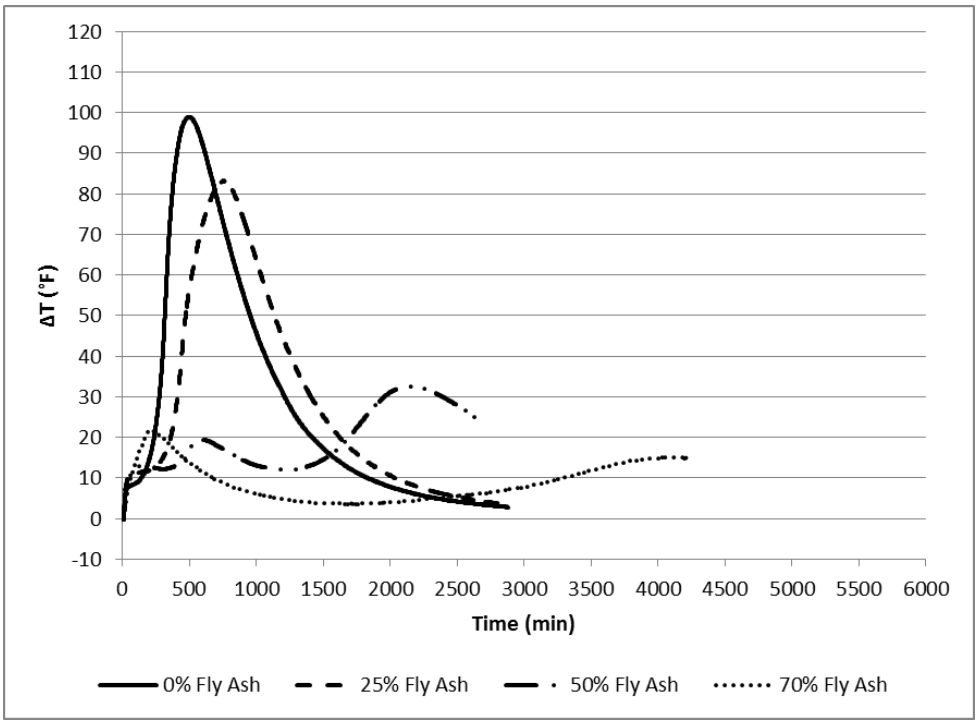

Figure D.5. Thermal Curve Plots for Combination 1-5

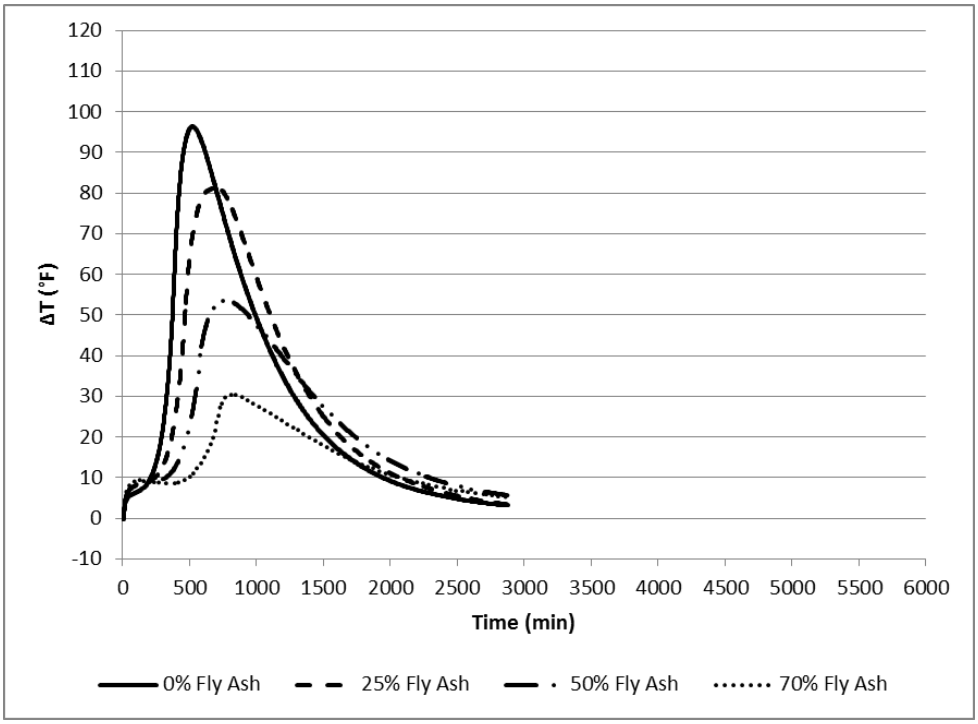

Figure D.6. Thermal Curve Plots for Combination 2-1

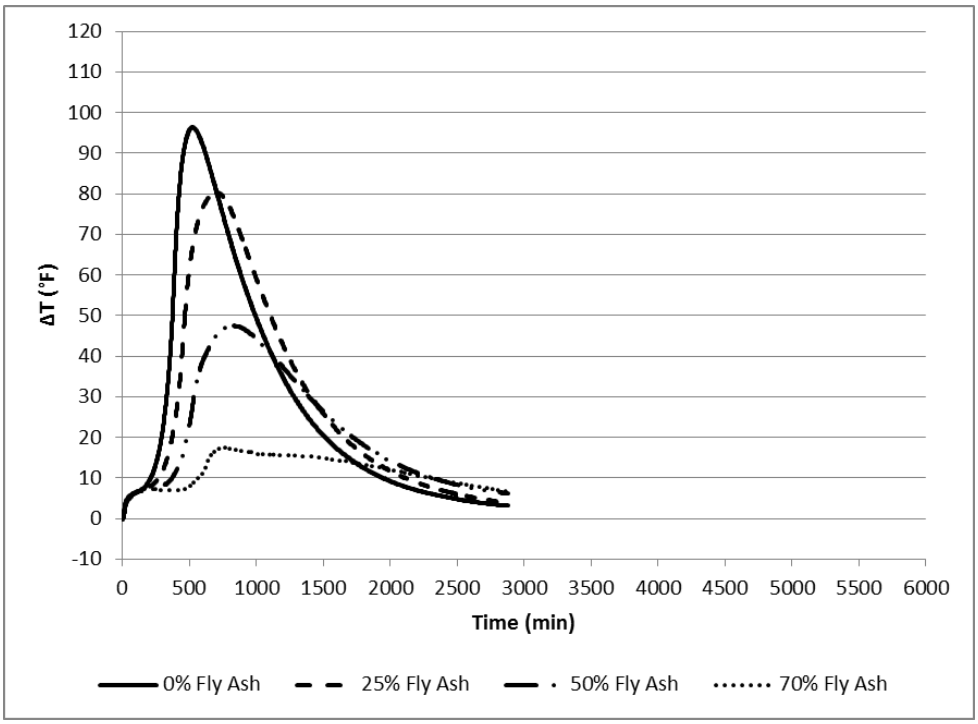

Figure D.7. Thermal Curve Plots for Combination 2-2

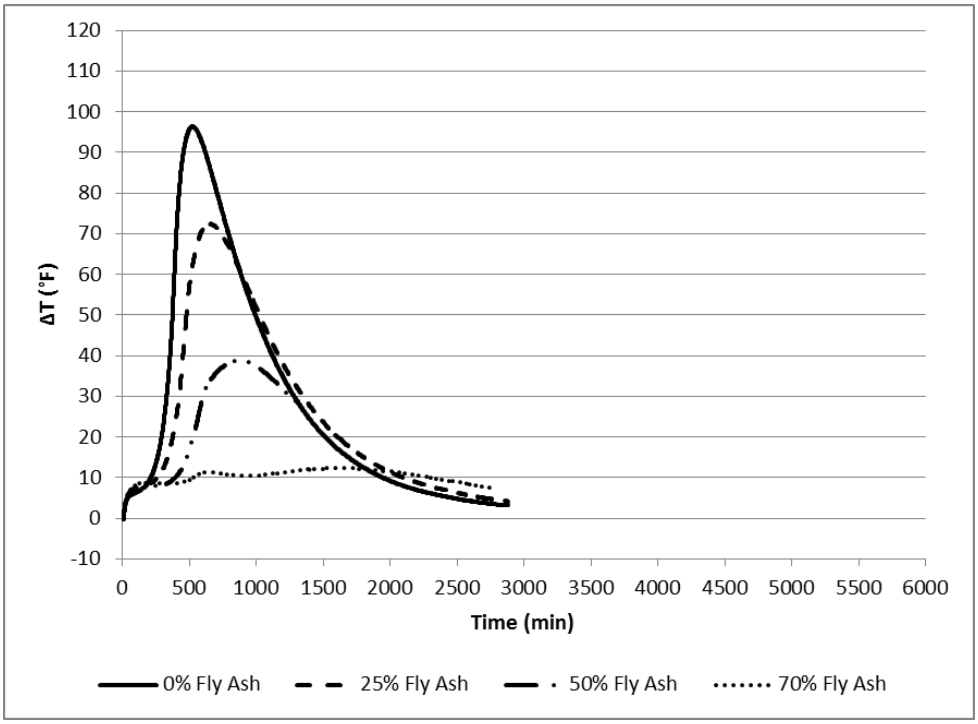

Figure D.8. Thermal Curve Plots for Combination 2-3

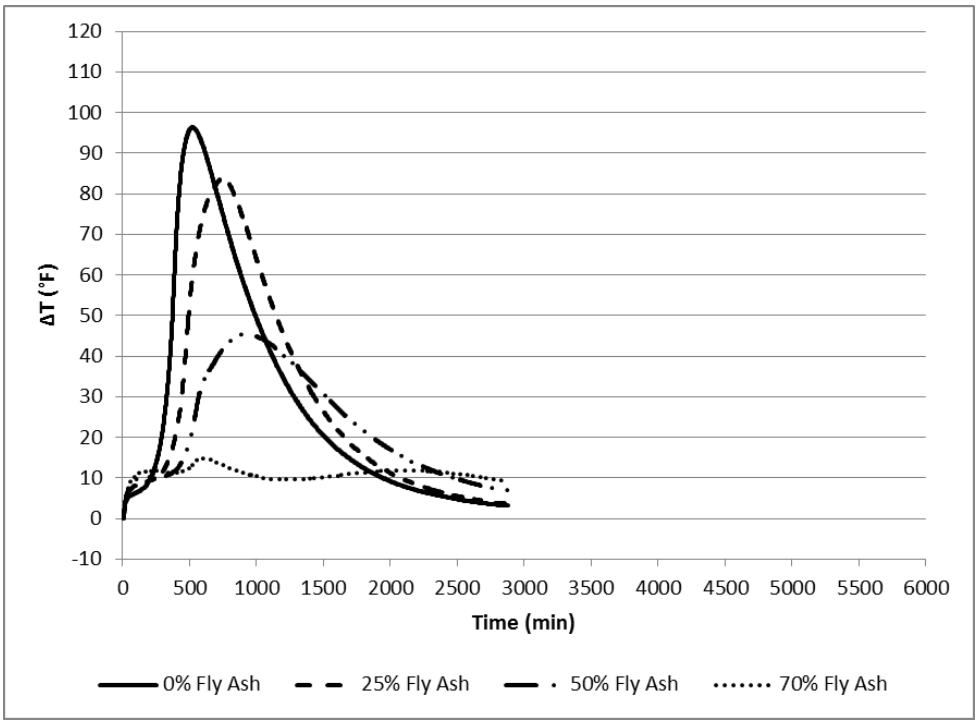

Figure D.9. Thermal Curve Plots for Combination 2-4

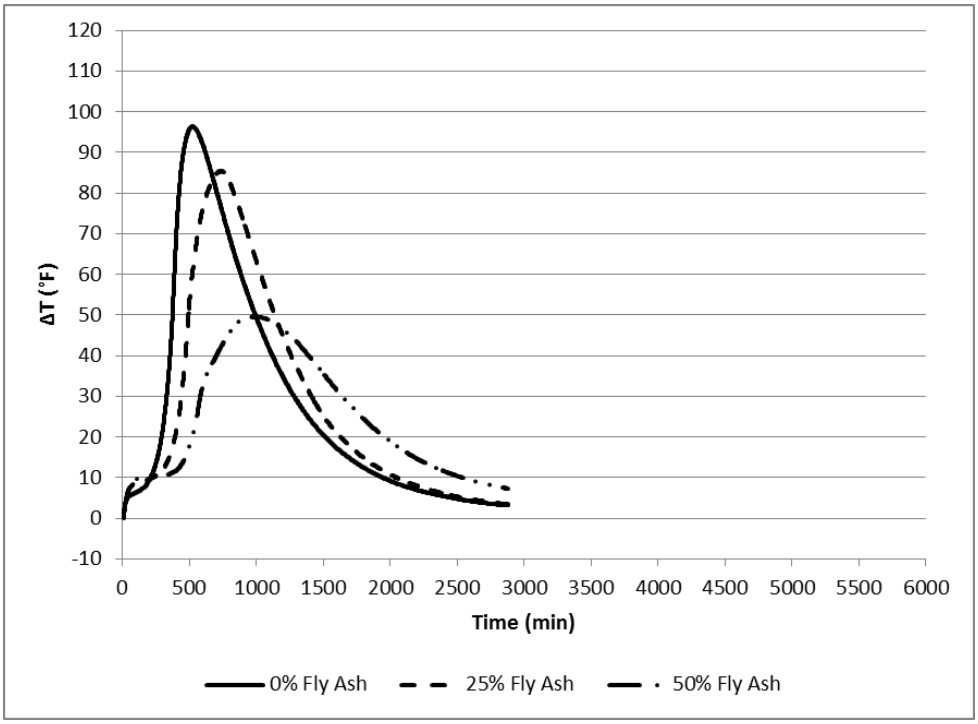

Figure D.10. Thermal Curve Plots for Combination 2-5

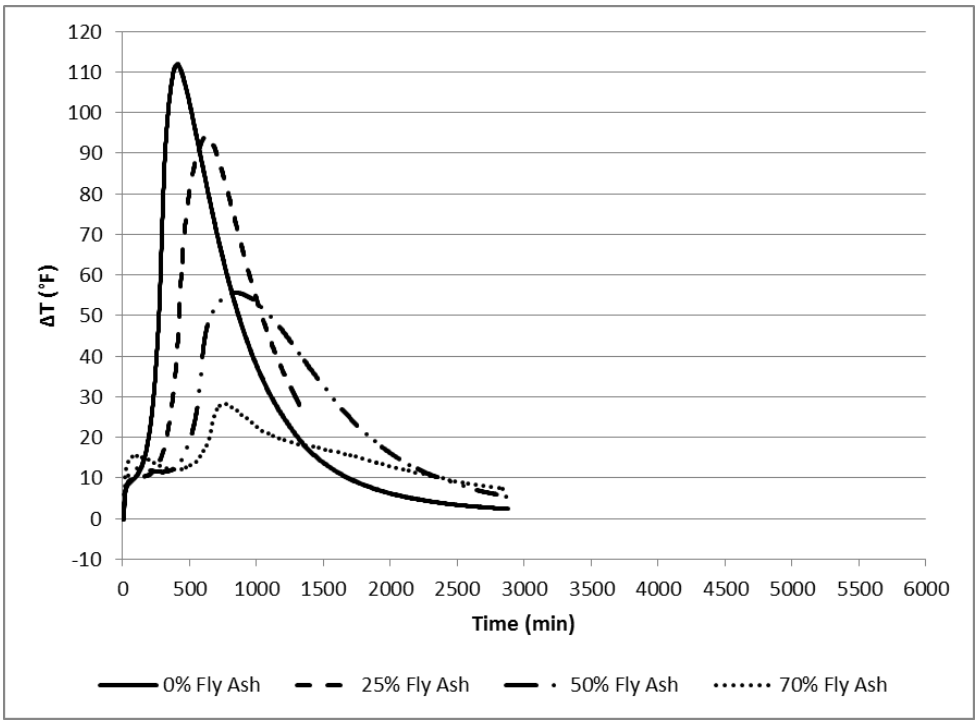

Figure D.11. Thermal Curve Plots for Combination 3-1

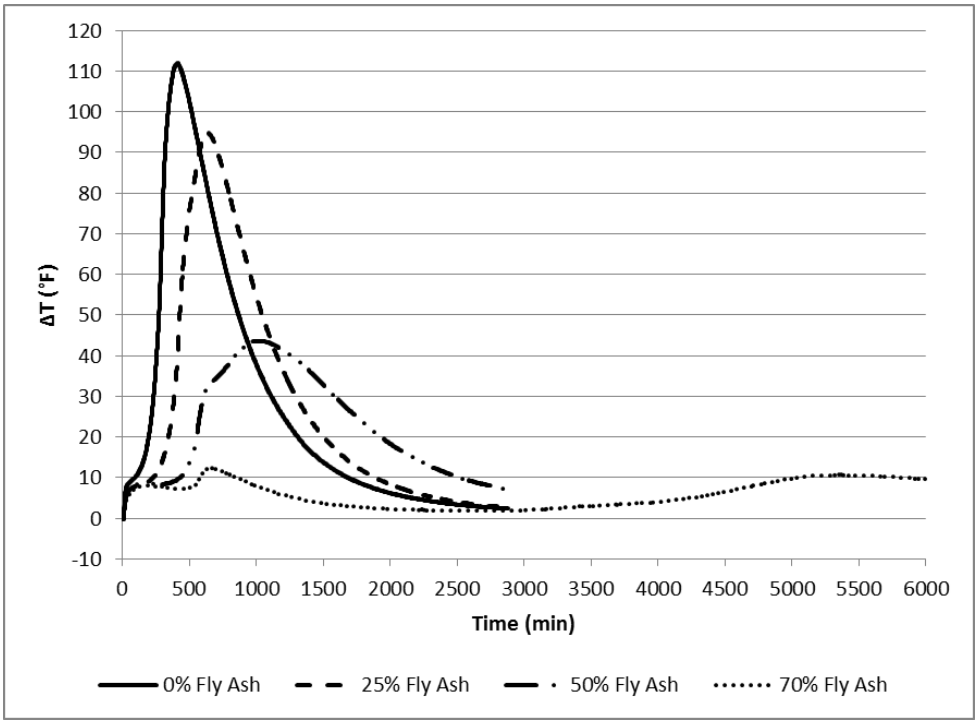

Figure D.12. Thermal Curve Plots for Combination 3-2

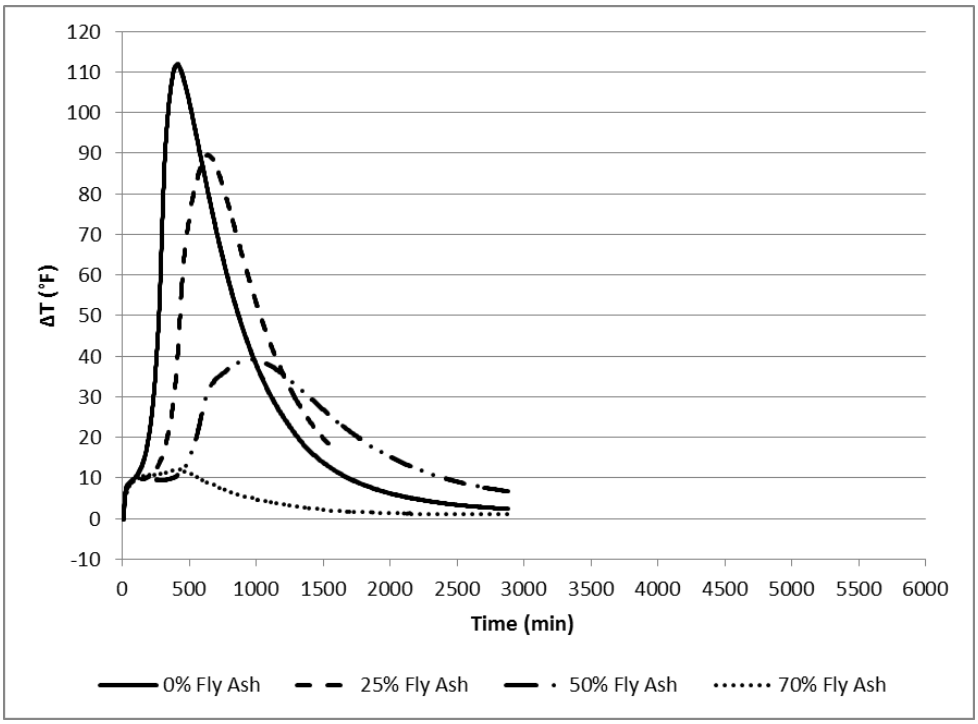

Figure D.13. Thermal Curve Plots for Combination 3-3

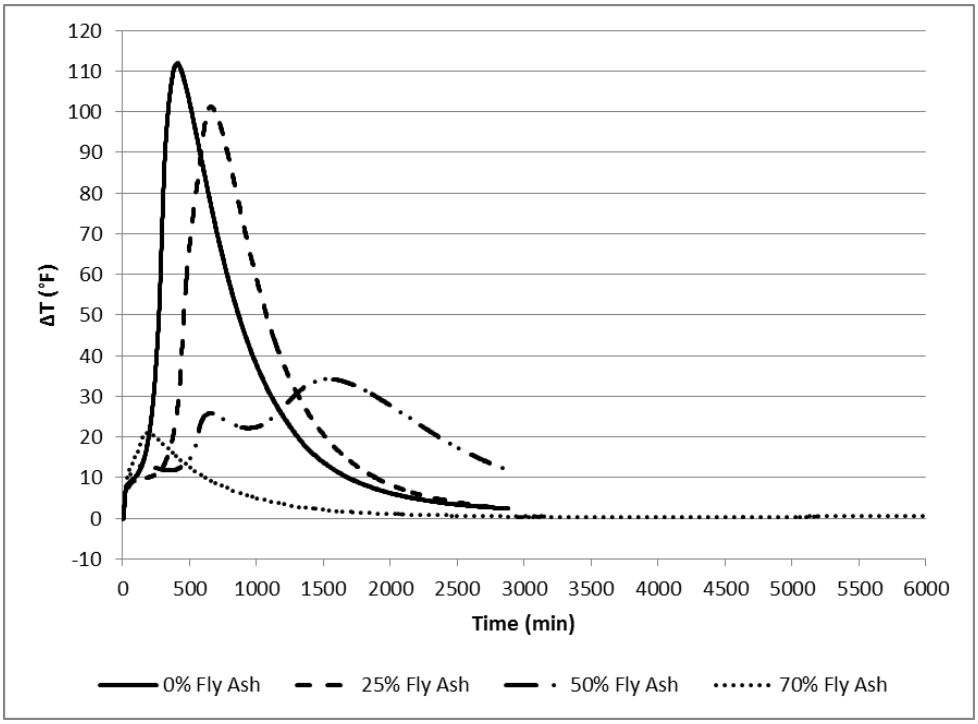

Figure D.14. Thermal Curve Plots for Combination 3-4

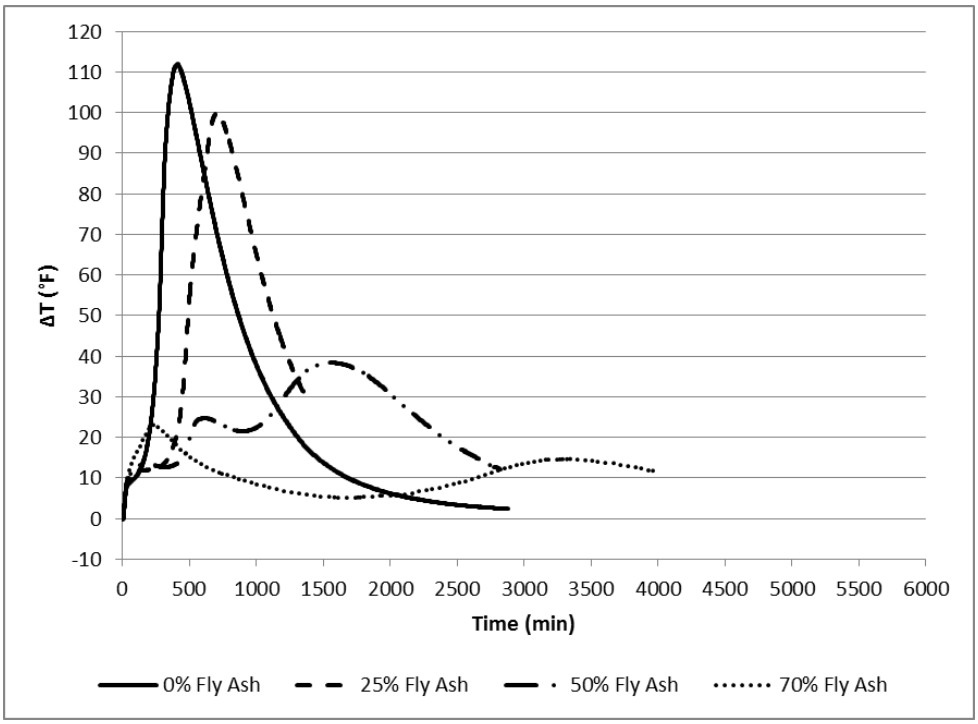

Figure D.15. Thermal Curve Plots for Combination 3-5

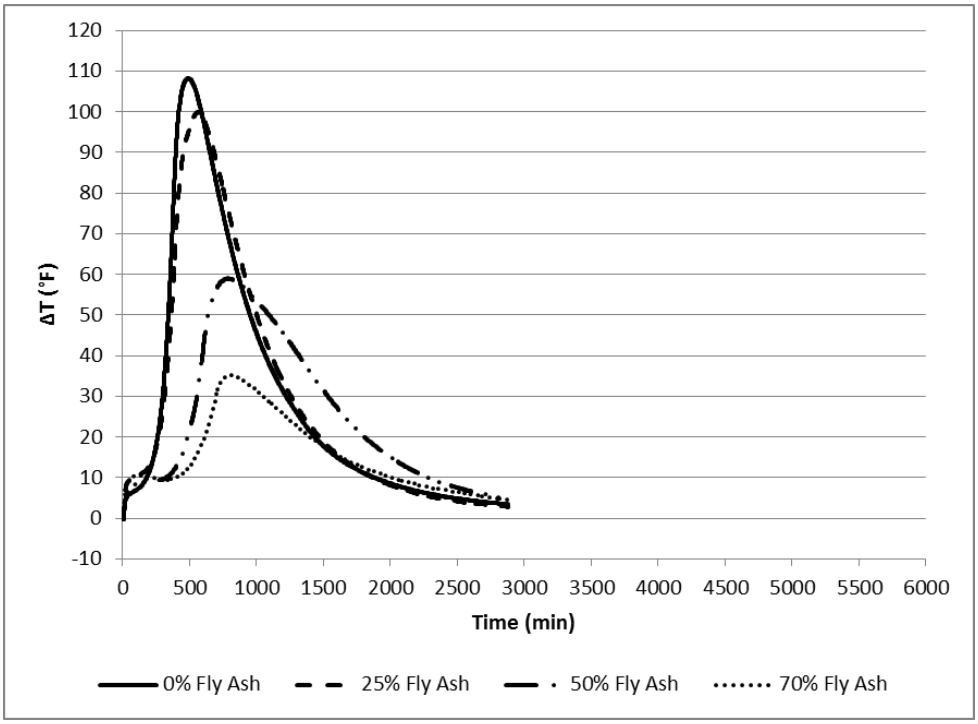

Figure D.16. Thermal Curve Plots for Combination 4-1

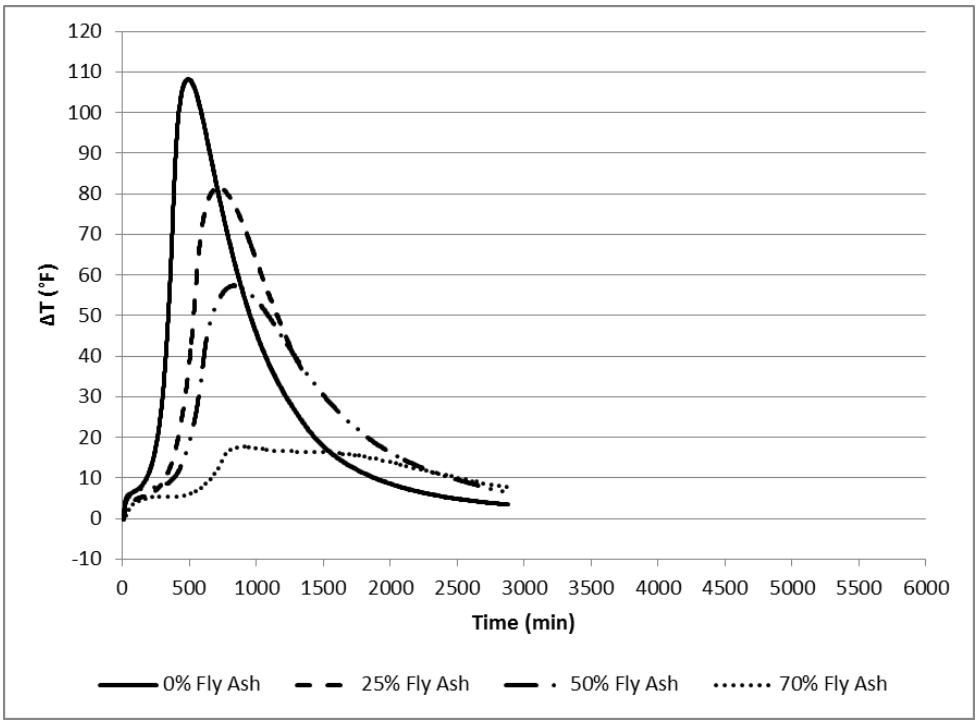

Figure D.17. Thermal Curve Plots for Combination 4-2

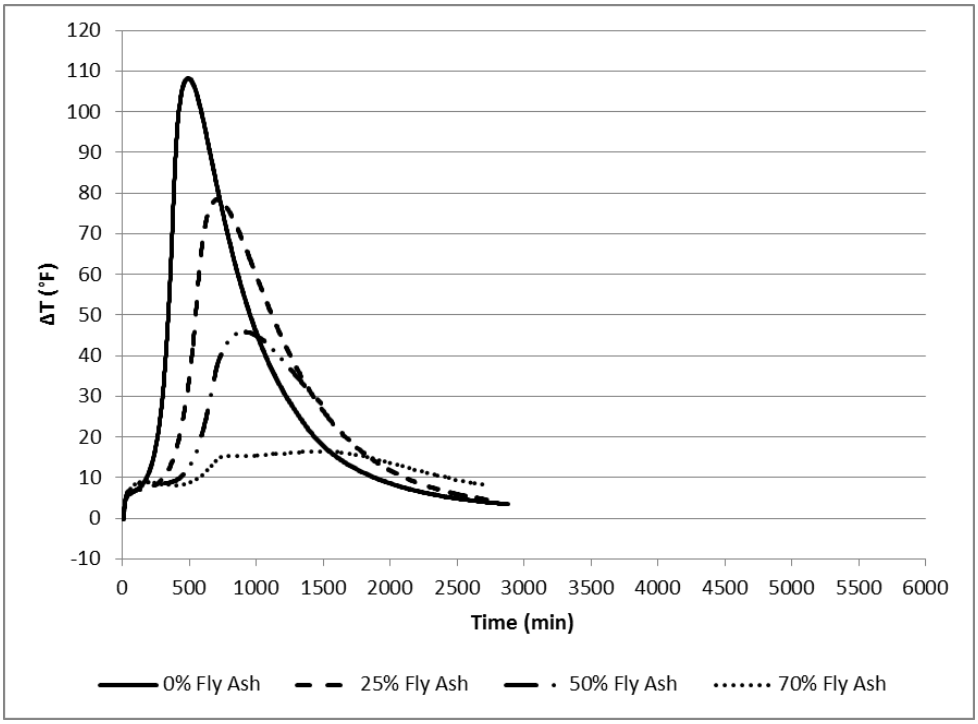

Figure D.18. Thermal Curve Plots for Combination 4-3

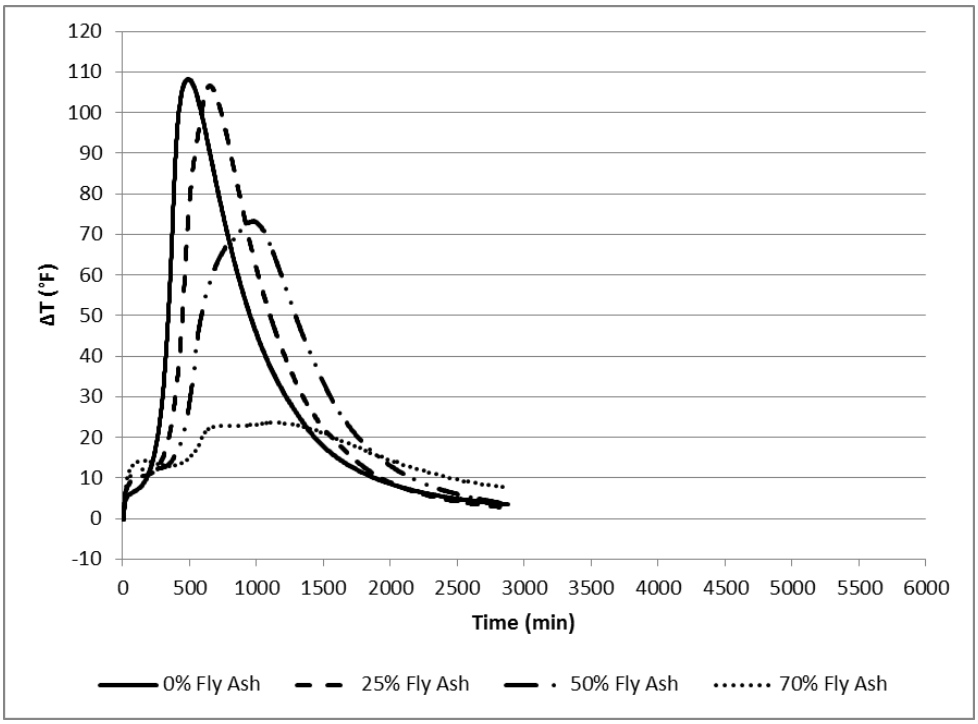

Figure D.19. Thermal Curve Plots for Combination 4-4

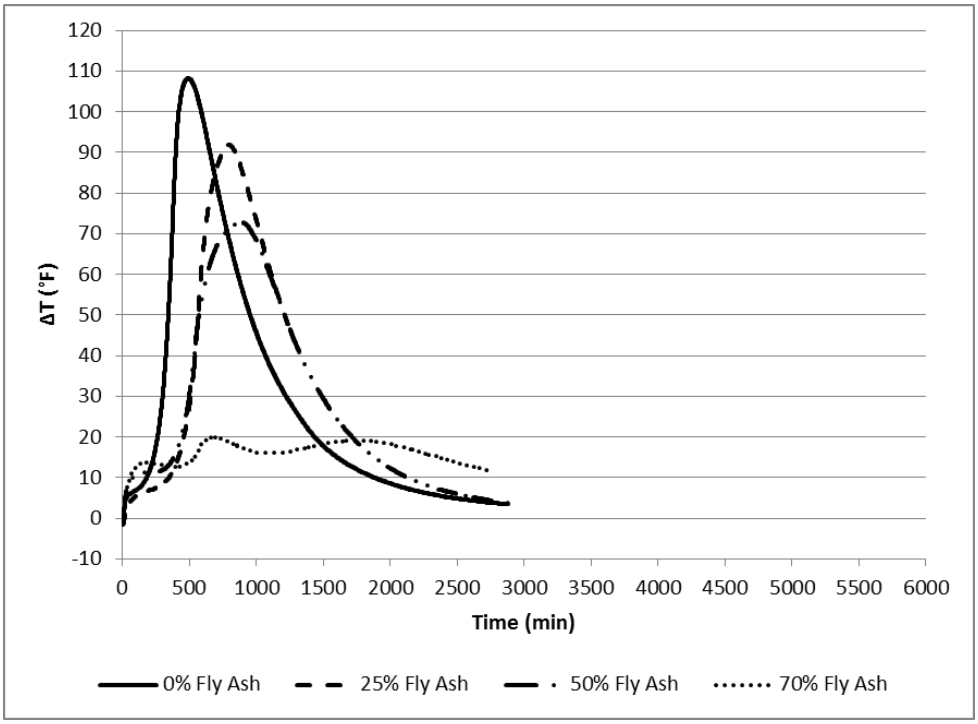

Figure D.20. Thermal Curve Plots for Combination 4-5

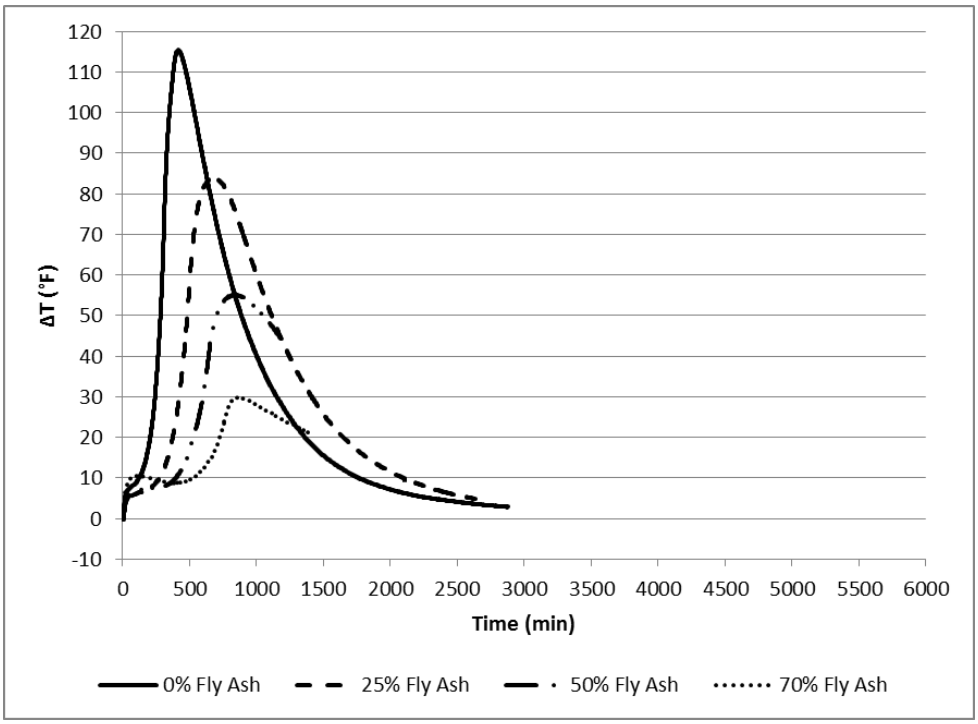

Figure D.21. Thermal Curve Plots for Combination 5-1

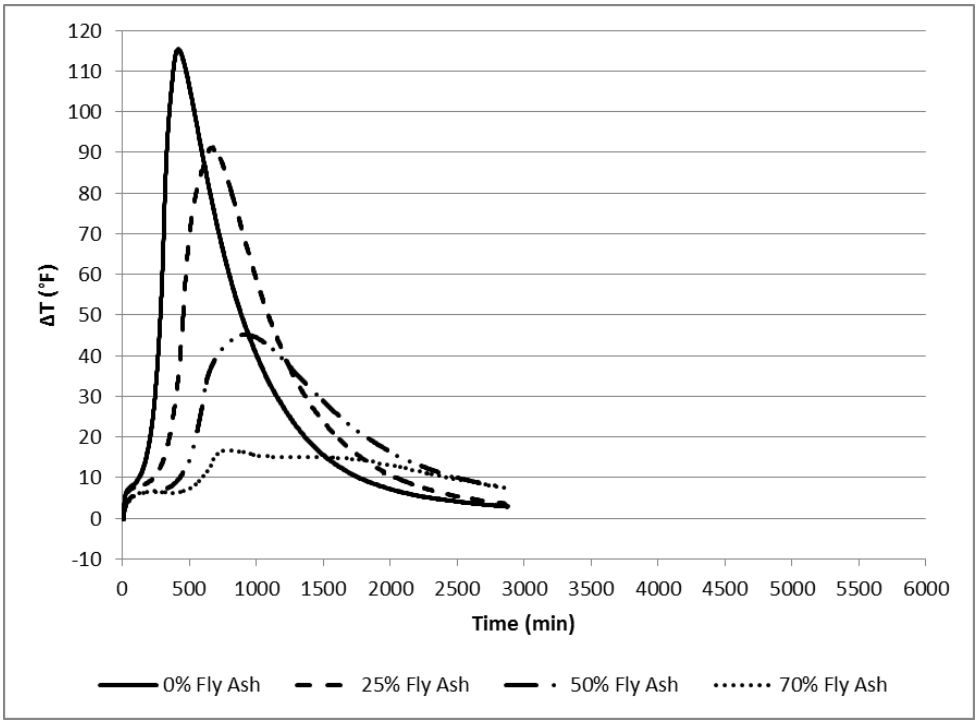

Figure D.22. Thermal Curve Plots for Combination 5-2

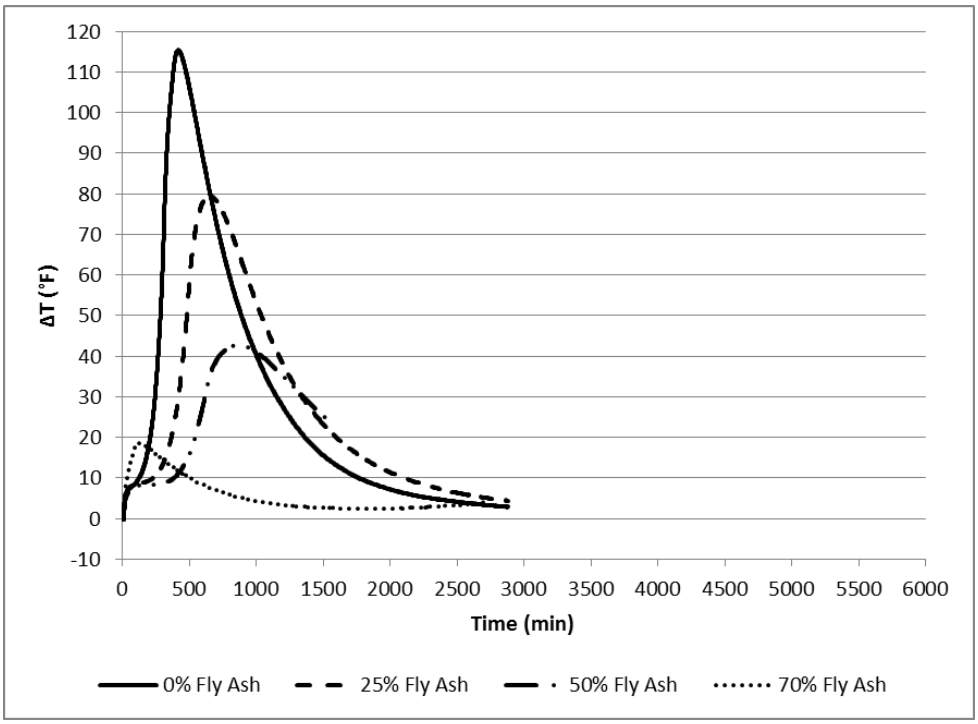

Figure D.23. Thermal Curve Plots for Combination 5-3

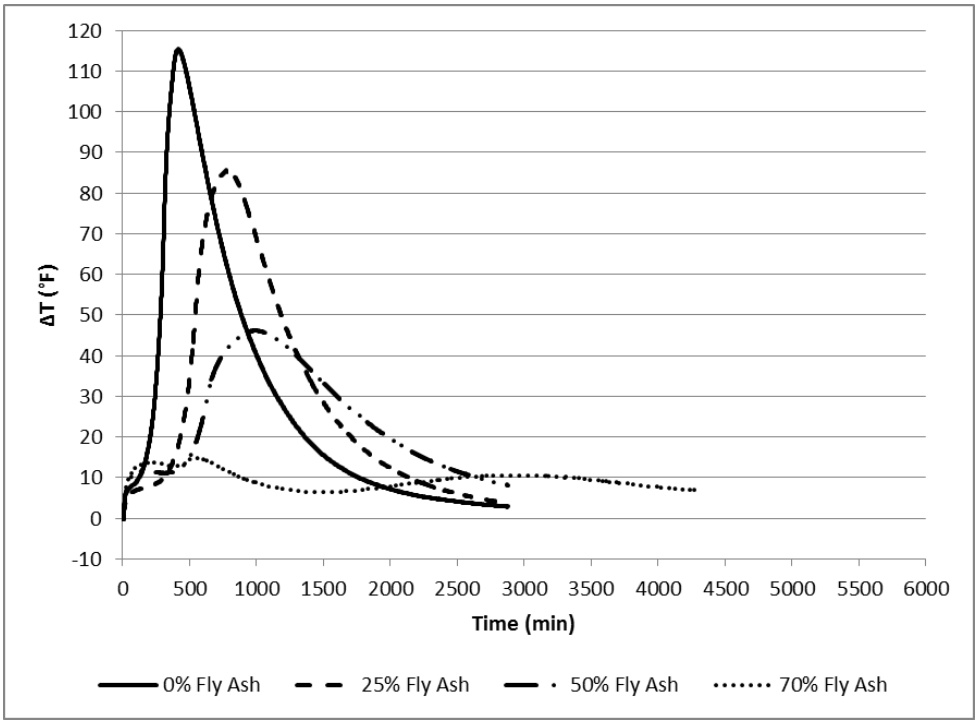

Figure D.24. Thermal Curve Plots for Combination 5-4

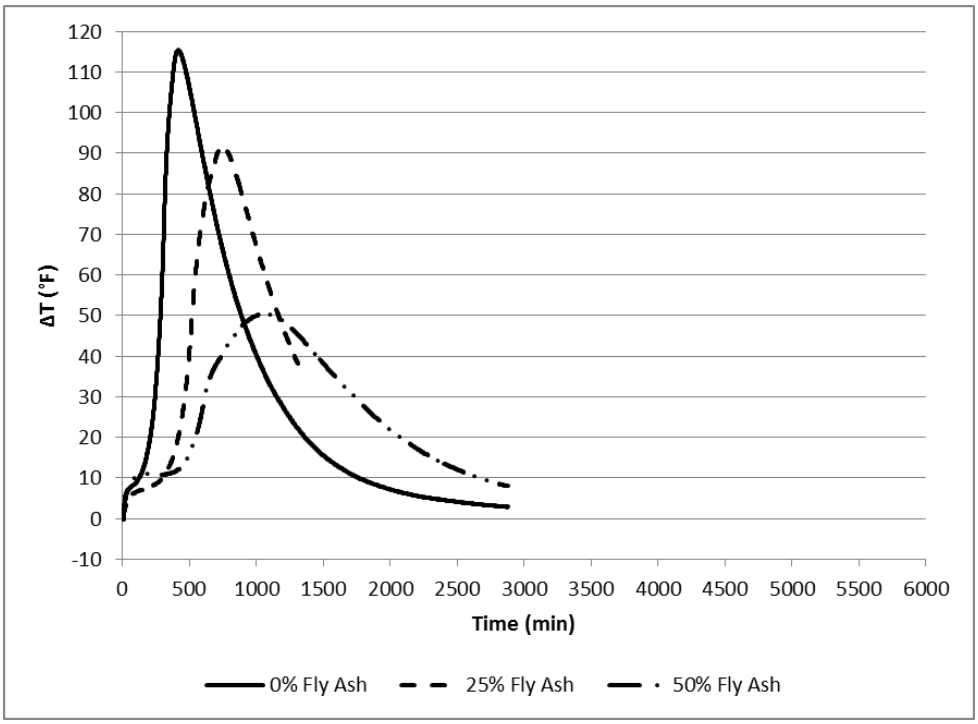

Figure D.25. Thermal Curve Plots for Combination 5-5

APPENDIX E

THERMAL CURVE PLOTS FROM THE MAIN EFFECTS PASTE STUDY

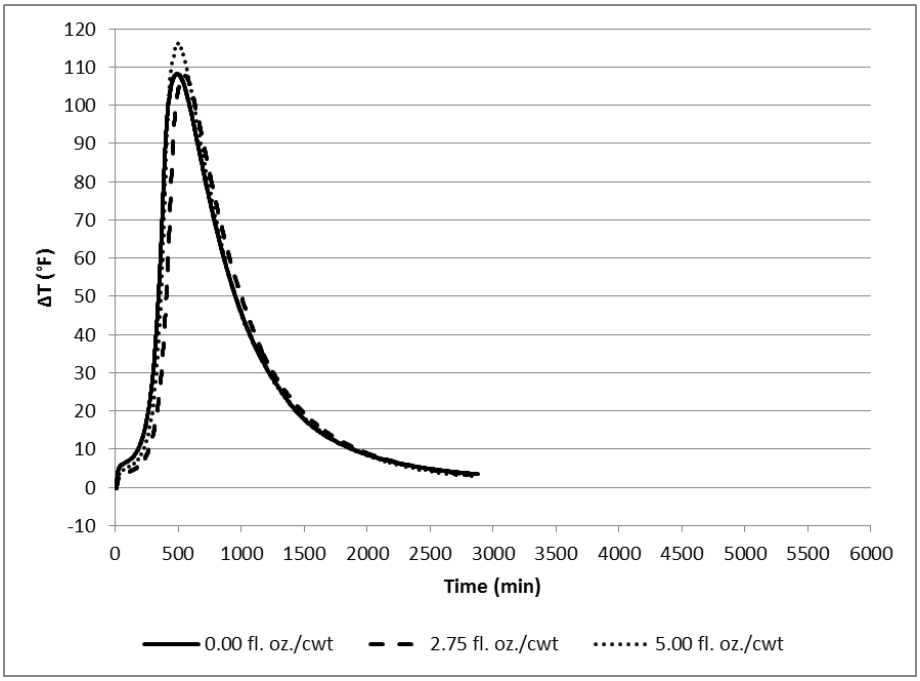

Figure E.1. Effect of Water Reducer on Combination 4-1 with 0% Fly Ash

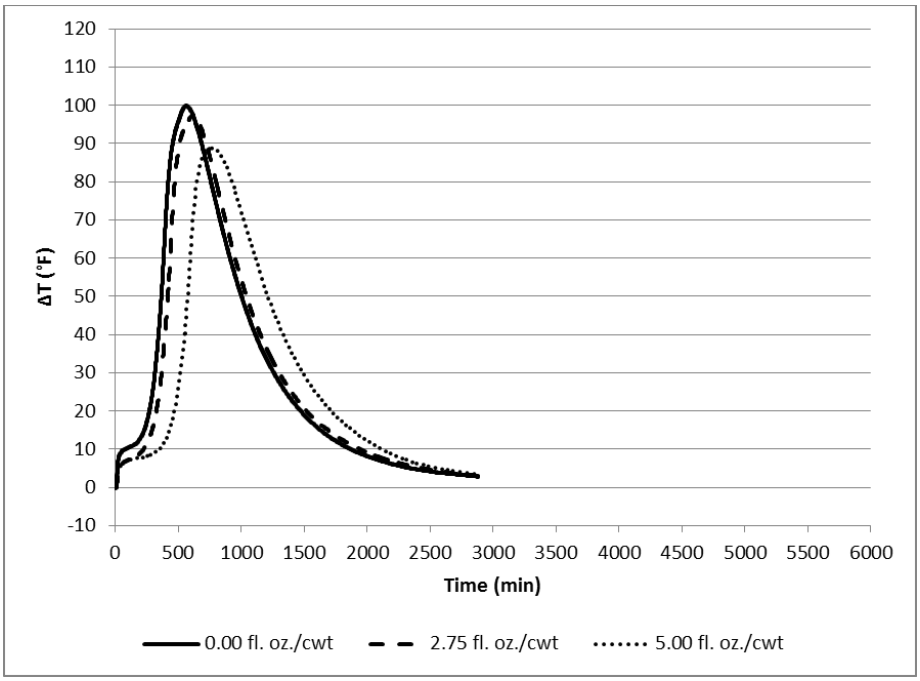

Figure E.2. Effect of Water Reducer on Combination 4-1 with 25% Fly Ash

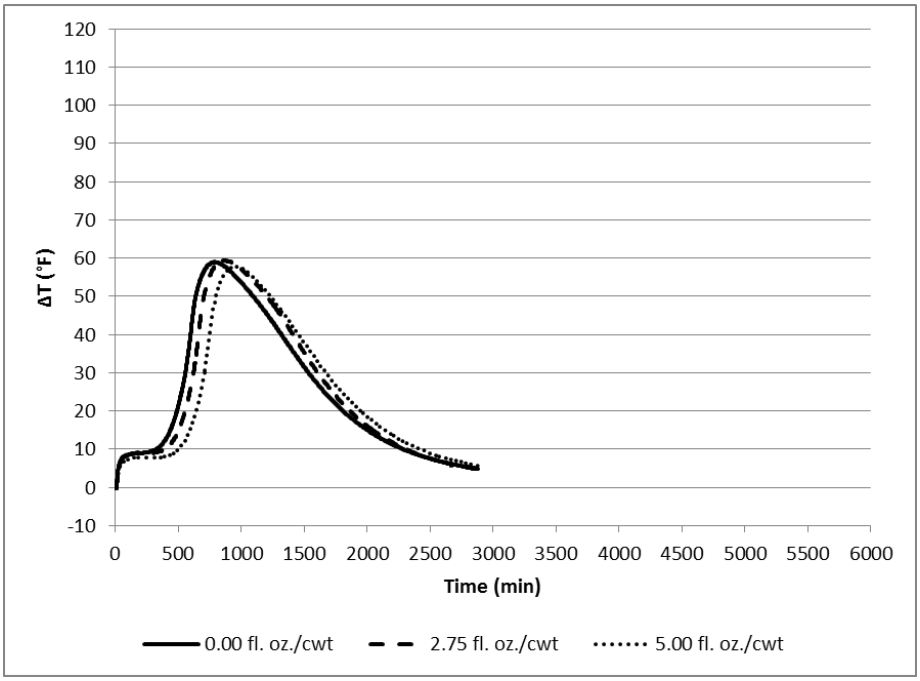

Figure E.3. Effect of Water Reducer on Combination 4-1 with 50% Fly Ash

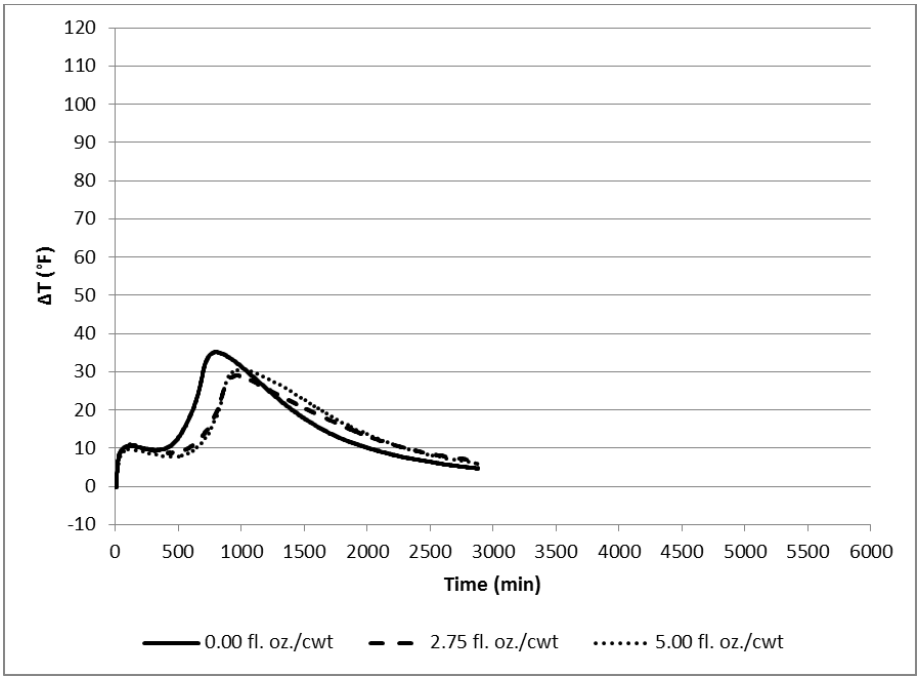

Figure E.4. Effect of Water Reducer on Combination 4-1 with 70% Fly Ash

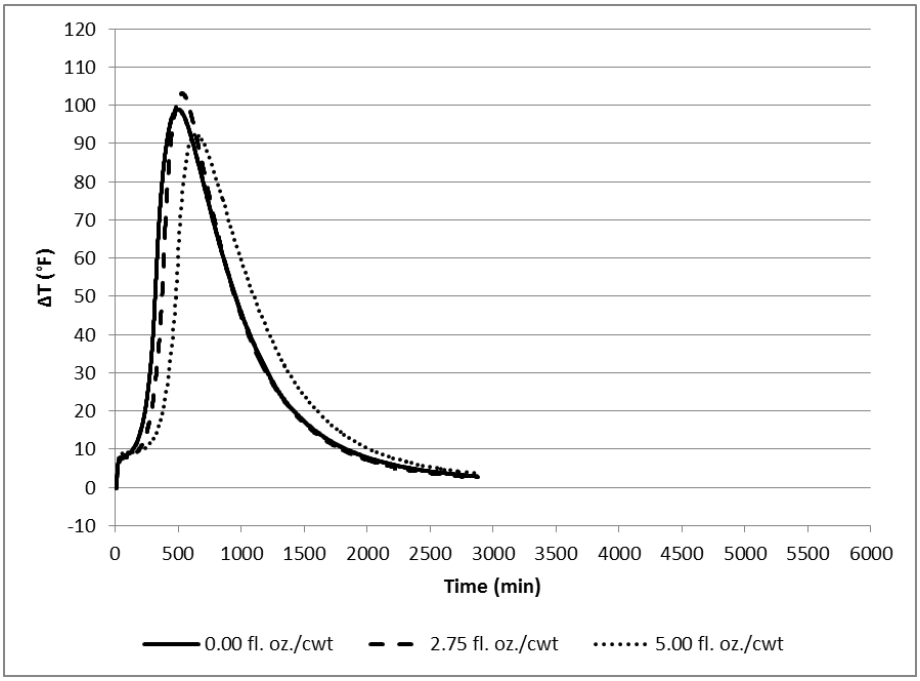

Figure E.5. Effect of Water Reducer on Combination 1-3 with 0% Fly Ash

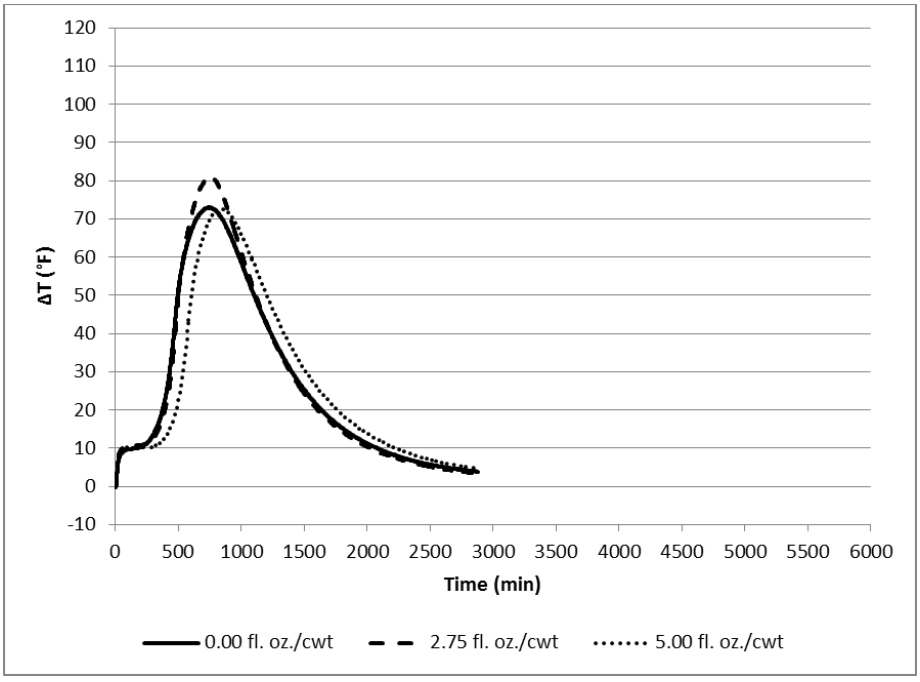

Figure E.6. Effect of Water Reducer on Combination 1-3 with 25% Fly Ash

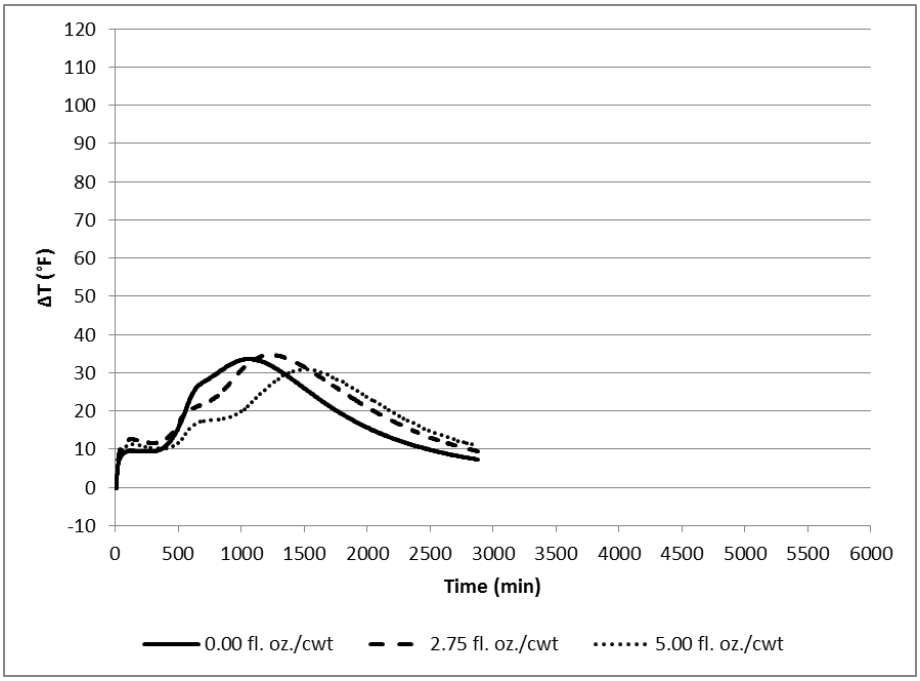

Figure E.7. Effect of Water Reducer on Combination 1-3 with 50% Fly Ash

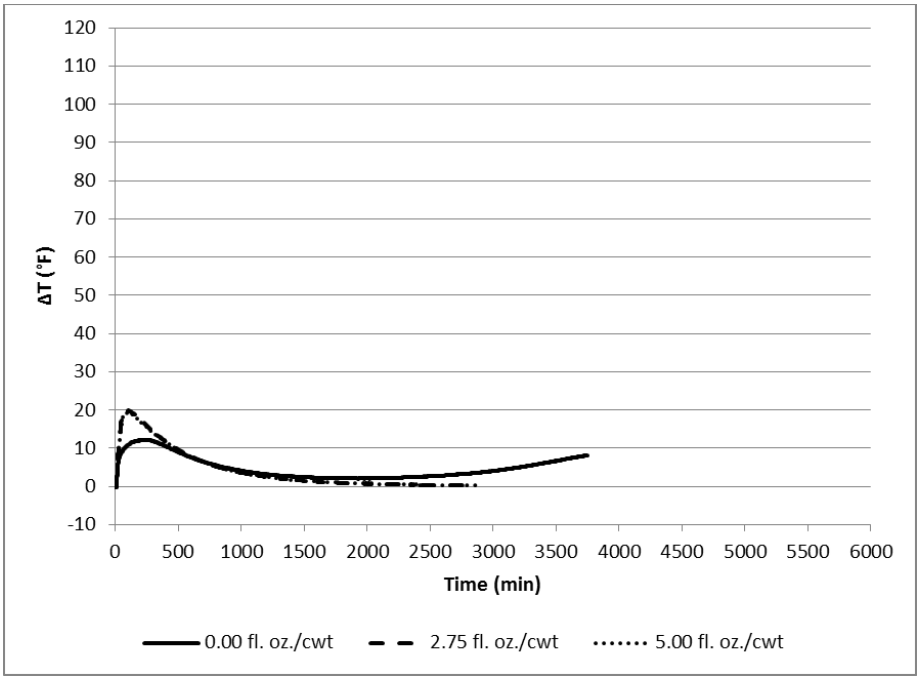

Figure E.8. Effect of Water Reducer on Combination 1-3 with 70% Fly Ash

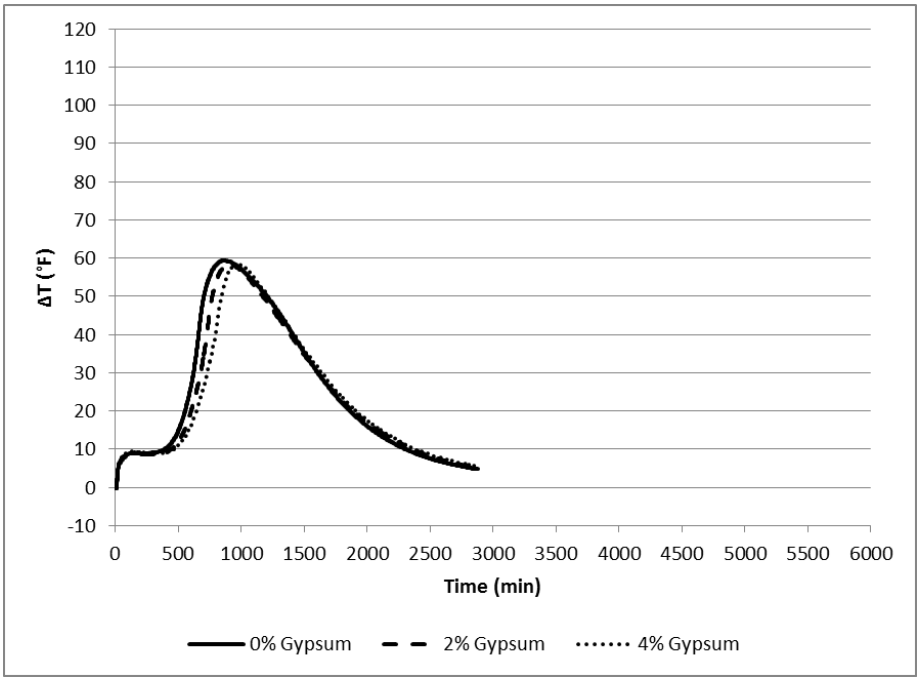

Figure E.9. Effects of Gypsum on Combination 4-1 with 50% Fly Ash and Low Dosage of Water Reducer

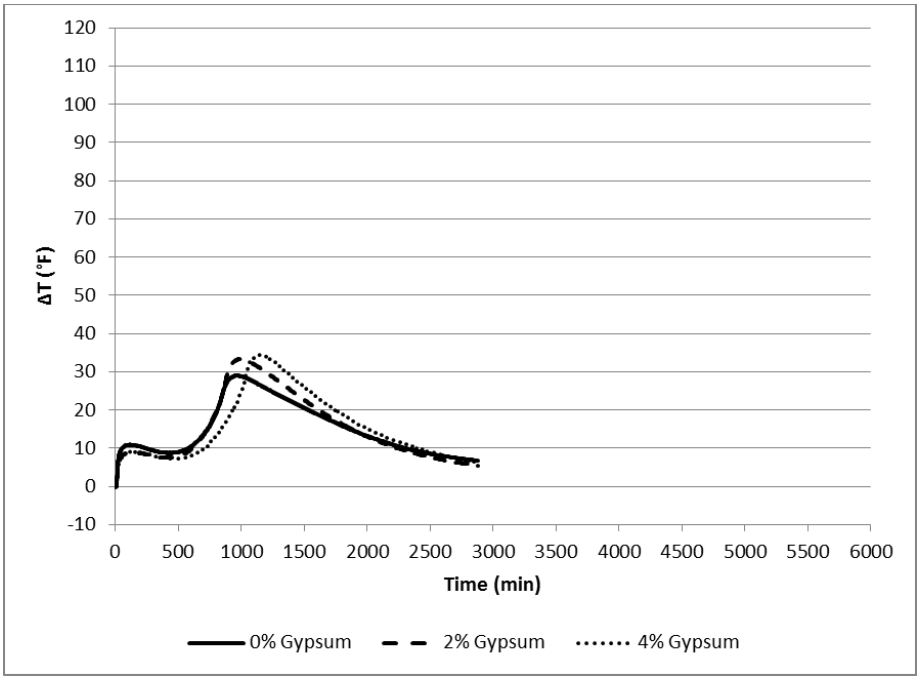

Figure E.10. Effects of Gypsum on Combination 4-1 with 70% Fly Ash and Low Dosage of Water Reducer

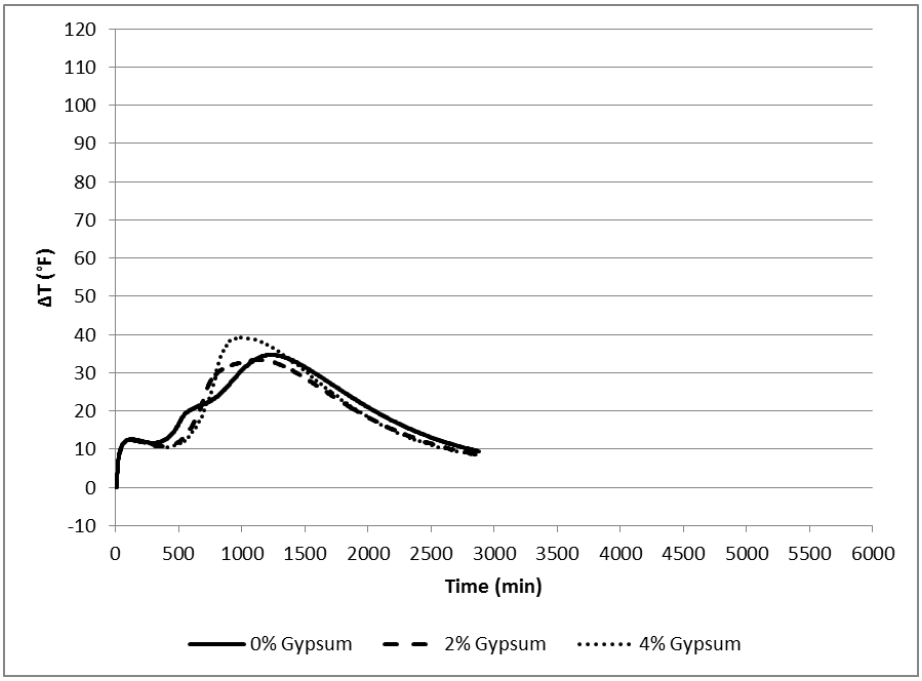

Figure E.11. Effects of Gypsum on Combination 1-3 with 50% Fly Ash and Low Dosage of Water Reducer

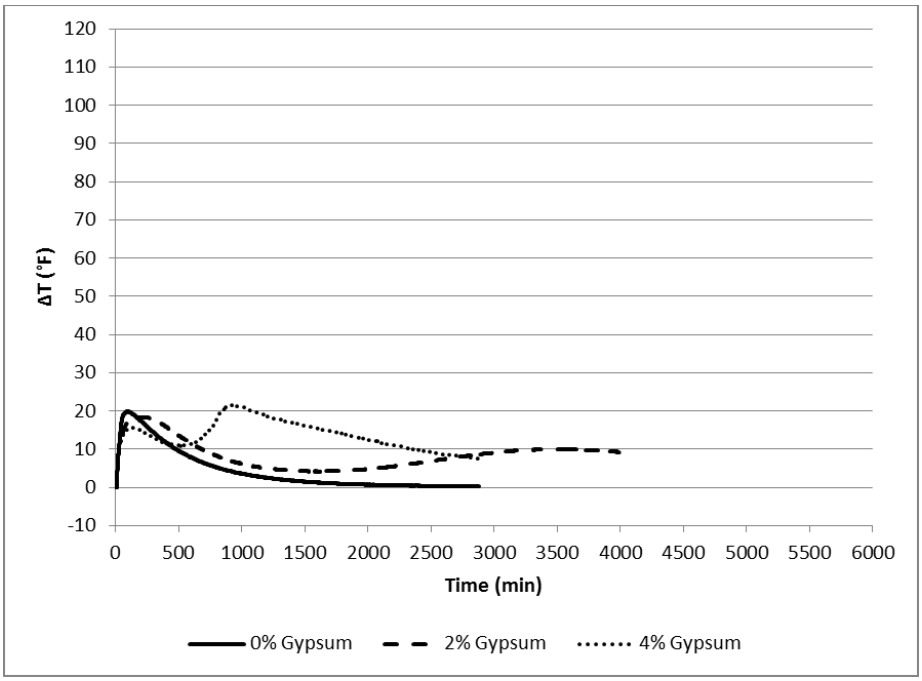

Figure E.12. Effects of Gypsum on Combination 1-3 with 70% Fly Ash and Low Dosage of Water Reducer

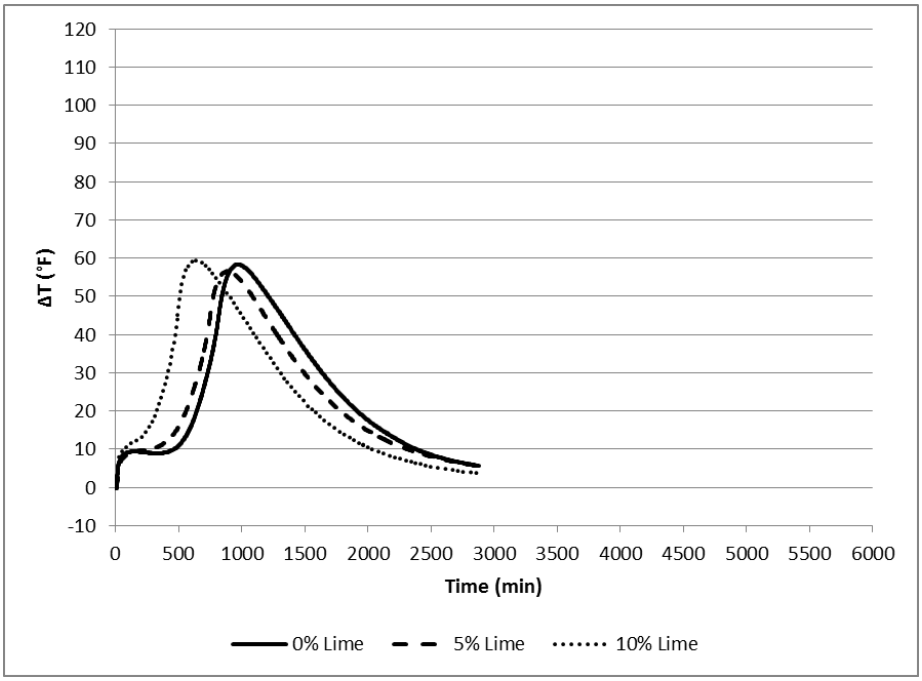

Figure E.13. Effects of Lime on Combination 4-1 with 50% Fly Ash, 4% Gypsum, and Low Dosage of Water Reducer

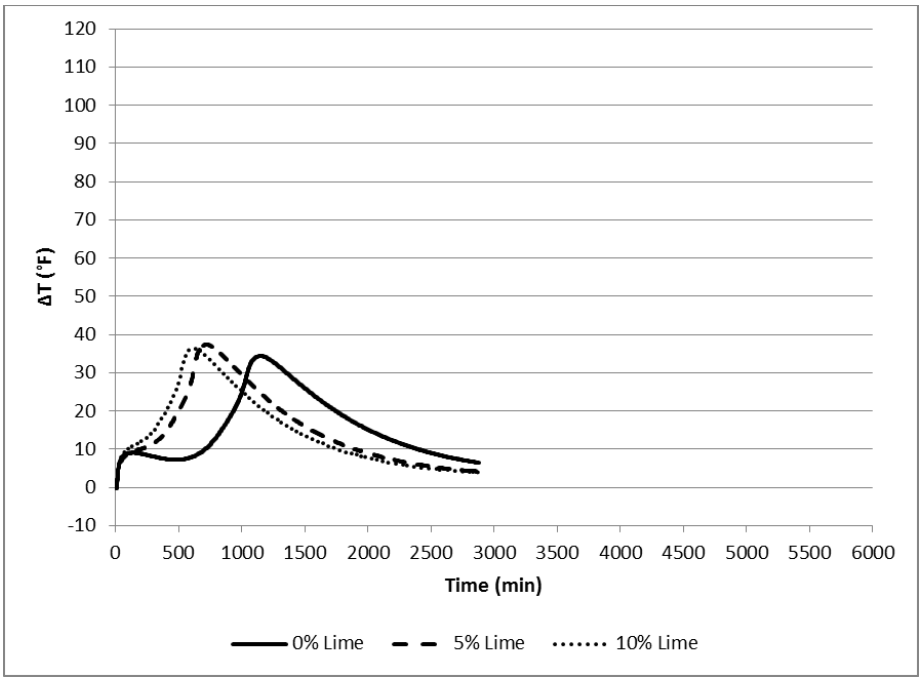

Figure E.14. Effects of Lime on Combination 4-1 with 70% Fly Ash, 4% Gypsum, and Low Dosage of Water Reducer

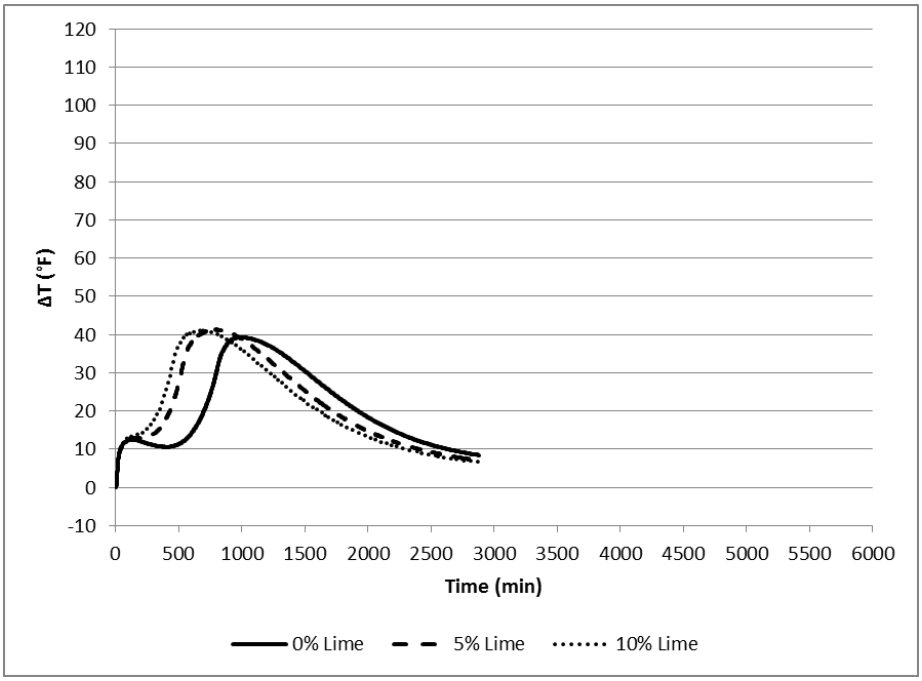

Figure E.15. Effects of Lime on Combination 1-3 with 50% Fly Ash, 4% Gypsum, and Low Dosage of Water Reducer

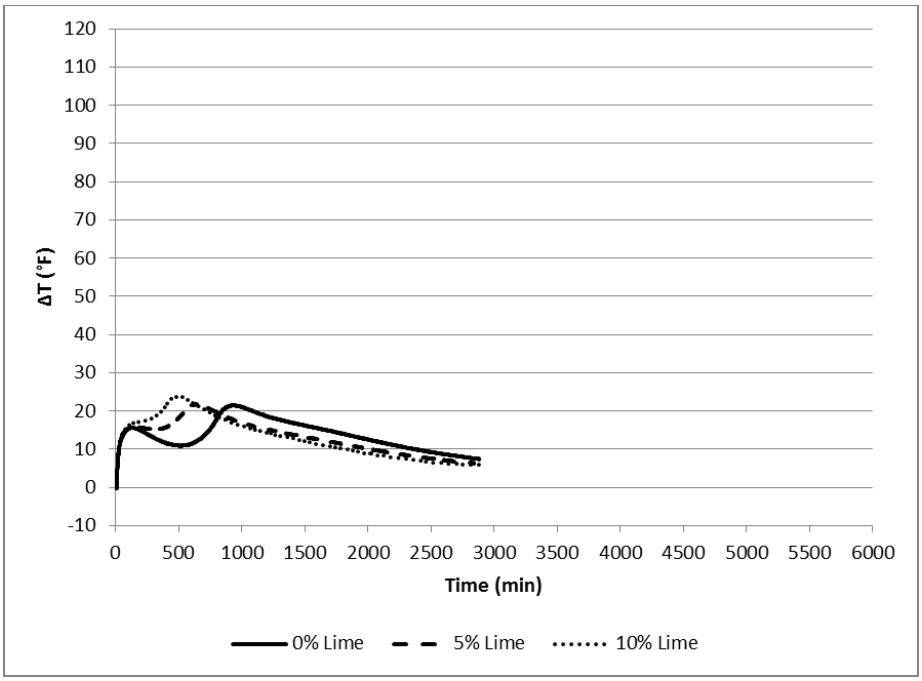

Figure E.16. Effects of Lime on Combination 1-3 with 70% Fly Ash, 4% Gypsum, and Low Dosage of Water Reducer

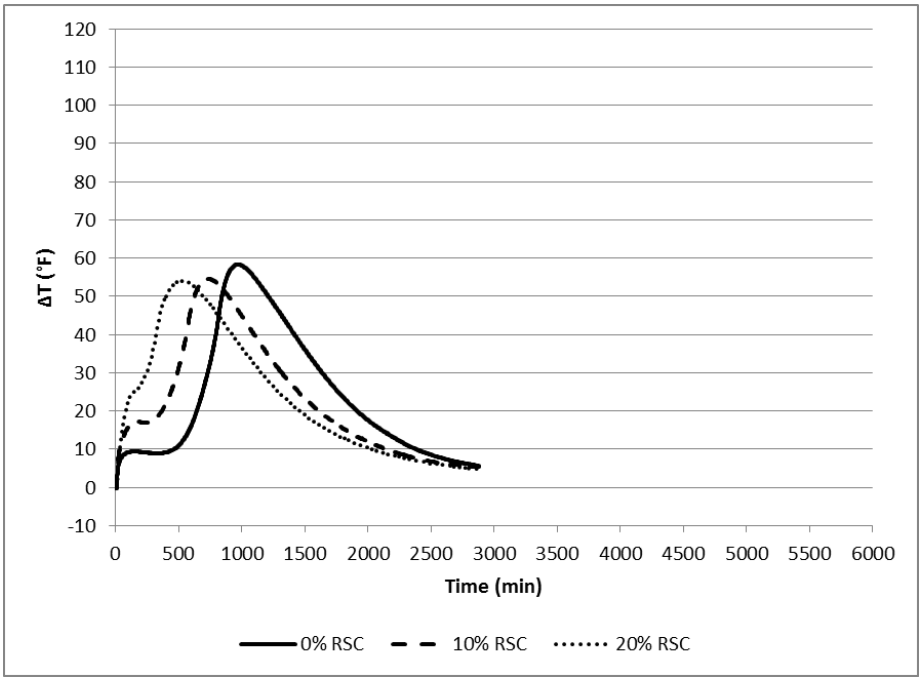

Figure E.17. Effects of Rapid Set Cement on Combination 4-1 with 50% Fly Ash, 4% Gypsum, and Low Dosage of Water Reducer

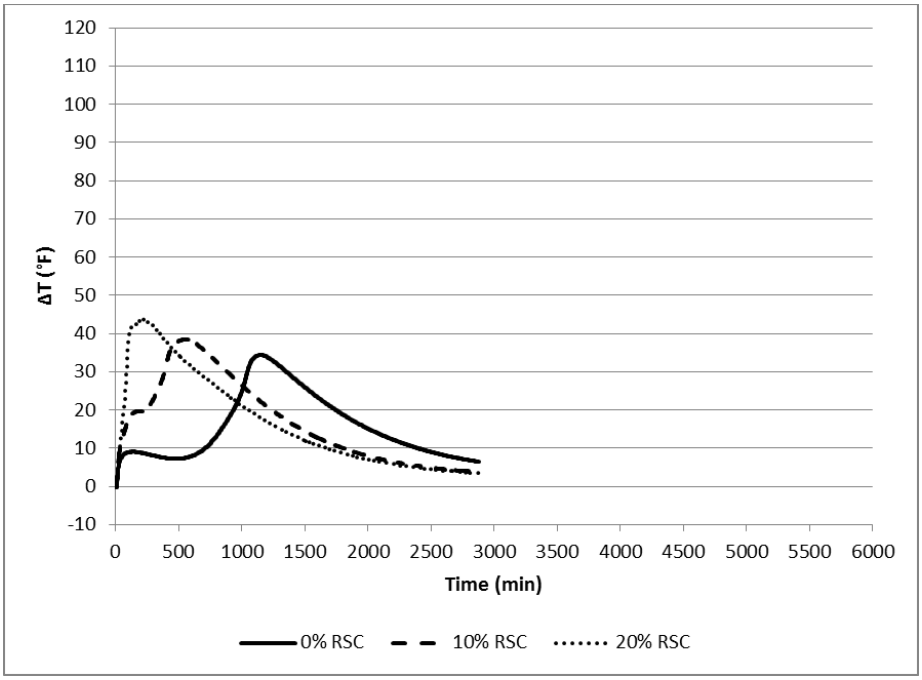

Figure E.18. Effects of Rapid Set Cement on Combination 4-1 with 70% Fly Ash, 4% Gypsum, and Low Dosage of Water Reducer

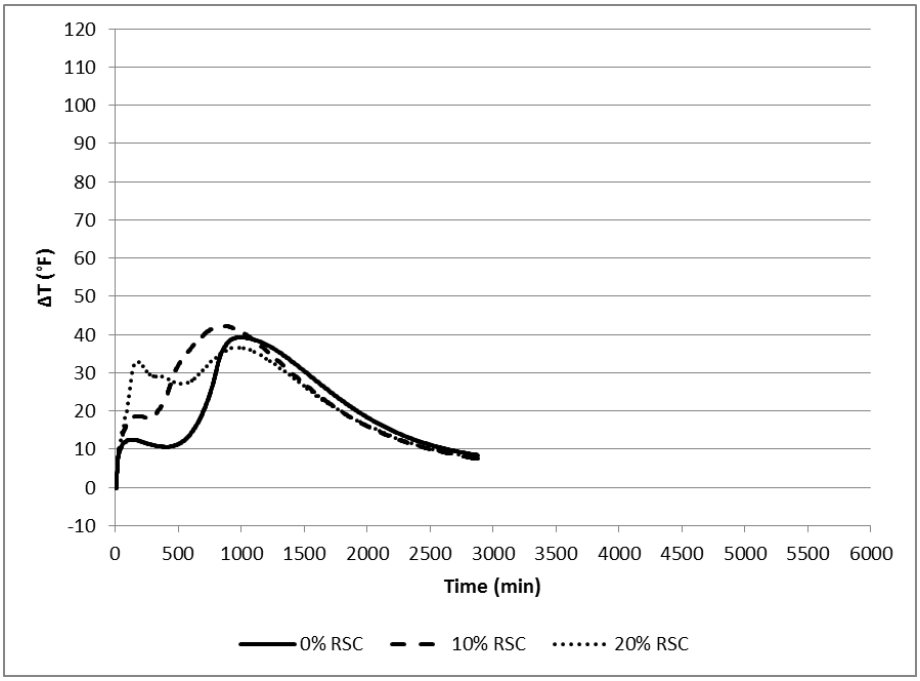

Figure E.19. Effects of Rapid Set Cement on Combination 1-3 with 50% Fly Ash, 4% Gypsum, and Low Dosage of Water Reducer

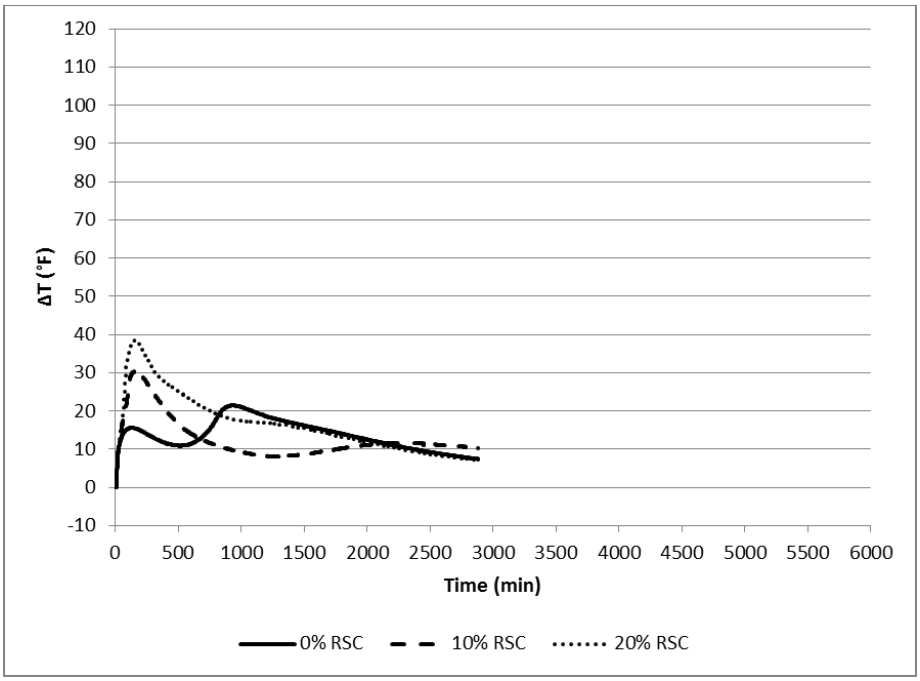

Figure E.20. Effects of Rapid Set Cement on Combination 1-3 with 70% Fly Ash, 4% Gypsum, and Low Dosage of Water Reducer

APPENDIX F

SCREENING STUDY RESULTS

Vicat Setting Time

Combination	Proportions		Vicat Results		Combination	Proportions		Vicat Results	
	Cement (%)	Fly Ash (%)	Initial Set (min)	Final Set (min)		Cement (%)	Fly Ash (%)	Initial Set (min)	Final Set (min)
Baseline 1	100	0	170	210	Baseline 4	100	0	81	180
1-1	75	25	184	345	4-1	75	25	132	270
1-1	50	50	95	390	4-1	50	50	107	300
1-1	30	70	34	405	4-1	30	70	14	285
1-2	75	25	218	390	4-2	75	25	213	450
1-2	50	50	208	510	4-2	50	50	78	525
1-2	30	70	87	450	4-2	30	70	53	480
1-3	75	25	171	375	4-3	75	25	238	435
1-3	50	50	142	435	4-3	50	50	101	660
1-3	30	70	49	525	4-3	30	70	48	300
1-4	75	25	203	450	4-4	75	25	125	360
1-4	50	50	47	360	4-4	50	50	34	270
1-4	30	70	15	135	4-4	30	70	12	105
1-5	75	25	178	480	4-5	75	25	123	255
1-5	50	50	33	180	4-5	50	50	15	195
1-5	30	70	11	45	4-5	30	70	11	60
Baseline 2	100	0	158	255	Baseline 5	100	0	146	285
2-1	75	25	182	360	5-1	75	25	158	300
2-1	50	50	67	375	5-1	50	50	100	405
2-1	30	70	20	420	5-1	30	70	21	465
2-2	75	25	154	345	5-2	75	25	179	360
2-2	50	50	71	435	5-2	50	50	175	435
2-2	30	70	57	495	5-2	30	70	59	495
2-3	75	25	151	390	5-3	75	25	149	315
2-3	50	50	40	650	5-3	50	50	54	390
2-3	30	70	12	150	5-3	30	70	13	150
2-4	75	25	92	360	5-4	75	25	167	345
2-4	50	50	35	300	5-4	50	50	48	375
2-4	30	70	12	90	5-4	30	70	14	120
2-5	75	25	80	345	5-5	75	25	136	345
2-5	50	50	13	90	5-5	50	50	13	135
2-5	30	70	11	45	5-5	30	70	11	45
Baseline 3	100	0	78	180					
3-1	75	25	170	315					
3-1	50	50	85	360					
3-1	30	70	31	225					
3-2	75	25	146	315					
3-2	50	50	101	435					
3-2	30	70	59	435					
3-3	75	25	123	300					
3-3	50	50	96	450					
3-3	30	70	40	375					
3-4	75	25	172	375					
3-4	50	50	33	300					
3-4	30	70	12	60					
3-5	75	25	124	345					
3-5	50	50	12	75					
3-5	30	70	11	30					

Compressive Strength

Combination	Proportions		1-Day Cube Strength (psi)	28-Day Cube Strength (psi)	Combination	Proportions		1-Day Cube Strength (psi)	28-Day Cube Strength (psi)
	Cement (%)	Fly Ash (%)				Cement (%)	Fly Ash (%)		
Baseline 1	100	0	4593	12300	Baseline 4	100	0	4114	11261
1-1	75	25	2805	10992	4-1	75	25	3671	10535
1-1	50	50	1246	7912	4-1	50	50	1935	8500
1-1	30	70	332	4108	4-1	30	70	665	4144
1-2	75	25	2881	9925	4-2	75	25	3625	10053
1-2	50	50	810	7980	4-2	50	50	1302	8000
1-2	30	70	70	4081	4-2	30	70	277	3842
1-3	75	25	2774	10703	4-3	75	25	3230	9921
1-3	50	50	655	7874	4-3	50	50	1564	7849
1-3	30	70	16	2475	4-3	30	70	316	2897
1-4	75	25	2767	9889	4-4	75	25	3618	10698
1-4	50	50	335	8803	4-4	50	50	1483	8088
1-4	30	70	88	5037	4-4	30	70	382	4953
1-5	75	25	2924	11342	4-5	75	25	3783	10525
1-5	50	50	515	8323	4-5	50	50	1658	8148
1-5	30	70	100	5685	4-5	30	70	538	4926
Baseline 2	100	0	4562	11708	Baseline 5	100	0	4815	12207
2-1	75	25	2722	10107	5-1	75	25	3111	11087
2-1	50	50	1094	7241	5-1	50	50	1407	8005
2-1	30	70	407	3078	5-1	30	70	612	4321
2-2	75	25	2491	5916	5-2	75	25	3069	10911
2-2	50	50	934	4221	5-2	50	50	998	8001
2-2	30	70	178	2647	5-2	30	70	293	3730
2-3	75	25	2521	8888	5-3	75	25	2943	11481
2-3	50	50	537	5850	5-3	50	50	855	7709
2-3	30	70	52	2702	5-3	30	70	105	2412
2-4	75	25	2657	10476	5-4	75	25	2958	12079
2-4	50	50	1052	7905	5-4	50	50	1101	7625
2-4	30	70	90	4133	5-4	30	70	100	4010
2-5	75	25	2511	7915	5-5	75	25	3006	11671
2-5	50	50	1091	7828	5-5	50	50	1180	8725
2-5	30	70	285	4264	5-5	30	70	325	4309
Baseline 3	100	0	5182	11806					
3-1	75	25	3182	9885					
3-1	50	50	1271	5993					
3-1	30	70	308	4316					
3-2	75	25	3522	10514					
3-2	50	50	804	5718					
3-2	30	70	55	3818					
3-3	75	25	3154	9678					
3-3	50	50	917	5813					
3-3	30	70	22	2351					
3-4	75	25	3108	10421					
3-4	50	50	339	7692					
3-4	30	70	139	5353					
3-5	75	25	3329	8991					
3-5	50	50	926	5056					
3-5	30	70	137	5479					

Calorimeter Results

Combination	Proportions		ΔT_{max} (°F)	Time at ΔT_{max} (min)	Time at 20% ΔT_{max} (min)	Time at 50% ΔT_{max} (min)	Combination	Proportions		ΔT_{max} (°F)	Time at ΔT_{max} (min)	Time at 20% ΔT_{max} (min)	Time at 50% ΔT_{max} (min)
	Cement (%)	Fly Ash (%)						Cement (%)	Fly Ash (%)				
Baseline 1	100	0	98.91	501	264	321	Baseline 4	100	0	108.25	486	288	353
1-1	75	25	71.81	685	369	445	4-1	75	25	99.92	567	306	371
1-1	50	50	45.50	885	506	592	4-1	50	50	58.97	785	475	575
1-1	30	70	24.13	882	611	730	4-1	30	70	35.17	791	537	640
1-2	75	25	75.56	773	354	436	4-2	75	25	81.61	673	402	513
1-2	50	50	31.39	1236	188	571	4-2	50	50	37.11	837	483	578
1-2	30	70	10.05	599	493	519	4-2	30	70	17.74	885	591	696
1-3	75	25	72.96	749	392	469	4-3	75	25	78.41	705	431	526
1-3	50	50	33.58	1050	477	572	4-3	50	50	45.85	917	545	642
1-3	30	70	22.25	94	26	41	4-3	30	70	16.53	1489	591	649
1-4	75	25	78.15	829	425	500	4-4	75	25	106.63	642	391	462
1-4	50	50	20.04	642	445	511	4-4	50	50	73.23	980	477	553
1-4	30	70	19.99	197	61	104	4-4	30	70	23.63	1150	503	570
1-5	75	25	87.17	756	391	463	4-5	75	25	91.93	691	474	566
1-5	50	50	19.11	597	126	186	4-5	50	50	72.94	881	463	541
1-5	30	70	21.68	704	64	108	4-5	30	70	19.85	683	513	567
Baseline 2	100	0	96.10	521	305	371	Baseline 5	100	0	115.10	111	237	298
2-1	75	25	81.29	705	380	455	5-1	75	25	83.82	678	382	471
2-1	50	50	53.69	763	455	548	5-1	50	50	55.05	844	494	605
2-1	30	70	30.52	819	573	671	5-1	30	70	29.81	868	619	720
2-2	75	25	80.25	714	374	452	5-2	75	25	91.18	674	372	452
2-2	50	50	47.50	822	438	520	5-2	50	50	45.15	900	488	583
2-2	30	70	17.89	757	541	612	5-2	30	70	16.81	1184	548	617
2-3	75	25	72.13	644	376	422	5-3	75	25	79.11	657	378	461
2-3	50	50	38.92	861	462	552	5-3	50	50	47.17	854	447	584
2-3	30	70	11.11	627	171	526	5-3	30	70	18.16	129	36	58
2-4	75	25	83.87	744	413	484	5-4	75	25	85.66	788	446	514
2-4	50	50	43.17	927	181	536	5-4	50	50	46.15	980	511	625
2-4	30	70	14.71	588	471	512	5-4	30	70	14.80	530	448	476
2-5	75	25	85.44	738	414	486	5-5	75	25	91.07	743	434	513
2-5	50	50	49.62	977	508	581	5-5	50	50	50.45	1063	533	617
2-5	30	70	-----	-----	-----	-----	5-5	30	70	-----	-----	-----	-----
Baseline 3	100	0	111.38	413	228	284							
3-1	75	25	94.79	622	364	427							
3-1	50	50	55.61	839	512	581							
3-1	30	70	28.74	767	582	627							
3-2	75	25	91.90	632	369	429							
3-2	50	50	41.65	1010	521	582							
3-2	30	70	12.26	661	316	376							
3-3	75	25	89.61	635	364	428							
3-3	50	50	39.26	966	506	583							
3-3	30	70	12.15	400	179	316							
3-4	75	25	101.17	664	413	469							
3-4	50	50	25.77	660	500	550							
3-4	30	70	20.99	185	38	86							
3-5	75	25	99.82	703	116	505							
3-5	50	50	24.73	607	452	493							
3-5	30	70	23.04	232	62	116							

Miniature Slump Results

Combination	Proportions		Early Stiffening Index (30-min/5-min)	Combination	Proportions		Early Stiffening Index (30-min/5-min)
	Cement (%)	Fly Ash (%)			Cement (%)	Fly Ash (%)	
Baseline 1	100	0	0.93	Baseline 4	100	0	0.92
1-1	75	25	1.02	4-1	75	25	0.91
1 1	50	50	0.84	1 1	50	50	0.72
1 1	30	70	0.69	1 1	30	70	0.64
1 2	75	25	0.87	1 2	75	25	1.08
1 2	50	50	0.79	1 2	50	50	0.73
1 2	30	70	0.55	1 2	30	70	0.54
1 3	75	25	0.95	1 3	75	25	0.88
1 3	50	50	0.83	1 3	50	50	0.7.
1 3	30	70	0.59	1 3	30	70	0.57
1 4	75	25	0.89	1 4	75	25	0.77
1-4	50	50	0.59	4-4	50	50	0.65
1 4	30	70	0.50	1 4	30	70	0.57
1 5	75	25	0.87	1 5	75	25	0.64
1 5	50	50	0.68	1 5	50	50	0.55
1 5	30	70	0.36	1 5	30	70	0.35
Baseline 2	100	0	0.98	Baseline 5	100	0	0.77
2 1	75	25	0.95	5 1	75	25	0.85
2 1	50	50	0.75	5 1	50	50	0.7.
2 1	30	70	0.49	5 1	30	70	0.56
2 2	75	25	0.78	5 2	75	25	0.77
2 2	50	50	0.66	5 2	50	50	0.69
2 2	30	70	0.50	5 2	30	70	0.5.
2-3	75	25	0.76	5-3	75	25	0.77
2-3	50	50	0.58	5-3	50	50	0.74
2 3	30	70	0.49	5 3	30	70	0.58
2 4	75	25	0.72	5 4	75	25	0.7.
2 4	50	50	0.49	5 4	50	50	0.58
2 4	30	70	0.30	5 4	30	70	0.48
2 5	75	25	0.75	5 5	75	25	0.72
2 5	50	50	0.46	5 5	50	50	0.57
2 5	30	70	0.27	5 5	30	70	0.26
Baseline 3	100	0	1.00				
3-1	75	25	0.90				
3-1	50	50	0.81				
3-1	30	70	0.63				
3-2	75	25	0.90				
3-2	50	50	0.83				
3-2	30	70	0.75				
3 3	75	25	0.96				
3 3	50	50	0.79				
3 3	30	70	0.61				
3 4	75	25	0.93				
3-4	50	50	0.79				
3-4	30	70	0.47				
3-5	75	25	0.86				
3-5	50	50	0.61				
3-5	30	70	0.50				

APPENDIX G

PASTE MAIN EFFECTS STUDY

Vicat Setting Time Results

	Nominal Proportions						Vicat Results	
Combination	Cement (%)	Fly Ash (%)	Gypsum (%)	Lime (%)	RSC (%)	WR (fl.oz./cwt)	Initial Set (min)	Final Set (min)
4-1	100	0	0	0	0	0.00	81	180
4-1	100	0	0	0	0	2.75	138	255
4-1	100	0	0	0	0	5.00	167	375
4-1	75	25	0	0	0	0.00	132	270
4-1	75	25	0	0	0	2.75	137	255
4-1	75	25	0	0	0	5.00	190	420
4-1	50	50	0	0	0	0.00	107	300
4-1	50	50	0	0	0	2.75	87	345
4-1	50	50	0	0	0	5.00	126	450
4-1	50	50	2	0	0	2.75	136	405
4-1	50	50	4	0	0	2.75	123	510
4-1	50	50	4	5	0	2.75	111	360
4-1	50	50	4	10	0	2.75	101	315
4-1	50	50	4	0	10	2.75	15	360
4-1	50	50	4	0	20	2.75	13	180
4-1	30	70	0	0	0	0.00	14	285
4-1	30	70	0	0	0	2.75	18	420
4-1	30	70	0	0	0	5.00	38	450
4-1	30	70	2	0	0	2.75	48	405
4-1	30	70	4	0	0	2.75	39	450
4-1	30	70	4	5	0	2.75	80	345
4-1	30	70	4	10	0	2.75	92	345
4-1	30	70	4	0	10	2.75	12	135
4-1	30	70	4	0	20	2.75	12	90
1-3	100	0	0	0	0	0.00	110	210
1-3	100	0	0	0	0	2.75	147	315
1-3	100	0	0	0	0	5.00	171	360
1-3	75	25	0	0	0	0.00	171	375
1-3	75	25	0	0	0	2.75	214	510
1-3	75	25	0	0	0	5.00	238	555
1-3	50	50	0	0	0	0.00	142	435
1-3	50	50	0	0	0	2.75	65	495
1-3	50	50	0	0	0	5.00	73	510
1-3	50	50	2	0	0	2.75	77	570
1-3	50	50	4	0	0	2.75	83	675
1-3	50	50	4	5	0	2.75	63	465
1-3	50	50	4	10	0	2.75	46	360
1-3	50	50	4	0	10	2.75	44	450
1-3	50	50	4	0	20	2.75	31	165
1-3	30	70	0	0	0	0.00	49	525
1-3	30	70	0	0	0	2.75	17	135
1-3	30	70	0	0	0	5.00	12	90
1-3	30	70	2	0	0	2.75	15	240
1-3	30	70	4	0	0	2.75	24	300
1-3	30	70	4	5	0	2.75	25	285
1-3	30	70	4	10	0	2.75	14	195
1-3	30	70	4	0	10	2.75	12	120
1-3	30	70	4	0	20	2.75	12	75

Compressive Strength Results

Combination	Nominal Proportions						Cube Compressive Strength (psi)				
	Cement (%)	Fly Ash (%)	Gypsum (%)	Lime (%)	RSC (%)	WR (fl.oz./cwt)	1-Day	3-Day	7-Day	28-Day	56-Day
4-1	100	0	0	0	0	0.00	4124	8111	9572	11251	12863
4-1	100	0	0	0	0	2.75	4199	8192	10232	11576	13625
4-1	100	0	0	0	0	5.00	5243	8808	10502	13116	13291
4-1	75	25	0	0	0	0.00	3671	6190	7842	10535	11125
4-1	75	25	0	0	0	2.75	3487	6779	7873	11015	12554
4-1	75	25	0	0	0	5.00	2857	6136	7513	10883	12989
4-1	50	50	0	0	0	0.00	1935	3535	4963	8500	8710
4-1	50	50	0	0	0	2.75	1381	3281	4855	6327	8071
4-1	50	50	0	0	0	5.00	1217	3580	4978	6574	8457
4-1	50	50	2	0	0	2.75	1284	4351	4871	6841	8162
4-1	50	50	4	0	0	2.75	710	3329	5118	6916	8361
4-1	50	50	4	5	0	2.75	822	3163	4871	6510	7204
4-1	50	50	4	10	0	2.75	1234	3134	4610	6150	7521
4-1	50	50	4	0	10	2.75	774	2940	5299	7191	8218
4-1	50	50	4	0	20	2.75	1202	3343	5311	7821	8185
4-1	30	70	0	0	0	0.00	665	1101	1740	4144	4125
4-1	30	70	0	0	0	2.75	409	1036	2036	3078	4360
4-1	30	70	0	0	0	5.00	369	1157	2075	3224	4422
4-1	30	70	2	0	0	2.75	462	1289	2088	3158	3626
4-1	30	70	4	0	0	2.75	212	1613	2441	3611	4267
4-1	30	70	4	5	0	2.75	557	1433	2157	3229	3405
4-1	30	70	4	10	0	2.75	541	1261	1992	2774	3256
4-1	30	70	4	0	10	2.75	675	1674	2793	3854	4691
4-1	30	70	4	0	20	2.75	802	1885	3067	4442	5207
1-3	100	0	0	0	0	0.00	4893	7892	8998	11300	11655
1-3	100	0	0	0	0	2.75	4176	7905	9015	12668	13979
1-3	100	0	0	0	0	5.00	3086	7790	9059	11673	13814
1-3	75	25	0	0	0	0.00	2774	4762	7034	10703	11838
1-3	75	25	0	0	0	2.75	2031	5387	7517	10577	11877
1-3	75	25	0	0	0	5.00	1642	4961	8276	11201	11913
1-3	50	50	0	0	0	0.00	655	2337	4218	7874	7480
1-3	50	50	0	0	0	2.75	239	2417	4289	5828	6915
1-3	50	50	0	0	0	5.00	135	2159	3932	6059	7252
1-3	50	50	2	0	0	2.75	348	2131	3971	5622	7354
1-3	50	50	4	0	0	2.75	315	2232	4193	5828	6986
1-3	50	50	4	5	0	2.75	656	2616	4399	5969	6393
1-3	50	50	4	10	0	2.75	697	2743	4185	5399	5972
1-3	50	50	4	0	10	2.75	660	2901	4587	6667	8249
1-3	50	50	4	0	20	2.75	506	2931	4785	7150	8480
1-3	30	70	0	0	0	0.00	16	75	93	2475	3168
1-3	30	70	0	0	0	2.75	58	71	104	2588	4867
1-3	30	70	0	0	0	5.00	59	76	98	2504	3414
1-3	30	70	2	0	0	2.75	64	457	1459	2837	4768
1-3	30	70	4	0	0	2.75	212	998	1696	2890	3750
1-3	30	70	4	5	0	2.75	244	913	1596	2659	3291
1-3	30	70	4	10	0	2.75	240	781	1432	2685	3118
1-3	30	70	4	0	10	2.75	275	1012	1875	3544	4331
1-3	30	70	4	0	20	2.75	443	567	2431	4352	5965

Calorimeter Results

Combination	Nominal Proportions						ΔT_{max} (°F)	Time at ΔT_{max} (min)	Time at 20% ΔT_{max} (min)	Time at 50% ΔT_{max} (min)
	Cement (%)	Fly Ash (%)	Gypsum (%)	Lime (%)	RSC (%)	WR (fl.oz./cwt)				
4-1	100	0	0	0	0	0.00	108.25	186	288	353
4-1	100	0	0	0	0	2.75	107.74	551	347	413
4-1	100	0	0	0	0	5.00	118.16	501	314	374
4-1	75	25	0	0	0	0.00	99.92	567	306	374
4-1	75	25	0	0	0	2.75	97.39	618	345	420
4-1	75	25	0	0	0	5.00	88.80	753	483	569
4-1	50	50	0	0	0	0.00	58.97	782	475	573
4-1	50	50	0	0	0	2.75	59.37	846	513	639
4-1	50	50	0	0	0	5.00	57.82	948	621	722
4-1	50	50	2	0	0	2.75	58.36	908	588	697
4-1	50	50	4	0	0	2.75	58.34	962	630	756
4-1	50	50	4	5	0	2.75	58.58	886	534	678
4-1	50	50	4	10	0	2.75	59.37	631	325	444
4-1	50	50	4	0	10	2.75	54.61	726	433	564
4-1	50	50	4	0	20	2.75	51.13	520	251	318
4-1	30	70	0	0	0	0.00	35.17	794	537	640
4-1	30	70	0	0	0	2.75	28.98	964	680	795
4-1	30	70	0	0	0	5.00	30.61	984	707	812
4-1	30	70	2	0	0	2.75	34.32	995	684	817
4-1	30	70	4	0	0	2.75	34.39	1148	787	947
4-1	30	70	4	5	0	2.75	34.37	720	394	547
4-1	30	70	4	10	0	2.75	35.38	613	285	401
4-1	30	70	4	0	10	2.75	35.50	544	303	378
4-1	30	70	4	0	20	2.75	43.67	210	58	81
1-3	100	0	0	0	0	0.00	95.91	501	264	321
1-3	100	0	0	0	0	2.75	104.14	532	314	378
1-3	100	0	0	0	0	5.00	92.43	636	407	481
1-3	75	25	0	0	0	0.00	72.96	749	392	469
1-3	75	25	0	0	0	2.75	80.95	757	423	490
1-3	75	25	0	0	0	5.00	72.64	836	502	577
1-3	50	50	0	0	0	0.00	33.58	1050	477	572
1-3	50	50	0	0	0	2.75	34.69	1245	493	778
1-3	50	50	0	0	0	5.00	30.88	1497	564	1020
1-3	50	50	2	0	0	2.75	33.35	1130	590	686
1-3	50	50	4	0	0	2.75	39.27	991	644	756
1-3	50	50	4	5	0	2.75	41.25	792	406	497
1-3	50	50	4	10	0	2.75	41.02	702	317	414
1-3	50	50	4	0	10	2.75	42.30	852	394	473
1-3	50	50	4	0	20	2.75	32.86	171	55	100
1-3	30	70	0	0	0	0.00	22.25	94	28	41
1-3	30	70	0	0	0	2.75	19.85	92	27	36
1-3	30	70	0	0	0	5.00	19.26	96	27	38
1-3	30	70	2	0	0	2.75	18.41	209	26	41
1-3	30	70	4	0	0	2.75	15.62	126	25	37
1-3	30	70	4	5	0	2.75	21.69	820	439	508
1-3	30	70	4	10	0	2.75	23.83	483	289	372
1-3	30	70	4	0	10	2.75	30.32	162	50	84
1-3	30	70	4	0	20	2.75	38.42	149	39	71

Miniature Slump Results

Combination	Nominal Proportions						Early Stiffening Index
	Cement (%)	Fly Ash (%)	Gypsum (%)	Lime (%)	RSC (%)	WR (fl.oz./cwt)	(30-min/5-min)
4-1	100	0	0	0	0	0.00	0.92
4-1	100	0	0	0	0	2.75	0.83
4-1	100	0	0	0	0	5.00	1.14
4-1	75	25	0	0	0	0.00	0.91
4-1	75	25	0	0	0	2.75	0.73
4-1	75	25	0	0	0	5.00	1.01
4-1	50	50	0	0	0	0.00	0.72
4-1	50	50	0	0	0	2.75	0.76
4-1	50	50	0	0	0	5.00	0.94
4-1	50	50	2	0	0	2.75	0.71
4-1	50	50	4	0	0	2.75	0.72
4-1	50	50	4	5	0	2.75	0.84
4-1	50	50	4	10	0	2.75	0.61
4-1	50	50	4	0	10	2.75	0.59
4-1	50	50	4	0	20	2.75	0.42
4-1	30	70	0	0	0	0.00	0.64
4-1	30	70	0	0	0	2.75	0.48
4-1	30	70	0	0	0	5.00	0.81
4-1	30	70	2	0	0	2.75	0.46
4-1	30	70	4	0	0	2.75	0.61
4-1	30	70	4	5	0	2.75	0.53
4-1	30	70	4	10	0	2.75	0.62
4-1	30	70	4	0	10	2.75	0.29
4-1	30	70	4	0	20	2.75	0.20
1-3	100	0	0	0	0	0.00	0.93
1-3	100	0	0	0	0	2.75	1.35
1-3	100	0	0	0	0	5.00	1.65
1-3	75	25	0	0	0	0.00	0.95
1-3	75	25	0	0	0	2.75	0.84
1-3	75	25	0	0	0	5.00	1.17
1-3	50	50	0	0	0	0.00	0.83
1-3	50	50	0	0	0	2.75	0.47
1-3	50	50	0	0	0	5.00	0.80
1-3	50	50	2	0	0	2.75	0.53
1-3	50	50	4	0	0	2.75	0.56
1-3	50	50	4	5	0	2.75	0.59
1-3	50	50	4	10	0	2.75	0.59
1-3	50	50	4	0	10	2.75	0.42
1-3	50	50	4	0	20	2.75	0.37
1-3	30	70	0	0	0	0.00	0.59
1-3	30	70	0	0	0	2.75	
1-3	30	70	0	0	0	5.00	0.17
1-3	30	70	2	0	0	2.75	0.39
1-3	30	70	4	0	0	2.75	0.42
1-3	30	70	4	5	0	2.75	0.45
1-3	30	70	4	10	0	2.75	-----
1-3	30	70	4	0	10	2.75	0.38
1-3	30	70	4	0	20	2.75	-----

APPENDIX H

Abrasion Resistance of Concrete

ASTM C 944

7/3/12

Equipment

Equipment includes a drill press, an abrasion head conforming to ASTM C 944, a weight applied to the drill press arm conforming to a 44 pound double load, the 32 kg Ohaus balance, digital calipers, and a stopwatch.

Procedure

1. Remove the abrasion resistance test specimen from the moist room 15 minutes before testing, drying the surface with a cloth to remove free water.
2. Secure the abrasion head into the drill press and tighten down.
3. Check that the drill press is set for 300 RPM.
4. Set the drill press table to an appropriate height so that when the abrasion head is flush with the concrete surface, the drill press arm is parallel to the ground.
5. Record the time.
6. Obtain and record the initial weight of the sample.
7. Position the test specimen in the clamp on the drill press table so that there is adequate space to conduct the test. (IE, the specimen should be placed so that the abrasion head is grinding against the concrete specimen at all times during the test.)
8. Bring the head down into contact with the specimen. Hang the weight corresponding to a 44 pound double load from the arm of the drill press.

9. Turn the drill press on, and begin timing with the stop watch.
10. Turn the drill press off after two minutes of abrasion.
11. Carefully remove the test specimen from the clamp, taking care not to damage it. Remove dust from the surface with clean air.
12. Weigh the test specimen and record.
13. Replace the test specimen in the clamp, taking care to reposition it exactly beneath the abrasion head.
14. Bring the abrasion head down manually to check position. Do this at at least two degrees of rotation to ensure positioning.
15. Repeat steps 8 through 14 twice more, so that the test specimen has been abraded in the same location three times.
16. Using the digital calipers, check the depth of wear.

a. An average depth of wear is calculated by checking the depth of wear at eight points.
b. The eight points correspond to the 12 o’clock, 3 o’clock, 6 o’clock, and 9 o’clock positions on the test specimen at both the innermost and outermost abraded rings on the specimen.

17. Calculate mass loss for each of the abrasion periods.
18. Sum each mass loss and record a total mass loss for that replicate.
19. This abrasion procedure is conducted three times on the specimen, for a total of three replicate tests.

		28 Day	56 Day
Replicate 1	Start Time	3:30	2:57
	Initial Weight	13192.4	13456.4
	Weight 1	13169	13431.3
	Mass Loss 1	23.4	25.1
	Weight 2	13159	13422.1
	Mass Loss 2	10	9.2
	Weight 3	13150.5	13414.8
	Mass Loss 3	8.5	7.3
	Total Mass Loss	41.9	41.6
	Depth of wear	1.91	2.49
Replicate 2	Start Time	3:39	3:08
	Initial Weight	13150.5	13414.8
	Weight 1	13122.9	13392.4
	Mass Loss 1	27.6	22.4
	Weight 2	13112.6	13382.4
	Mass Loss 2	10.3	10
	Weight 3	13104.9	13375.5
	Mass Loss 3	7.7	6.9
	Total Mass Loss	45.6	39.3
	Depth of wear	2.29	2.31
Replicate 3	Start Time	3:48	3:20
	Initial Weight	13104.9	13374.1
	Weight 1	13077.1	13349.9
	Mass Loss 1	27.8	24.2
	Weight 2	13067.1	13342.6
	Mass Loss 2	10	7.3
	Weight 3	13060.1	13335.4
	Mass Loss 3	7	7.2
	Total Mass Loss	44.8	38.7
	Depth of wear	2.35	2.0425
Average Mass Loss		44.10	39.87
Average Depth of Wear		2.18	2.28

APPENDIX I

Testing Shrinkage Specimens

7/3/12

Equipment

Equipment includes DEMEC points, metal/concrete epoxy, and a DEMEC gauge with reference bar.

Procedure

20. 24 hours after casting, demold the specimens by use of a dremel tool with a cutting head.
21. Mark the shrinkage specimens with name and number with a black sharpie.
22. Using the DEMEC reference tool, mark the specimens with locations to place the DEMEC points, ensuring that they are placed in a vertical fashion. The first DEMEC point is placed 4 inches from the top of the specimen, and subsequent DEMEC points are placed the distance of the reference tool apart.
23. Apply a small amount of metal/concrete epoxy to the surface of the shrinkage specimen, where the DEMEC points are to be placed.
24. Press the DEMEC point into the epoxy.
25. Repeat steps 4 and 5 until all DEMEC points are applied to the specimen. For HVFA study, this is 10 DEMEC points, in lines of 5 at 180 degrees from each other.
26. Take initial readings as soon as possible after demolding and applying the DEMEC points.

Testing

1. Before taking readings, use the DEMEC gauge to take a length reading of the reference bar. Record this on the data sheet.
2. Record the temperature and relative humidity.
3. Record the time.

4. Fit the DEMEC gauge onto the points, rocking the gauge from side to side. The largest reading on the dial occurs when the gauge is perpendicular to the points, and this is the reading that should be recorded.
5. Readings should be taken on each specimen every day until 14 days of age, every 2 days until 28 days, every 4 days until 56 days, and every week thereafter.

Data

1. To obtain the shrinkage for each day, first subtract the reference bar reading from the day's length reading for each reading. These are the adjusted readings.
    a. *Example: Day 1 reading—1020. Day 2 reading—1018. Reference bar reads 800 for both days. Adjusted reading for Day 1 is 1020-800=220. Adjusted reading for Day 2 is 1018-800=218.*
2. The difference between two days (for instance, day 2 and day 1) provides the shrinkage for day 2 in dial reading increments.
    a. *Example: 220-218=2.*
3. Multiply the shrinkage in dial reading increments by the adjustment factor provided with the DEMEC gauge to convert to shrinkage in microstrain.
    a. *Example: 2*7.6 microstrain/dial reading = 15.2 microstrain.*
4. Average the microstrain for a given day.
    a. Each specimen will consist of 6 readings, averaged to determine an average strain.
5. Summing each day's strain, calculate the accumulative strain. Numbers will be negative due to calculation method.
6. Take the absolute value of these numbers to convert to a positive number, and plot accumulative strain versus age in days.

Cast Date													
3-26-12	Read Date:	3-27-12	3-28-12	3-29-12	3-30-12	3-31-12	4-01-12	4-02-12	4-03-12	4-04-12	4-05-12	4-06-12	4-07-12
	Time:	3:12	2:05	1:43	5:12	3:53	11:39	4:00	1:18	4:11	1:17	2:29	3:27
	Temp:	72	70	70	72	72	72	72	72	72	72	72	78
	Rel Humid:	55.00%	63.00%	61.00%	60.00%	60.00%	68.00%	60.00%	63.00%	70.00%	56.00%	36.00%	38.00%

Specimen	Reading	1	2	3	4	5	6	7	8	9	10	11	12
Refer Bar		806	806	807	807	807	807	806	807	807	806	807	808
Hbase 2	1--1	583	583	583	583	580	578	576	573	572	570	569	568
Hbase 2	1--2	976	975	973	970	968	965	961	958	955	954	953	948
Hbase 2	1--3	1070	1069	1065	1061	1058	1056	1052	1049	1048	1047	1042	1036
Hbase 2	2--1	470	466	463	457	456	454	451	449	448	447	444	443
Hbase 2	2--2	1268	1261	1258	1256	1251	1249	1246	1241	1238	1237	1236	1236
Hbase 2	2--3	706	697	689	682	677	675	674	671	668	668	669	663

Shrinkage Calcs:

Specimen	Reading												
Age		1	2	3	4	5	6	7	8	9	10	11	12
Hbase 2	1--1		0	-7.84	0	-23.52	-15.68	-7.84	-31.36	-7.84	-7.84	-15.68	-15.68
Hbase 2	1--2		-7.84	-23.52	-23.52	-15.68	-23.52	-23.52	-31.36	-23.52	0	-15.68	-47.04
Hbase 2	1--3		-7.84	-39.2	-31.36	-23.52	-15.68	-23.52	-31.36	-7.84	0	-47.04	-54.88
Hbase 2	2--1		-31.36	-31.36	-47.04	-7.84	-15.68	-15.68	-23.52	-7.84	0	-31.36	-15.68
Hbase 2	2--2		-54.88	-31.36	-15.68	-39.2	-15.68	-15.68	-47.04	-23.52	0	-15.68	-7.84
Hbase 2	2--3		-70.56	-70.56	-54.88	-39.2	-15.68	0	-31.36	-23.52	7.84	0	-54.88
		Average	-28.7467	-33.9733	-28.7467	-24.8267	-16.9867	-14.3733	-32.6667	-15.68	0	-20.9067	-32.6667
		Acc. Strain	-28.75	-62.72	-91.47	-116.29	-133.28	-147.65	-180.32	-196.00	-196.00	-216.91	-249.57
		Plot	28.74667	62.72	91.46667	116.2933	133.28	147.6533	180.32	196	196	216.9067	249.5733

APPENDIX J
CONCRETE STUDY RESULTS

Table J.1 Concrete Setting Time

	Combination 4-1		Combination 1-3	
	Initial Set	Final Set	Initial Set	Final Set
Baseline	314	403	272	349
50% FA w/CH	461	579	556	733
50% FA w/RSC	388	566	582	797
70% FA w/CH	483	673	656	952
70% FA w/RSC	219	422	336	561

Table J.2 Concrete Compressive Strength (4-1)

	Combination 4-1				
Compressive Strength	Baseline	50% FA with CH	70% FA with CH	50% FA with RSC	70% FA with RSC
1 Day	2636	993	385	1063	548
7 Day	4440	3174	2017	3823	2045
28 Day	4909	4466	2916	4807	2962
56 Day	5651	5703	3470	5849	3686

Table J.3 Concrete Compressive Strength (1-3)

	Combination 1-3				
Compressive Strength	Baseline	50% FA with CH	70% FA with CH	50% FA with RSC	70% FA with RSC
1 Day	2586	624	158	525	264
7 Day	4750	3202	1304	3037	1748
28 Day	5634	4778	2696	4746	3376
56 Day	5663	5485	3139	5001	3033

Table J.4 Compressive Strength, MOR, Splitting tensile Strength, and MOE (4-1)

	Combination 4-1				
	Baseline	50% FA with CH	70% FA with CH	50% FA with RSC	70% FA with RSC
28 Day Comp. Str.	4909	4466	2916	4807	2962
Modulus of Rupture	727	695	460	698	546
Splitting Tensile	437	458	313	485	379
Modulus of Elasticity	4716461	5193245	4254350	5058505	4677422

Table J.5 Compressive Strength, MOR, Splitting tensile Strength, and MOE (1-3)

	Combination 1-3				
	Baseline	50% FA with CH	70% FA with CH	50% FA with RSC	70% FA with RSC
28 Day Comp. Str.	5634	4778	2696	4746	3376
Modulus of Rupture	796	637	395	622	455
Splitting Tensile	486	462	276	459	346
Modulus of Elasticity	5046413	4980308	3953000	5279370	4551751

Table J.6 Durability (4-1)

	4-1 Combinations				
	Baseline	50% FA with CH	70% FA with CH	50% FA with RSC	70% FA with RSC
RCP	2846	1339	5537	1139	3678
Durability Factor	78.16	92.97	96.66	93.47	96.49
Scaling @ 50 cycles	1	5	5	5*	5*

*Scaling @ 40 cycles

Table J.7 Durability (1-3)

	1-3 Combinations				
	Baseline	50% FA with CH	70% FA with CH	50% FA with RSC	70% FA with RSC
RCP	2438	3081	NA	2339	4669
Durability Factor	87.25	92.31	96.71	90.86	95.38
Scaling @ 50 cycles	2	5*	5*	4*	3*

*Scaling @ 40 cycles

Table J.8 Abrasion Resistance (4-1)

		Combination 4-1				
		Baseline	50% FA w/CH	50% FA w/RSC	70% FA w/CH	70% FA w/RSC
28 Day	Mass Loss	11.2	19.6	44.1	23.4	44.2
	Depth of Wear	0.8	1.2	2.2	1.6	2.6
56 Day	Mass Loss	12.7	15.4	39.9	17.8	31.2
	Depth of Wear	0.9	1.1	2.3	1.4	1.9

Table J.9 Abrasion Resistance (1-3)

		Combination 1-3				
		Baseline	50% FA w/CH	50% FA w/RSC	70% FA w/CH	70% FA w/RSC
28 Day	Mass Loss	13.8	24.9	48.2	23.5	42.3
	Depth of Wear	0.9	1.7	2.8	1.5	2.2
56 Day	Mass Loss	14.2	17.9	33.9	21.7	34.5
	Depth of Wear	1.1	1.3	2.1	1.5	2.1

Table J.10 Scaling Results

Blend	% Fly Ash	Additive	Rating
4-1	**0**	**---**	**1**
4-1	**50**	**Lime**	**5**
4-1	**70**	**Lime**	**5**
4-1	**50**	**RSC**	**5**
4-1	**70**	**RSC**	**5**
1-3	**0**	**---**	**2**
1-3	**50**	**Lime**	**5**
1-3	**70**	**Lime**	**5**
1-3	**50**	**RSC**	**4 at 40 cycles**
1-3	**70**	**RSC**	**3 at 40 cycles**